TECHNIQUES FOR THE TUNING OF HELICOPTER MULTIVARIABLE FLIGHT CONTROL SYSTEMS AND HANDLING QUALITIES

A Thesis Submitted to the

Faculty of Engineering

University of Glasgow

for the Degree of

Doctor of Philosophy

by

Michael Arnold Manness, B.A.Sc. (Hons.)

December 1988

ProQuest Number: 10999317

ProQuest 10999317

To my parents.

ACKNOWLEDGEMENTS

TABLE OF CONTENTS

SUMMARY

Helicopter flight control systems are often developed using low order linear descriptions of the plant. Unfortunately, unmodelled high order dynamics, such as those of the actuators and the main rotor, can have an adverse effect on stability and cross couplings when the design is tested on the aircraft. Hence, the flight controller may require tuning during commissioning trials in order to yield a system with acceptable handling qualities.

As the sophistication of flight control systems is enhanced, the currently used trial and error optimization techniques will lose effectiveness. Anticipating the difficulties which will arise in the implementation of active control technology to helicopters, a study has been made of systematic procedures for adjusting the control system gains. The tuning processes which have been developed rely upon the signal convolution method to generate sensitivity functions of the state variables with respect to control system gains. State variable sensitivities allow one to predict what effects changing a controller gain will have on the system response. The beauty of the signal convolution method is that the sensitivity information is generated without knowledge of the helicopter plant. Therefore, by using data collected during flight trials, it is possible to calculate the sensitivity functions with respect to the dynamics of the actual system plant, including the unmodelled modes.

The sensitivity information is used by an adjustment algorithm which employs Newton—Raphson techniques to predict how the system response will change with a trial set of perturbations to the controller gains. For each set of perturbations, an estimate is made of the modifed response which, in turn, is assigned a figure of merit. The set of perturbation values which yields the best figure of merit is then used to update the initial values of the control system gains. Since the characteristics of the optimized system response are determined by the type of figure of merit used in the adjustment algorithm, two distinct performance indices have been evaluated during the study.

In model reference tuning, the Least Integral Error Square Performance Index is calculated to provide the figure of merit for each projected system response. The controller gains are altered to minimize the difference between the response of the actual system and a desirable response which is generated by a computer simulation model. However, in using a reference model, care must be taken to ensure that the desirable response is consistent with a Level 1

handling qualities rating so that pilots find the tuned system acceptable to fly.

In contrast, the Handling Qualities Performance Index allows system responses to be compared explicitly in terms of whether or not they satisfy the handling quality requirements. As these requirements form the starting point for many control system designs, the use of the Handling Qualities Performance Index should guarantee an improvement in system response. This new performance index uniquely links the values of control system gains to the helicopter's handling quality ratings.

Computer simulation has been used to validate both the application of the signal convolution method to multivariable control systems and the ability of the two performance indices to tune a helicopter's flight controller. The flight control systems considered during these simulations were developed using modal control theory and have been used with both linear and nonlinear representations of the helicopter plant. The results of a real—time simulation have reinforced the notion that the flight controller's structure and parameter values must be determined with respect to desirable flight handling qualities rather than purely on the basis of mathematical control system design techniques.

CHAPTER 1: INTRODUCTION

1.1) Helicopter Operations

The helicopter's unique ability to hover efficiently has made it an invaluable component of modern military operations and of civil tasks such as medical evacuation, public transport, and search and rescue. While civil operators are looking for increased safety, the military is primarily concerned with increased performance and ease of operations. NATO countries are placing greater emphasis on helicopters because of their mobility and fire– power [1]. Future land battles will see battlefield helicopters used to engage armoured vehicles in both the front line and rearward areas, with weapons ranging from missiles to light cannons. Current senarios envisage three distinct phases in a typical anti– armour operation [2]. High speed contour flight to and from the combat zone will involve the aircraft flying at a fairly constant speed at a prescribed height above ground level to avoid obstacles. Upon reaching the combat zone, where concealment is of prime importance, pilots will use *'nap of the earth'* (NOE) flight to minimize exposure to enemy forces. Since the use of armour for protection on helicopters limits their usable payloads, the main defensive tactic employed must be to use trees, buildings and terrain features for concealment [2],[3]. The third phase of the anti– armour mission is the hover which is extensively used for target acquisition and weapons firing. Battlefield helicopters are forced to fly as low as possible during all operations because of the lethality of modern air defense systems.

The performance demands of military operations are most severe during NOE flight and the emerging realm of air to air combat between opposing helicopters. Although air to air combat tactics are still being developed [4], standard NOE manoeuvres are currently being used to compare different helicopters, and handling quality criteria are being developed with reference to NOE manoeuvres. These standard manoeuvres are designed to test the aircraft's ability to minimize exposure to threats when moving between two or more concealed positions [5]. The *'slalom'* involves moving laterally during forward flight to take advantage of objects lining the intended flight path (Figure 1.1), while the *'dolphin'* involves changing height to minimize the time spent above objects blocking the flight path (Figure 1.2). Three manoeuvres which are initiated and terminated in a hover are: the *'bob up/ bob down'*, the *'sidestep*

– 1 –
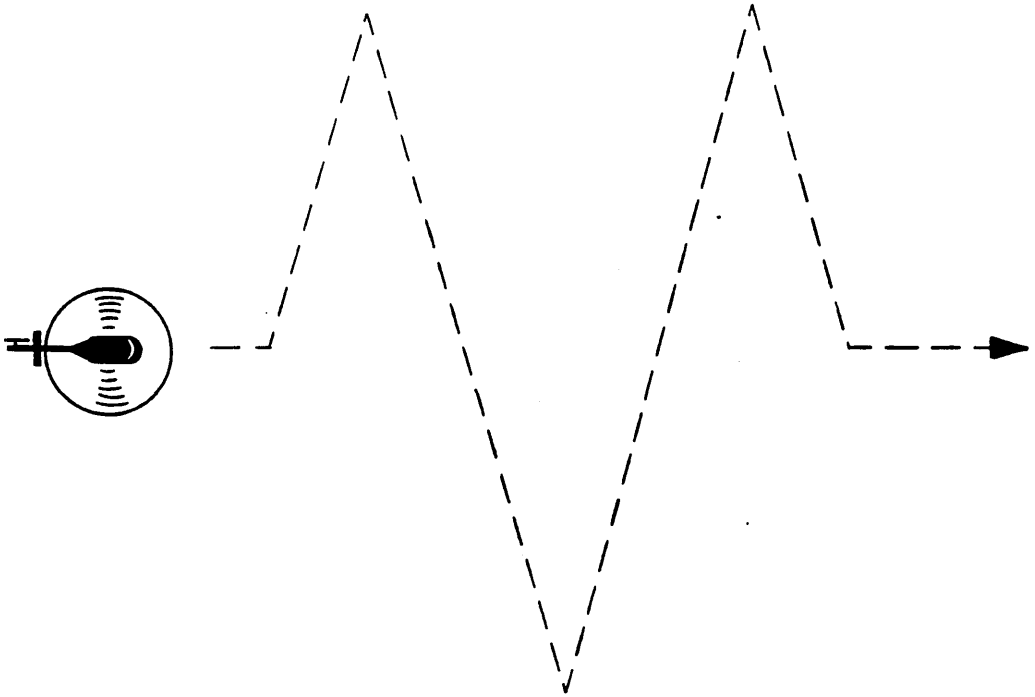
Figure 1.1: An idealized representation of the slalom manoeuvre.
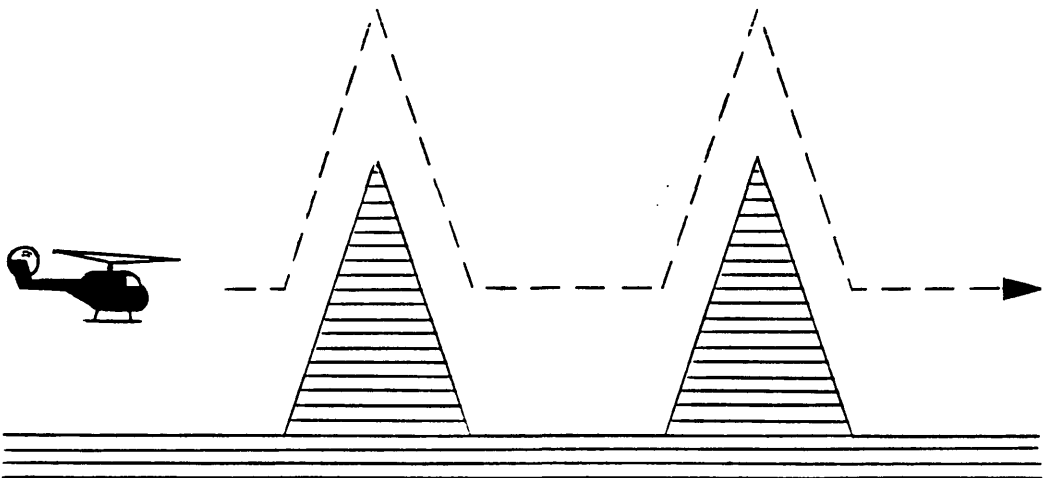
Figure 1.2: An idealized representation of the dolphin manoeuvre.

unmask/remask', and the *'dash/quickstop'*. The bob up/bob down is used for weapons firing while the sidestep and dash are used to change the hover position in a lateral and longitudinal sense with regard to the fuselage heading.

To maximize the effectiveness of NOE tactics, and hence the survivability of the vehicle, the pilot must have tight control over the helicopter's motions. Agility is the term used to describe how easily a helicopter makes the rapid and precise changes of velocity necessary in aggressive manoeuvres [5]. Agility is improved by increasing the amount of thrust available for manoeuvres and by easing the control of this excess thrust for the pilot. Although agility depends on the availability of excess rotor thrust, studies have shown that the authority which a pilot has over the excess rotor thrust will have a far greater influence on the precision of NOE manoeuvres [5]. Aggressive manoeuvring will require large and rapid pilot inputs and thus the flight control system must have a bandwidth which is commensurate with these inputs. Hence, NOE flight is motivating a drive towards high bandwidth flight controllers.

1.2) Handling Qualities

Handling qualities describe the ease or difficulty with which a pilot can perform manoeuvres and are of primary concern in the development of flight control systems. To simply increase the thrust available for manoeuvring without providing adequate means of controlling the excess power can increase the pilot's workload. Indeed, one of the main objectives of flight controller design is to yield a vehicle which is easier to fly. Improved handling qualities (control over the excess rotor thrust) will reduce the pilot's workload in terms of flying the aircraft, leading to greater mission effectiveness [2]. By improving the handling, manoeuvres are flown at higher speeds, and closer to the ground and obstacles: all of which results in a greater degree of concealment and increased survivability [6].

If handling qualities are improved such that NOE flight can be carried out at the minimum power speed (well above the currently used hover and taxi speeds) many operational benefits will arise [2]. At the minimum power speed, fuel consumption is reduced and power management is simplified because the energy expended in keeping the aircraft airborne is at a minimum. Thus, the excess thrust available for manoeuvring is at a maximum resulting in maximum absolute agility. Handling qualities determine the usable agility — that which the pilot will make use of during flight. Ideally, the ratio of usable to absolute

agility will be increased to 1.0 which will yield a helicopter with *'carefree manoeuvring'*. Carefree manoeuvring exists when a pilot can fly the vehicle to the edge of the flight envelope without losing control and without causing excessive fatique damage to the aircraft [5]. The flight envelope is bounded by the flight conditions beyond which the helicopter cannot remain airborne. Therefore a helicopter possessing good handling qualities as measured by useable agility will allow the safe use of more of the vehicle's performance in terms of flight near to the edge of the flight envelope.

1.3) Active Control Technology

Modern flight control systems make use of *'active control technology'* (ACT) for several reasons. By having a computer dynamically involved in flight control, ACT systems promise to improve both the usable and absolute agility of helicopters [5]. The use of a computer allows raw dynamics of helicopters to be modified such that the pilot is less aware of nonlinearities and cross— couplings. Examples of helicopter nonlinearities are the hysteresis present in hydraulic actuators and mechanical linkages and the rate limits on the motion of the actuators. Although ACT will allow the removal of many mechanical parts used for flight control, actuators will continue to be used to change the pitch on individual rotor blades and hence the magnitude and direction of the main rotor's thrust vector. Cross— couplings between longitudinal and lateral dynamics are more severe on helicopters with hingeless as opposed to articulated rotors. While increasing the absolute agility of helicopters, the dynamics of hingeless rotors can increase the pilot's workload in manoeuvring the aircraft. Modern control theories and techniques are required to design flight controllers which decouple system dynamics from the pilot's point of view. By implementing these control laws with onboard computers, the vehicle is made easier to fly. Therefore, ACT allows an increase in usable agility by improving the system's handling qualities.

On battlefield helicopters, one aim is to develop single pilot crewstations in order to reduce training time, weight and costs. Present handling qualities are such that the workload of flying, navigation, launching weapons, and keeping a lookout for threats is excessive, even for a two man crew. Training time is reduced with a single pilot crewstation because the need to develop teamwork between the pilot and a copilot/gunner is eliminated.

Active control technology is being used in two closely related areas to achieve the single person crewstation objective. As noted previously, computers

allow a tailoring of the raw vehicle dynamics to make the aircraft easier to fly. At the same time, ACT allows a complete redesign of the man—machine interface in the cockpit. It is no longer necessary to have a collective lever controlling the total rotor thrust and a large cyclic stick to provide the leverage needed to tilt the rotor's thrust vector. Because pilot inputs are being fed directly into a computer, it is possible to have small sidearm inceptors rather than conventional controls [7]. Since these inceptors can be smaller, valuable cockpit space is saved for other uses. In addition, displacements of these inceptors can be interpreted in several ways. For example, with a traditional cyclic stick the position of the stick specifies the position of the longitudinal and lateral cyclic rotor blade actuators. The positions of these actuators, in turn, determine the direction of the thrust vector and hence the steady state flight condition. In contrast to this attitude demand system, sidearm controller displacement can be interpreted as a demand for rates of change of aircraft motion. In a rate demand system, the lateral position of a sidearm inceptor might be proportional to a demanded roll rate. The flight computer will then move the rotor blade actuators in order to achieve this roll rate demand. In this way the pilot's inputs are related more directly to aircraft states of motion than has been possible in the past. These inceptor characteristics can have a large bearing on how pilots judge a helicopter's handling qualities on the Cooper—Harper scale [7]. Other improvements to the man—machine interface can be made by increasing the information displayed to the pilot on 'Head Up Displays' (HUD). A HUD is a projection of the flight path/vehicle attitude information on to either the glass canopy of the cockpit or on to the visor of the pilot's helmet and allows the pilot to perform various functions while continuing to look at the outside world.

In terms of absolute agility, the use of ACT can be of benefit because the speed of the natural modes of motion of the system can be increased. These natural modes determine the stability of the helicopter and how quickly it will respond to pilot inputs and disturbances, such as wind gusts.

In summary, ACT can be used to expand the usable flight envelope by reducing cross—couplings, improving the man—machine interface, and increasing agility. These advantages of ACT systems can be recorded as improved flight handling qualities. Although the cost and weight motives behind the introduction of ACT to helicopters are not as important as for fixed wing aircraft [5], full authority manoeuvre demand flight control systems are essential for NOE operations and the survivability of the battlefield helicopter.

1.4) The Tuning Requirement

The need to tune fly by wire flight control systems on new helicopters persists despite ACT due to current design techniques. Computer simulation of the aircraft dynamics through the use of mathematical models is the basis of most flight control system designs. Since the simulation models do not incorporate all of the dynamics of the helicopter to be controlled, errors are introduced into the design of the flight controller from a very early stage. Such errors are important as they appear during real–time piloted flight simulations and test flights as handling quality deficiencies.

Flight control systems are traditionally designed around eighth order, six degree of freedom models of the helicopter fuselage dynamics. Models of this type use the quasi–static rotor approximation in which the dynamics of the tip path plane of the rotor blades are ignored [8]. Essentially, the blades are treated collectively as a lifting disc, rather than looking at the flapping, lagging, and feathering motions of the blades as they revolve about the rotor shaft axis. Since the pitch on each blade is varied sinusoidally about a constant value during each revolution for stability and control purposes on the actual aircraft, various secondary blade motions tend to be excited. In addition to neglecting the complex rotor motions, low order linear models also ignore actuator dynamics which are responsible for considerable delays in system response.

When developing the high bandwidth flight controllers needed for NOE operations, the natural resonances of the fuselage in flight are moved closer to those of the main rotor. The interactions which result lead to compromises in the system's static and dynamic stability. In a comprehensive study of the effects of high order system dynamics on the bandwidth of helicopter flight controllers, Chen and Hindson [9] showed that increasing roll rate and roll attitude feedback caused the regressing flapping rotor mode of a CH47 helicopter to migrate towards a right half plane zero. As system bandwidth is extended by the increasing feedback, the stability of the regressing flapping mode decreases.

The dynamics of the rotor, sensors, filters, and actuators have traditionally been referred to as high order dynamics because the poles characterizing their motion were well separated from the slower dynamics of the fuselage. Since high order dynamics place restrictions on the gains which can be used in controllers, they should be considered in all designs of high bandwidth flight systems. Unfortunately, rotor models are notoriously inaccurate, particularly during manoeuvres. In addition, the nonlinear actuator dynamics are commonly represented by simple first order linear lags. The control engineer is presently

faced with making a decision between using a simple, understandable model of the fuselage dynamics, or a much more complex description which he knows to be flawed. The danger in using the simpler model is that by neglecting high order dynamics, the controller may cause instabilities when used with the actual system thereby creating the need for tuning. Even if new flight control systems are developed with the currently inaccurate descriptions of the rotor dynamics, they will need to be optimized with regard to the actual system.

Although inaccuracies in mathematical descriptions of the helicopter are responsible for most of the need for tuning, fixed wing experience indicates that flying quality deficiencies will persist even with accurate models. Despite the use of advanced control system design methods allowed by ACT, fixed wing aircraft prototypes continue to suffer from problems with control sensitivity, pilot induced oscillations, and sluggish responses. These continuing handling deficiencies have been attributed to an over reliance on piloted flight simulation and a communication gap which exists between handling quality engineers and control system engineers [10]. Contrary to previously held beliefs that advances in flight control would eliminate deficient handling qualities, there is evidence to indicate that hardware and software capabilities are not being properly utilized because handling quality criteria have not matured at a rate which will give direction to control system design. As in most aspects of development, it is expected that the helicopter community will follow its fixed wing counterpart in this respect, and will suffer from similar problems in the future. If this is the case, the need for tuning will be reinforced by the development of helicopters which have handling quality deficiencies.

Tuning will be needed for ACT systems for two reasons. First, the presence of unmodelled dynamics can be responsible for the instability of a system employing a controller designed on the basis of low order linear descriptions. The design of high bandwidth systems requires the use of accurate high bandwidth models which are presently not available. Second, it is expected that control concepts will continue to be developed without adequate regard to the handling quality requirements. As the complexity of ACT flight controllers increases, the use of trial and error tuning techniques will cease to be a viable proposition. In the future, even the engineer responsible for the controller's design will find it difficult to say with any accuracy that increasing or decreasing particular gains will remove an undesirable response characteristic.

To clarify when and how the tuning process will be used, it is necessary to consider the steps involved in the design and commissioning of a new flight control system. Given the desired handling quality specifications for the design

and a representation of the helicopter's plant in terms of force and moment equations, the first task is to decide on a control strategy or control law which is to be used to design the flight control system. Following the procedures which are prescribed by the chosen control theory, a controller is developed and tested on computer simulation models, both linear and nonlinear. These computer simulations are used to validate the control theory implementation in terms of very simple pre—programmed test inputs, such as pulses, steps, and doublets. Once the performance is satisfactory in response to these inputs, the controller will be used in a real—time piloted flight simulation which will test its performance with regard to the pilot demands which it is likely to encounter on the real aircraft. Real—time flight simulation allows an investigation of how the pilot reacts with the controller. The results of testing at this stage will indicate if there are inadequacies in terms of handling quality specifications, that is, whether the pilot finds the dynamics of the controlled system easy or difficult to use. It may be the case that the controller needs tuning at this stage just to take into account the adaptive nature of the control inputs which a pilot will use. It should be remembered that up to this stage, the controller is essentially having to cope with the same plant dynamics which were modelled for the design. Additional dynamics of the real—time simulation facility should be well above the controller's bandwidth in order to prevent problems. Once difficulties with the pilot—flight control system interfacing have been rectified, the controller will be implemented on a test aircraft for flight trials. At this stage, handling quality deficiencies which are attributable to unmodelled high order dynamics will become apparent. A tuning process promises the most, in terms of improving a controller's performance, at this jump from simulation models to the actual plant.

In the following, the word 'tuning' will be used in preference to 'optimization' since the latter tends to be associated with procedures used during controller design with simulation models. In contrast, the techniques which are presented herein are directed at optimizing controller gains once the flight control system is actually flying.

In developing tuning procedures for ACT systems, there are several attributes which the method should possess. The first is that the tuning process should be quantitative. It must be possible to show that increasing a particular controller gain, α_i, by the amount $\Delta\alpha_i$ will lead to an improvement in system response. Furthermore, it must be possible to judge that one response is better than another in precise terms, and this implies using a quantitative performance measure to rate the relative merit of particular system responses. Trial and error techniques suffer because controller parameters are being altered without prior

knowledge of the effects of the changes on the system's response. With the large number of adjustable gains in ACT systems, the costs of trial and error tuning during inflight trials would be prohibitive. A systematic and quantitative tuning algorithm will minimize the amount of inflight testing which is needed to optimize controller settings.

The second aspect of the tuning process which must be considered is the fact that precise knowledge of the dynamics of the actual plant will not be available. This lack of knowledge creates the need for tuning in the first place, and forces the tuning algorithm to base its optimization on information provided by the response of the actual controlled system. If one considers the objective of the tuning process to be that of nullifying the adverse effects of unmodelled high order dynamics, then information concerning these effects must be available. However, the only valid source of information concerning unmodelled dynamics is the system response to pilot inputs. In other words, the tuning process must work with the response of the actual system in order to gain the information needed to decide how the controller's parameters should be adjusted.

Other desirable attributes are for the tuning process to work on nonlinear systems and for the process to be capable of real—time implementation. However, the tuning algorithm which has been developed relies upon sensitivity functions to show how each control system parameter affects the system response. With the constraints that inflight testing is to be minimized, and that knowledge of the system plant is inaccurate, one is forced to use signal convolution techniques to generate the sensitivities. Unfortunately, the multivariable application of the signal convolution technique precludes a real—time implementation and hard nonlinearities, such as actuator rate limits, must be avoided.

The remaining seven chapters of this thesis present the theoretical basis for the techniques which have been developed and the results which were obtained. Although the tuning processes are generally applicable, they are presented with regard to flight path controllers developed using modal control theory. The design techniques used for these flight control systems are presented in Chapter 2. Chapter 3 details the signal convolution method of calculating sensitivity functions which provide the quantitative information lacking in trial and error tuning methods. Apart from the collection of flight trials data, the tuning process consists of a parameter adjustment algorithm which projects how the controller's gains should be changed in order to improve system performance. Chapter 4 presents the adjustment algorithm theory which makes use of either of the two performance index measures of Chapter 5 and 6. Model reference tuning uses

the Least Integral Error Square Performance Index (Chapter 5), while the handling qualities tuning algorithm uses a performance index which is based on quantitative handling quality requirements (Chapter 6). The results of a real—time simulation of one of the flight path controllers of Chapter 2 are presented in Chapter 7, helping to show how complex and important the man—machine interface is to good handling qualities. The conclusions of Chapter 8 summarize the results which have been obtained during the current study and propose future areas of research.

CHAPTER 2: HELICOPTER DYNAMICS AND FLIGHT CONTROL SYSTEM DESIGN

2.1) Helicopter Dynamics

The equations of motion of the single rotor helicopter are derived by summing the force and moment contributions of various structural components of the helicopter system. The most important of these components are the main rotor, the tail rotor, and the fuselage. The difficulties encountered in attempting to model helicopters arise in two areas. First, the dynamics of the main rotor are complex, particularly during transient manoeuvres, and in addition, aerodynamic coupling is considerably more pronounced for helicopters than for fixed wing aircraft. This increased level of coupling is a result of using the rotor to generate both lift and control moments.

The coordinate system used to describe the single rotor helicopter system throughout this thesis will be the body fixed axes of Padfield [11]. Figure 2.1 shows the x, y, and z axes of this coordinate system along with the X, Y, and Z components of total force and the L, M, and N components of the total moment. The derivation of forces and moments is given by Padfield [11] along with the nonlinear equations of motion of the fuselage at the centre of gravity (Equations 2.1).

$$\dot{u} = - (wq - vr) + \frac{X}{m} - g \sin\theta$$

$$\dot{w} = - (vp - uq) + \frac{Z}{m} + g \cos\theta \cos\varphi$$

$$\dot{q} = \frac{1}{I_{yy}} \left[\left[I_{zz} - I_{xx} \right] rp + I_{xz} \left[r^2 - p^2 \right] + M \right]$$

$$\dot{\theta} = q \cos\theta - r \sin\varphi$$

$$\dot{v} = - (ur - wp) + \frac{Y}{m} + g \cos\theta \sin\varphi$$

$$\dot{p} = \frac{1}{I_{xx}} \left[\left[I_{yy} - I_{zz} \right] qr + I_{xz} \left[\dot{r} + pq \right] + L \right]$$

$$\dot{\varphi} = p + q \sin\varphi \tan\theta + r \cos\varphi \tan\theta$$

$$\dot{r} = \frac{1}{I_{zz}} \left[\left[I_{xx} - I_{yy} \right] pq + I_{xz} \left[\dot{p} - qr \right] + N \right]$$

$$\dot{\psi} = q \sin\varphi \sec\theta + r \cos\varphi \sec\theta \qquad \text{Equations 2.1}$$
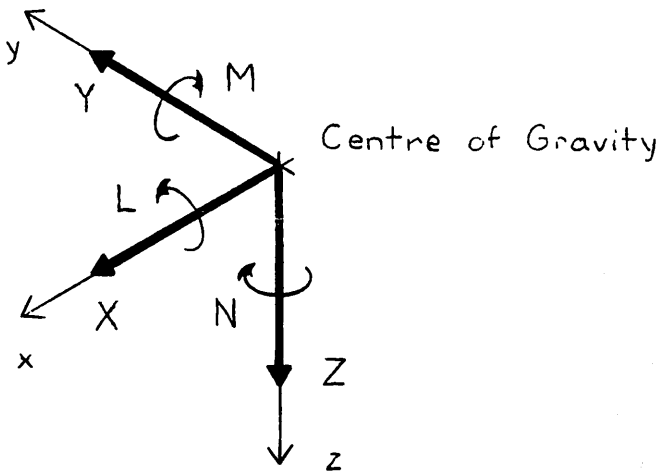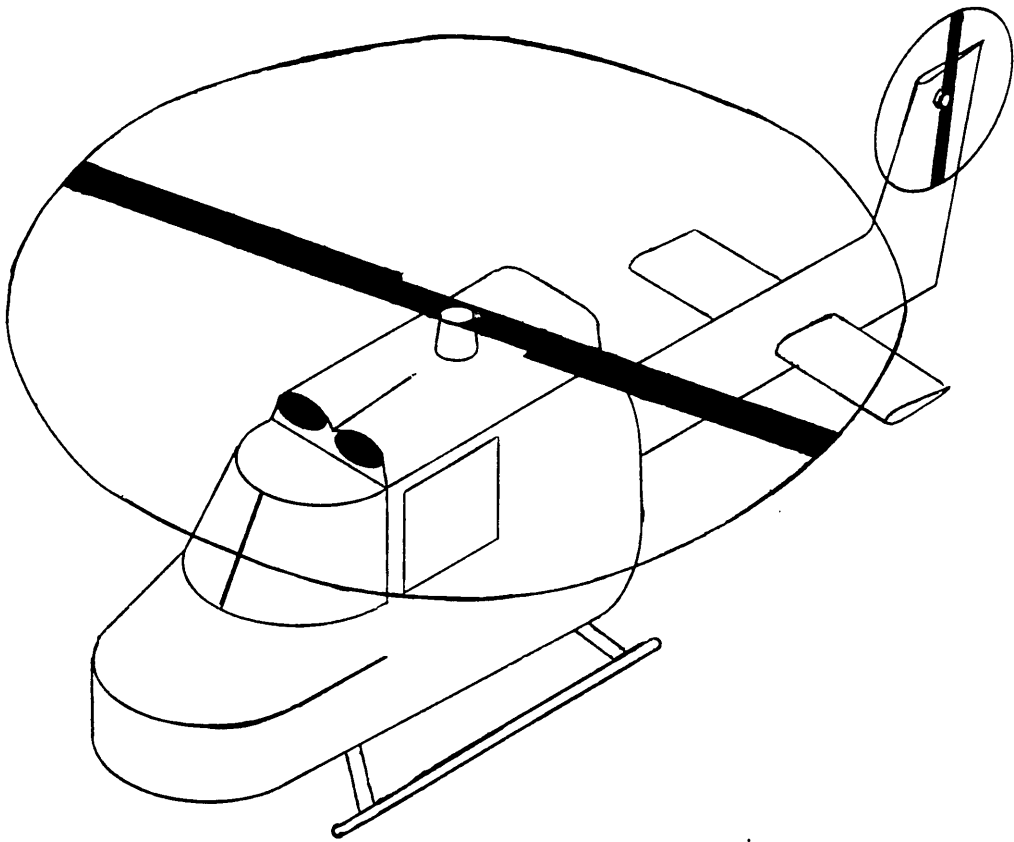
Figure 2.1: Helicopter Force and Moment Vectors in Body Axes

```
Where u  = forward velocity
      w  = vertical velocity
      q  = pitch rate
      θ  = pitch angle
      v  = lateral velocity
      p  = roll rate
      φ  = roll angle
      r  = yaw rate
      ψ  = yaw angle
      m  = the aircraft mass
      g  = the gravitational constant
      I_xx = the moment of inertia about the x axis
      I_yy = the moment of inertia about the y axis
      I_zz = the moment of inertia about the z axis
      I_xz = the product of inertia about the x and z axes
```

For flight control system design, it is a common and useful practice to use linearized equations of motion to describe the vehicle's dynamics near a prescribed operating point in the flight envelope. This representation of the aircraft lends itself readily to physical interpretation. The need to reduce the equations of motion into a form which is more easily interpreted is fully explained by Houston and Horton [12]. The standard method of linearizing the equations of motion is through the use of stability and control derivatives [13]. The nonlinear force and moment equations are described as a Taylor series expansion about the desired operating point in terms of the degrees of freedom of the aircraft. By truncating each series to first order terms, a linear model of the system is derived. The stability and control derivatives are the coefficients of the linear terms of this Taylor series expansion. The truncated series of this linear representation can be arranged into state space canonical form.

$$\underline{\dot{x}}(t) = [A]\underline{x}(t) + [B]\underline{u}(t) \qquad\qquad \text{Equation 2.2}$$

$$\underline{z}(t) = [C]\underline{x}(t) \qquad\qquad \text{Equation 2.3}$$

The stability and control derivatives are used to derive the elements of the system matrix, [A], and the input distribution matrix, [B], respectively. Since the development of a control law was not the primary objective of the project, the helicopter plant used for design work did not include rotor dynamics and was represented as a six degree of freedom, eighth order system.

The state vector, $\underline{x}(t)$, is made up of the eight rigid body states of the fuselage.

$$
\underline{x}(t) = \begin{bmatrix} u(t) \\ w(t) \\ q(t) \\ \theta(t) \\ v(t) \\ p(t) \\ \varphi(t) \\ r(t) \end{bmatrix}
\qquad \text{Equation 2.4}
$$

Following standard practice, the yaw angle is not included as a state variable because the heading on which an aircraft is flying does not affect its stability or control. This can be deduced from the nonlinear equations of motion in which heading or yaw angle, ψ, does not appear in the equations for the other states. However, as will be shown, heading feedback may be necessary in terms of providing decoupled spiral mode stability.

For single main rotor helicopters, the control input vector, $\underline{u}(t)$, is made up of the four actuator blade angles.

$$
\underline{u}(t) = \begin{bmatrix} \Theta_{0E} & - \text{ main rotor collective blade angle} \\ \Theta_{1S} & - \text{ longitudinal cyclic blade angle} \\ \Theta_{1C} & - \text{ lateral cyclic blade angle} \\ \Theta_{0T} & - \text{ tail rotor collective blade angle} \end{bmatrix}
$$

$$\text{Equation 2.5}$$

Traditionally, the pilot's collective lever is mechanically linked to the collective actuator controlling total thrust, while his centre stick is linked to the cyclic actuators controlling the direction of the thrust. The pedals are linked to the tail rotor actuator which controls the tail rotor thrust used to counter the torque of the main rotor. ACT is used to eliminate these traditional control channels and replace them with with pilot inceptor demands for angular rates of motion and linear velocities. This fundamental change in the man—machine interface is the driving force behind current helicopter flight control research.

Equation 2.3 defines the system output vector, $\underline{z}(t)$, and the output matrix, [C] for a general system. For the design of control laws in Section 2.2, it has been assumed that the states of the helicopter are observable and hence the output vector, $\underline{z}(t)$, is equivalenced to the state vector, $\underline{x}(t)$, by making the output matrix, [C], equal to the eighth order identity matrix.

Representations of the helicopter plant have been supplied by the Royal Aerospace Establishment (Bedford). The HELISTAB software package [11],[14] generates a system matrix, [A], and an input distribution matrix, [B], given an

initial flight condition.   These matrices are used in Equation 2.2 to represent the helicopter plant for all of the control system design work described herein.   The stability and control derivatives calculated by HELISTAB are valid for limited manoeuvres which do not require large and rapid movements [11].   Although the HELISTAB package has been correlated with flight test data, it has been shown that discrepancies exist at both ends of the flight envelope: at speeds below 50 knots, the impingement of the rotor downwash on the fuselage becomes increasingly important;   above 120 knots speed, stall begins to appear on the retreating blades.   As neither of these phenomena are mathematically modelled by HELISTAB, its use for design purposes is essentially restricted to the range of speeds between 50 knots and 120 knots.   Other anomalies which occur within this range have been reported in the literature [11],[12].   Furthermore, the system matrix, [A], and input distribution matrix, [B], are only valid over a limited portion of the flight envelope because the elements of these matrices change with flight condition — with forward speed, for example.   This is a consequence of the nonlinearity of the equations of motion.   Because [A] and [B] are only locally valid, the linearized model is a perturbation model and the nominal, unperturbed values of the states and actuator blade angles will be zero.

In contrast, the HELISIM3 software package is a full envelope nonlinear helicopter plant model.   As such, the plant is described by the nonlinear equations of motion (Equations 2.1).   Although the nonlinear plant model simulates the vehicle's dynamics with greater fidelity, it too suffers from deficiencies because both models (HELISTAB and HELISIM3) were developed from the same theoretical basis.

2.2) Flight Control Systems

An unaugmented helicopter presents the pilot with certain open loop modes. In manoeuvring a helicopter, a pilot will input signals to his inceptors which will excite these natural modes of motion.   Through experience, the pilot will learn how to excite these modes such that the aircraft responds in a desirable manner. Since the raw plant dynamics of single rotor helicopters are highly coupled, flight control systems attempt to change the nature of these open loop modes.

The helicopter which is being used as a basis in this study has six rigid body modes.   Because of the asymmetry of the single rotor helicopter, it is not as easy to separate these rigid body modes into longitudinal and lateral modes as is done for fixed wing aircraft.   Nevertheless, the helicopter community classifies

— 15 —

the raw dynamics in a form consistent with fixed wing nomenclature. The traditional longitudinal modes are the pitching mode and the phugoid mode. On the helicopter of interest, the pitching motion is actually characterized by a fast pitch and a slow pitch mode. These pitching modes describe the natural motions of the helicopter in response to a perturbation in pitch from the trimmed value. If these modes are stable, any deviations in pitch will decay. The phugoid is a different type of motion which involves a periodic exchange of the kinetic energy of forward flight and the potential energy of aircraft altitude. The three classical lateral modes are referred to as: the roll; the spiral; and the Dutch roll mode. The tendency of the helicopter to return to a level flight condition with a perturbation in roll angle is described as the roll mode. The spiral mode is an indication of the helicopter's predisposition to wander off its course (essentially in a horizontal plane). The Dutch roll motion can be described as a complicated interchange of sideslip and rolling energy. If the aircraft is given an initial sideslip as a result of a wind gust, for example, aerodynamic forces will be such as to turn the aircraft into the flight path producing a differential lift across the lifting surface whether it be a wing or a rotor. This differential lift will then roll the aircraft towards the change in heading caused by the reduction in sideslip, thus establishing an oscillation. These descriptions are only superficial and the the modes vary from aircraft to aircraft. There are a number of texts on the subject [15],[16],[17] which provide more in depth discussions of flight dynamics.

In the past, the modes of helicopters were determined through the aerodynamic and structural design. Following trends in the fixed wing community, current practice is to design the raw plant for greater performance and then to use flight control systems to tailor the system modes such that the aircraft is stable. Present helicopters are difficult enough to fly: greater performance without flight control systems would only serve to exhaust pilots at a faster rate. The objective of all flight control systems is then to modify the natural modes in order that they are more managable for the pilot. Flight controllers attempt to improve the raw dynamics by relocating closed loop system poles and zeros to desirable locations. Different control theories position these poles and zeros according to different criteria, and at present, the most commonly used theories are modal control, optimal control, and model following techniques.

Of these three linear control theories, modal control theory can be seen as the most direct and visible method of pole—zero placement. This control strategy has been used for flight control systems both in isolation [18] and as part

of a more sophisticated design criteria [19],[20],[21]. Modal control will be described in detail in the following sections.

Optimal control or Linear Quadratic Gaussian (LQG) control involves the formulation of a performance index, J, which, when minimized, yields a fairly robust, if somewhat conservative, control system. The simplest form of optimal control involves finding a control function $\underline{u}(t)$ (the plant input signal) which minimizes the following performance index [22].

$$J = \int_0^t \left[\underline{x}^T(t) \ [Q] \ \underline{x}(t) + \underline{u}^T(t) \ [R] \ \underline{u}(t) \right] dt$$

Equation 2.6

Both control input activity as specified by $\underline{u}(t)$ and large system transients as given by $\underline{x}(t)$ are penalized by minimizing the performance index in Equation 2.6. The weighting matrices [Q] and [R] are generally diagonal and their nonzero elements are assigned by the designer on the basis of his experience. This leads to an iterative design process. The feedback matrix to be used to provide the controlling action is then determined from the solution of a matrix Riccati equation.

The main difficulty in the application of optimal control is that the use of the performance index of Equation 2.6 obscures what is happening to the system's poles and zeros. Although it may be argued that pole– zero locations are chosen with regard to a control theory working at a higher level of abstraction, it must be remembered that handling quality specifications (Chapter 6) are described directly in terms of damping ratios and natural frequencies, which can be related to pole positions with relative ease. Nevertheless, optimal control has been used by Murphy and Narendra [23] to design a stability augmentation system for a Sikorsky SH–3D Sea King in hover and by Miyajima [24] in a full envelope stability and control augmentation system.

Model following controllers make use of a model of the helicopter's plant dynamics as part of the control system. The essence of the method is that the inputs of the helicopter plant are excited by the outputs of an inverse plant model. The desired state vector which is input to the inverse model should be reproduced by the aircraft state vector. Pilot inputs to the inverse model are augmented by control signals derived from differences in the desired and actual state vectors. The method has been used on a Bell UH–1H [25] and a MBB BO–105 [21].

Other, less commonly used control techniques include H−∞ control and adaptive control. The motivation behind H−∞ control is that stability margins can be guaranteed for the design model. The techniques used are designed to provide a robust controller design. Adaptive control schemes, on the other hand, modify control system parameters with respect to the flight condition [26],[27].

2.2.1) Modal Control Design Philosophy

The objective of modal control is to provide a means of controlling the transient modes of a system. Modal control theory has rapidly evolved from being a procedure for the placement of the eigenvalues of controllable system modes to a design process which allows extensive tailoring of the system's pole− zero locations. By allowing the designer some flexibility in the location of the response zeros, it is possible to decouple the modes in terms of their distribution among the state variables of the system. This fact makes modal control particularly attractive for use in helicopter flight control systems where coupling between the axes of motion can be severe. The argument for the use of modal control theory in the helicopter context is further strengthened when one considers the flight handling quality specifications for helicopters (see Chapter 6). As previously mentioned, the flight handling quality criteria dealing with system transients are largely specified in terms of natural frequencies, damping ratios and time constants which can be readily transformed into eigenvalues. Thus, modal control theory will allow handling quality specifications to be an integral component of the design process [18].

There are four concepts which are central to modal control theory. The first of these is that state feedback or output feedback can be used to move plant eigenvalues so that the closed loop system has a desirable rate of transient response to perturbations [28]. Secondly, since the use of a feedback matrix in a closed loop system gives the designer more degrees of freedom than he needs to reassign the system eigenvalues, it is possible to use the feedback matrix to partially assign system eigenvectors [29],[30],[31]. Third, by assigning a desirable closed loop eigenvalue, the designer defines an assignable subspace in which the closed loop eigenvectors must lie [32]. The fourth concept is that the difference between desirable closed loop eigenvectors and those which are assignable can be minimized in a least squares sense through the use of principal angles [33],[18]. These ideas will be explained in the following section which shows how modal control theory has been applied to the single rotor helicopter by Parry and

Murray–Smith [18].

2.2.2) Modal Control Design Methods

As explained, the equations of motion for helicopters are linearized for design purposes. Recall Equations 2.2 and 2.3 which give the state space representation of the helicopter plant in terms of: the state vector, $\underline{x}$; the control vector, $\underline{u}$; the output vector, $\underline{z}$; the system matrix, $[A]$; the input distribution matrix, $[B]$; and the output matrix, $[C]$.

$$\dot{\underline{x}} = [A]\underline{x} + [B]\underline{u} \qquad\qquad \text{Equation 2.2}$$

$$\underline{z} = [C]\underline{x} \qquad\qquad \text{Equation 2.3}$$

In the above equations it is assumed that the rank of all three system matrices: $[A]$, $[B]$, and $[C]$, is full. That is, $r([A]) = n$, $r([B]) = m$, and $r([C]) = k$.

When the output signal, $\underline{z}$, is fed back through an $m \times k$ matrix $[K]$ to provide control, the control signal, $\underline{u}$, is given by,

$$\underline{u} = \underline{r} - [K]\underline{z} \qquad\qquad \text{Equation 2.7}$$

Where $\underline{r}$ is a reference control input. Substitution of Equations 2.3 and 2.7 into Equation 2.2 gives,

$$\dot{\underline{x}} = \Big\{\ [A] - [B][K][C]\ \Big\}\underline{x} + [B]\underline{r} \qquad\qquad \text{Equation 2.8}$$

If,

$$[A_c] = [A] - [B][K][C] \qquad\qquad \text{Equation 2.9}$$

Then Equation 2.8 reduces to,

$$\dot{\underline{x}} = [A_c]\underline{x} + [B]\underline{r} \qquad\qquad \text{Equation 2.10}$$

The location of the poles are given by the eigenvalues of $[A]$ for the open loop system and by the eigenvalues of $[A_c]$ for the closed loop system. The eigenvalues of the closed loop system matrix, $[A_c]$, are a function of the feedback matrix, $[K]$. Since the location of the poles determines the stability and rise times of the system in response to perturbations, the use of the feedback matrix,

[K], allows the elimination of undesirable slower dynamics in the closed loop system [31], thereby improving the vehicle's agility.

In their discussion of output feedback, Andry et. al. [33] have shown for the system being considered, that with the states both controllable and observable, it is possible to assign max(m,k) closed loop eigenvalues. Furthermore, max(m,k) closed loop eigenvectors can be partially assigned with min(m,k) degrees of freedom. This is a result of the m×k degrees of freedom provided by the feedback matrix, [K].

If it is advantageous for the system to have the desired eigenvalue/eigenvector pair ($\lambda_i, \underline{\nu}_i$), then the modal control problem can be expressed as the need to find a real feedback matrix, [K], such that,

$$\left[\ [A] - [B][K][C] \ \right] \underline{\nu}_i = \lambda_i \underline{\nu}_i \qquad \text{Equation 2.11}$$

When the closed loop eigenvalues are distinct from the open loop eigenvalues, it is possible to rearrange Equation 2.11 into the form,

$$\underline{\nu}_i = \left[\ [A] - \lambda_i [I] \ \right]^{-1} [B][K][C]\underline{\nu}_i \qquad \text{Equation 2.12}$$

If the two sets of eigenvalues were not distinct, it would not be possible to invert ($[A] - \lambda_i[I]$) since it would be singular.

One of the major contributions to modal control theory was made by Sinswat and Fallside [32] by defining an m dimensional vector $\underline{m}_i$ as,

$$\underline{m}_i = [K][C]\underline{\nu}_i \qquad \text{Equation 2.13}$$

For a nonzero eigenvector, $\underline{\nu}_i$, it is possible to consider the vector $\underline{m}_i$ as arbitrary in m−space. Therefore, rewriting Equation 2.12 as,

$$\underline{\nu}_i = \left[\ [A] - \lambda_i [I] \ \right]^{-1} [B]\underline{m}_i \qquad \text{Equation 2.14}$$

It becomes clear that the closed loop system eigenvector must lie in an m dimensional subspace of the n dimensional system space. Parry and Murray−Smith [18] state that the closed loop eigenvectors must be contained in the subspace $\mathbb{U}(\lambda_i, [A], [B])$ spanned by the columns of $([A] - \lambda_i)^{-1}[B]$. Hence, the assignable subspace for each eigenvector, $\underline{\nu}_i$, is a function of the input distribution matrix, [B], the system matrix, [A], and the eigenvalue, λ_i, for that particular eigenvector.

Assuming that the closed loop eigenvalues have been chosen (on the basis of handling quality criteria), it is necessary to select an assignable eigenvector for each of the system modes. While the eigenvalues determine the location of a system's poles, the eigenvectors determine the locations of response zeros and hence the response shape [33]. The amplitudes of the elements in an eigenvector determine the strength of that particular mode on each of the system states. If it is desirable to eliminate a mode on particular states, the elements of the eigenvector corresponding to those states should then have amplitudes which are much smaller than the amplitudes for the elements corresponding to the states on which the mode is to be present. Ideally, the small amplitudes on the unwanted states will be zero. It is therefore necessary to have a clear idea about how the rigid body modes of the helicopter are to be distributed among the states before system eigenvectors can be assigned.

In order to ease the pilot's workload, it is beneficial to decouple the longitudinal and lateral dynamics as much as possible. To this end, desirable subspaces are defined for each particular mode. For the helicopter flight control systems discussed in the following sections the desirable subspaces are defined by the basis vectors shown in Table 2.1 [18].

Table 2.1: The state distribution of the system modes.

Mode		Subspace Eigenvector Elements							
		u	w	q	θ	v	p	φ	r
Fast Pitch	$v_1^T =$	0	1	0	0	0	0	0	0
Slow Pitch	$v_2^T =$	1	0	0	0	0	0	0	0
		0	0	1	0	0	0	0	0
		0	0	0	1	0	0	0	0
Phugoid	$v_3^T =$	1	0	0	0	0	0	0	0
		0	0	1	0	0	0	0	0
		0	0	0	1	0	0	0	0
Roll	$v_4^T =$	0	0	0	0	0	1	0	0
Spiral	$v_5^T =$	0	0	0	0	0	0	1	0
Dutch Roll	$v_6^T =$	0	0	0	0	1	0	0	0
		0	0	0	0	0	0	0	1

The choice of basis vectors for each subspace is not arbitrary since the modes must be associated with their relevant rigid body states. Table 2.1 shows that the fast pitch mode would ideally be confined to the vertical velocity state, w, while the slow pitch and phugoid modes would be present on the forward velocity, u, pitch rate, q, and pitch angle, θ, states. The desired roll mode would be found solely on the roll rate, p. The roll angle state, φ, is the only channel excited by the desired spiral mode. The Dutch roll mode would ideally be found on the lateral velocity, v, and the yaw rate, r. Any eigenvectors which are spanned by the above desirable subspaces, $\mathbb{U}_i$, would eliminate coupling between longitudinal and lateral states for that particular mode.

On the actual closed loop system, it is not possible to achieve the complete decoupling of longitudinal and lateral states. It is therefore necessary to assign the feedback gain elements so as to minimize the difference between the assignable eigenvectors and those which are desired, thereby minimizing the coupling between states. Principal angles measure the amount by which two subspaces are inclined to each other [34]. The desired subspaces, $\mathbb{U}_i$, are as decoupled as ideal helicopter plant dynamics would allow. The assignable subspaces, Γ_i, define the subspace over which the system eigenvectors, $\underline{\nu}_i$, may reside. By choosing the eigenvector, $\underline{\nu}_i$, in the assignable subspace, Γ_i, such that the first principal angle, θ_{i1}, between $\underline{\nu}_i$ and the desired subspace, $\mathbb{U}_i$, is minimized, the amount of coupling in the system is also minimized. Parry and Murray—Smith [18] demonstrate that the use of principal angles allows one to measure the amount of mode coupling between states in addition to providing a means of minimizing the coupling.

For the problem at hand, let the two subspaces, Γ_i and $\mathbb{U}_i$, have dimensions such that,

$$n \geq p = \dim(\Gamma_i) \geq \dim(\mathbb{U}_i) = q \geq 1 \qquad \text{Equation 2.15}$$

By defining Γ_i and $\mathbb{U}_i$ as subspaces of the n dimensional unitary space E^n, the q principal angles, θ_{ik}, between Γ_i and $\mathbb{U}_i$ are defined by Björck and Golub [35] to be,

$$\cos\theta_{ik} = \max_{\underline{u}_i \epsilon \Gamma_i} \max_{\underline{v}_i \epsilon \mathbb{U}_i} \underline{u}_i^H \underline{v}_i = \underline{u}_{ik}^H \underline{v}_{ik} \qquad \text{Equation 2.16}$$

$$\left\| \underline{u}_{ik} \right\|_2 = 1, \ \left\| \underline{v}_{ik} \right\|_2 = 1 \qquad \text{Equation 2.17}$$

Where the $\underline{u}_{ik}$ and $\underline{v}_{ik}$ are constrained by,

$$\underline{u}_{ij}^{H} \, \underline{u}_{ik} = 0, \quad \underline{v}_{ij}^{H} \, \underline{v}_{ik} = 0, \quad j = 1,2,\ldots,k\text{-}1 \quad \text{Equation 2.18}$$

The set of vectors $\underline{u}_{ik}$ and $\underline{v}_{ik}$ are defined as the q principal vectors of the pair of subspaces Γ_i and $\mathbb{U}_i$. The subset of principal vectors, $\underline{u}_{i1}$, is the set of assignable eigenvectors, $\underline{\nu}_i$, which will minimize the coupling in the system.

An alternate approach to understanding the above is presented by Andry et. al. [33]. If the desired subspace, $\mathbb{U}_i$, is of one dimension, then the projection of the desired eigenvector, $\underline{\mathbb{U}}_i$, onto the assignable subspace Γ_i, finds the assignable eigenvector, $\underline{\nu}_i$, which will minimize the coupling in the system. Consider Figure 2.2 which shows a two dimensional assignable subspace, Γ_i, and a one dimensional desired subspace, $\mathbb{U}_i$.
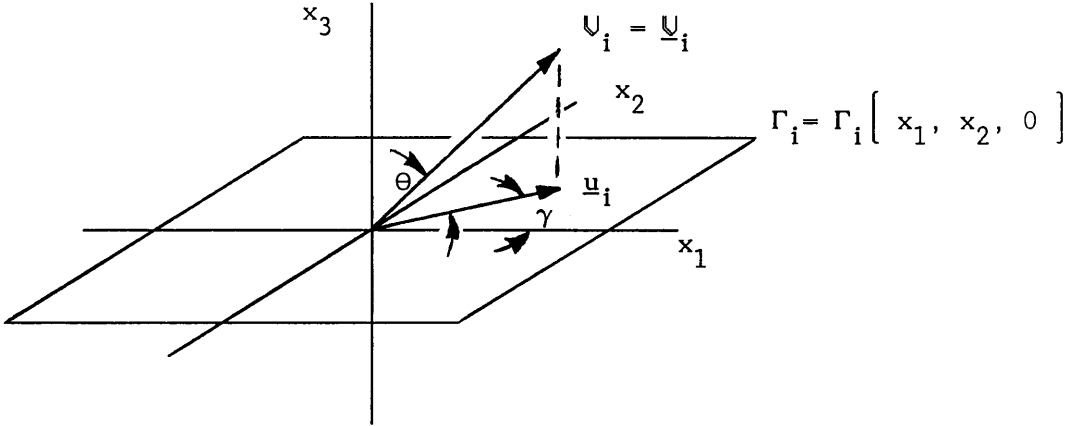
Figure 2.2: The projection of a desirable one dimensional subspace, $\mathbb{U}_i$, onto an assignable two dimensional subspace, Γ_i.

The principal vector, $\underline{u}_i$, is simply the projection of the desired subspace, $\mathbb{U}_i$, onto Γ_i. Although principal angles give a direct measure of the inclination between subspaces, the solution of the problem from the viewpoint of projections allows one to see that this method of eigenvector assignment reduces coupling in a least squares sense. This follows from the fact that minimizing the first principal angle between the assignable and desired eigenvectors brings these vectors as close to each other as possible for a least squares solution [33].

The calculation of principal angles, Θ_{ik}, and principal vectors, $\underline{u}_{ik}$, is most accurately accomplished using singular values. Björck and Golub [35] give the following theorem relating the singular value decomposition (SVD) of a matrix to

the principal angles and principal vectors of the two subspaces used to form the matrix.

Assume that the columns of $[Q_{\Gamma i}]$ and $[Q_{\cup i}]$ form unitary bases for two subspaces of a unitary space E^n. Put

$$[M_i] = [Q_{\Gamma i}]^H [Q_{\cup i}],$$

and let the SVD of this $p \times q$ matrix be

$$[M_i] = [Y_i][C_i][Z_i]^H \;,\; [C_i] = diag\left[\sigma_{i1}, \sigma_{i2}, \ldots, \sigma_{iq}\right]$$

where $[Y_i]^H[Y_i] = [Z_i]^H[Z_i] = [Z_i][Z_i]^H = [I_q]$. If we assume that $\sigma_{i1} \geq \sigma_{i2} \geq \ldots \geq \sigma_{iq}$, then the principal angles and principal vectors associated with this pair of subspaces are given by

$$\cos \Theta_{ik} = \sigma_{ik}([M_i]), \quad [U_i] = [Q_{\Gamma i}][Y_i], \quad [V_i] = [Q_{\cup i}][Z_i]$$

For the applications discussed here, $[Q_{\Gamma i}]$ is a unitary basis for Γ_i and $[Q_{\cup i}]$ is a unitary basis for $\cup_i$. Klema and Laub [36] show that the singular values of the matrix, $[M_i]$, are the positive square roots of the eigenvalues of the matrix, $[M_i]^T[M_i]$. The assignable eigenvectors, $\underline{v}_i$, of the system are given by the orthonormal eigenvector of $[M_i][M_i]^T$ corresponding to the largest singular value σ_{i1}, for each of the i pairs of desirable and assignable subspaces.

At this stage, the eigenvalues have been chosen on the grounds of giving the system acceptable rates of transient response and the eigenvectors have been selected in order to minimize the coupling in the system. The only task remaining in the design of the modal controller is the calculation of the feedback gains which will yield the designed eigenvalue/eigenvector pair $(\lambda_i, \underline{v}_i)$. Recall Equation 2.11,

$$\left[\; [A] - [B][K][C] \;\right] \underline{v}_i = \lambda_i \underline{v}_i \qquad\qquad \text{Equation 2.11}$$

Restating Equation 2.11 in terms of the $k \times k$ diagonal eigenvalue matrix, $[\Lambda]$, and the $n \times k$ eigenvector matrix, $[V]$, one derives Equation 2.19. Modified Jordan canonical form is used for $[\Lambda]$ and $[V]$ when there are multiple eigenvalues.

$$\Big[\ [A] - [B][K][C] \ \Big] \ [V] = [V][\Lambda] \qquad\qquad \text{Equation 2.19}$$

Rearrangement gives,

$$[B][K][C][V] = \Big[\ [A][V] - [V][\Lambda] \ \Big] \qquad\qquad \text{Equation 2.20}$$

Solving for the feedback matrix, [K], yields,

$$[K] = [B]^{\dagger} \Big[\ [A][V] - [V][\Lambda] \ \Big] \Big[\ [C][V] \ \Big]^{-1} \qquad \text{Equation 2.21}$$

The psuedo—inverse of the input distribution matrix, $[B]^{\dagger}$, is found from calculating the matrix product,

$$[B]^{\dagger} = \Big[\ [B]^{T}[B] \ \Big]^{-1}[B]^{T} \qquad\qquad \text{Equation 2.22}$$

Modal control techniques have been used in the design of two flight control systems which will be discussed in the following sections.

2.2.3) The Parry Modal Controller

A flight control system using modal control theory as discussed above has been developed by Parry and Murray—Smith [18]. The structure of the controller consists of a feedback matrix which provides the desired eigenstructure assignment and an input precompensator matrix which is designed to decouple the pilot inputs as much as possible. The flight control system is shown in Figure 2.3 for a linear time invariant system plant.
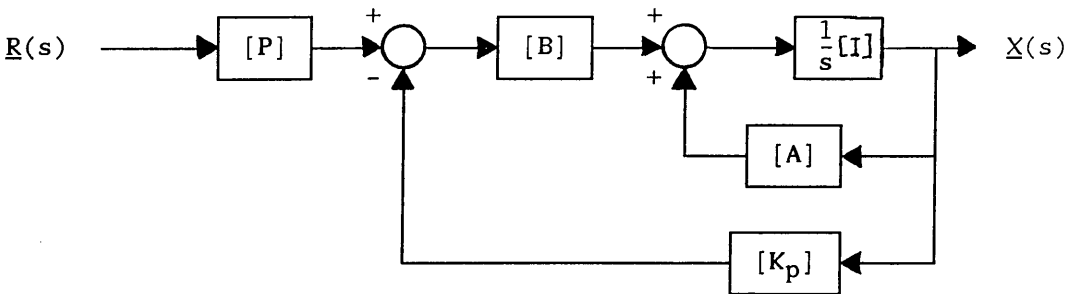
Figure 2.3: The structure of the Parry Modal Controller.

The equations governing the above system are a straightforward extension of the modal control equations (Equations 2.2 and 2.7).

$$\dot{x} = [A]\underline{x} + [B]\underline{u} \qquad\qquad \text{Equation 2.2}$$

$$\underline{u} = [P]\underline{r} - [K_p]\underline{x} \qquad\qquad \text{Equation 2.23}$$

An implicit assumption concerning the structure of the controller in Figure 2.3 is that all states are observable. Since full state feedback is used, there is no need for an output matrix in the above system since it would merely be the identity matrix. From the theory presented by Andry et. al. [33], it will be possible to arbitarily reassign all 8 eigenvalues and 4 degrees of freedom for each of the 8 eigenvectors using full state feedback. The closed loop equation governing the system is,

$$\dot{x} = \left[\; [A] - [B][K_p] \; \right] \underline{x} + [B][P]\,\underline{r} \qquad\qquad \text{Equation 2.24}$$

The design of the controller was carried out for a flight condition of 80.0 knots forward speed. This speed was chosen because future military helicopters will need to perform NOE manoeuvres at relatively high velocities. In addition, it was hoped that selecting a design point in the middle of the forward flight envelope would minimize the amount of gain scheduling which would be necessary. As the elements of [A] and [B] migrate, the gains of the feedback matrix, [K], will need to change if the system eigenvalues and eigenvectors are to remain constant.

At 80.0 knots level flight, the open loop eigenvalues and eigenvectors for an eighth order representation of the helicopter are given in Table 2.2. The uncontrolled aircraft has several undesirable characteristics. Examination of the open loop eigenvalues shows that the phugoid mode is unstable with a time to double amplitude of 5.2 seconds and a frequency of 0.060 Hz. [18]. The second adverse characteristic is the light damping of the Dutch roll mode. Although stable, Dutch roll oscillations do not decay rapidly. In terms of the eigenvectors, mode coupling between longitudinal and lateral states is high. The fast pitch mode is strong on the vertical velocity, w, and the lateral velocity, v. The phugoid mode is spread out across the three linear velocities, u, w, and v. The roll mode shows coupling between lateral velocity, v, roll rate, p, and vertical velocity, w. The spiral mode is present on u, v, and φ. The open loop eigenvectors show a considerable degree of coupling between the longitudinal and lateral dynamics.

Table 2.2: The open loop system eigenvalues and eigenvectors.

Mode	Fast Pitch	Slow Pitch	Phugiod	Roll	Spiral	Dutch Roll
Eigenvalue	-3.199	-0.0406	0.134 ±j0.376	-10.54	-0.031	-0.654 ±j2.255
Eigenvector						
u	0.0382	-.5837	0.8070 ±j0.0000	0.0138	-.3917	-.0002 ∓j.0046
w	0.9591	0.8088	0.2617 ∓j0.495	0.3015	-.0057	-.0109 ∓j.0166
q	-.0168	0.0025	0.0033 ∓j0.0028	-.0177	-.0010	0.0003 ∓j.0002
θ	0.0052	-.0059	-.0039 ∓j0.0100	0.0015	0.0000	-.0004 ∓j.0001
v	0.2797	0.0703	0.1076 ∓j0.1518	0.8879	0.9106	0.9996 ±j.0000
p	0.0118	0.0056	-.0002 ∓j0.0021	0.3394	-.0046	-.0049 ±j.0015
φ	-0.004	-.0137	-.0051 ∓j0.0011	-.0323	0.1283	0.0011 ±j.0018
r	0.0057	-.0031	-.0019 ∓j0.0003	0.0630	0.0299	0.0039 ∓j.0164

The choice of eigenvalues for the closed loop system is often a compromise between decreasing coupling and increasing the rate of response [18]. By plotting the variation of the first principal angle, Θ_{1i}, for each mode versus the corresponding eigenvalue, λ_i, it is possible to choose the eigenvalues, λ_i, with relative ease. Once the eigenvalues, λ_i, have been assigned, the closed loop eigenvectors which yield minimal coupling are calculated. The results of this procedure are displayed in Table 2.3. The closed loop eigenstructure is much better behaved than its open loop counterpart. All of the eigenvalues, except the spiral mode, are stable and the oscillations of the phugoid and Dutch roll modes are much more heavily damped. The spiral mode eigenvalue was placed at 0.00 in order to minimize coupling. Coupling on the spiral mode is particularly strong because the heading angle, ψ, is not used for stability augmentation. Tests have shown that spiral mode coupling can be greatly decreased if ψ is fed back to provide stability. However, the use of ψ for stability augmentation causes difficulties when a pilot wishes to execute a turn. The most efficient means of

turning a helicopter is by rolling the aircraft into a turn and flight controllers are designed acknowledging this fact. Because the pilot's roll command affects heading indirectly, a sophisticated turn coordination controller would be required if heading angle, ψ, is part of the feedback signal. Since the spiral mode divergence is slow, it is well within a pilot's ability to control. Therefore, the spiral mode eigenvalue of 0.00 was deemed acceptable. The closed loop eigenvectors show a great improvement in the decoupling of longitudinal and lateral dynamics. The modes are confined to the desired states. This is borne out by the first principal angle for each mode — the values are small.

Table 2.3: The closed loop system eigenvalues, eigenvectors and principal angles.

Mode	Fast Pitch	Slow Pitch	Phugoid	Roll	Spiral	Dutch Roll
Eigenvalue	-4.000	-2.000	-3.000 ±j1.732	-11.00	0.0000	-6.000 ±j3.465
Eigenvector						
u	-.0031	0.9963	0.9825 ∓j0.0000	-.0005	-.0000	-.0001 ∓j.0001
w	0.9999	-.0000	0.0000 ±j0.0000	0.0000	0.0001	-.0000 ∓j0.000
q	-.0001	-.0768	-.1405 ±j0.1108	0.0007	-.0076	-.0004 ∓j0.000
θ	0.0036	0.0384	0.0511 ∓j0.0074	0.0000	0.0008	-.0000 ±j.0000
v	-.0000	0.0000	0.0000 ∓j0.0000	0.0034	0.0001	0.9986 ∓j.0001
p	0.0000	-.0001	-.0001 ±j0.0000	0.9952	-.0050	-.0000 ±j.0000
φ	-.0000	0.0001	0.0001 ∓j0.0001	-.0904	0.9728	-.0000 ±j.0000
r	0.0001	-.0024	-.0042 ±j0.0040	-.0382	0.2316	0.0451 ∓j0.287
Principal Angles	0.8813°	0.1355°	0.3332°	5.634°	13.40°	0.0284°

The feedback matrix, $[K_p]$, is then calculated using Equation 2.21

The design of the precompensator matrix, $[P]$, shown in Figure 2.3, is based on the rows of the input distribution matrix, $[B]$, corresponding to the 4 states which are to be controlled directly from the pilot's inceptors. The philosophy behind the distribution of the pilot inputs was: the collective lever would command changes in vertical velocity, the longitudinal inceptor would command changes in forward velocity, the lateral inceptor would command roll rates, and the pedals would command changes in lateral velocity.

The first step in the design of the precompensator, $[P]$, was the creation of a matrix, $[B_1]$, containing the appropriate rows of the input distribution matrix, $[B]$, as given by Equation 2.25.

$$\left[B_1\right] = \begin{bmatrix} 0 & 1 & 0 & 0 & 0 & 0 & 0 & 0 \\ 1 & 0 & 0 & 0 & 0 & 0 & 0 & 0 \\ 0 & 0 & 0 & 0 & 0 & 1 & 0 & 0 \\ 0 & 0 & 0 & 0 & 1 & 0 & 0 & 0 \end{bmatrix} [B] \qquad \text{Equation 2.25}$$

By defining the precompensator matrix, $[P]$, as the inverse of $[B_1]$ (Equation 2.26), the rows of the pilot–controlled states of the modified input distribution matrix, $[B_c]$, (Equation 2.27) approximate the identity matrix [18].

$$[P] = [B_1]^{-1} \qquad \text{Equation 2.26}$$

$$[B_c] = [B][P] \qquad \text{Equation 2.27}$$

With this precompensator design, the pilot inputs are fed through the system to the outputs of the input distribution matrix, $[B]$, where they act as a reference signal for the system plant loop of the integrators and system matrix, $[A]$. Since the precompensator matrix, $[P]$, is external to the feedback loop, its design has no effect on the system eigenstructure.

For implementation as a computer simulation model, an important change was made to the structure as shown in Figure 2.3. The inputs to the input distribution matrix correspond to the outputs of the swash plate actuators. These actuators have dynamics of their own which are conveniently modelled as first order delays with time constant τ. Thus, the simulation model of the modal controller of Parry and Murray–Smith has the structure shown in Figure 2.4.
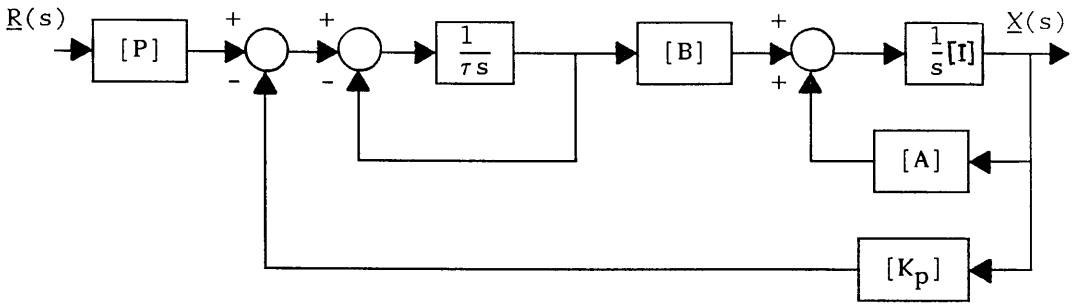
Figure 2.4: The structure of the Parry Modal Controller as implemented for computer simulation.

The simulated state responses to a step input of full amplitude 1.0 (standard test amplitude) on the vertical inceptor are shown in Figure 2.5. This input will be used to move between two steady state vertical velocities. The 0.25 ft/s change in vertical velocity, w, is made rapidly with a small amount of overshoot. Although the amplitudes of the responses are small, it can be seen that coupling is minimal in terms of pitch, roll and yaw. The pitching response, θ, is less than 0.005 radians, while the longitudinal and lateral velocities change by 0.07 ft/s and 0.03 ft/s respectively.

Figure 2.6 shows the simulated state responses to a step input of amplitude 1.0 on the longitudinal inceptor. The resulting change in forward velocity, u, only begins to occur after a delay of 0.5 seconds from the application of the input. The nature of this response is due to the slower phugoid and slow pitch modes which are excited during the manoeuvre. Transients in vertical velocity, w, are approximately half the amplitude of the forward velocity, u, change. However, coupling to the lateral states is minimal.

A doublet input with pulses of standard 1.0 second duration on the lateral (roll) inceptor generates the simulated responses of Figure 2.7. The input is tracked successfully by the system roll rate, p, as expected by the roll eigenvalue of −11.00. However, the yaw rate, r, is far from smooth, with the higher harmonics of the input showing through in the response.

A step input on the pedals (lateral velocity inceptor) generates a sideslip as shown in Figure 2.8. The system response is confined to the forward velocity, u, the lateral velociy, v, and the yaw rate, r, channels. Once again, it can be seen that coupling is minimal.

The Parry Modal Controller has also been used to control a nonlinear HELISIM3 plant. The system responses to vertical, longitudinal, roll, and lateral (pedal) inceptor inputs are shown in Figures 2.9 to 2.12 respectively. In
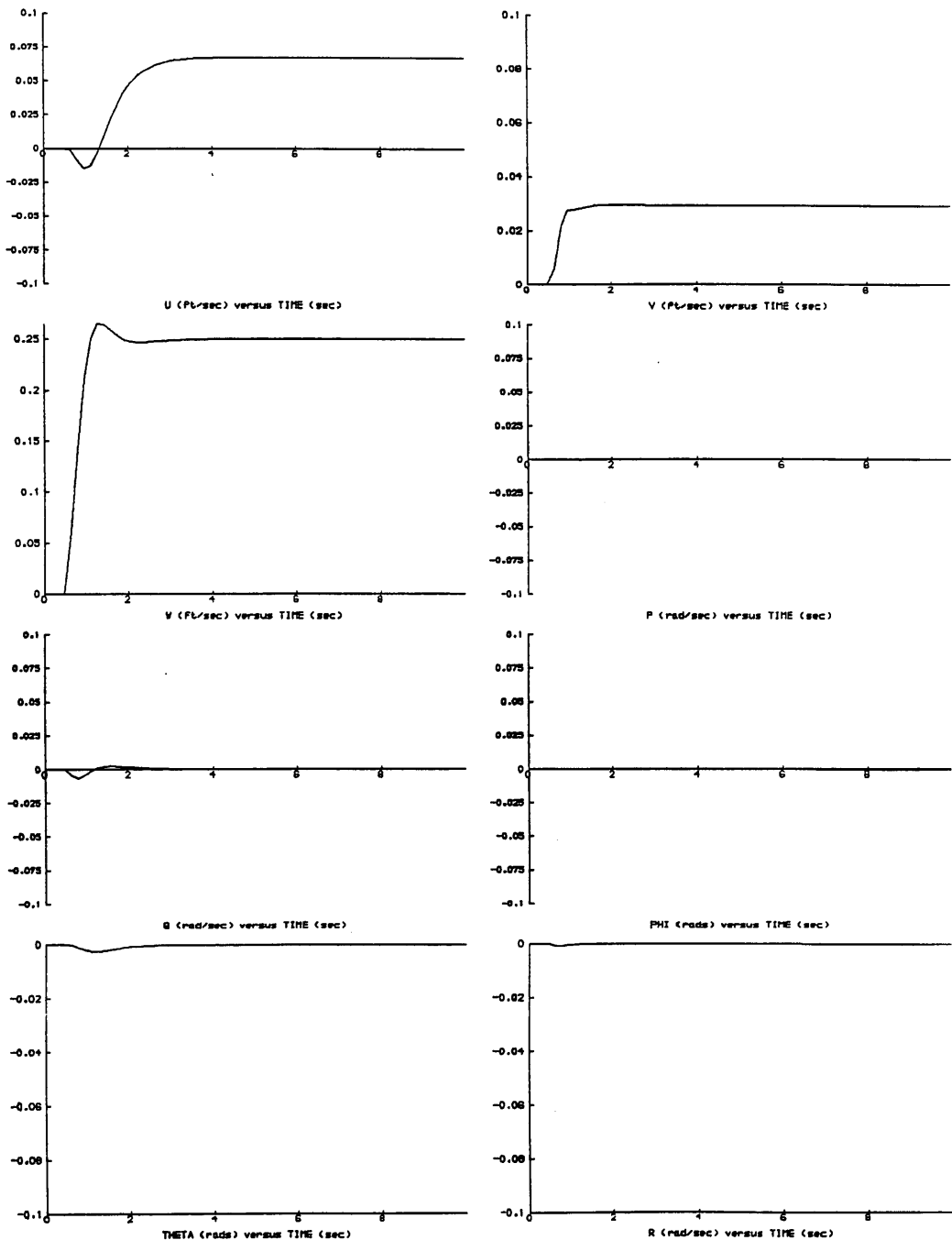
Figure 2.5: Parry Modal Controlled — Linear System Responses to Vertical Inceptor, Step Input
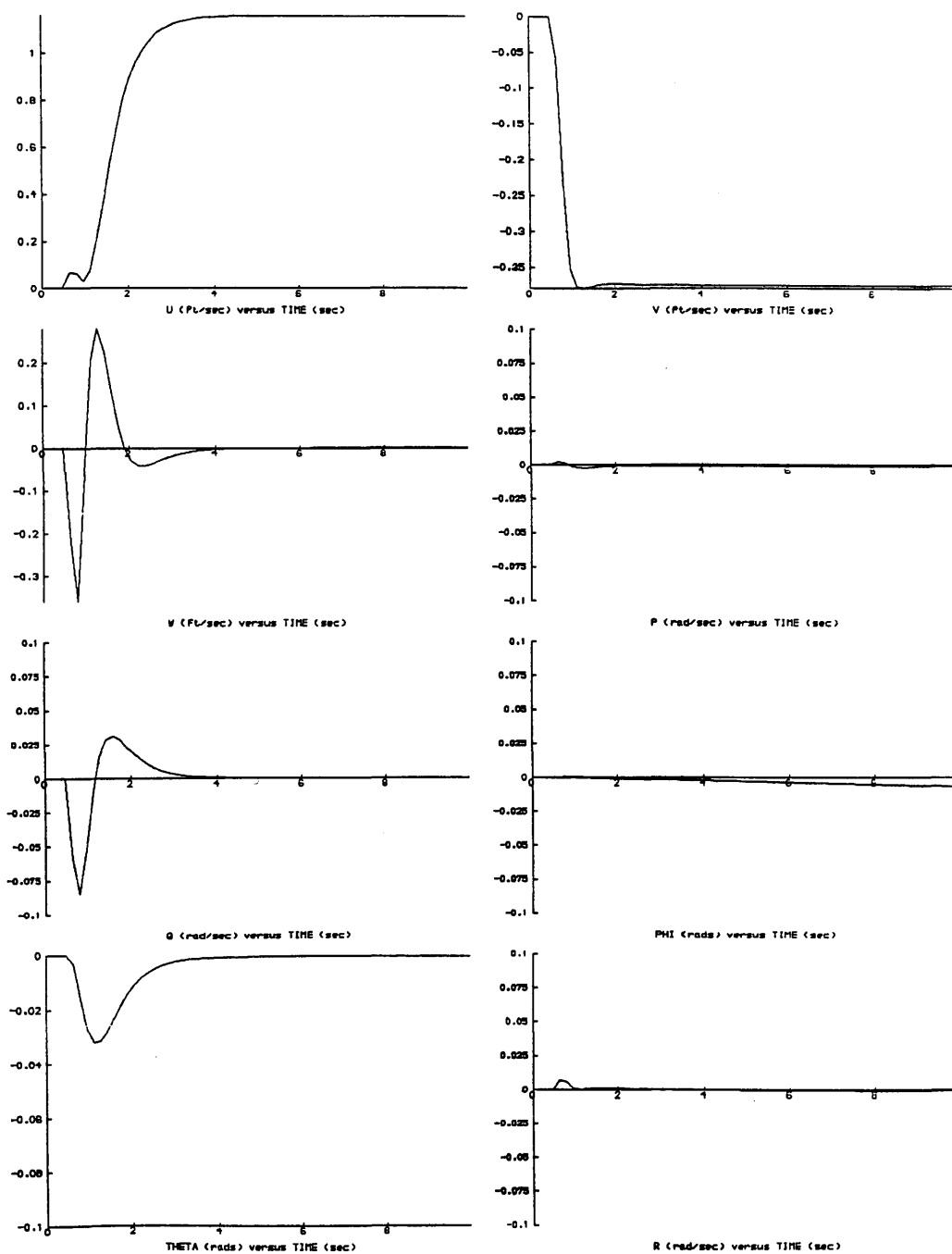
Figure 2.6: Parry Modal Controlled — Linear System Responses to Longitudinal Inceptor, Step Input
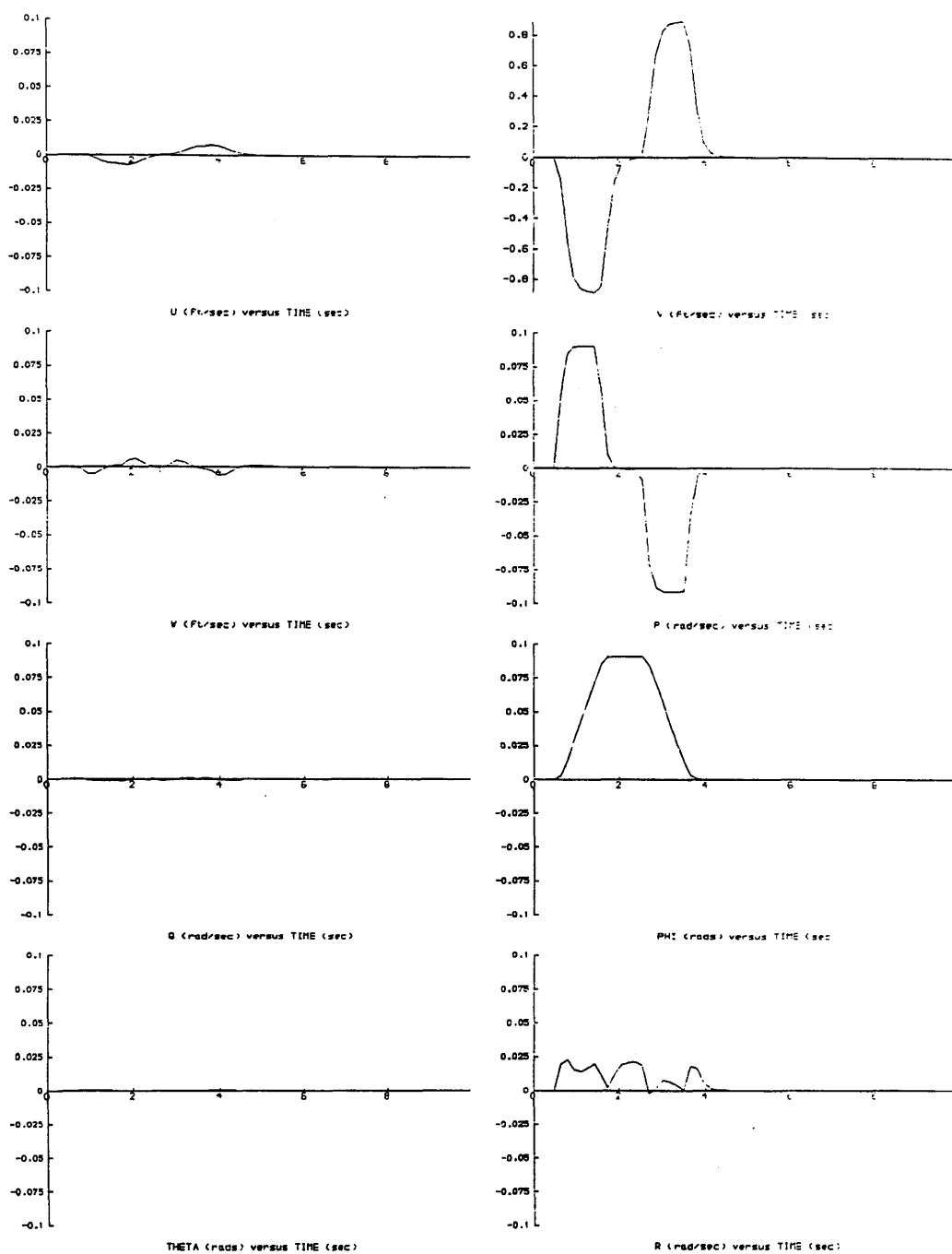
Figure 2.7: Parry Modal Controlled — Linear System Responses to Lateral (Roll) Inceptor, Doublet Input
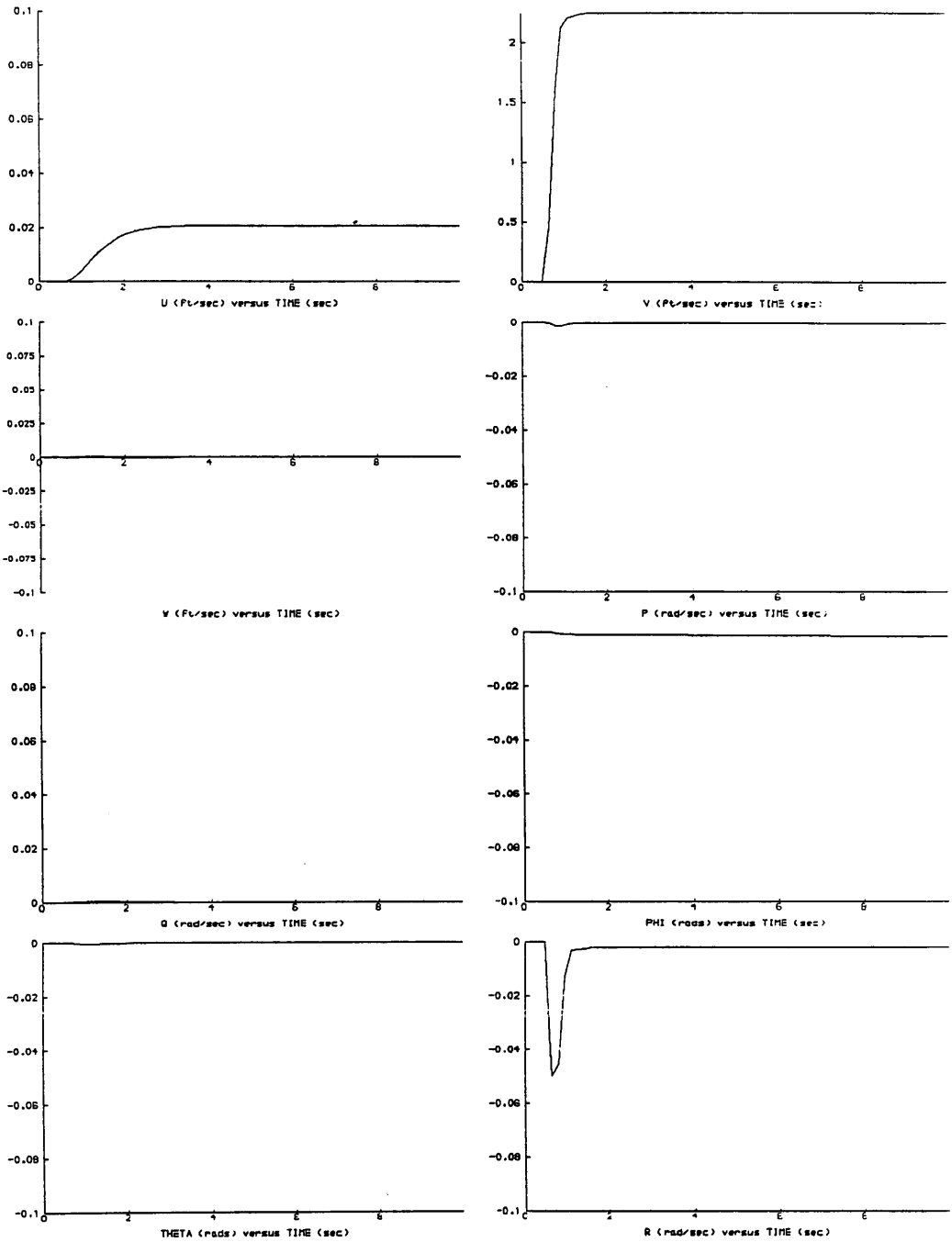
Figure 2.8: Parry Modal Controlled — Linear System Responses to Pedal (Lateral Velocity) Inceptor, Step Input
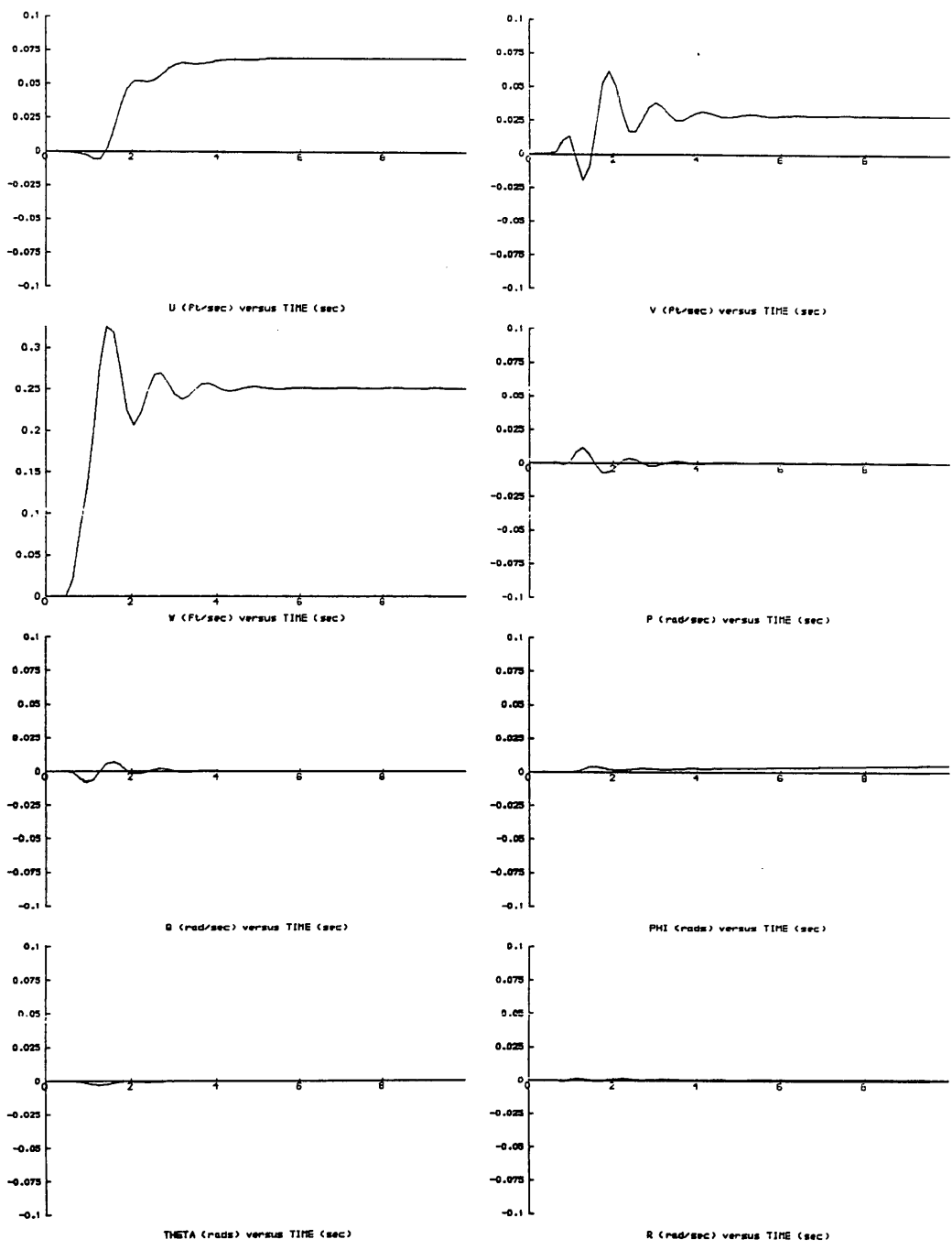
Figure 2.9: Parry Modal Controlled — Nonlinear System Responses to Vertical Inceptor, Step Input
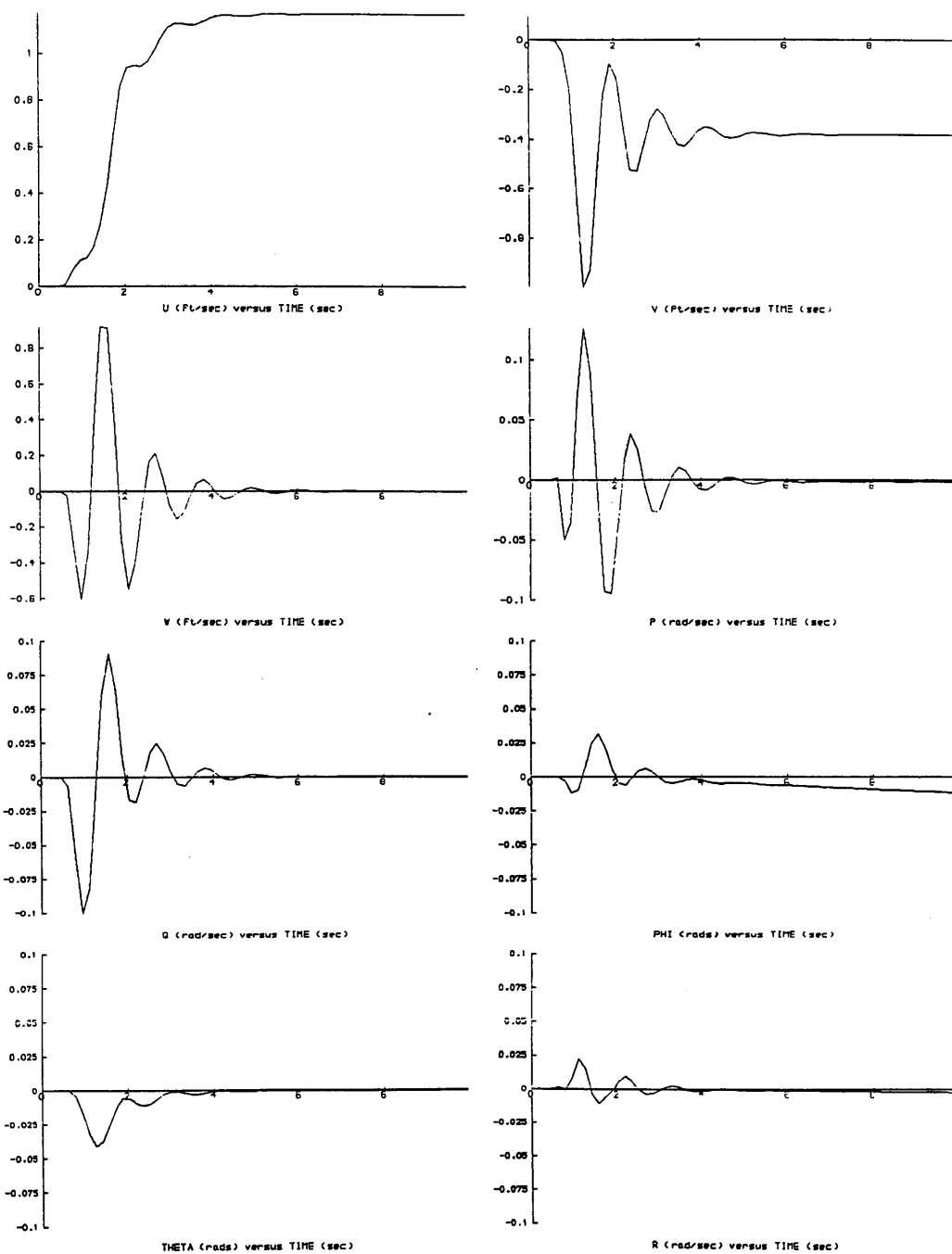
Figure 2.10: Parry Modal Controlled — Nonlinear System Responses to Longitudinal Inceptor, Step Input
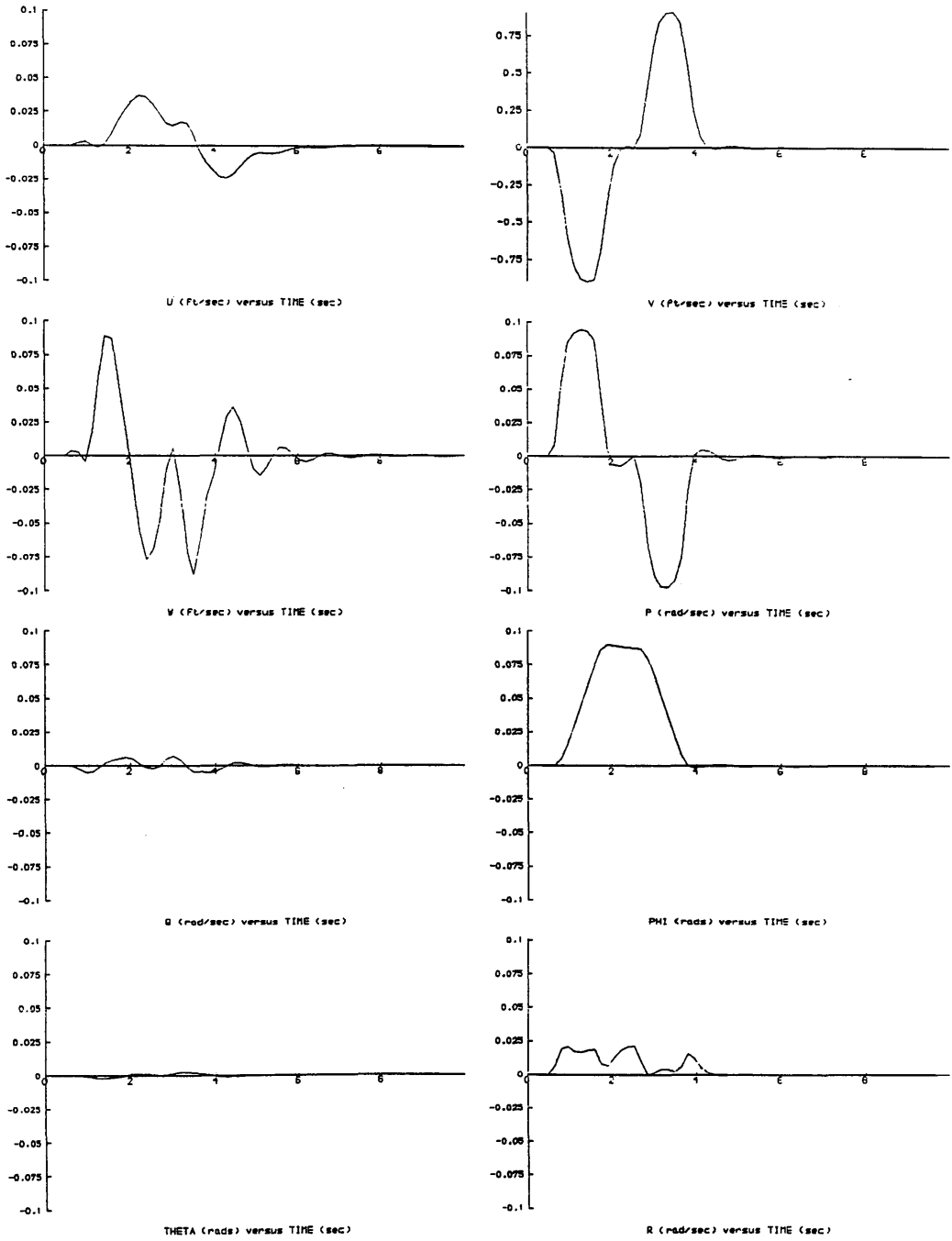
Figure 2.11: Parry Modal Controlled − Nonlinear System Responses to Lateral (Roll) Inceptor, Doublet Input
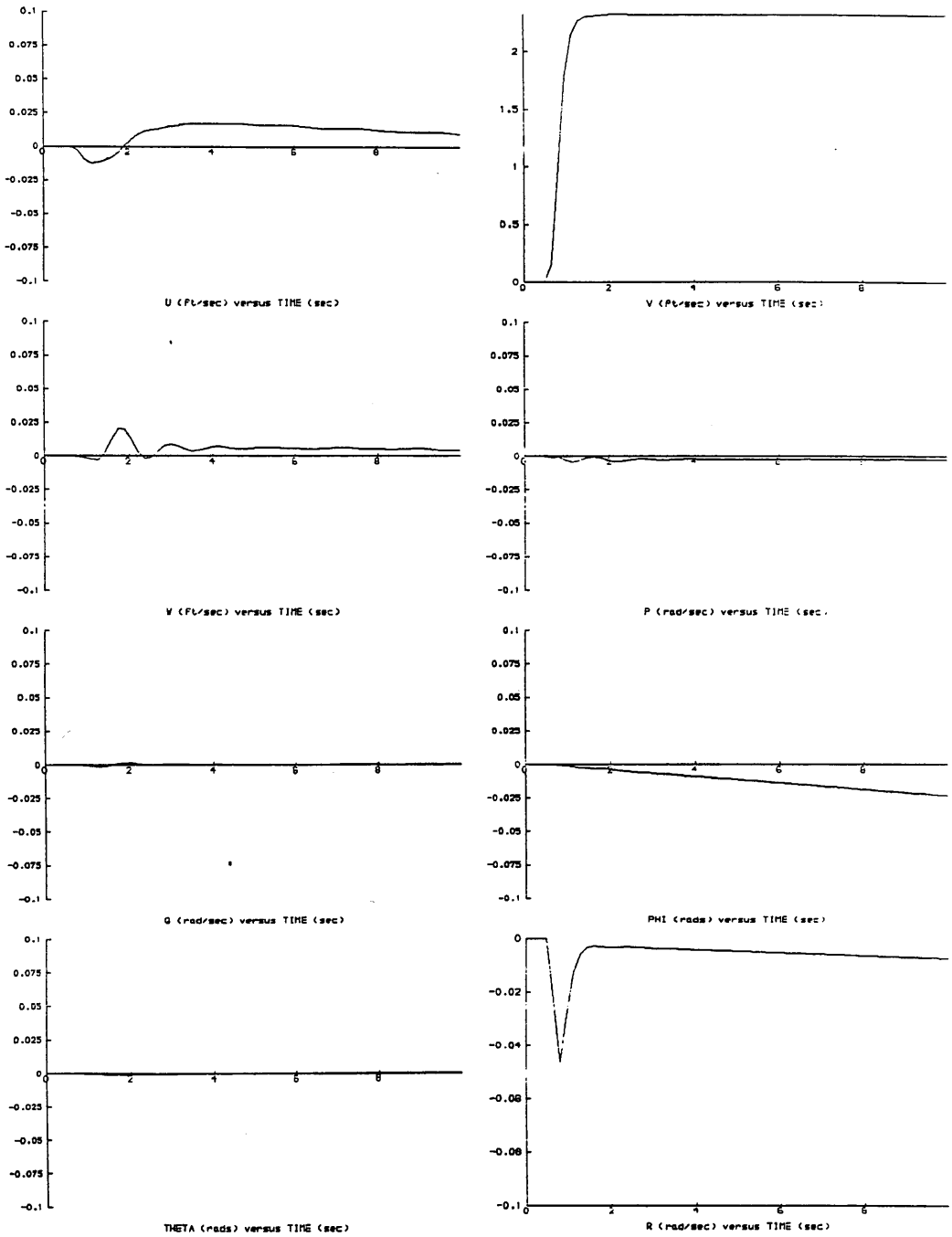
Figure 2.12: Parry Modal Controlled — Nonlinear System Responses to Pedal (Lateral Velocity) Inceptor, Step Input

response to steps on the vertical and longitudinal inceptors (Figures 2.9 and 2.10), the system shows a lightly damped oscillation. The combination of rotor and actuator dynamics moves the phugoid eigenvalue from $-3.0 \pm j1.7$ to $-1.7 \pm j5.5$. The delay in forward velocity response is again in evidence in Figure 2.10. Figure 2.11 shows once more that the yaw rate in response to a roll command doublet is not consistent with a steady turn. Another problem which arises with the inclusion of rotor dynamics concerns the stability of the spiral mode which has migrated to 0.001. The roll angle, φ, and yaw rate, r, in Figure 2.12 show that the spiral mode is unstable.

The responses of the Parry Modal Controller as shown by Figures 2.5− 2.12 are encouraging. Although problems exist, coupling between longitudinal and lateral states is minimal. Stability has been enhanced, but as reported by other authors [9], high order dynamics can adversely affect stability: the phugoid and spiral modes in this example. Vertical, roll, and lateral responses are quick, but the delay in the longitudinal response will probably be unacceptable for pilots. In addition the yaw rate response to roll inputs is far from desirable. For these reasons, it is concluded that although the Parry Modal Controller is effective in stabilizing the system, some sort of command augmentation would greatly facilitate control. Command augmentation could also be designed to yield desirable levels of response; the Parry Modal Controller, as presented here, does not have enough input authority due to a lack of scaling of the precompensator matrix.

2.2.4) An Acceleration Demand Flight Path Controller

In an attempt to provide the command augmentation lacking with the Parry Modal Controller, an acceleration demand flight path controller was developed during preparations for a real− time flight simulation trial (Chapter 7). There were three constraints which were imposed on the structure of the new Flight Path Controller. First, the flight control system was to be based on eigenstructure assignment in a similar manner to the original Parry Modal Controller design. Second, the pilot inputs were required to pass through an integrator before they were input to the actuators. By passing the inputs through an integrator, it would be possible for the pilot to employ a pulse width modulation control strategy. Changes in steady state velocities would be proportional to the amplitude of inceptor displacements and the length of time that the displacement was present. It was hoped that this control strategy would allow sidearm controllers to be used on all input channels since these inceptors

have advantages over conventional helicopter controls [37]. Finally, the Flight Path Controller should regulate the quantities demanded by the pilot. In this case, the pilot input demands are for: vertical acceleration, $\dot{w}$; forward acceleration, $\dot{u}$; roll rate, p; and lateral acceleration, $\dot{v}$, in earth fixed axes. As will be demonstrated in the following, the structure was built up in a rather heuristic manner. Nevertheless, the results of computer simulation tests are good.

2.2.4.1) Acceleration Demand Flight Path Controller Theory

The structure of the Acceleration Demand Flight Path Controller results from the pilot input strategy which is to be employed during flight. Since one of the design aims was to regulate the linear accelerations and the roll rate, it was apparent that a feedback loop in addition to the stability augmentation loop of the Parry Modal Controller would be required. This command augmentation feedback loop would allow a regulator structure to be applied to the acceleration demands and, at the same time, allow the integration of pilot inputs to be carried out as part of a closed loop. Open loop integrators are undesirable for aircraft flight controllers because they are more prone to saturation and must be zeroed before the aircraft takes off. Prior to the summing junction of the command regulator, the pilot inputs would be converted from inceptor displacements to earth axis acceleration demands by the diagonal pilot input gain matrix, [G], and then into body axis demands by the conversion matrix, [η]. The following diagram shows the control structure which was implemented as the Flight Path Controller.
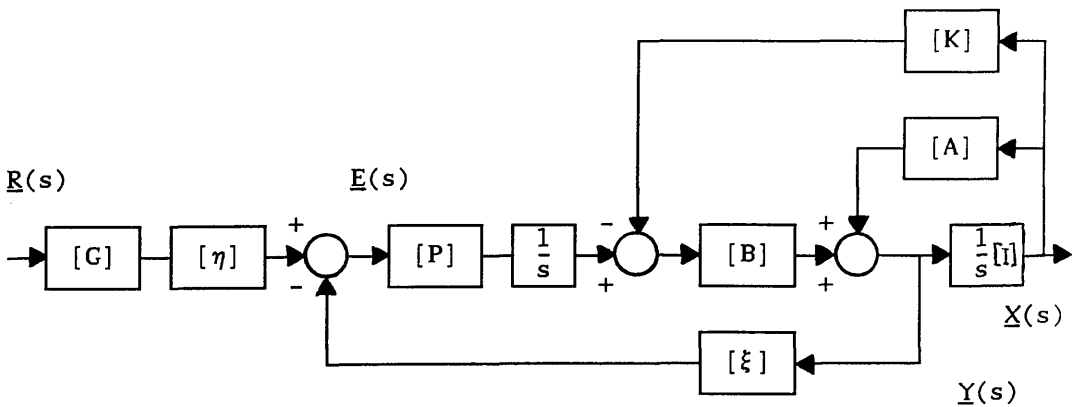
Figure 2.13: The Structure of the Flight Path Controller.

In the above, the feedback distribution matrix, $[\xi]$, is used to select the particular quantities from the acceleration vector, $\underline{Y}(s)$, which are to be compared with the pilot inputs in the body axes coordinate system.

$$[\xi] \equiv \begin{bmatrix} 0 & 1 & 0 & 0 & 0 & 0 & 0 & 0 \\ 1 & 0 & 0 & 0 & 0 & 0 & 0 & 0 \\ 0 & 0 & 0 & 0 & 0 & 0 & 1 & 0 \\ 0 & 0 & 0 & 0 & 1 & 0 & 0 & 0 \end{bmatrix} \qquad \text{Equation 2.28}$$

The conversion matrix, $[\eta]$, is a matrix containing the appropriate Euler angle relationships to map the pilot's earth axes demands onto the body axes of the vehicle. If the earth axes demand vector is,

$$\begin{bmatrix} \dot{w}_E \\ \dot{u}_E \\ p_E \\ \dot{v}_E \end{bmatrix} = \begin{bmatrix} \text{Earth axis vertical acceleration} \\ \text{Earth axis forward acceleration} \\ \text{Roll rate} \\ \text{Earth axis lateral acceleration} \end{bmatrix}$$

Equation 2.29

Then, with the body axis demand vector defined as,

$$\begin{bmatrix} \dot{w}_B \\ \dot{u}_B \\ p_B \\ \dot{v}_B \end{bmatrix} = \begin{bmatrix} \text{Body axis vertical acceleration} \\ \text{Body axis forward acceleration} \\ \text{Roll rate} \\ \text{Body axis lateral acceleration} \end{bmatrix}$$

Equation 2.30

The conversion matrix is defined by,

$$\begin{bmatrix} \dot{w}_B \\ \dot{u}_B \\ p_B \\ \dot{v}_B \end{bmatrix} = \begin{bmatrix} \eta \end{bmatrix} \begin{bmatrix} \dot{w}_E \\ \dot{u}_E \\ p_E \\ \dot{v}_E \end{bmatrix} \qquad \text{Equation 2.31}$$

The elements of the conversion matrix, $[\eta]$, are given by Tomlinson [38] to be,

$$[\eta] = \begin{bmatrix} \cos\theta\ \cos\psi & \cos\theta\ \sin\psi & 0 & -\sin\theta \\ \begin{array}{c}\sin\varphi\ \sin\theta\ \cos\psi \\ -\cos\varphi\ \sin\psi\end{array} & \begin{array}{c}\sin\varphi\ \sin\theta\ \sin\psi \\ +\cos\varphi\ \cos\psi\end{array} & 0 & \sin\varphi\ \cos\theta \\ 0 & 0 & 1 & 0 \\ \begin{array}{c}\cos\varphi\ \sin\theta\ \cos\psi \\ +\sin\varphi\ \sin\psi\end{array} & \begin{array}{c}\cos\varphi\ \sin\theta\ \sin\psi \\ -\sin\varphi\ \cos\psi\end{array} & 0 & \cos\varphi\ \cos\theta \end{bmatrix}$$

Equation 2.32

Where θ = pitch attitude

φ = roll angle

ψ = heading angle

The equations governing the Flight Path Controller of Figure 2.13 are,

$$\underline{E}(s) = [\eta][G]\ \underline{R}(s) - [\xi]\ \underline{Y}(s)$$ Equation 2.33

$$\underline{Y}(s) = [A]\ \underline{X}(s) + [B]\frac{1}{s}[P]\ \underline{E}(s) - [B][K]\ \underline{X}(s)$$

Equation 2.34

$$\underline{X}(s) = \frac{1}{s}\ \underline{Y}(s)$$ Equation 2.35

Rearranging Equation 2.35 and substituting Equations 2.33 and 2.34 for $\underline{E}(s)$ and $\underline{Y}(s)$, the resulting equation for the velocity state vector, $\underline{X}(s)$, is,

$$\underline{X}(s) = \left\{ s[I] - [A] + [B][K] + [B][P][\xi] \right\}^{-1} [B]\frac{1}{s}[P][\eta][G]\ \underline{R}(s)$$

Equation 2.36

The closed loop transfer function matrix for the Flight Path Controller is given by,

$$[W(s)] = \left\{ s[I] - [A] + [B][K] + [B][P][\xi] \right\}^{-1} [B]\frac{1}{s}[P][\eta][G]$$

Equation 2.37

At this point, it is worth considering the characteristic equation for the Flight Path Controller, which is given by,

$$\epsilon(s) = s[I] - [A] + [B][K] + [B][P][\xi] \qquad \text{Equation 2.38}$$

By equating the Flight Path Controller's characteristic polynomial to the characteristic polynomial for the Parry Modal Controller, it is possible to ensure that the Flight Path Controller retains the same eigenstructure assignment.

$$s[I] - [A] + [B][K] + [B][P][\xi] = s[I] - [A] + [B][K_p]$$

$$\text{Equation 2.39}$$

Equation 2.39 can be simplified to yield,

$$[K_p] = [K] + [P][\xi] \qquad \text{Equation 2.40}$$

To solve Equation 2.40, a second expression for the feedback matrix, [K], and the precompensator matrix, [P], must be found. This second equation can be deduced by using the final value theorem to define the desired steady state accelerations of the system to the pilot inputs.

The final value theorem is,

$$\lim_{t \to \infty} [y(t)] = \lim_{s \to 0} s[Y(s)] \qquad \text{Equation 2.41}$$

It should be noted that [y(t)] is the 8×4 matrix made up of the four acceleration vectors, y(t), which result from each of the four pilot inceptors being individually excited by a unit step input. Using Equations 2.35 and 2.36 from above, the following simplifications can be made,

$$\lim_{t \to \infty} [y(t)] = \lim_{s \to 0} s^2[X(s)] \qquad \text{Equation 2.42}$$

$$\lim_{t \to \infty} [y(t)] = \lim_{s \to 0} s^2 \left\{ s[I] - [A] + [B][K] + [B][P][\xi] \right\}^{-1}$$

$$\times [B]\frac{1}{s}[P][\eta][G][R(s)] \qquad \text{Equation 2.43}$$

As stated, the pilot input matrix, [R(s)], is a diagonal matrix representing a unit step on each of the four pilot inceptors,

$$[R(s)] = \frac{1}{s} [I] \qquad\qquad\qquad \text{Equation 2.44}$$

Where [I] is the identity matrix. Further simplification of Equation 2.43 gives,

$$\lim_{t \to \infty} [y(t)] = \lim_{s \to 0} s^2 \left\{ s[I] - [A] + [B][K] + [B][P][\xi] \right\}^{-1}$$

$$\times [B]\frac{1}{s}[P][\eta][G] \frac{1}{s} \qquad \text{Equation 2.45}$$

$$\lim_{t \to \infty} [y(t)] = \lim_{s \to 0} \left\{ s[I] - [A] + [B][K] + [B][P][\xi] \right\}^{-1}$$

$$\times [B][P][\eta][G] \qquad \text{Equation 2.46}$$

$$\lim_{t \to \infty} [y(t)] = \left\{ - [A] + [B][K] + [B][P][\xi] \right\}^{-1} [B][P][\eta][G]$$

$$\text{Equation 2.47}$$

Remembering that the desired steady state accelerations are given by the diagonal pilot input gain matrix, [G], in steady state,

$$\lim_{t \to \infty} [\xi][y(t)] = [G] \qquad\qquad \text{Equation 2.48}$$

And therefore,

$$[G] = [\xi] \left\{ - [A] + [B][K] + [B][P][\xi] \right\}^{-1} [B][P][\eta][G]$$

$$\text{Equation 2.49}$$

Rearranging gives,

$$[\eta]^{-1}[P]^{-1} = [\xi] \left\{ - [A] + [B][K] + [B][P][\xi] \right\}^{-1} [B]$$

$$\text{Equation 2.50}$$

And,

$$[P]^{-1} = [\eta][\xi] \left\{ - [A] + [B][K] + [B][P][\xi] \right\}^{-1} [B]$$

$$\text{Equation 2.51}$$

Recalling Equation 2.40, it is possible to solve for the elements of the precompensator matrix, [P], in terms of the elements of the feedback matrix of

the Parry Modal Controller, $[K_p]$.

$$[P]^{-1} = [\eta][\xi] \left\{ -[A] + [B][K_p] \right\}^{-1} [B] \qquad \text{Equation 2.52}$$

Substitution of the resulting precompensator matrix into Equation 2.40, allows the feedback matrix for the Flight Path Controller, [K], to be determined.

$$[K] = [K_p] - [P][\xi] \qquad \text{Equation 2.53}$$

As stated above, the pilot input gain matrix, [G], is diagonal. The gains are chosen to yield reasonable rates of acceleration. The lateral inceptor gain controlling roll rate amplitude had to be set through trial and error because of a poor transmittance of roll command inputs to the lateral cyclic actuator. Part of the problem is that the command augmentation loop feedback signal is based on roll angle, φ, rather than on roll rate, p. Since the lateral cyclic actuator has a weak authority over roll angle, φ, in comparison to roll rate, p, the energy of the pilot's roll comand is ineffective in terms of generating a roll rate.

Although the eigenstructure of the Parry Modal Controller was used as a basis for the design of the Flight Path Controller, two of the deficiencies of the former were rectified by relocating the closed loop phugoid and spiral mode eigenvalues. Phugoid oscillations were controlled by reducing the gain such that the phugoid eigenvalue was designed as $-1.0 \pm j0.58$. As will be seen in the results of the following section, phugoid oscillations are absent. Indeed, the inclusion of rotor and actuator dynamics only pushes the location of this pole to $-1.0 \pm j0.57$. Spiral mode divergence was eliminated by relocating the designed, closed loop pole from 0.0 to -0.25.

The values for all elements of the control matrices of the Flight Path Controller, for a design point of 80.0 knots level flight are listed in Appendix 1.

2.2.4.2) Acceleration Demand Flight Path Controller Simulation Results

The Flight Path Controller has been tested using both linear and nonlinear representations of the helicopter plant in a computer simulation study. The plots of Figures 2.14 through 2.17 show the simulated body axes responses of the system with an eighth order linear plant. Figure 2.14 shows the response with respect to a 1.0 second full amplitude pulse on the vertical inceptor. Within a second, the vertical velocity has changed by 10 feet per second. The response is

Figure 2.14: Flight Path Controlled — Linear System Responses to Vertical Inceptor, Pulse Input

Figure 2.15: Flight Path Controlled — Linear System Responses to Longitudinal Inceptor, Pulse Input

Figure 2.16: Flight Path Controlled — Linear System Responses to Lateral (Roll) Inceptor, Doublet Input

Figure 2.17: Flight Path Controlled — Linear System Responses to Pedal (Lateral Velocity) Inceptor, Pulse Input

— 49 —

acceptable because the overshoot is negligible and the amount of coupling to other states for the input is small. The transient in forward velocity has an amplitude of less than 0.7 feet per second, which is acceptable. The responses of Figure 2.15 for a 1.0 second pulse on the longitudinal inceptor show that slower modes are present on the forward velocity channel. Whereas the change in vertical velocity to the vertical inceptor input reaches its steady state value in approximately 1 second, the rise time for forward velocity is greater than 3 seconds. Although the delay in the forward velocity response is still a cause for concern, the change in velocity is monotonically smooth. Figure 2.16 shows the system response to a doublet of 10% amplitude on the lateral inceptor. Coupling to the longitudinal states with a roll inceptor input is small, and the yaw rate response, r, is more indicative of a smooth turn than was the yaw response of the Parry Modal Controller. The lateral velocity, v, follows the input quite well, showing very little steady state offset, as desired for a doublet input. The roll rate, p, and roll angle, φ, responses of Figure 2.16 show undesirable features. At the end of the positive roll acceleration demand at 1.5 seconds, the vehicle's roll rate begins to decay. This decay results from the feedback in the command augmentation loop. Since the doublet input has amplitude 0.0 between 1.5 seconds and 2.5 seconds, the finite, nonzero roll rate feedback will try to drive the system to zero roll rate. When the negative pulse of the doublet is applied at 2.5 seconds the roll rate, p, has decreased. Unfortunately, because of the decay in roll rate between 1.5 and 2.5 seconds, the negative pulse of the input drives the system to a negative roll rate, rather than to a zero roll rate. At the end of the negative doublet pulse, at 3.5 seconds, the command loop feedback again starts to drive the roll rate back to zero. The roll rate feedback in the command augmentation loop is responsible for the undesirable roll characteristics. The amount of decay in roll rate will be dependent on the length of the deadband between the positive and negative pulses of the doublet. If the doublet deadband were zero, the decay would not be noticeable to a pilot, but it is clear that further work remains to be done in terms of developing a command augmentation system to complement the Parry Modal Controller. The system response to a pulse input on the pedals is almost ideal (Figure 2.17). The step change in lateral velocity, v, of over 9 feet per second is accomplished rapidly and without overshoot. In addition, coupling is almost nonexistent, except for a vertical velocity change of less than 0.35 feet per second.

When the same controller is used with the HELISIM3 plant, the adverse effects of rotor dynamics become clear. Figures 2.18 to 2.21 are the HELISIM3 equivalents of Figures 2.14 to 2.17. Figure 2.18 shows the closed loop system
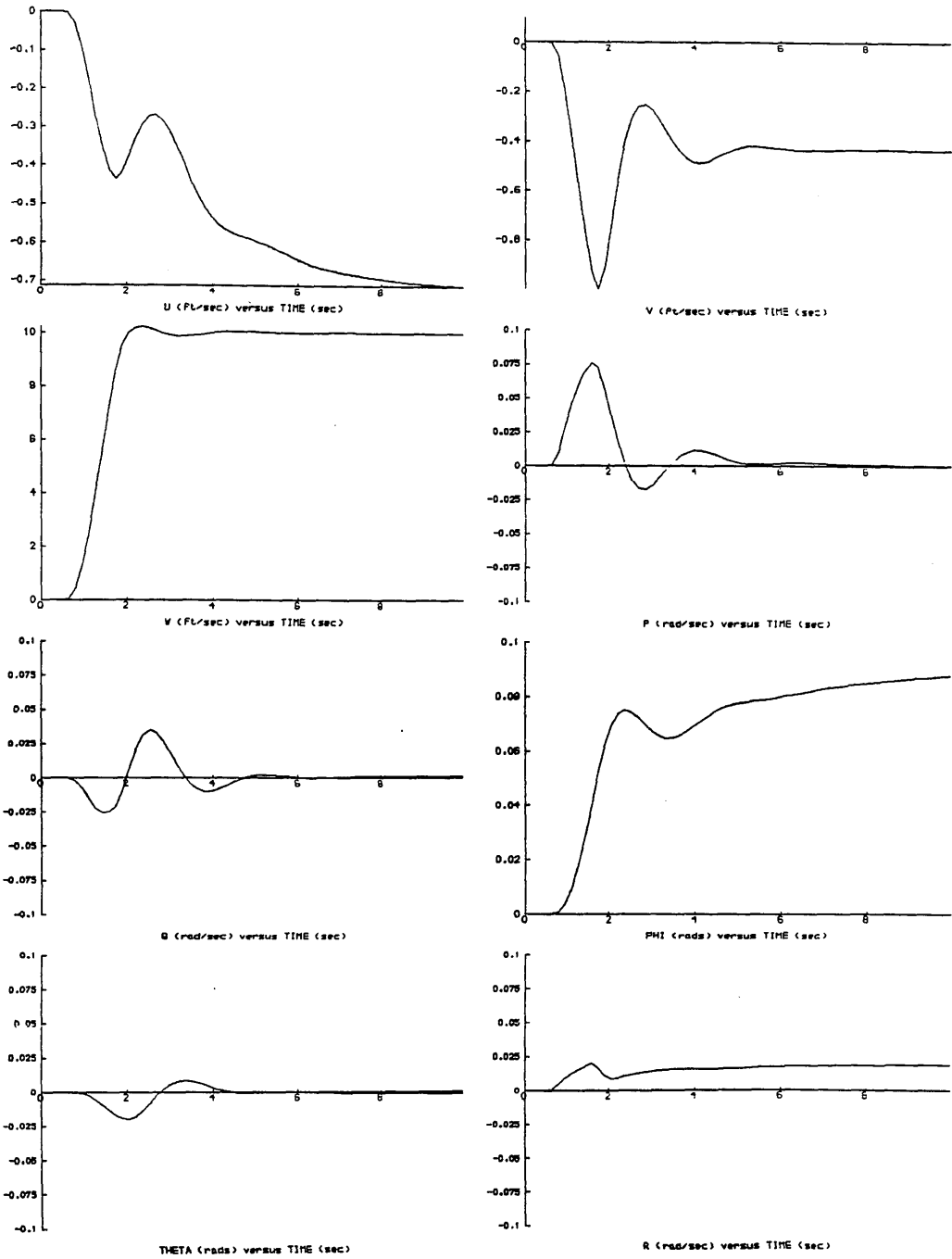
Figure 2.18: Flight Path Controlled — Nonlinear System Responses to Vertical Inceptor, Pulse Input
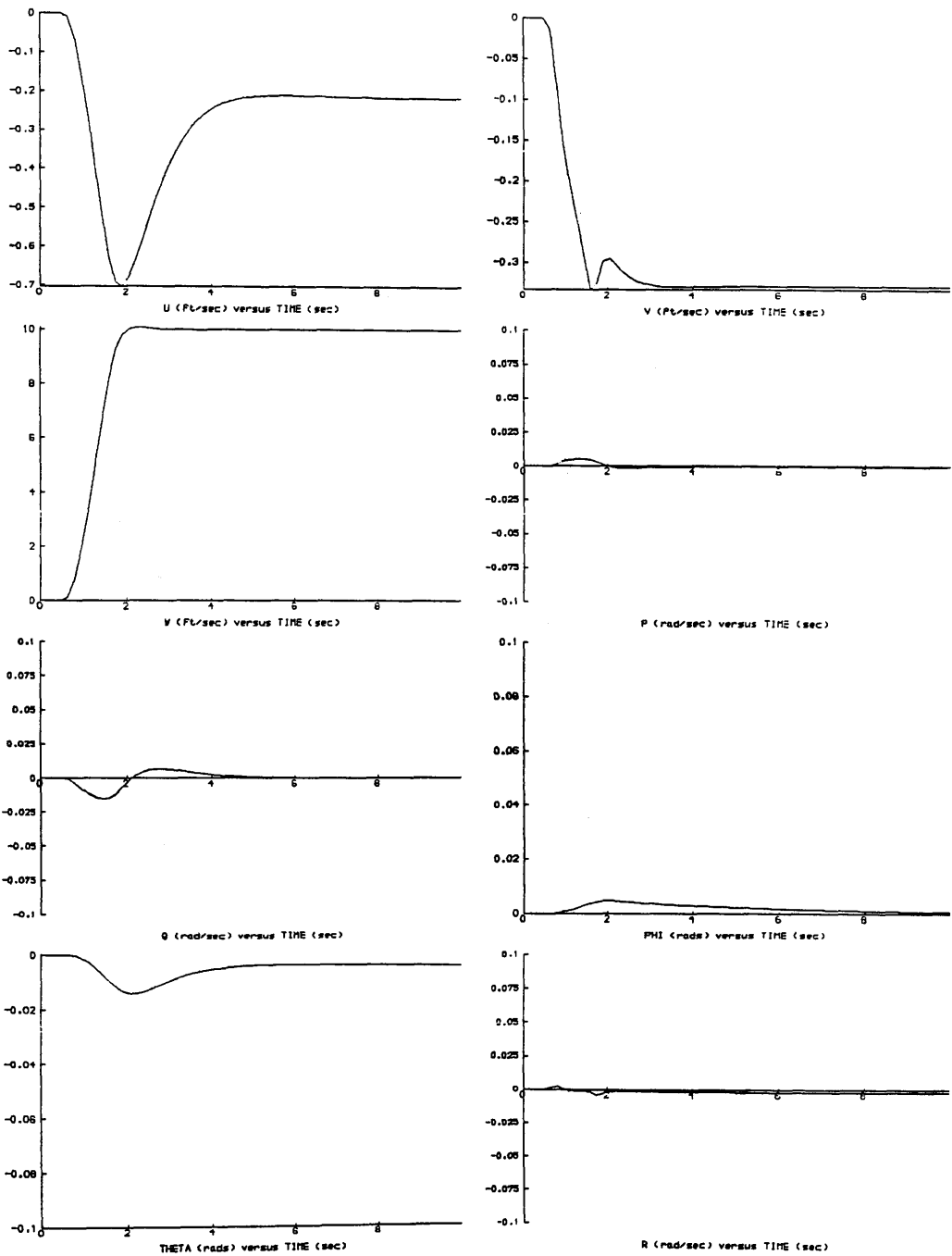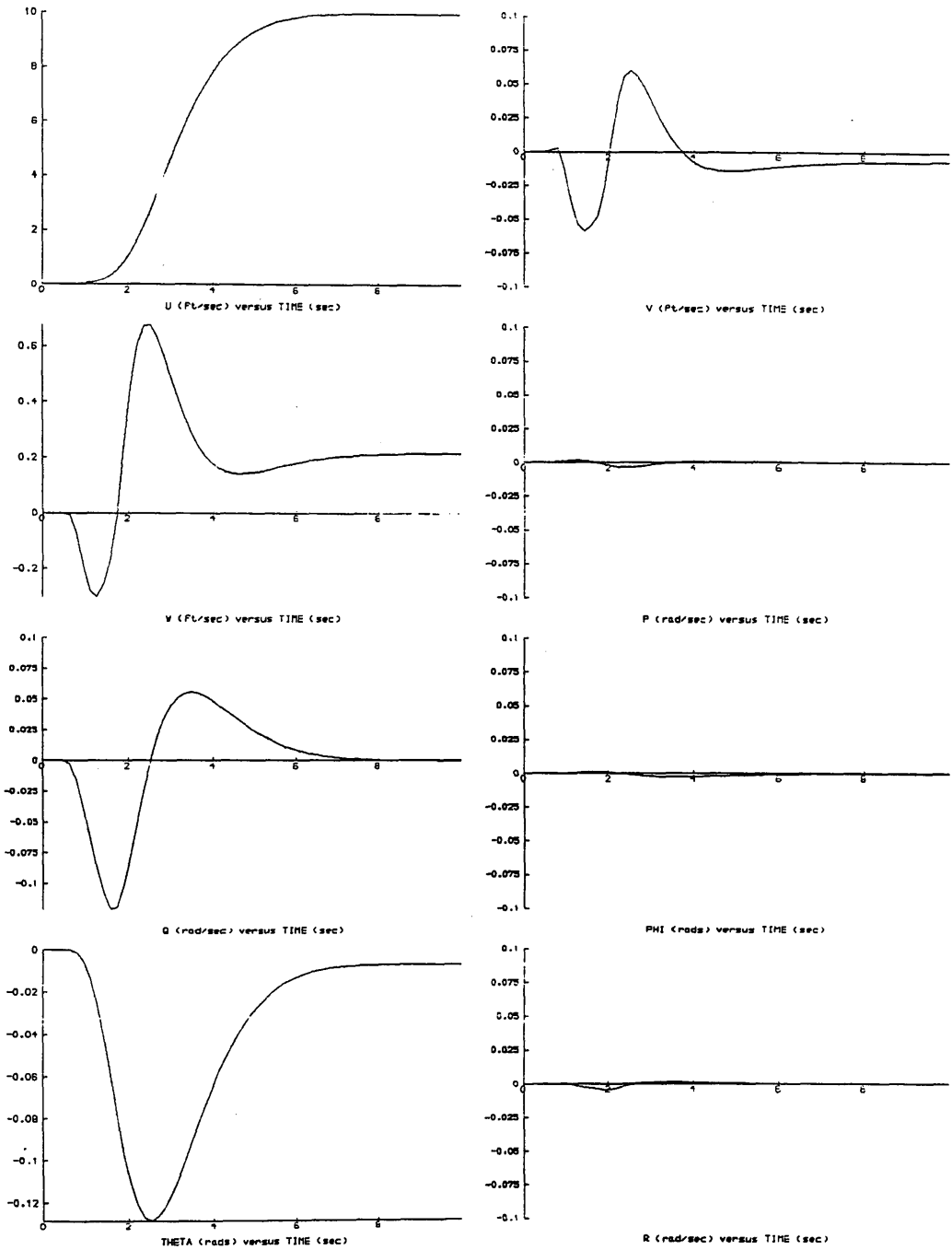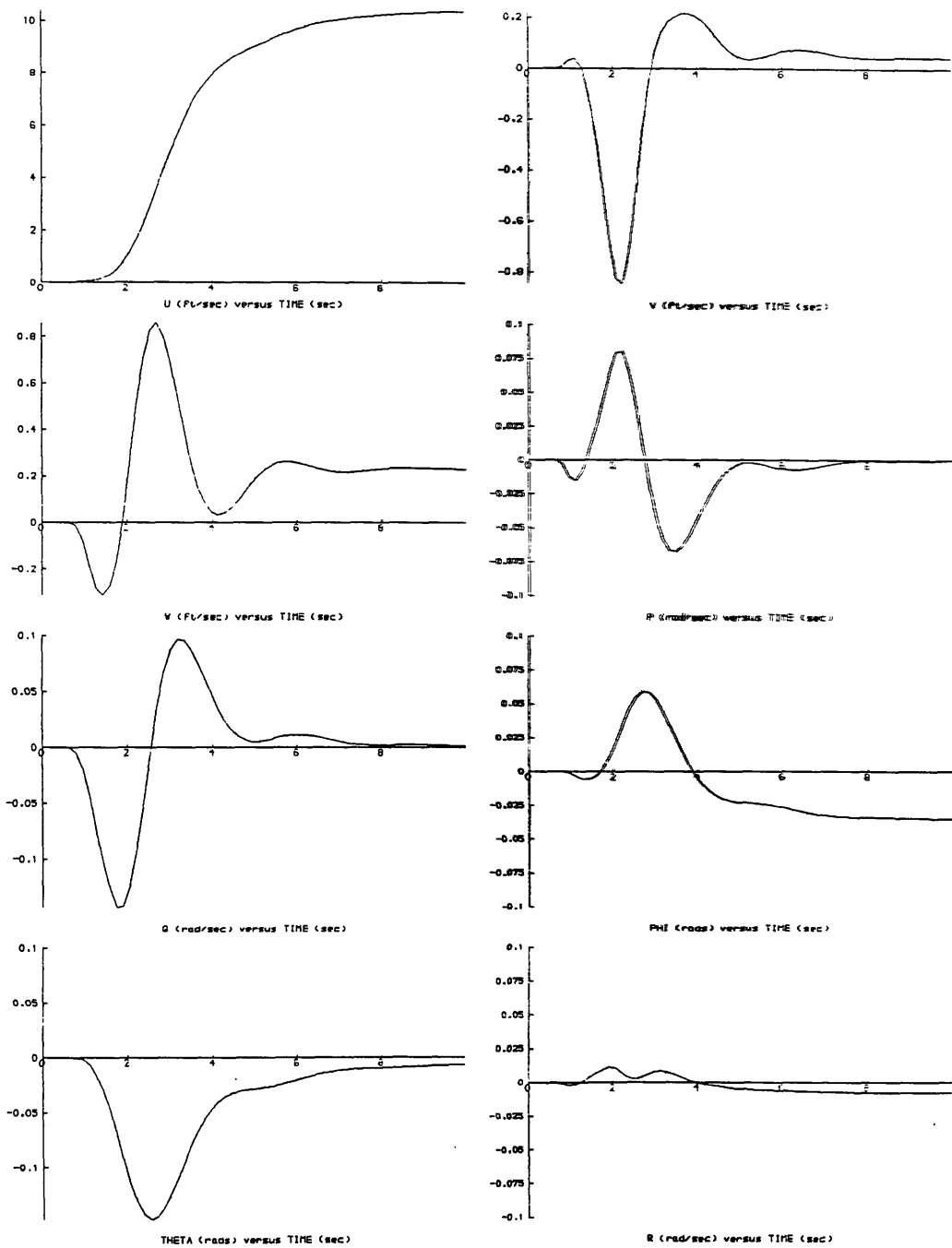
Figure 2.19: Flight Path Controlled — Nonlinear System Responses to Longitudinal Inceptor, Pulse Input
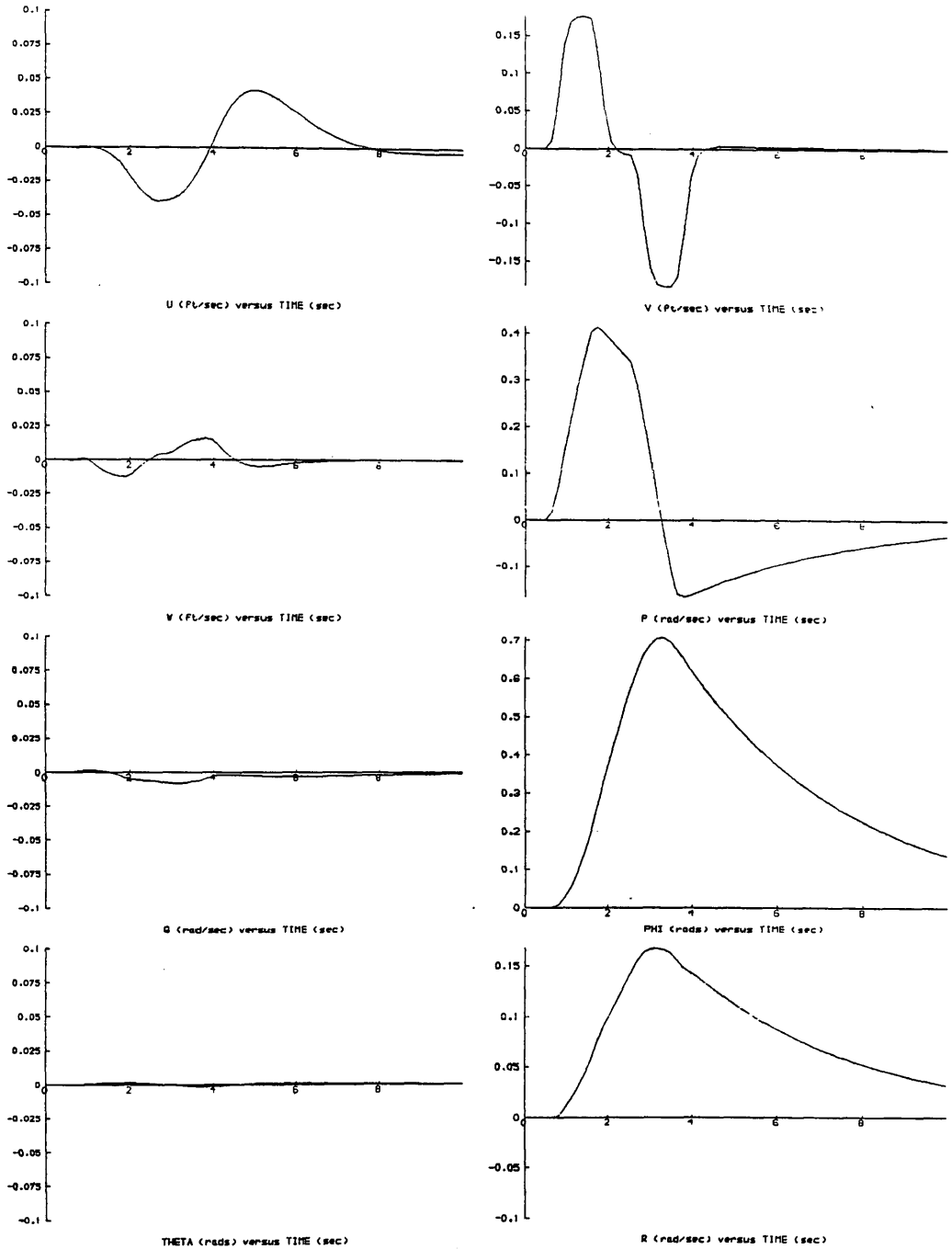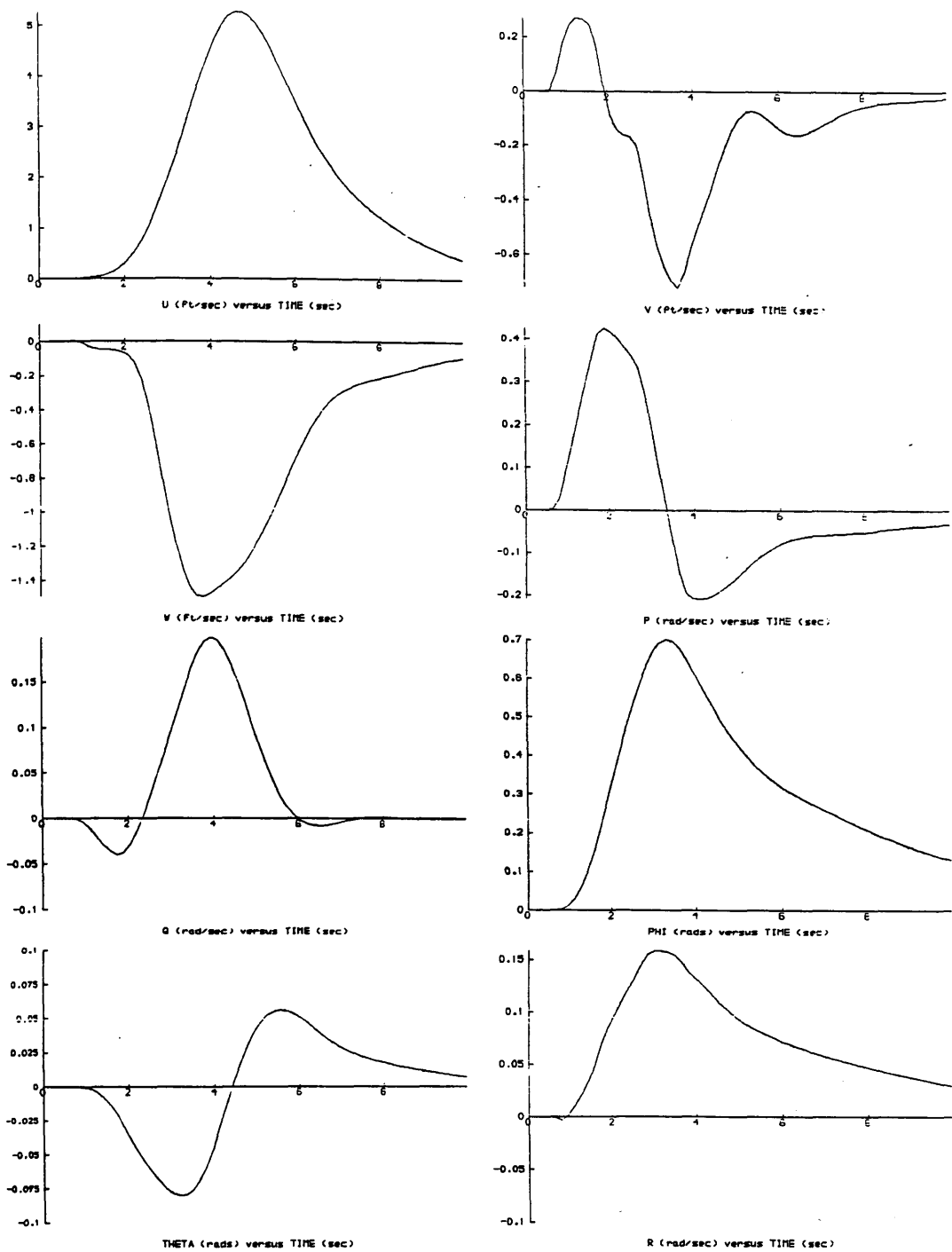
Figure 2.20: Flight Path Controlled — Nonlinear System Responses to Lateral (Roll) Inceptor, Doublet Input
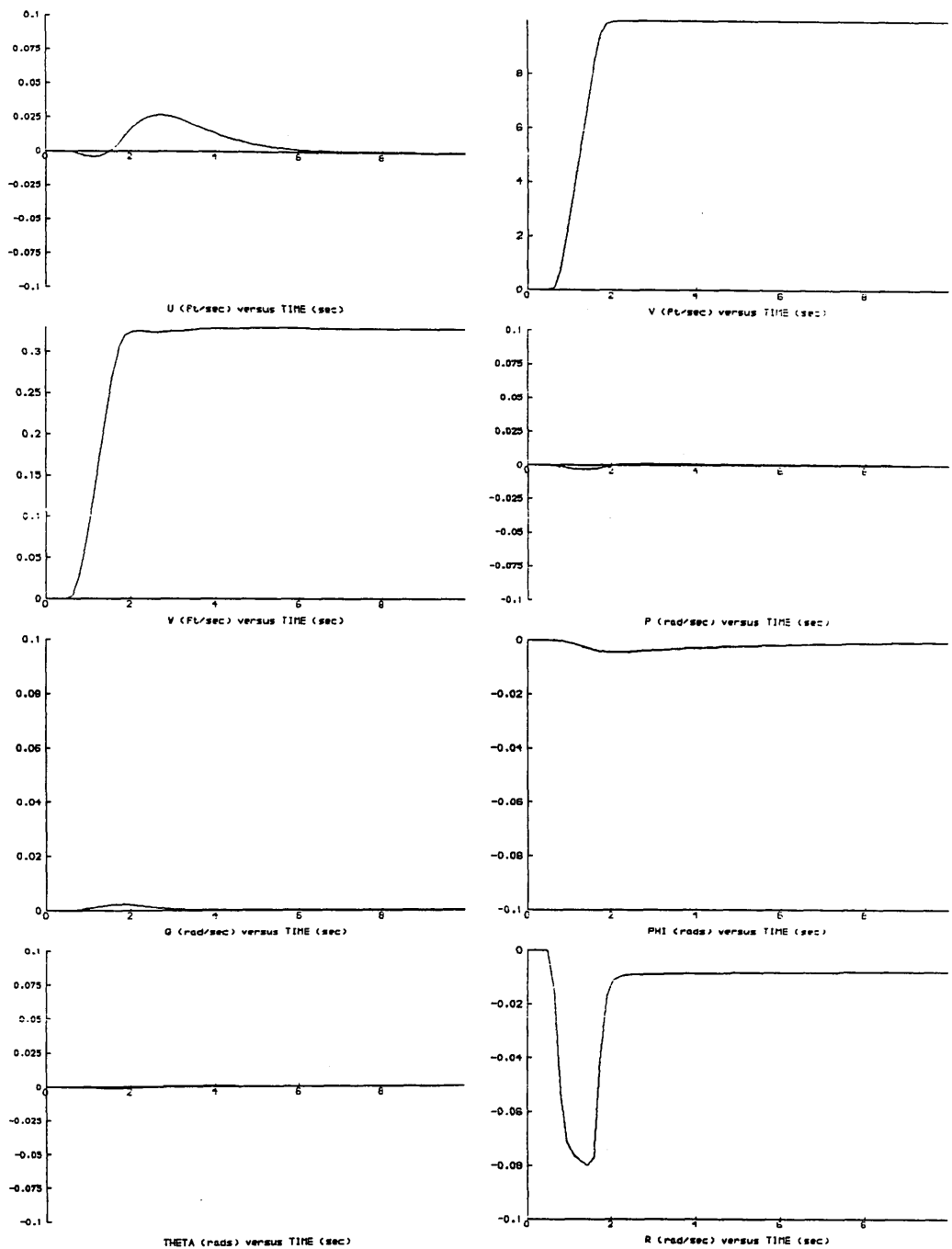
— 53 —
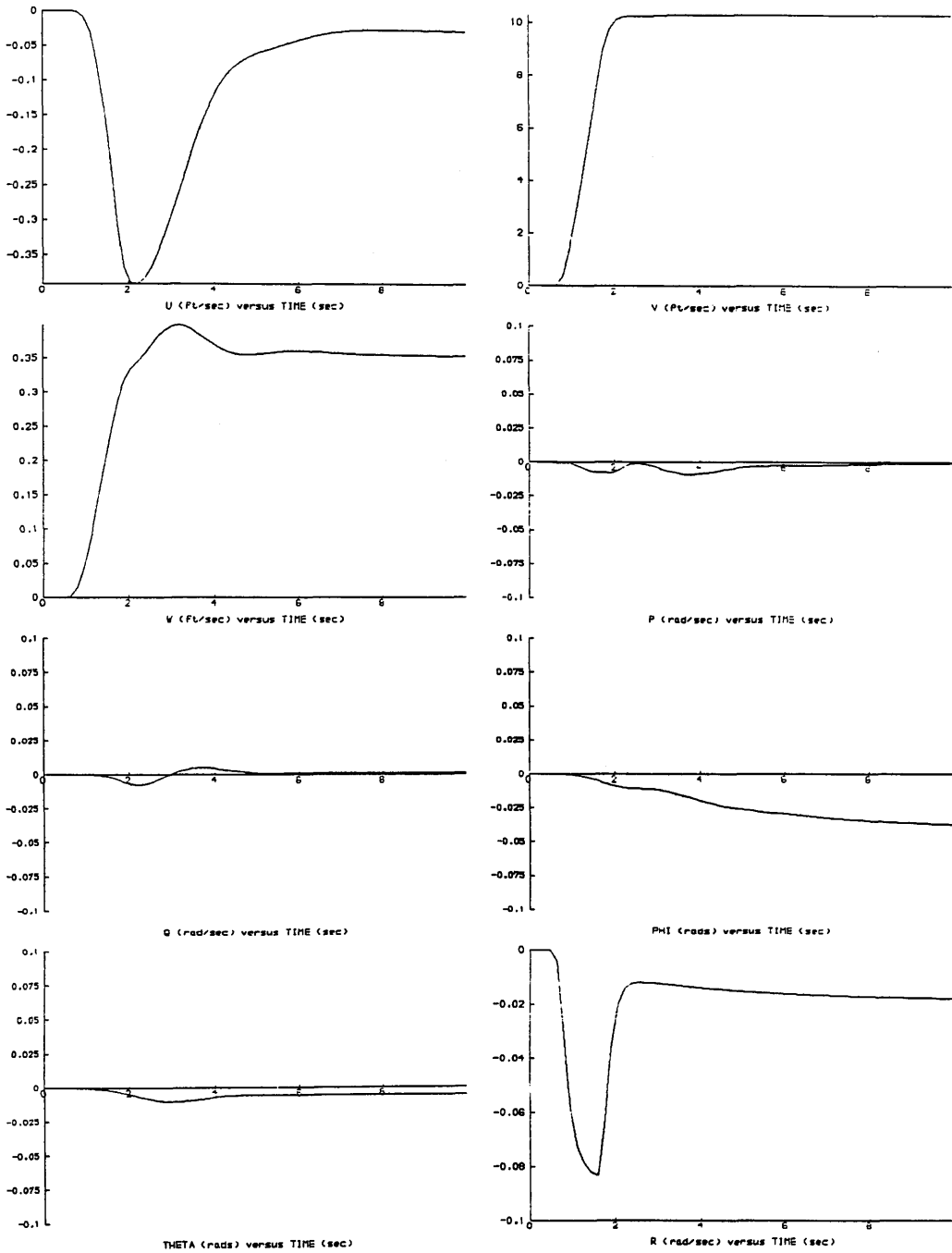
Figure 2.21: Flight Path Controlled — Nonlinear System Responses to Pedal (Lateral Velocity) Inceptor, Pulse Input

response (nonlinear HELISIM3 plant) to a 1.0 second pulse on the vertical inceptor. The lateral states are not only coupled to the longitudinal states to a much higher degree, but the responses of the nonlinear system also differ from those of the linear system 2 seconds after the input has been initiated. This indicates that the nonlinear system is moving away from the controller's design point.

Figure 2.19 is the nonlinear response to a longitudinal inceptor pulse (1.0 second duration). Once again coupling is more pronounced when the Flight Path Controller is used with a nonlinear plant than with a linear plant. Figure 2.19 also shows the higher order rotor dynamics coming through on the longitudinal state responses (compared with the linear system responses shown in Figure 2.15).

The effects of system nonlinearities are clearly in evidence if one compares the linear roll command responses of Figure 2.16 with their nonlinear counterparts in Figure 2.20. The most striking difference is that the rotor dynamics and nonlinearities have coupled the roll command energy into the forward velocity channel, u. The vertical velocity also has a transient of 1.5 feet per second. Although the roll rate, p, roll angle, φ, and yaw rate, r, responses are similar for nonlinear and linear plants, the lateral velocity, v, is more oscillatory using the HELISIM3 nonlinear plant model.

The response of the nonlinear HELISIM3 plant — Flight Path Controller system to a pulse input on the pedals is shown in Figure 2.21. The responses show increased levels of coupling to the longitudinal states, particularly on forward velocity, u, and the divergence of the spiral mode which is evident on the roll angle, φ, and yaw rate, r, responses. The command is designed to produce a step change in lateral velocity, v, and the controller accomplishes this for both linear and nonlinear plants.

The time domain responses of the Flight Path Controlled system show that improvements can be made to the original Parry Modal Controller. The vertical velocity response is improved through the elimination of overshoot. The improvement in forward velocity response is questionable since, although the change in forward velocity is effected monotonically (without acceleration reversals) with the Flight Path Controller, the change is made much more slowly and with larger pitch attitude transients. The Flight Path Controller has helped to reduce coupling from the longitudinal inceptor to lateral velocity, v, for this input. The command augmentation loop has helped to improve the turning abilities of the aircraft but it is clear that further work needs to be carried out on the development of the command augmentation strategy and structure. Another adverse characteristic of the Flight Path Controller is that the pedal inceptors are

coupled to vertical velocity.

Since the closed loop dynamics of the two systems (Parry Modal Controller versus Flight Path Controller) are equivalent, the differences in coupling between the two is due to the pilot command strategy/command augmentation loop. The pilot command strategy affects the structure of the command augmentation of the controller in an intimate way. Movement of the pilot's inceptors feeds energy to the system in different ways for the two controller structures and hence coupling between states will be different, as has been shown. Assuming that the controller requires both stability and command augmentation, if a decision is made to use two feedback loops in the controller, it might then be profitable to use the stability loop to ensure plant stability, and to use the command loop to give decoupled responses. The stability augmentation loop would yield stable eigenvalues and decoupled eigenvectors, while the command augmentation loop could be used to decouple pilot input energy such that individual closed loop modes were excited by each inceptor. Modal control could be used in a two tiered approach; first to provide plant stability, and second to provide command decoupling. One of the problems with the Flight Path Controller is that the structure is designed in such a way that plant stability and decoupling are the sole criteria for the eigenstructure assignment. This led to weak authority over roll and some undesirable couplings between inceptors and states. The design of command augmentation might be improved if the system eigenstructure could be described in terms of a static stability eigenstructure and a dynamic (or command) stability eigenstructure.

One of the distinguishing features of the HELISIM3 results with the Flight Path Controller is the increased level of coupling in the system. Although a portion of this coupling will be due to high order dynamics and nonlinearities, part may be a result of the fact that the nonlinear system is moving away from its design point and hence the eigenvectors may not have optimal orientation. Study of the movement of eigenvalues and eigenvectors would be an appropriate starting point for work on an adaptive controller. Such work was considered beyond the scope of the current project.

The frequency responses of the nonlinear HELISIM3 plant controlled by the Flight Path Controller are shown in Figures 2.22 to 2.29. The responses were obtained by exciting the system with a step input of amplitude 0.025 so as not to drive the system too far away from a linear region about the design point. The magnitude plots are in decibels while the phase plots are in units of degrees. Frequency is plotted on a logarithmic scale in Hertz. Each of the figures shows the frequency responses of a state with respect to the four pilot inceptors. The
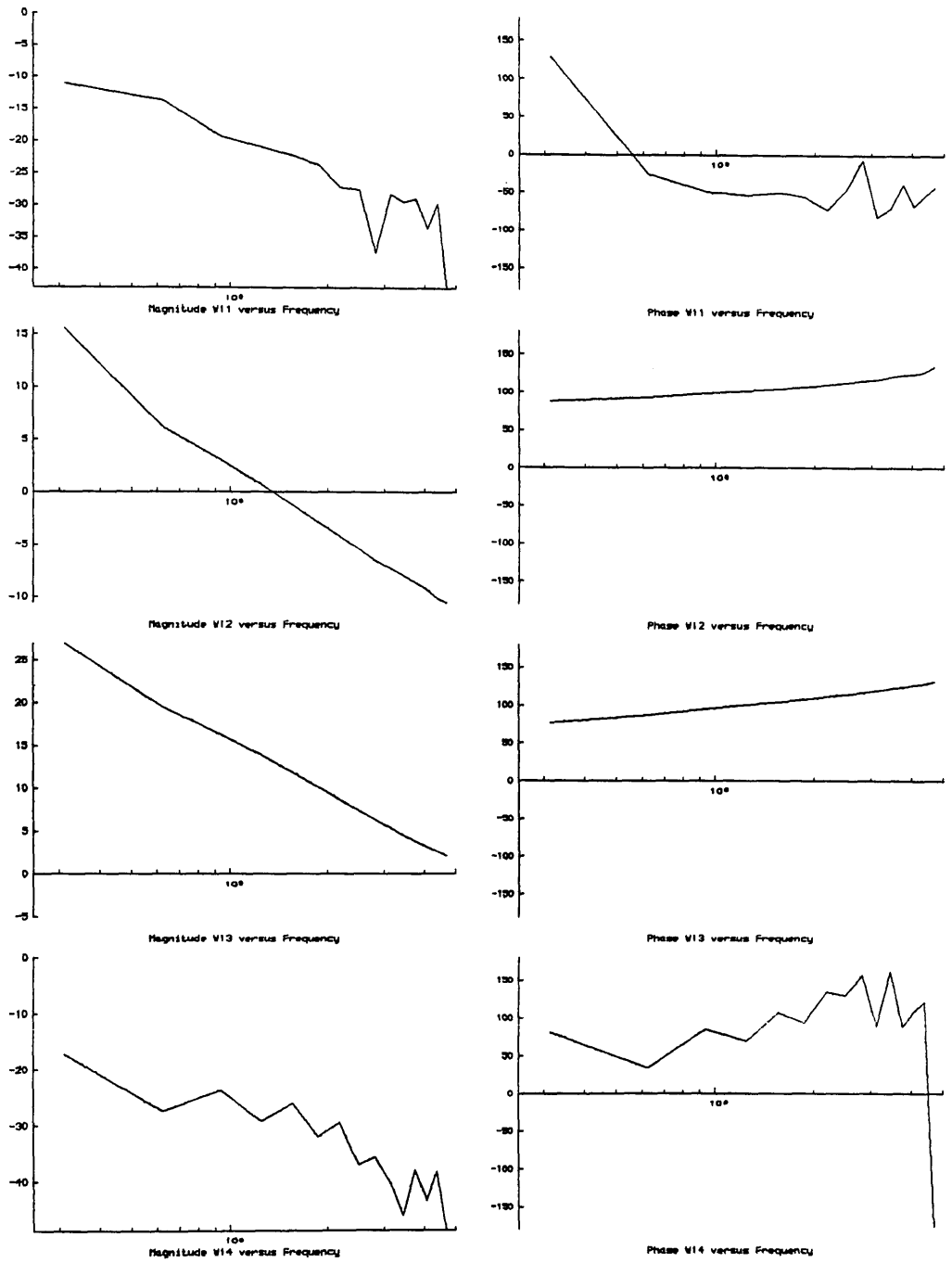
Figure 2.22: Flight Path Controlled — Nonlinear System, Forward Velocity Frequency Responses
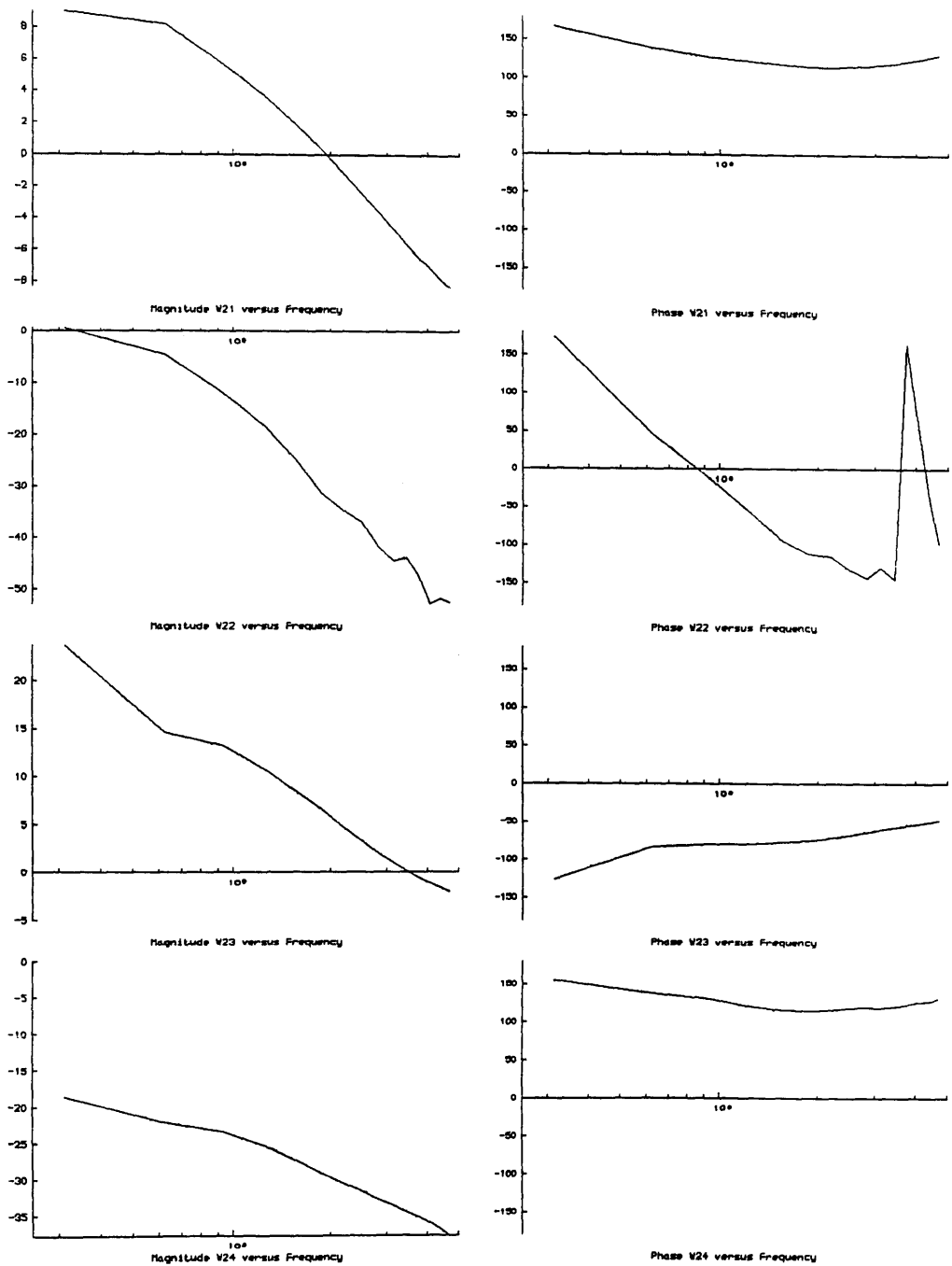
Figure 2.23: Flight Path Controlled — Nonlinear System, Vertical Velocity
Frequency Responses
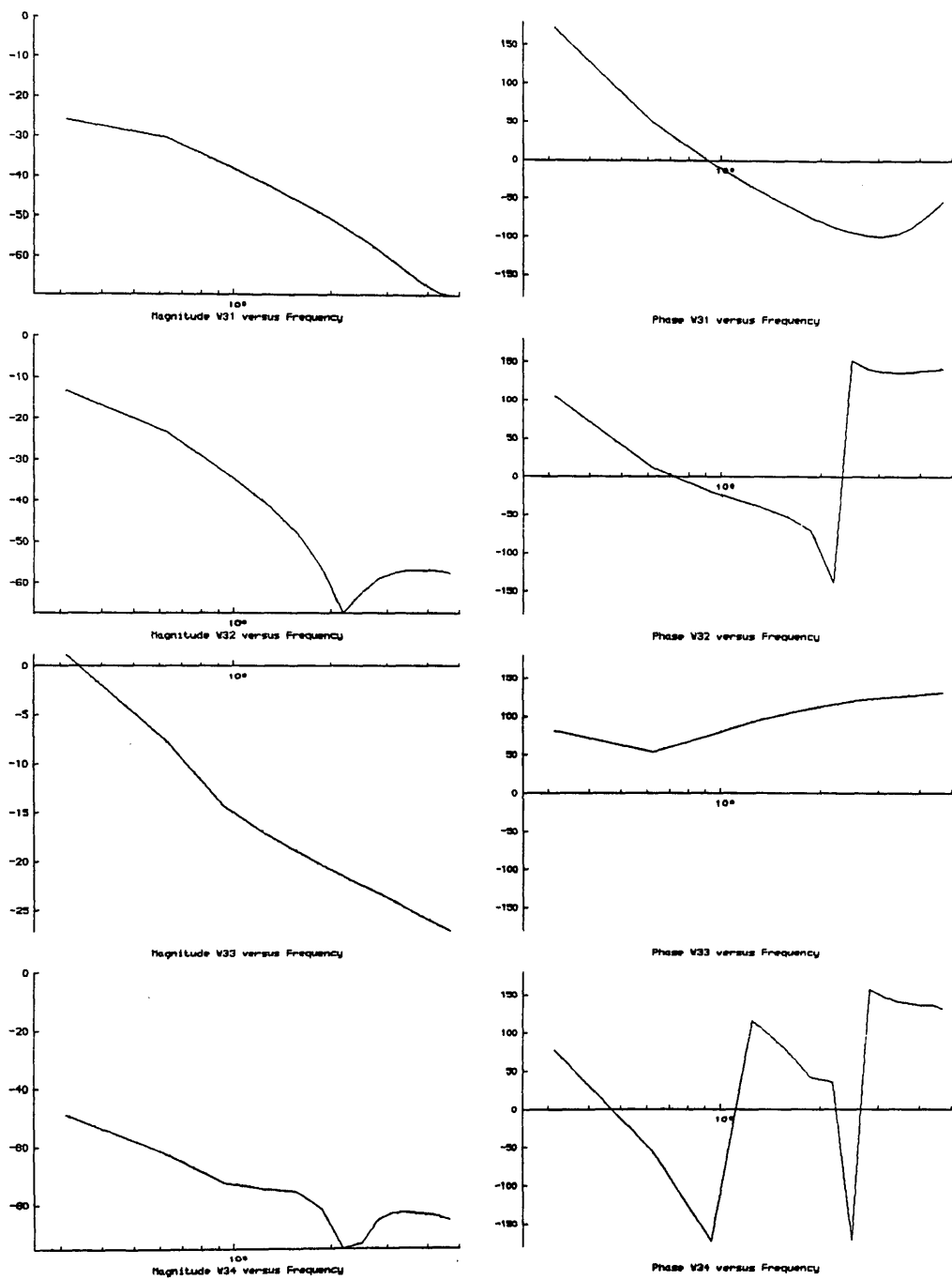
Figure 2.24: Flight Path Controlled — Nonlinear System, Pitch Rate Frequency Responses
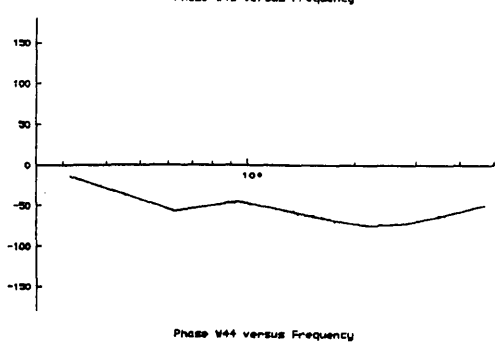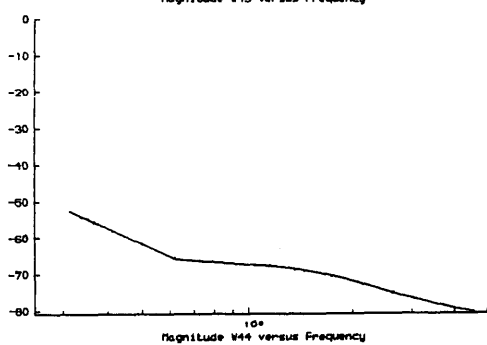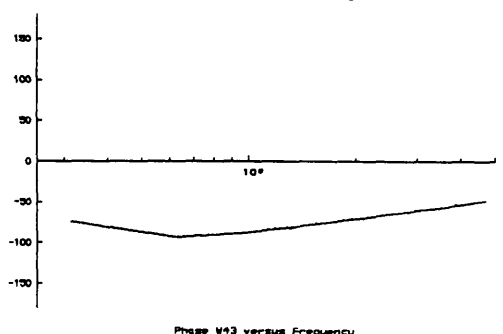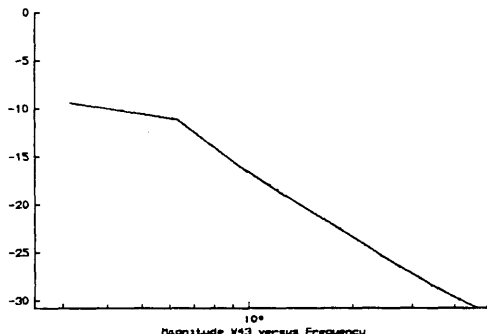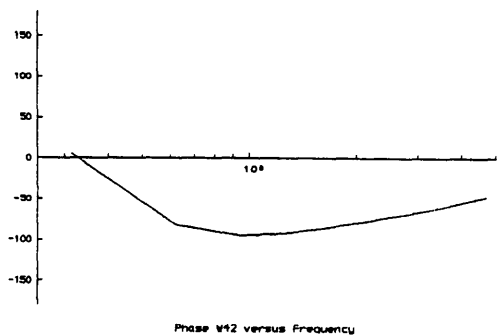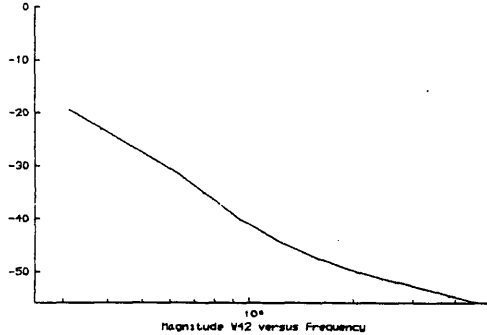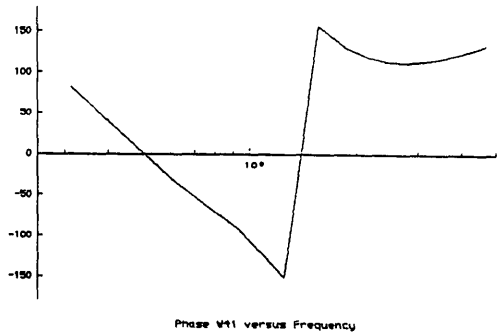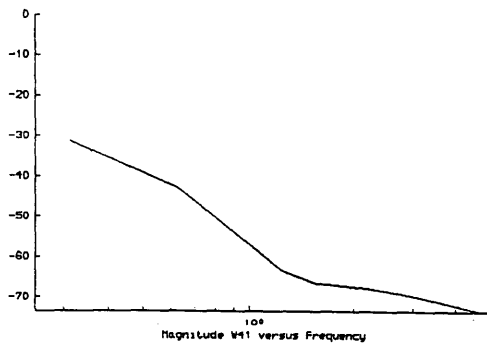
Figure 2.25: Flight Path Controlled — Nonlinear System, Pitch Angle Frequency Responses
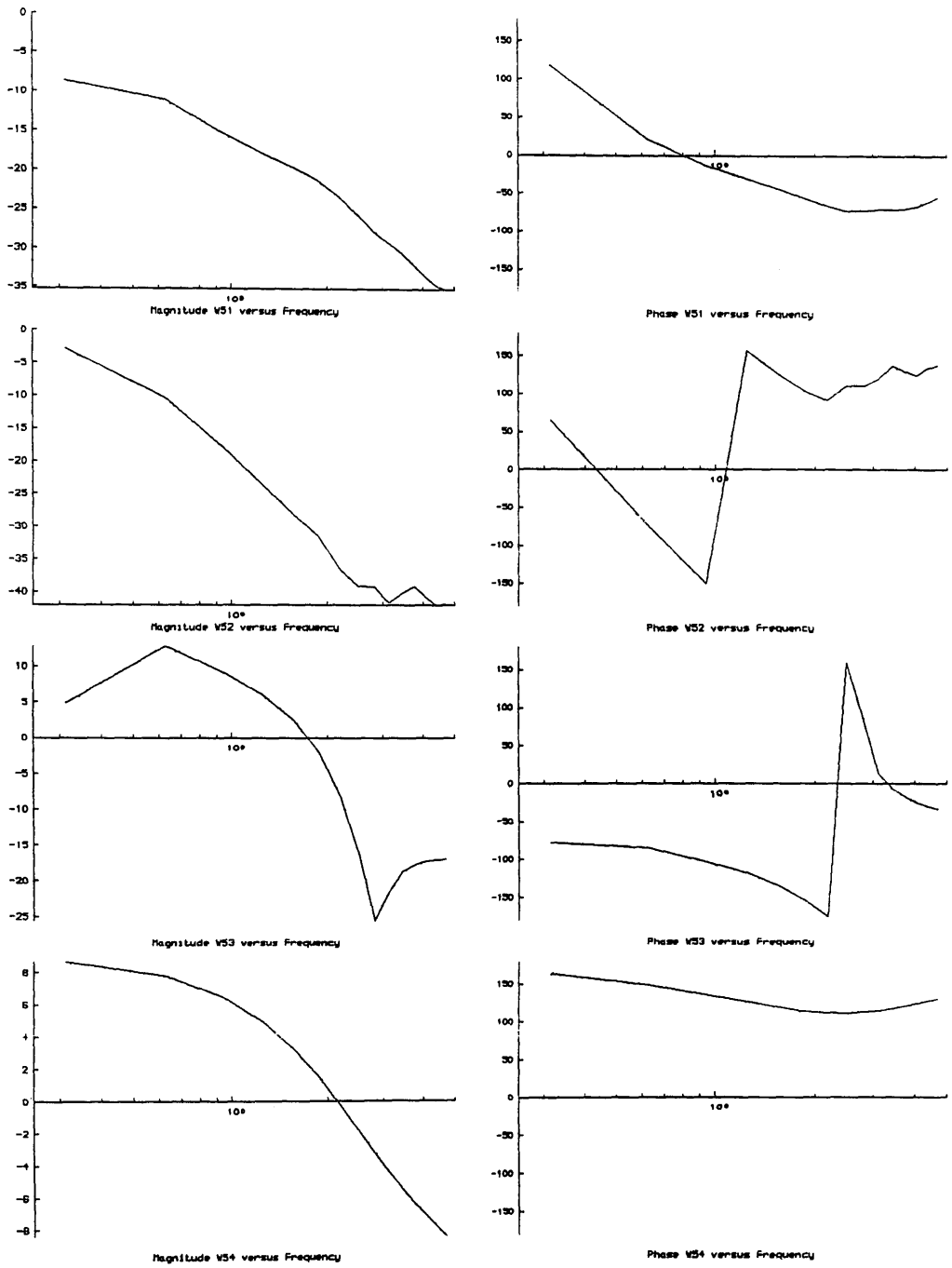
Figure 2.26: Flight Path Controlled — Nonlinear System, Lateral Velocity
Frequency Responses
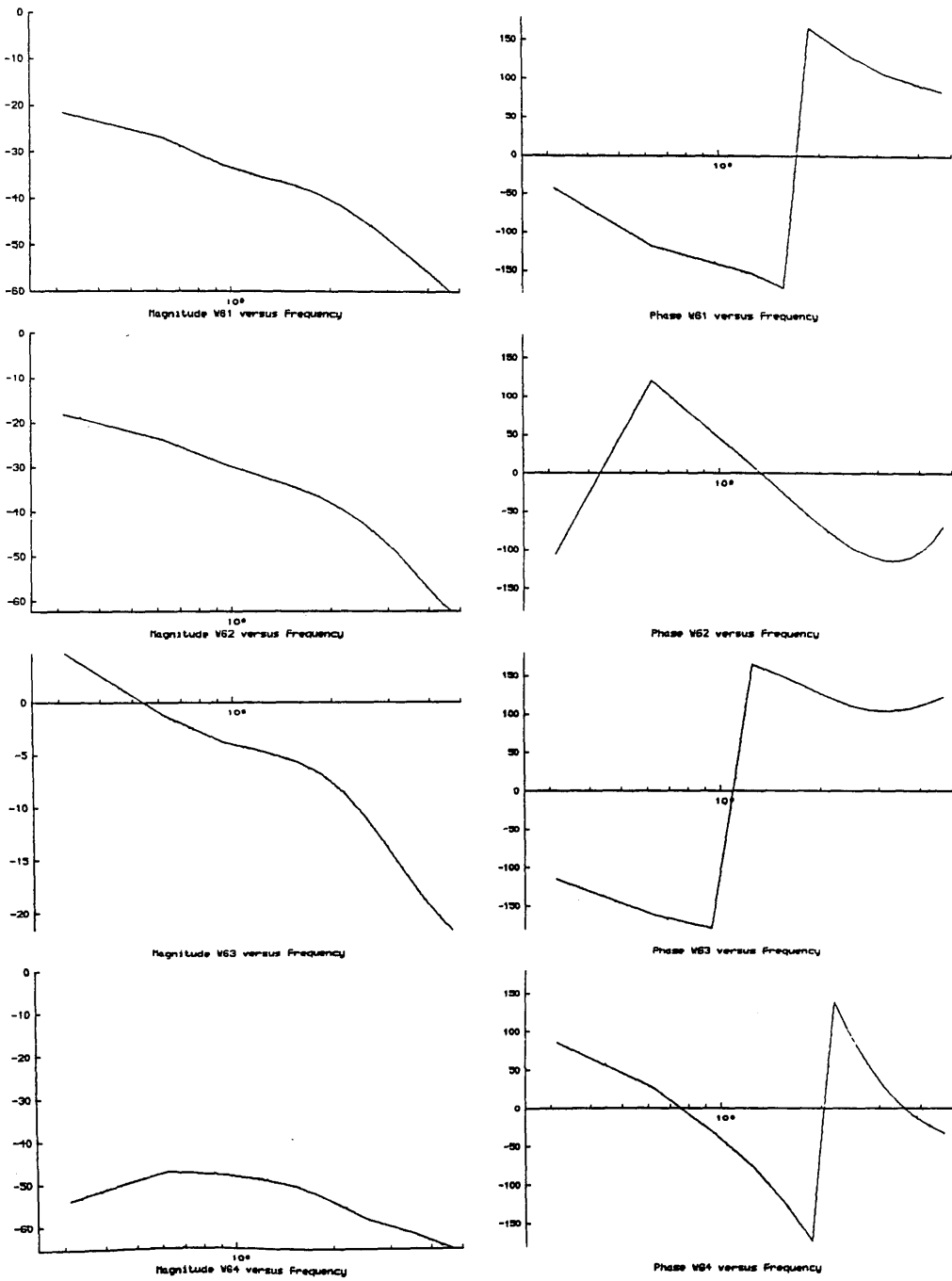
Figure 2.27: Flight Path Controlled — Nonlinear System, Roll Rate Frequency
Responses
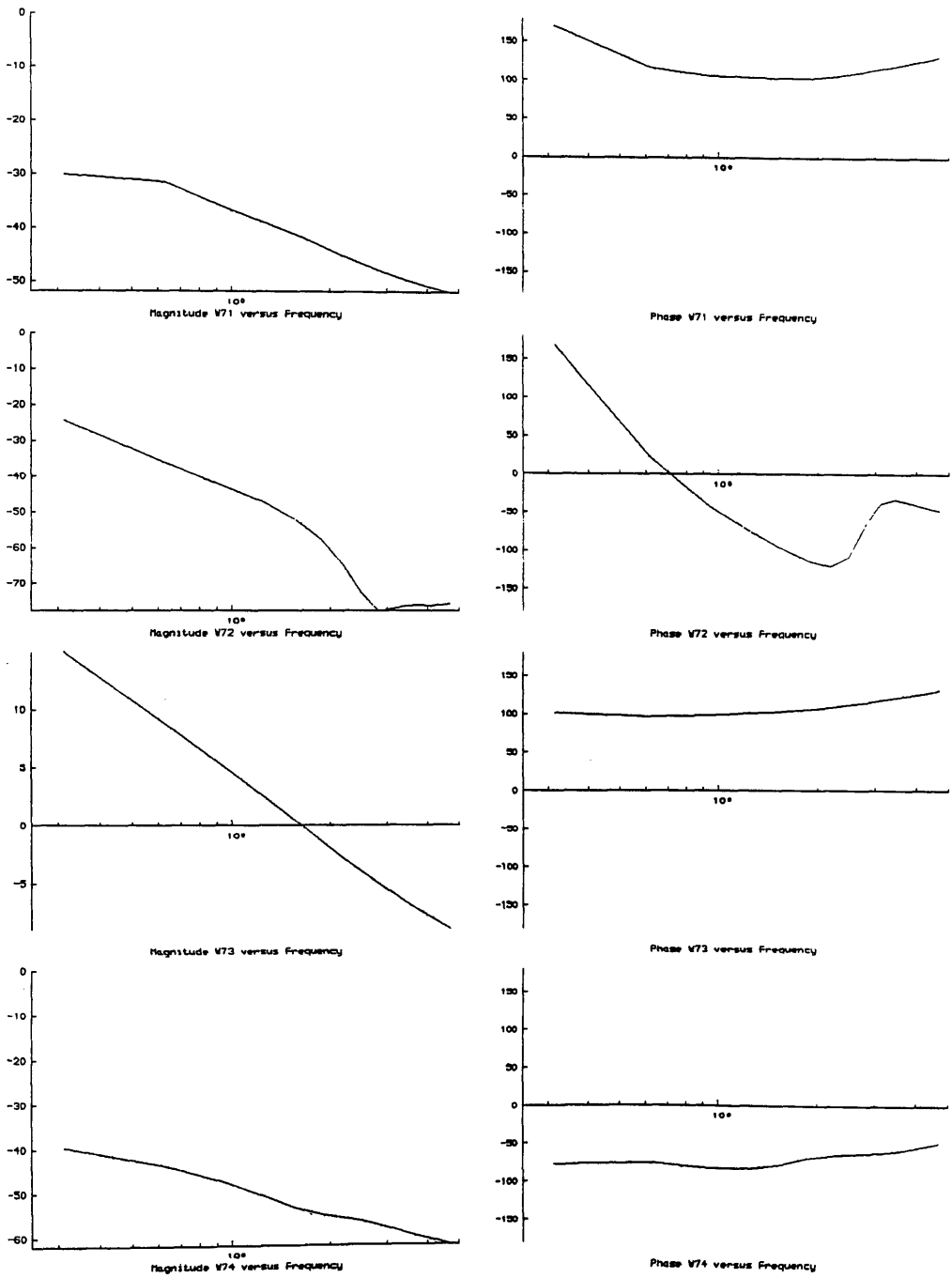
Figure 2.28: Flight Path Controlled — Nonlinear System, Roll Angle Frequency Responses
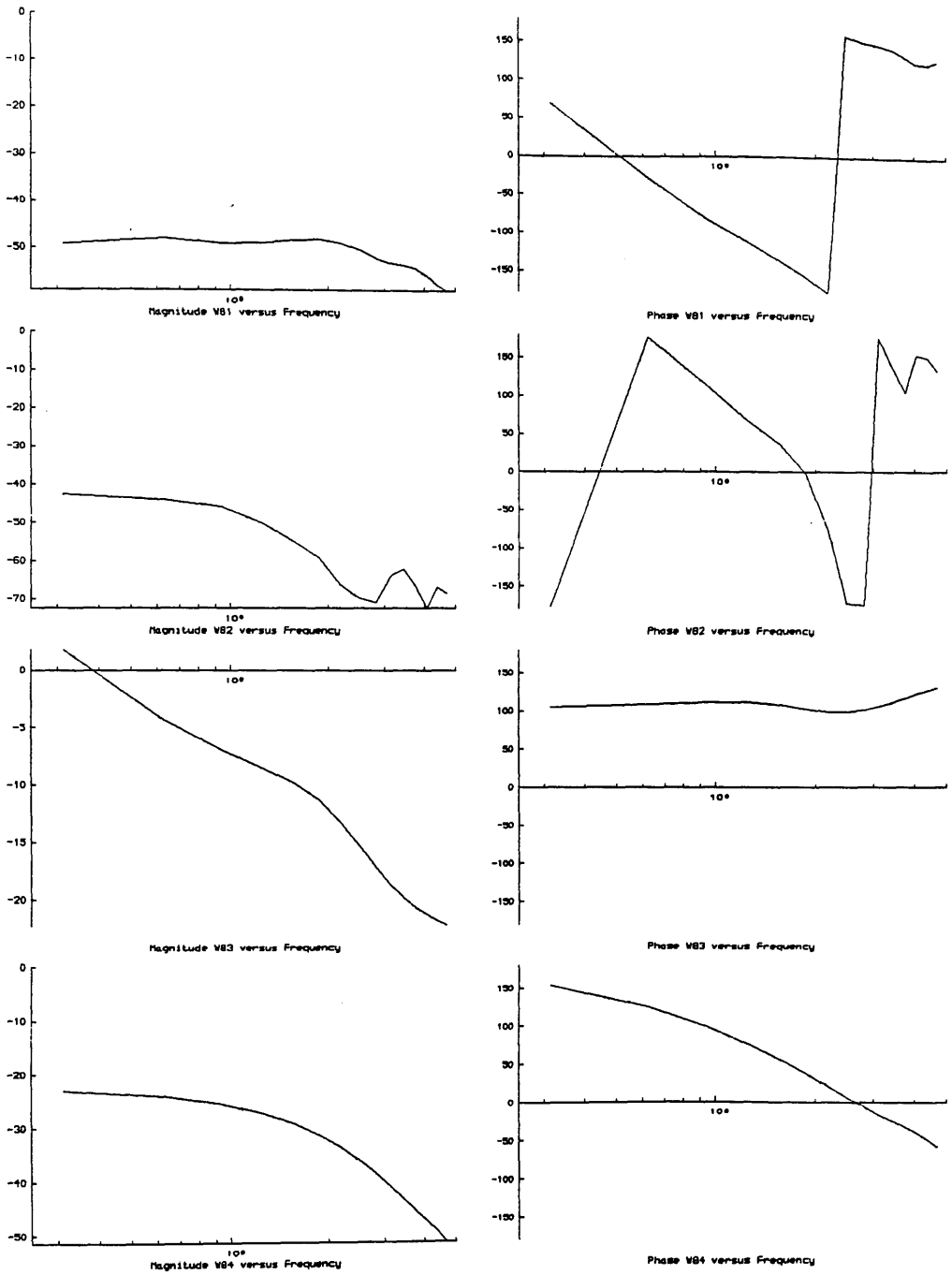
Figure 2.29: Flight Path Controlled − Nonlinear System, Yaw Rate Frequency Responses

forward velocity, u, is responsive to both longitudinal and roll inceptor inputs as shown by positive magnitudes in Figure 2.22. This confirms the results of the time history analysis. Figure 2.23 shows that the vertical velocity, w, is affected by the vertical inceptor and the roll inceptor. The most important inceptor in terms of the pitch rate, q, (Figure 2.24) and the pitch angle, θ, (Figure 2.25) is the roll inceptor. The importance of the roll inceptor to these states is a result of the fact that the input gain on the roll inceptor was increased in relation to the other gains of the pilot input gain matrix, [G], in an attempt to yield a system with reasonable authority over roll. The frequency responses of the lateral states (Figures 2.26 to 2.29) all demonstrate large roll inceptor authority. Not surprisingly, Figures 2.27 and 2.29 showing the roll rate response and the yaw rate response to roll inceptor, respectively, have smaller magnitudes than other channels linking a command inceptor with the output state it is attempting to control. This underlines the problems with the roll command channel authority and confirms the need for more work on the command augmentation issues involved in implementing a modal controller. Figure 2.26 illustrating the lateral velocity responses indicates a good response to the pedal inceptors as designed. The response is relatively flat in comparison with the forward velocity response to the longitudinal inceptor and the vertical velocity response to the vertical inceptor. Figures 2.27 and 2.28 show that the roll response to the roll inceptor is poor with a cutoff frequency of less than 0.5 Hz. The yaw rate response of Figure 2.29 exhibits very low levels of coupling from the vertical, longitudinal and pedal inceptors, but once again the bandwidth of the response is less than 0.5 Hz.

CHAPTER 3: SENSITIVITY FUNCTIONS

Sensitivity functions provide the quantitative information necessary for systematic tuning of helicopter flight control systems. Sensitivities measure the rate of change of system output responses in the time and frequency domains with changes in system parameters. For the purposes of tuning flight controllers, only the sensitivity functions of the output responses with respect to the flight control system parameters are needed.

The methods used to calculate sensitivity functions are discussed in this chapter, while Chapters 4,5 and 6 describe the use of sensitivity functions. Section 3.1 reviews the standard methods of generating sensitivity functions. The signal convolution method is described in detail in section 3.2. Both the time and frequency domain implementations of the signal convolution method are explained. Theory governing the use of transfer function sensitivities in the selection of which control system parameters are to be adjusted is outlined in section 3.3, while section 3.4 discusses eigenstructure sensitivities.

3.1) Methods of Generating Sensitivity Functions

Of the traditional approaches to generating the sensitivity functions of state variables with respect to controller parameters, there are drawbacks to both a sensitivity cosystem approach [39] and parameter perturbation techniques. To use a sensitivity cosystem, one must have accurate knowledge of both the structure and parameters of the plant, but such knowledge is not available for helicopters. As previously stated, one of the reasons why tuning is of such importance in the development of helicopter flight control systems is that the controllers must cope with unmodelled high order dynamics, such as those of the rotor. An accurate model of rotor dynamics is not available and hence precludes the use of the sensitivity cosystem approach. In parameter perturbation methods, on the other hand, the sensitivity functions are approximated through calculations of differences between system responses before and after a small change in a control system parameter. Although a detailed plant model is not necessary in this case, the calculations can be critically affected by the amplitude of the perturbations, and for a system with many parameters, the generation of all of the sensitivity functions can require a large number of tests on the system. In helicopter

applications, it is beneficial to minimize the amount of inflight testing which must be performed, which argues against the use of parameter perturbation techniques. In addition, signals measured during flight tests on helicopters are significantly corrupted by noise, which could lead to instabilities in the calculation of sensitivity functions using parameter perturbation techniques.

3.2) The Signal Convolution Method

An alternative approach which generates the sensitivity functions has been developed for the special case of controller parameters in closed− loop systems [40],[41],[42],[43],[44]. Research involving the signal convolution (direct assessment) method with single− input single− output system applications has already been reported [40],[41],[43] but multivariable applications have remained largely unexplored. The sensitivity functions are generated in a three part process. First, the closed loop impulse response function matrix, [w(t)], is identified; second, the sensitivity signals, $z_{\alpha i}(t)$, are generated; and third, a matrix convolution is performed.

Because the signal convolution method does not rely on knowledge of the plant and since it does not require a large number of tests on the system, this technique for generating state variable sensitivity functions is ideally suited for use in the proposed adjustment algorithm for helicopter flight controllers. In addition, the effects of measurement noise are diminished by the presence of a convolution integral in the procedure. Signal convolution techniques can be used to generate sensitivities in the time domain (Section 3.2.1) and the frequency domain (Section 3.2.2).

The theory governing the signal convolution method is described in the next few sections of this chapter. Although the theory is developed with respect to the Flight Path Controller described in Chapter 2, the signal convolution method can be applied to other controllers designed with other control strategies. The signal convolution method of generating sensitivity functions is in no way linked to the control strategy, however, it will be seen that the structure of the flight controller will affect the implementation of the signal convolution theory.

3.2.1) State Variable Sensitivity Functions

State variable sensitivity functions give the rate of change of the state responses to parameter variations. The signal convolution method is being used to calculate the state variable sensitivity functions with respect to parameters in the control matrices. The signals to be convolved in this direct assessment method of parameter sensitivity analysis are obtained directly from the system and hence it is possible to use sensitivity information to optimize controller parameters in the presence of unmodelled dynamics. This section describes the theory of the signal convolution method as applied to a linear helicopter simulation model and presents the results which have been obtained in simulation studies.

Since the theory behind the signal convolution method is best explained with reference to a particular controller, the following shows how state variable sensitivity functions are calculated with respect to the Flight Path Controller of Section 2.3.4, Figure 2.13. The equations governing sensitivity functions for the Parry Modal Controller (Section 2.3.3) are given in Appendix 2.

Recall Equation 2.36 which governs the the flight path control system,

$$\underline{X}(s) = \left\{ s[I] - [A] + [B][K] + [B][P][\xi] \right\}^{-1} [B]\frac{1}{s}[P][\eta][G] \ \underline{R}(s)$$

<div align="right">Equation 3.1</div>

The closed loop transfer function matrix is,

$$[W(s)] = \left\{ s[I] - [A] + [B][K] + [B][P][\xi] \right\}^{-1} [B]\frac{1}{s}[P][\eta][G]$$

<div align="right">Equation 3.2</div>

Equation 2.35 will also be useful in this section and is given here as Equation 3.3

$$\underline{Y}(s) = s \ \underline{X}(s)$$ <div align="right">Equation 3.3</div>

The equations which describe the sensitivity functions are found by successive implicit differentiations of Equation 3.1. In order to perform these differentiations easily, it is beneficial to rearrange Equation 3.1 into the form given by Equation 3.4.

$$\left\{ s[I] - [A] + [B][K] + [B][P][\xi] \right\} \underline{X}(s) = [B]\frac{1}{s}[P][\eta][G]\underline{R}(s)$$

<div align="right">Equation 3.4</div>

3.2.1.1) First Order State Variable Sensitivities

3.2.1.1.1) First Order Sensitivity Function Theory

The first order sensitivity functions of the state variables with respect to the flight control system parameter, α_i, can be found by implicitly differentiating Equation 3.4. The result is Equation 3.5.

$$\left\{ [B]\frac{\partial[K]}{\partial\alpha_i} + [B]\frac{\partial[P]}{\partial\alpha_i}[\xi] + [B][P]\frac{\partial[\xi]}{\partial\alpha_i} \right\} \underline{X}(s) +$$

$$\left\{ s[I] - [A] + [B][K] + [B][P][\xi] \right\} \frac{\partial\underline{X}(s)}{\partial\alpha_i}$$

$$= [B]\frac{1}{s}\frac{\partial[P]}{\partial\alpha_i}[\eta][G]\underline{R}(s) + [B]\frac{1}{s}[P]\frac{\partial[\eta]}{\partial\alpha_i}[G]\underline{R}(s) + [B]\frac{1}{s}[P][\eta]\frac{\partial[G]}{\partial\alpha_i}\underline{R}(s)$$

<div align="right">Equation 3.5</div>

Since the feedback distribution matrix, $[\xi]$, is defined to allow a comparison of the system response with the pilot's commands, it will not be involved in the tuning process and therefore it is not necessary to calculate sensitivities with respect to parameters in this matrix. Similarly, it will not be necessary to calculate sensitivities with respect to parameters in the axes conversion matrix, $[\eta]$, and the pilot input gain matrix, $[G]$, because they do not affect the dynamics of the flight control system. Therefore, set the partial derivatives of these matrices with respect to the control system parameter, α_i, to be zero.

$$\frac{\partial[\xi]}{\partial\alpha_i} = 0 \qquad\qquad\qquad \text{Equation 3.6}$$

$$\frac{\partial[\eta]}{\partial\alpha_i} = 0 \qquad\qquad\qquad \text{Equation 3.7}$$

$$\frac{\partial[G]}{\partial\alpha_i} = 0 \qquad\qquad\qquad \text{Equation 3.8}$$

It is now possible to simplify Equation 3.5 to Equation 3.9.

$$\left\{ [B]\frac{\partial[K]}{\partial\alpha_i} + [B]\frac{\partial[P]}{\partial\alpha_i}[\xi] \right\} \underline{X}(s) +$$

$$\left\{ s[I] - [A] + [B][K] + [B][P][\xi] \right\} \frac{\partial\underline{X}(s)}{\partial\alpha_i}$$

$$= [B]\frac{1}{s}\frac{\partial[P]}{\partial\alpha_i}[\eta][G]\underline{R}(s) \qquad \text{Equation 3.9}$$

Rearranging to solve for the first order sensitivity functions gives,

$$\frac{\partial\underline{X}(s)}{\partial\alpha_i} = \left\{ s[I]-[A]+[B][K]+[B][P][\xi] \right\}^{-1} [B] \times$$

$$\left\{ -\frac{\partial[K]}{\partial\alpha_i}\underline{X}(s) - \frac{\partial[P]}{\partial\alpha_i}[\xi]\underline{X}(s) + \frac{1}{s}\frac{\partial[P]}{\partial\alpha_i}[\eta][G]\underline{R}(s) \right\}$$

$$\text{Equation 3.10}$$

Since the precompensator matrix, the axes transformation matrix, and the pilot input gain matrix are invertible, Equation 3.10 can be simplified using Equation 3.2.

$$\frac{\partial\underline{X}(s)}{\partial\alpha_i} = [W(s)][G]^{-1}[\eta]^{-1}[P]^{-1} \times$$

$$\left\{ -s\frac{\partial[K]}{\partial\alpha_i}\underline{X}(s) - s\frac{\partial[P]}{\partial\alpha_i}[\xi]\underline{X}(s) + \frac{\partial[P]}{\partial\alpha_i}[\eta][G]\underline{R}(s) \right\}$$

$$\text{Equation 3.11}$$

At this point, it is convenient to consider the sensitivity function equation as the product of the closed loop transfer function matrix, [W(s)], and a sensitivity signal vector, $\underline{Z}^1_{\alpha i}(s)$.

$$\frac{\partial\underline{X}(s)}{\partial\alpha_i} = [W(s)] \underline{Z}^1_{\alpha_i}(s) \qquad \text{Equation 3.12}$$

Where,

$$\underline{Z}^1_{\alpha_i}(s) = [G]^{-1}[\eta]^{-1}[P]^{-1} \times$$

$$\left\{ -s\frac{\partial[K]}{\partial\alpha_i}\underline{X}(s) - s\frac{\partial[P]}{\partial\alpha_i}[\xi]\underline{X}(s) + \frac{\partial[P]}{\partial\alpha_i}[\eta][G]\underline{R}(s) \right\}$$

$$\text{Equation 3.13}$$

The appearance of the Laplace transform variable, s, in the equation for the sensitivity signal, $\underline{Z}^1_{\alpha i}(s)$, implies that during the processing of measured data (namely $\underline{X}(s)$) it will be necessary to find the time derivative of the helicopter's output states. As these states will be corrupted by noise when measured experimentally, numerical errors will be introduced in the calculation of the sensitivity functions. However, realizing that the expression for the sensitivity signal vector is linear, and recalling equation 3.3, it is possible to use Equation 3.14 to find the sensitivity signal vector without the need for differentiation of measured signals.

$$\underline{Z}^1_{\alpha_i}(s) = [G]^{-1}[\eta]^{-1}[P]^{-1} \times$$

$$\left\{ -\frac{\partial[K]}{\partial\alpha_i} \underline{Y}(s) - \frac{\partial[P]}{\partial\alpha_i}[\xi] \underline{Y}(s) + \frac{\partial[P]}{\partial\alpha_i}[\eta][G] \underline{R}(s) \right\}$$

<div align="right">Equation 3.14</div>

Implicit in this step is the belief that it is possible to measure the rates of change of the helicopter states, $\underline{Y}(s)$. The above shows that the sensitivity signals are generated by applying signals taken directly from the system ($\underline{Y}(s)$ and $\underline{R}(s)$ in this example) to a filter which has a form depending only upon the controller. The structure of the sensitivity filter is dependent on the structure of the system under investigation. The most important aspect of the sensitivity filters, $[F_{\alpha i}(s)]$, is that they are independent of the system plant matrices, $[A]$ and $[B]$. Since the control matrices will be known quantities, if one is able to estimate the closed loop transfer function matrix, $[W(s)]$, then the sensitivity functions can be generated without precise knowledge of the system plant. This result will hold for any linear system independent of the plant structure, however, dynamic elements in the control system can complicate the form of the sensitivity filters.

The theory, so far, has been developed in terms of the Laplace transform variable, s. Sensitivity functions are most often generated and used in the time domain. Assuming that the closed loop impulse response function matrix, $[w(t)]$, has been identified, the sensitivity signal is found by exciting the system with a desired input and recording $\underline{z}^1_{\alpha i}(t)$ which is the output from the sensitivity filter. The time domain equivalent of Equation 3.12 is then given by,

$$\frac{\partial\underline{x}(t)}{\partial\alpha_i} = \int_0^t [w(\tau)] \, \underline{z}^1_{\alpha_i}(t-\tau) \, d\tau \qquad\qquad \text{Equation 3.15}$$

Thus, the sensitivity functions in the time domain are found by convolving signals which are directly obtained from the system. In practice, it can be easier to generate the sensitivity signals in software rather than in hardware. In the simulation trials which have been performed, observable system signals have been recorded and subsequently fed through software representations of the sensitivity filters, thereby generating the sensitivity signals, $\underline{z}^1{}_{\alpha i}(t)$.

The convolution of the data sequences representing the time histories can be carried out efficiently using Fast Fourier Transform (FFT) techniques [45]. The time sequences representing $[w(t)]$ and $\underline{z}^1{}_{\alpha i}(t)$ are padded with zeros, transformed into the frequency domain, and multiplied together. The inverse transform of this product yields the convolution of the two signals. The padding of the data sequences with zeros is necessary because of the periodic nature of the FFT operation.

Implicit in the use of the FFT convolution technique is the premise that the signals to be convolved are generated by a stable system. The signal convolution method makes use of the FFT to calculate the product of a matrix, $[W(s)]$, and a vector, $\underline{Z}^1{}_{\alpha i}(s)$, in the Laplace transform domain. In order for the inverse Laplace transform to be equivalent to an Inverse Fast Fourier Transform (IFFT), the contour integral used to calculate the inverse Laplace transform must enclose the right half plane with a boundary along the imaginary axis in the Laplace transform space. However, this contour integral is completely integrable if, and only if, it is to the right of any system poles — the contour cannot encircle singularities. Therefore, from a theoretical standpoint, all of the closed loop system poles must be in the left half plane which forces the system to be stable. However, it was found during tests that a slightly divergent spiral mode with an eigenvalue of 0.001 did not seriously affect the calculations of the sensitivity functions.

3.2.1.1.2) First Order Sensitivity Function Computer Simulation Results

The signal convolution method of calculating first order state variable sensitivity functions has been successfully implemented in the Sensitivity Adjustment Module (SAM) software package [46] for the two control structures presented in Sections 2.2.3, and 2.2.4. For a given system, the state variable sensitivities are a function of: the pilot input, the control system parameter of interest, and time. The amount of information contained in the sensitivity functions will depend on the pilot input used. The time dependency of the state

sensitivities shows up quite clearly in the results: most graphs show both transient and steady state components in the sensitivity functions. Consequently, it is difficult to analyze the results of the simulation study into the state sensitivities. Both of the flight control systems being studied have 32 gains in the feedback matrix and 16 gains in the precompensator matrix. These 48 controller parameters will affect each of the fuselage states which were modelled. An example of a set of first order sensitivities with respect to the parameter, P_{31}, of the precompensator matrix, [P], is given in Figure 3.1 for the Flight Path Controller of Section 2.2.4 controlling a linear HELISTAB plant. The input for this set of results was a pulse on the vertical inceptor.

The parameter, P_{31}, feeds vertical acceleration demands through to the lateral cyclic actuator and will be significant in terms of coupling in the system. Indeed, Figure 3.1 shows that the lateral velocity, v, and roll angle, φ, sensitivities to the parameter have larger amplitudes than the sensitivities of any of the longitudinal states for the pulse on vertical inceptor. In order to become acquainted with how the sensitivity functions are to be used, assume that P_{31} is to be increased from -3.0×10^{-3} to -2.0×10^{-3}. The effects of this change on the state responses can be deduced from the sensitivity functions. For the forward velocity, u, the negative transient (see Figure 2.14) will be decreased in amplitude and a steady state offset of approximately 0.1 will be added onto the state response. The vertical velocity, w, will show a greater degree of overshoot with the increase in P_{31}. The change in P_{31} will tend to accentuate the transients on the pitch rate, q, and the pitch angle, θ, possibly leading to divergent tendencies on these states. In a manner similar to the forward velocity state, u, the lateral velocity, v, and roll rate, p, will develop a more pronouced steady state offset for changes in P_{31}. The divergence of the sensitivities of roll angle, φ, and yaw rate, r, to P_{31} indicate that this parameter could be significant in controlling the stability of the spiral mode. For a smaller order system with a small set of adjustable controller parameters, this sort of qualitative analysis is probably of greater benefit than for the systems being considered in the present work.

A simulation study of the sensitivity functions of the Parry Modal Controller – HELISTAB system [18] is documented in Reference [47]. The results from this simulation study, using the signal convolution method, were checked with those generated using parameter perturbation techniques. The study [47] revealed that the signal convolution method, because of the smoothing nature of the convolution involved, was less sensitive to noise in the time sequences than was the parameter perturbation technique. Because the simulation model of the Parry
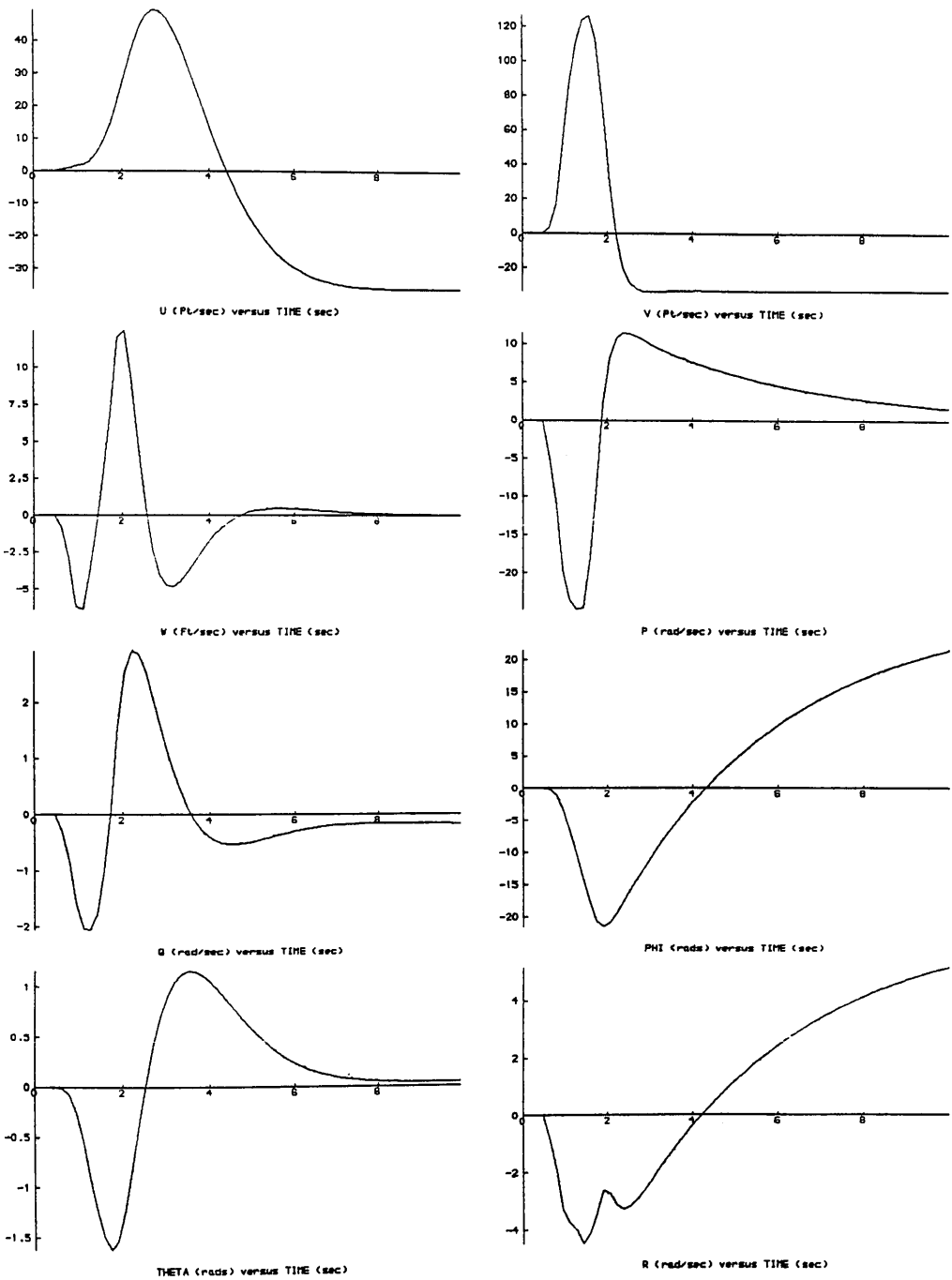
Figure 3.1: First Order State Variable Sensitivities to Flight Path Controller Parameter P_{31}, Linear Plant, Vertical Inceptor Pulse Input.

Modal Controlled helicopter system is linear, it is possible to narrow the choice of test inputs to a relatively small number. The principle of superposition holds for linear systems and this allows the formation of sensitivities to complicated pilot inputs from sensitivities generated by the excitation of individual pilot inceptors. The linearity of the model also means that step excitations do not yield sensitivity functions with additional information over those generated using pulse inputs. However, it must be stressed that for a helicopter, nonlinearities will always be present. This, in turn, will mean that superposition of state sensitivities will not hold and neither will the premise that the step and pulse input sensitivities contain equivalent information. On a helicopter, the state sensitivities will be truly input dependent. Even with the limited number of pilot inputs used in the simulation tests, the amount of information provided by the sensitivity functions to a small set of control system parameters was overwhelming. It was difficult to interpret the data in a concise manner and therefore the analysis was limited to the identification of general trends.

The superficial analysis of the state sensitivities of the Parry Modal Controller has shown that some parameters will affect the amplitudes of the state responses, while others will affect the response structure. If the shape of the sensitivity function of a particular parameter matches the shape of the state response, then that parameter will only affect the amplitude of the response. If the shapes of the state responses and the sensitivity functions are different, the structure of the state response will be affected by changing the parameter of interest.

Some states oscillate in response to certain inputs. If the corresponding parameter sensitivities of these states also oscillate, then adjusting the parameter will either increase or decrease the severity of the oscillations depending on the frequency content of the two signals.

Figure 3.2 shows the state variable sensitivities of the Flight Path Controller with respect to the precompensator gain, P_{31}, for a nonlinear HELISIM3 plant. At a first glance, the sensitivities of Figure 3.2 bear little resemblance to their linear counterparts in Figure 3.1. However, closer examination reveals that the nonlinear sensitivities are essentially correct for the first 2 seconds. After 2 seconds, the nonlinear sensitivities diverge rapidly. This divergence is caused by the system no longer operating near the design point of 80.0 knots and hence the plant's [A] and [B] matrices will have changed. The pilot input used to generate these sensitivity functions was a 1.0 second full amplitude pulse on the vertical inceptor, which changes the vehicle's forward velocity by 10 feet per second. Since this change in forward velocity is accomplished in 2 seconds (Figure 2.14),

Figure 3.2: First Order State Variable Sensitivities to Flight Path Controller Parameter P_{31}, Nonlinear Plant, Vertical Inceptor Pulse Input.

it is unreasonable to expect the response to behave in a linear fashion for the whole 10 seconds. The sensitivity functions will only be valid for nonlinear systems if the excitation input is chosen so that the system does not move away from a linear region about the trimmed operating point. In practice, it was found that doublet inputs were useful since they tended to bring the system back to its initial condition during the collection of data, thereby avoiding large excursions from the test's initial flight condition.

3.2.1.2) Second Order State Variable Sensitivities

3.2.1.2.1) Second Order Sensitivity Function Theory

The second order sensitivity functions are calculated using the same techniques as those used to calculate the first order sensitivity functions. Once again, it is assumed that the feedback distribution matrix, $[\xi]$, the pilot input gain matrix, $[G]$, and the axes conversion matrix, $[\eta]$, do not contain parameters of interest. The second order sensitivities are found from implicitly differentiating Equation 3.9 with respect to a second control system parameter, α_j.

$$\left\{ [B]\frac{\partial^2[K]}{\partial\alpha_j\partial\alpha_i} + [B]\frac{\partial^2[P]}{\partial\alpha_j\partial\alpha_i}[\xi] \right\} \underline{X}(s) +$$

$$\left\{ [B]\frac{\partial[K]}{\partial\alpha_i} + [B]\frac{\partial[P]}{\partial\alpha_i}[\xi] \right\} \frac{\partial\underline{X}(s)}{\partial\alpha_j} +$$

$$\left\{ [B]\frac{\partial[K]}{\partial\alpha_j} + [B]\frac{\partial[P]}{\partial\alpha_j}[\xi] \right\} \frac{\partial\underline{X}(s)}{\partial\alpha_i} +$$

$$\left\{ s[I] - [A] + [B][K] + [B][P][\xi] \right\} \frac{\partial^2\underline{X}(s)}{\partial\alpha_j\partial\alpha_i}$$

$$= [B]\frac{1}{s}\frac{\partial^2[P]}{\partial\alpha_j\partial\alpha_i}[\eta][G]\underline{R}(s)$$

<div align="right">Equation 3.16</div>

Since all of the control matrices are first order in the control system parameters, several simplifications in Equation 3.16 can be made. All terms containing second order partial derivatives of the control system matrices will be zero, as shown by Equations 3.17 and 3.18.

$$\frac{\partial^2 [K]}{\partial \alpha_j \partial \alpha_i} = 0 \qquad\qquad\qquad \text{Equation 3.17}$$

$$\frac{\partial^2 [P]}{\partial \alpha_j \partial \alpha_i} = 0 \qquad\qquad\qquad \text{Equation 3.18}$$

Therefore,

$$\left\{ [B]\frac{\partial [K]}{\partial \alpha_i} + [B]\frac{\partial [P]}{\partial \alpha_i}[\xi] \right\} \frac{\partial \underline{X}(s)}{\partial \alpha_j} +$$

$$\left\{ [B]\frac{\partial [K]}{\partial \alpha_j} + [B]\frac{\partial [P]}{\partial \alpha_j}[\xi] \right\} \frac{\partial \underline{X}(s)}{\partial \alpha_i} +$$

$$\left\{ s[I] - [A] + [B][K] + [B][P][\xi] \right\} \frac{\partial^2 \underline{X}(s)}{\partial \alpha_j \partial \alpha_i} = 0$$

$$\text{Equation 3.19}$$

Rearranging and simplifying with the aid of Equation 3.2, the second order sensitivity functions of the state variables of the flight path controller are,

$$\frac{\partial^2 \underline{X}(s)}{\partial \alpha_j \partial \alpha_i} = - [W(s)][G]^{-1}[\eta]^{-1}[P]^{-1}s \times$$

$$\left\{ \left[\frac{\partial [K]}{\partial \alpha_i} + \frac{\partial [P]}{\partial \alpha_i}[\xi] \right] \frac{\partial \underline{\dot{X}}(s)}{\partial \alpha_j} + \left[\frac{\partial [K]}{\partial \alpha_j} + \frac{\partial [P]}{\partial \alpha_j}[\xi] \right] \frac{\partial \underline{X}(s)}{\partial \alpha_i} \right\}$$

$$\text{Equation 3.20}$$

The appearance of the Laplace transform variable, s, in Equation 3.20 in the term corresponding to the sensitivity filter does not create a problem to the same extent as was the case for the first order sensitivities. This is because the sensitivity filters are excited by the first order sensitivity functions which will be relatively smooth due to the use of signal convolution techniques for their generation. The convolution integral which forms part of the signal convolution technique will help to reject noise from the sensitivity functions.

As a special case, if α_j is the same parameter as α_i then Equation 3.20 simplifies to,

$$\frac{\partial^2 \underline{X}(s)}{\partial \alpha_i^2} = - 2 [W(s)][G]^{-1}[\eta]^{-1}[P]^{-1}s \left\{ \frac{\partial [K]}{\partial \alpha_i} + \frac{\partial [P]}{\partial \alpha_i}[\xi] \right\} \frac{\partial \underline{\dot{X}}(s)}{\partial \alpha_i}$$

$$\text{Equation 3.21}$$

The second order sensitivity functions of Equations 3.20 and 3.21 are calculated in the same manner as the first order sensitivity functions. That is, a convolution integral is calculated as shown in Equation 3.22.

$$\frac{\partial^2 \underline{x}(t)}{\partial \alpha_j \partial \alpha_i} = \int_0^t [w(\tau)] \ \underline{z}^2_{\alpha_i \alpha_j}(t-\tau) \ d\tau \qquad \text{Equation 3.22}$$

Where, the Laplace transform of the second order sensitivity signal is given by,

$$\underline{z}^2_{\alpha_j \alpha_i}(s) = - [G]^{-1}[\eta]^{-1}[P]^{-1}s \times$$

$$\left\{ \left[\frac{\partial[K]}{\partial \alpha_i} + \frac{\partial[P]}{\partial \alpha_i}[\xi] \right] \frac{\partial \underline{X}(s)}{\partial \alpha_j} + \left[\frac{\partial[K]}{\partial \alpha_j} + \frac{\partial[P]}{\partial \alpha_j}[\xi] \right] \frac{\partial \underline{X}(s)}{\partial \alpha_i} \right\}$$

$$\text{Equation 3.23}$$

In practice, the second order sensitivity signals are generated using software since their sensitivity filters are excited by the first order sensitivity functions. Because the first order sensitivities must be calculated in an off—line manner with multivariable systems, it is not possible to generate the second order sensitivities by directly filtering system signals in hardware.

3.2.1.2.1) Second Order Sensitivity Function Computer Simulation Results

The second order sensitivities of the output states of the Flight Path Controlled helicopter to the precompensator parameters, P_{31} and P_{33}, are shown in Figures 3.3, 3.4 and 3.5 for a vertical inceptor pulse. Difficulties arise in visual analysis of the second order sensitivities to a degree that it is virtually impossible to make qualitative predictions concerning the effects on the system response, to second order, for changes in the controller parameters for all but the simplest of the second order sensitivity functions. However, the importance of the second order sensitivities will become apparent in Chapter 5 which discusses the results of tuning a system using model reference techniques. Figure 3.6 shows the nonlinear equivalent of Figure 3.3 and the divergence of the second order sensitivities for the nonlinear system is worse than for the first order senstivities. The use of nonlinear second order sensitivities in the adjustment algorithm must be done with care in order that the results of the tuning are valid. This translates into a statement that test inputs must be of low
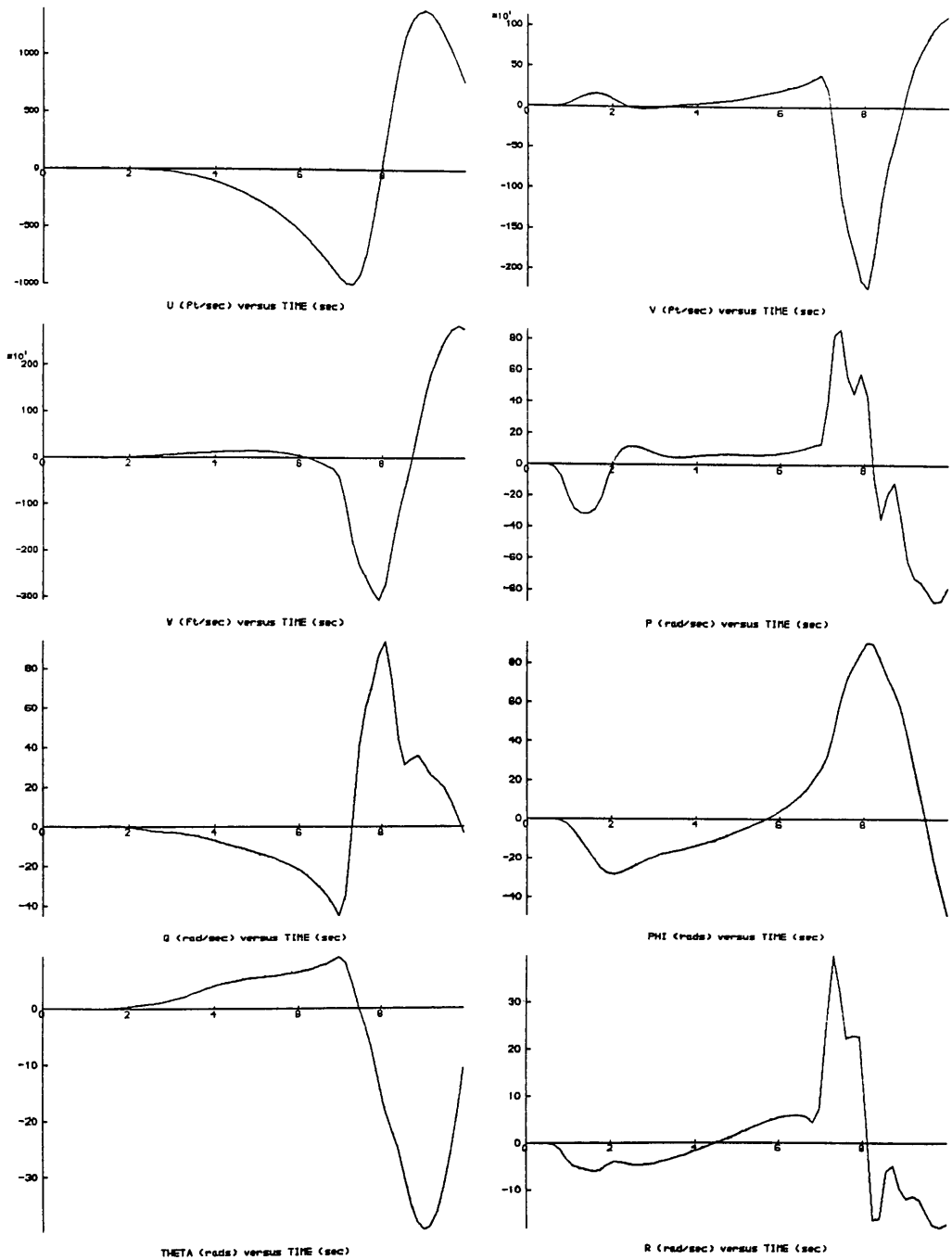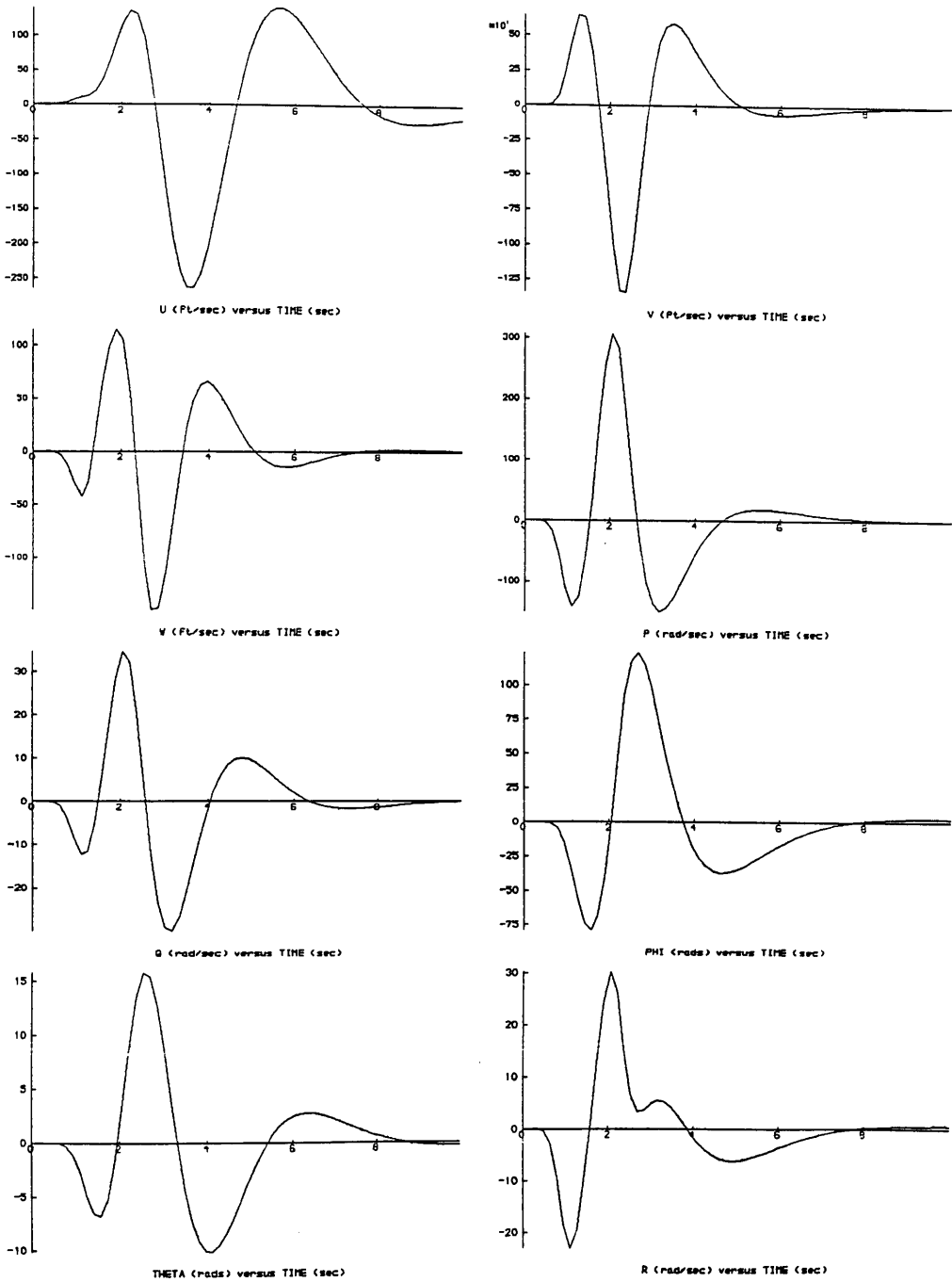
Figure 3.3: Second Order State Variable Sensitivities to Flight Path Controller Parameter P_{31}, Linear Plant, Vertical Inceptor Pulse Input.
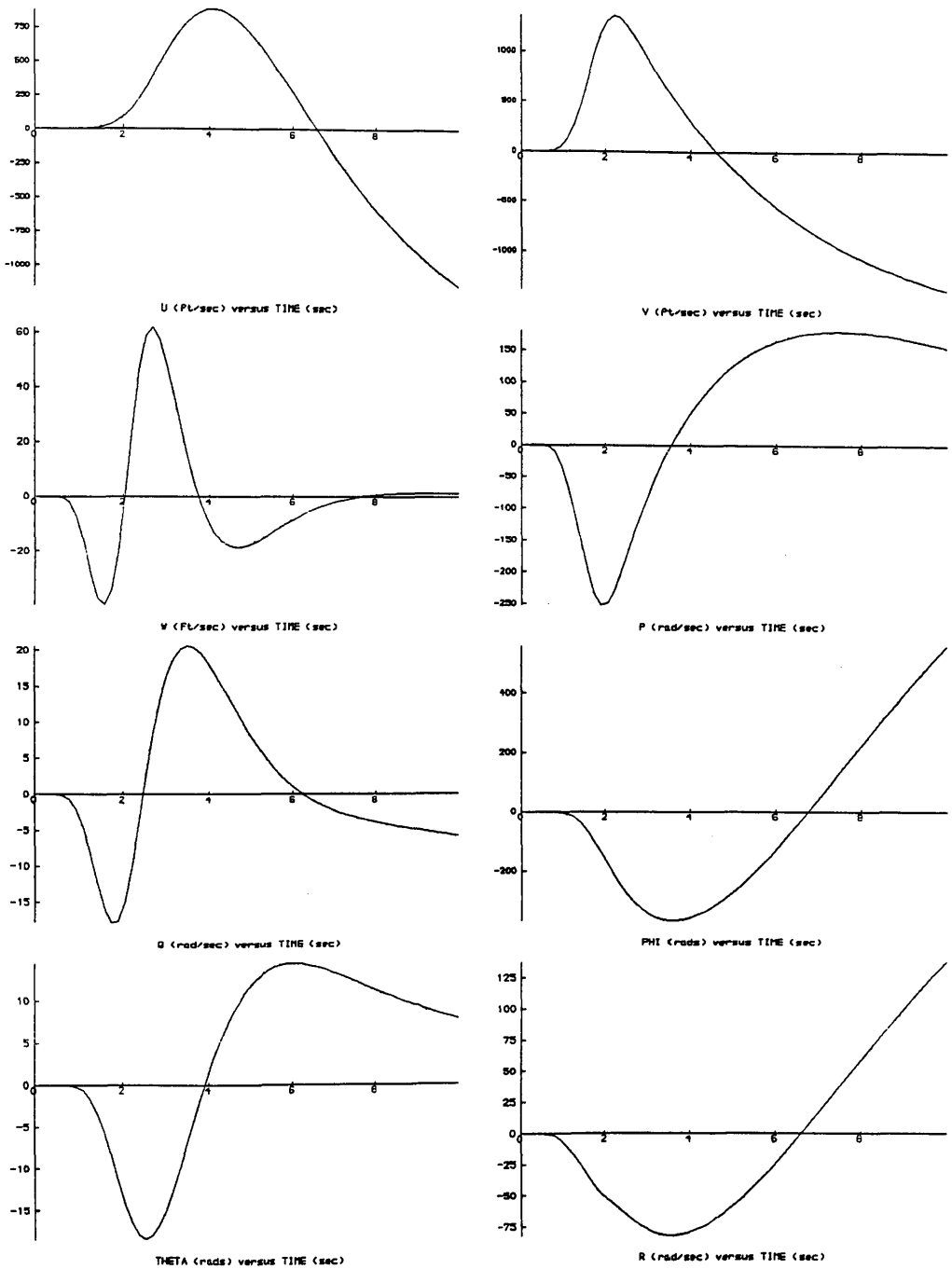
Figure 3.4: Second Order State Variable Sensitivities to Flight Path Controller Parameters P_{31} and P_{33}, Linear Plant, Vertical Inceptor Pulse Input.
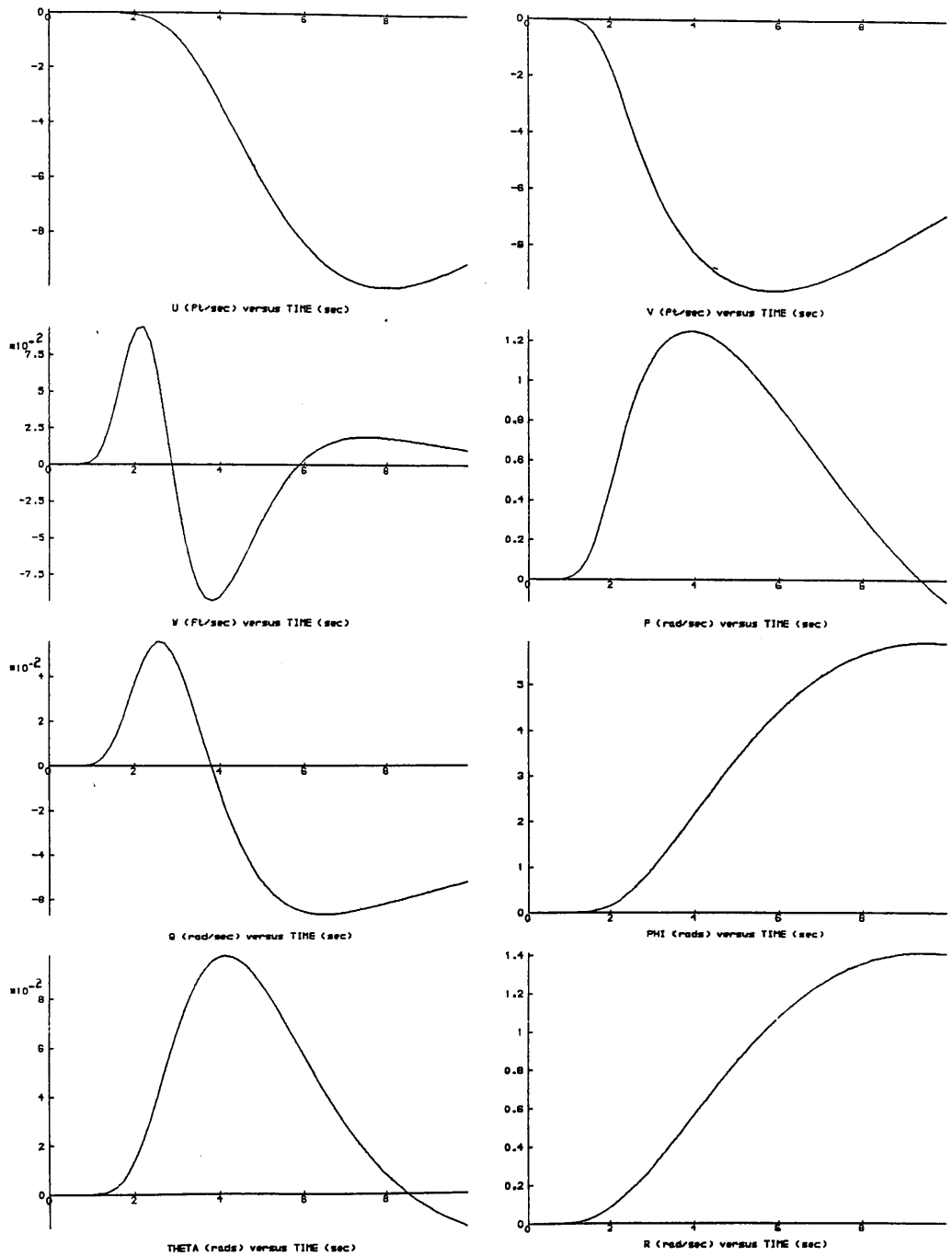
Figure 3.5: Second Order State Variable Sensitivities to Flight Path Controller Parameter P_{33}, Linear Plant, Vertical Inceptor Pulse Input.
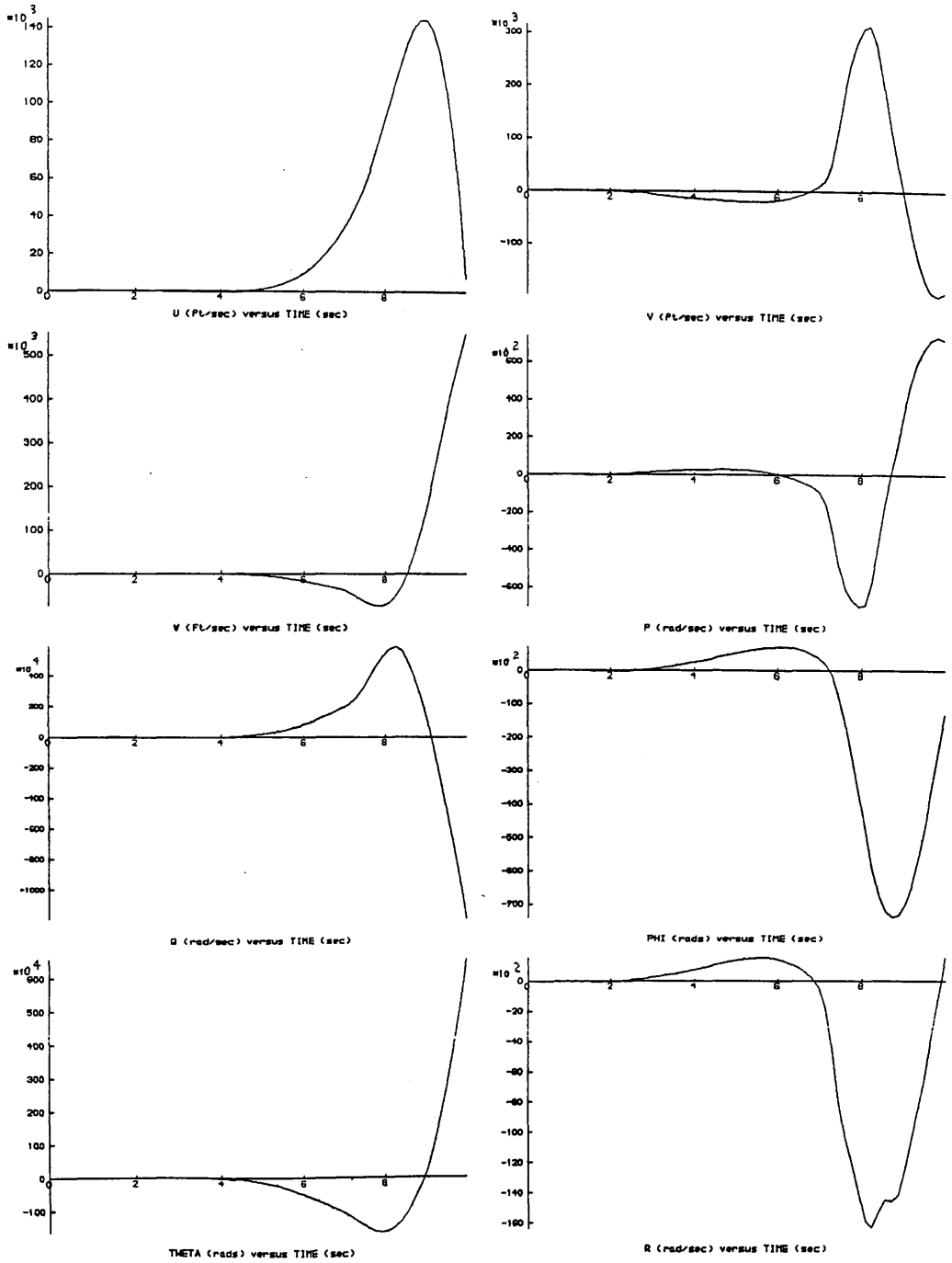
Figure 3.6: Second Order State Variable Sensitivities to Flight Path Controller Parameter P_{31}, Nonlinear Plant, Vertical Inceptor Pulse Input.

amplitude, such as 10% of the inceptor authority, so that system nonlinearities are avoided.

3.2.1.3) Identification of the Closed Loop Transfer Function Matrix

Because of the possibility of each input coupling into each output state in an unknown multivariable plant, [W(s)] cannot be identified simultaneously with the sensitivity signals. This may be seen by re—expressing the state variable responses, $x_i(t)$, in terms of individual elements of the transfer function matrix, $W_{ij}(s)$, and the input signal vector, $R_j(s)$.

$$X_i(s) = \sum_{j=1}^{4} W_{ij}(s) R_j(s) \qquad \text{Equation 3.24}$$

Rearranging Equation 3.24 to isolate the transfer function of interest gives,

$$W_{ij}(s) = \frac{X_i(s) - \sum_{h \ne j} W_{ih}(s) R_h(s)}{R_j(s)} \qquad \text{Equation 3.25}$$

Clearly, if we wish to identify $W_{ij}(s)$ solely from the input and output vectors, only one element of the input vector should be excited at a time. This will reduce Equation 3.25 to,

$$W_{ij}(s) = \frac{X_i(s)}{R_j(s)} \left\{ \text{all } R_h(s) = 0 \text{ for } h \ne j \right\} \quad \text{Equation 3.26}$$

Since all of the elements of [W(s)] are needed, the signal convolution method cannot be applied in real—time with multivariable systems.

In practice, [W(s)], or more precisely, its time domain equivalent, the impulse response function matrix, [w(t)], is determined by recording samples from time histories for each input. For a system with m inputs and n controller parameters, the generation of sensitivity functions to a particular pilot test input by the signal convolution method requires m+1 time periods. This can be accomplished by using, in parallel, a sensitivity filter for each parameter of interest to generate all of the sensitivity signals simultaneously. In a helicopter with the four conventional pilot inceptors, all of the necessary data can be collected in five time periods.

In contrast, the parameter perturbation technique would require n+1 time periods. For the flight control systems discussed in Chapter 2 with 48 adjustable

parameters, 49 time periods would be required to collect the data. The 49th time period is needed to determine the standard system response to the test input. For most ACT systems, there will be more controller parameters than inputs so the signal convolution method can be far more efficient than perturbation methods. Although less efficient than the sensitivity cosystem technique, the signal convolution method has the advantage that it does not require knowledge of the system plant. Therefore, directly assessing sensitivity functions from sensitivity signals is the method best suited for use in the adjustment of flight controllers.

The drawbacks of the signal convolution method are that the system should be linear and that in a multivariable system, [W(s)] cannot be determined simultaneously with the sensitivity signals for the reasons previously mentioned. Both of these adverse characteristics of the method centre around the identification of [W(s)]. If the system is nonlinear, then the closed loop impulse response function matrix, [W(s)], does not strictly exist. The helicopter system is nonlinear, but in practice, it has been shown that the linearity constraint can be relaxed to allow one to use the method at operating points in the flight envelope which are locally linear. For this reason the choice of test inputs must be made with care.

Three types of test inputs have been studied with regards to the identification of [w(t)]. If a pulse input is used on the jth input of Equation 3.26 then, since $R_j(s) = 1$ for a pulse, we obtain,

$$W_{ij}(s) = \frac{X_i(s)}{R_j(s)} = X_i(s) \qquad \text{Equation 3.27}$$

In the time domain, Equation 3.27 corresponds to,

$$w_{ij}(t) = x_i(t) \qquad \text{Equation 3.28}$$

Although the use of a pulse allows direct measurement of the elements of [w(t)], care must be exercised to ensure that the system is operating in a linear fashion. If the amplitude of the pulse is too large it may excite nonlinear system dynamics. The results of the simulation study have suggested that the sensitivity functions may still be valid if the nonlinearities are of a continuous form, described perhaps by a square law or other polynomial relationship, but exciting hard nonlinearities such as deadbands or rate-limits will lead to erroneous results.

If a step input is used then $R_j(s) = {}^1/_s$ and,

$$W_{ij}(s) = \frac{X_i(s)}{R_j(s)} = s\, X_i(s) \qquad \text{Equation 3.29}$$

Giving,

$$w_{ij}(t) = \frac{d}{dt}\, x_i(t) \qquad \text{Equation 3.30}$$

Thus, if a step is used to identify [w(t)], the output signals must be differentiated — an operation which can introduce noise to the results. In applications, the signals will be recorded as discrete samples. Initially, four of these sample points were used to approximate the derivatives of the time histories of each data sample [43]. This four point algorithm was tested against eight others. The five point method of Hildebrand [48] proved to be far more robust in the face of sharp discontinuities and required only a marginal increase in execution time. For the mth sample of the data sequence, $\underline{x}(n)$, (sampling period T), the derivative of the sequence is given as,

$$\frac{d\underline{x}(m)}{dt} \approx \frac{-8\underline{x}(m-1) + 8\underline{x}(m+1) - \underline{x}(m+2) + \underline{x}(m-2)}{12T}$$

$$\text{Equation 3.31}$$

Pseudo—random binary signal testing techniques [49] are used to identify [w(t)] in many systems. At present, application of these techniques in a helicopter system is not considered viable because test inputs must be injected manually by the pilot which would be very difficult with a practical pseudo—random binary sequence.

3.2.2) Transfer Function Sensitivities

Increasing emphasis is being placed on the use of frequency domain design techniques and the specification of desirable flight handling qualities in the frequency domain. This trend has motivated a study of the transfer function sensitivities with respect to the controller parameters. Signal convolution techniques are being used to generate the transfer function sensitivities.

3.2.2.1) Theory of Transfer Function Sensitivities

The theory needed to generate the transfer function sensitivities using signal convolution techniques is largely analogous to that describing the generation of state variable sensitivities.

Equation 3.32 shows Equation 3.2 rearranged into a form which is easier to differentiate. The reader will note that this is the equation governing the transfer functions of the Flight Path Controller (Section 2.2.4).

$$\left\{ s[I] - [A] + [B][K] + [B][P][\xi] \right\} [W(s)] = [B]\frac{1}{s}[P][\eta][G]$$

Equation 3.32

Implicitly differentiating Equation 3.32 with respect to the controller parameters, α_i, yields Equation 3.33 which describes the transfer function sensitivities.

$$\left\{ [B]\frac{\partial[K]}{\partial\alpha_i} + [B]\frac{\partial[P]}{\partial\alpha_i}[\xi] + [B][P]\frac{\partial[\xi]}{\partial\alpha_i} \right\} [W(s)] +$$

$$\left\{ s[I] - [A] + [B][K] + [B][P][\xi] \right\} \frac{\partial[W(s)]}{\partial\alpha_i} =$$

$$[B]\frac{1}{s}\frac{\partial[P]}{\partial\alpha_i}[\eta][G] + [B]\frac{1}{s}[P]\frac{\partial[\eta]}{\partial\alpha_i}[G] + [B]\frac{1}{s}[P][\eta]\frac{\partial[G]}{\partial\alpha_i}$$

Equation 3.33

If the control parameters of interest are again limited to being in either the feedback matrix, [K], or the precompensator matrix, [P], then Equation 3.33 can be simplified with Equation 3.2 in order to solve for the sensitivities of the transfer functions, $\partial[W(s)]/\partial\alpha_i$.

$$\frac{\partial[W(s)]}{\partial\alpha_i} = [W(s)] [G]^{-1}[\eta]^{-1}[P]^{-1} \times$$

$$\left\{ \left[\frac{\partial[K]}{\partial\alpha_i} + \frac{\partial[P]}{\partial\alpha_i}[\xi] \right] s [W(s)] + [B] \frac{\partial[P]}{\partial\alpha_i} [\eta][G] \right\}$$

Equation 3.34

Once again, it is preferable to work with the acceleration vector, $\underline{Y}(s)$, than with the state vector, $\underline{X}(s)$, in order to eliminate the Laplace transform variable

from Equation 3.34. Therefore, define the transfer function matrix between the pilot inputs, $\underline{R}(s)$, and the acceleration vector, $\underline{Y}(s)$, to be $[W_a(s)]$ where,

$$\underline{Y}(s) = [W_a(s)] \; \underline{R}(s) = s \; [W(s)] \; \underline{R}(s) \qquad \text{Equation 3.35}$$

The acceleration transfer function matrix, $[W_a(s)]$ can be experimentally determined in the same manner as the closed loop transfer function matrix, $[W(s)]$. The techniques for performing this operation were discussed in Section 3.2.1.3. Thus, Equation 3.34 can be rewritten in a form which does not imply differentiation of experimentally determined signals.

$$\frac{\partial [W(s)]}{\partial \alpha_i} = [W(s)] \; [G]^{-1} [\eta]^{-1} [P]^{-1} \quad \times$$

$$\left\{ \left[\; \frac{\partial [K]}{\partial \alpha_i} + \frac{\partial [P]}{\partial \alpha_i}[\xi] \; \right] \; [W_a(s)] + [B] \; \frac{\partial [P]}{\partial \alpha_i} \; [\eta][G] \right\}$$

$$\text{Equation 3.35}$$

In analogy with calculations of the state variable sensitivities, the transfer function sensitivities are then given by the multiplication of the closed loop transfer function matrix and a sensitivity signal matrix.

$$\frac{\partial [W(s)]}{\partial \alpha_i} = [W(s)] \; [Z_{\alpha_i}(s)] \qquad \text{Equation 3.36}$$

The sensitivity signal matrix is given by Equation 3.37.

$$[Z_{\alpha_i}(s)] = [G]^{-1} [\eta]^{-1} [P]^{-1} \quad \times$$

$$\left\{ \left[\; \frac{\partial [K]}{\partial \alpha_i} + \frac{\partial [P]}{\partial \alpha_i}[\xi] \; \right] \; [W_a(s)] + [B] \; \frac{\partial [P]}{\partial \alpha_i} \; [\eta][G] \right\}$$

$$\text{Equation 3.37}$$

When one considers the above equations, it becomes clear that the computation of transfer function sensitivities can be carried out with a minimum of system experimentation. Since the control matrices are known, the only data which must be experimentally determined are the elements of the closed loop transfer function matrix, $[W(s)]$, and of the acceleration transfer function matrix, $[W_a(s)]$. Therefore, not only does the method work without knowledge of the

plant, it can also help to minimize inflight experimentation since the data needed to calculate [W(s)] and [W_a(s)] can be found simultaneously.

The four stage computations which are used in practice, minimize the amount of data which must be recorded from the system, at the expense of computer processing time. As was the case for state variable sensitivities, the first step in the calculation of transfer function sensitivities is the inflight identification of the closed loop impulse response function matrix, [w(t)], and the acceleration impulse response function matrix, [w_a(t)]. The second step is the offline generation of the sensitivity signal matrix in the time domain, [$z_{\alpha i}$(t)]. The third step is a convolution of [w(t)] with [$z_{\alpha i}$(t)] to form the impulse response function sensitivity matrix, ∂[w(t)]/$\partial\alpha_i$, given by,

$$\frac{\partial[w(t)]}{\partial\alpha_i} = \int_0^t [w(\tau)] [z_{\alpha i}(t-\tau)] \, d\tau \qquad \text{Equation 3.38}$$

Finally, the impulse response function sensitivities are transformed into the frequency domain.

As previously mentioned, the convolution of the data sequences representing the time histories can be carried out efficiently using Fast Fourier Transform (FFT) techniques [45]. Realizing that FFT's are used to perform the convolution in Equation 3.38, the question of why the convolution and transform of the third and fourth steps of the calculations are not replaced by a multiplication of the FFT's of [w(t)] and [$z_{\alpha i}$(t)] arises. The answer to this concerns the periodic nature of the FFT — a multiplication of the FFT's of [w(t)] and [$z_{\alpha i}$(t)] would lead to an incorrect result. Attempting to linearize the FFT by adding zeros to the data sequences, as is done to produce linear convolutions, also distorts the frequency domain spectra. Without attempting to develop an algorithm to reconstruct the proper frequency domain product of [W(s)] and [$Z_{\alpha i}$(s)] from a distorted sequence, it was concluded that the most efficient procedure was, indeed, the one which is being used.

3.2.2.2) Transfer Function Sensitivities Computer Simulation Results

The signal convolution method of calculating transfer function sensitivities has been successfully implemented in a simulation study. The calculations of the transfer function sensitivities are performed by the Sensitivity Adjustment Module computer routines [46]. The results from the simulation study using the signal convolution method were compared with those generated using parameter

perturbation techniques. A further check on the results was made by transforming the state variable sensitivity functions: in analogy with the use of pulse inputs for the determination of [w(t)], a pulse can be used to generate state sensitivities which when transformed give a column of $\partial[W(s)]/\partial\alpha_i$.

For the systems being studied, the generation of the transfer function sensitivity matrix with respect to one parameter requires 128 convolutions (the state sensitivities to the same parameter would require 32 convolutions). Four convolutions are needed for each of the 32 transfer function sensitivities. The computational overhead of generating transfer function sensitivities is high and, at the present time, argues against their use.

The frequency responses (transfer functions) of the system can be displayed using magnitude and phase plots. Figures 2.22 to 2.29 contain the magnitude and phase plots for the transfer functions of the Flight Path Control system (Section 2.2.4) between each of the four pilot inceptors and the eight fuselage states. The magnitudes are plotted in decibels, while the phase angles are plotted in degrees. The helicopter system's transfer functions can be loosely categorized as being either low–pass or band–pass in nature. The high frequency cut–off is less than 1 Hz. for the fuselage states being examined.

The transfer function sensitivities show how a change in the value of a controller parameter will affect the system response. The transfer functions are displayed in terms of magnitude and phase and it would be convenient to be able to predict magnitude and phase changes that would result from a parameter change. For this reason, the transfer function sensitivities have been normalized.

Consider Equation 3.39 which is a first order approximation to the modified system transfer function matrix, $[W_m(s)]$, which will result from perturbations of the set of n controller parameters,

$$[W_m(s)] \approx [W(s)] + \sum_{i=1}^{n} \frac{\partial[W(s)]}{\partial\alpha_i} \Delta\alpha_i \qquad \text{Equation 3.39}$$

In the single–input single–output case in which there is only one controller parameter, Equation 3.39 simplifies to,

$$W_m(s) \approx W(s) + \frac{\partial W(s)}{\partial\alpha_i} \Delta\alpha_i \qquad \text{Equation 3.40}$$

which can be rewritten as,

$$W_m(s) \approx W(s) \left[1 + \frac{\Delta\alpha_i}{W(s)} \frac{\partial W(s)}{\partial\alpha_i} \right] \qquad \text{Equation 3.41}$$

The expression in the brackets on the right hand side gives the relative change in the transfer function W(s).

For small $\Delta\alpha_i$, the magnitude and phase changes to W(s) which result from changing α_i are approximately shown by the magnitude and phase plots of,

$$\frac{1}{W(s)} \frac{\partial W(s)}{\partial \alpha_i}$$

If one further normalizes the transfer function sensitivities with respect to the amplitude of the parameter, then it is possible to compare the sensitivities with respect to different parameters. This has been done to allow checks to be made on the relative importance of the controller parameters.

The normalized sensitivities were examined in an effort to determine which parameters significantly affect the system response. The first point to consider was the magnitude of the normalized transfer function sensitivities. The larger the magnitude for a parameter, the larger the effect of changing that parmeter. The phase of the sensitivities is not important for those parameters with small sensitivity magnitudes, since changes to these parameters will have little influence on the system's dynamics. The adjustment algorithm will be restricting the amount by which parameters may be changed. Assume that the changes in the controller parameters are restricted to being less than 10% (-20 dB) of their nominal values. For this amount of parameter shift, they might be considered as being significant if the resulting change in the transfer function magnitude is also 10% (-20 dB). Adopting this criterion, parameters will be significant if their normalized transfer function sensitivities have magnitudes greater than 0 dB.

The transfer function sensitivities to variations in the precompensator matrix parameter P_{31} of the Flight Path Controller with the linear HELISTAB plant are shown in Figures 3.7 through 3.14. Assuming that the only sensitivities which are of interest are those with large magnitudes (greater than 0dB), increasing P_{31} will increase the bandwidth of the following transfer functions:

$W_{14}(s)$ — Forward velocity due to pedal inceptor
$W_{51}(s)$ — Lateral velocity due to vertical inceptor
$W_{52}(s)$ — Lateral velocity due to longitudinal inceptor
$W_{61}(s)$ — Roll rate due to vertical inceptor
$W_{62}(s)$ — Roll rate due to longitudinal inceptor
$W_{64}(s)$ — Roll rate due to pedal inceptor
$W_{71}(s)$ — Roll angle due to vertical inceptor
$W_{72}(s)$ — Roll angle due to longitudinal inceptor
$W_{74}(s)$ — Roll angle due to pedal inceptor
$W_{81}(s)$ — Yaw rate due to vertical inceptor
$W_{82}(s)$ — Yaw rate due to longitudinal inceptor
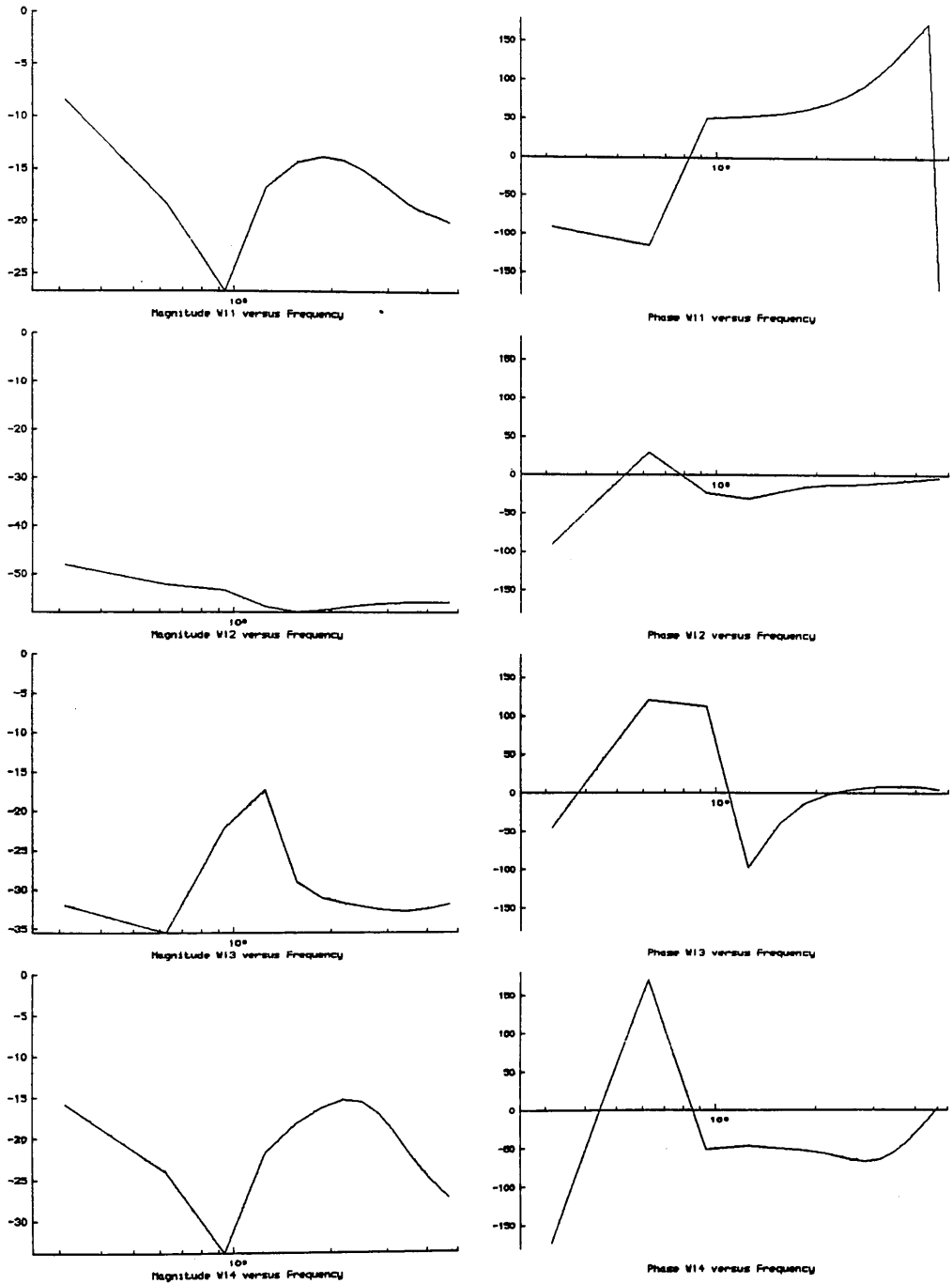
Figure 3.7: Forward Velocity Transfer Function Sensitivities, Flight Path Controller, Magnitude and Phase.
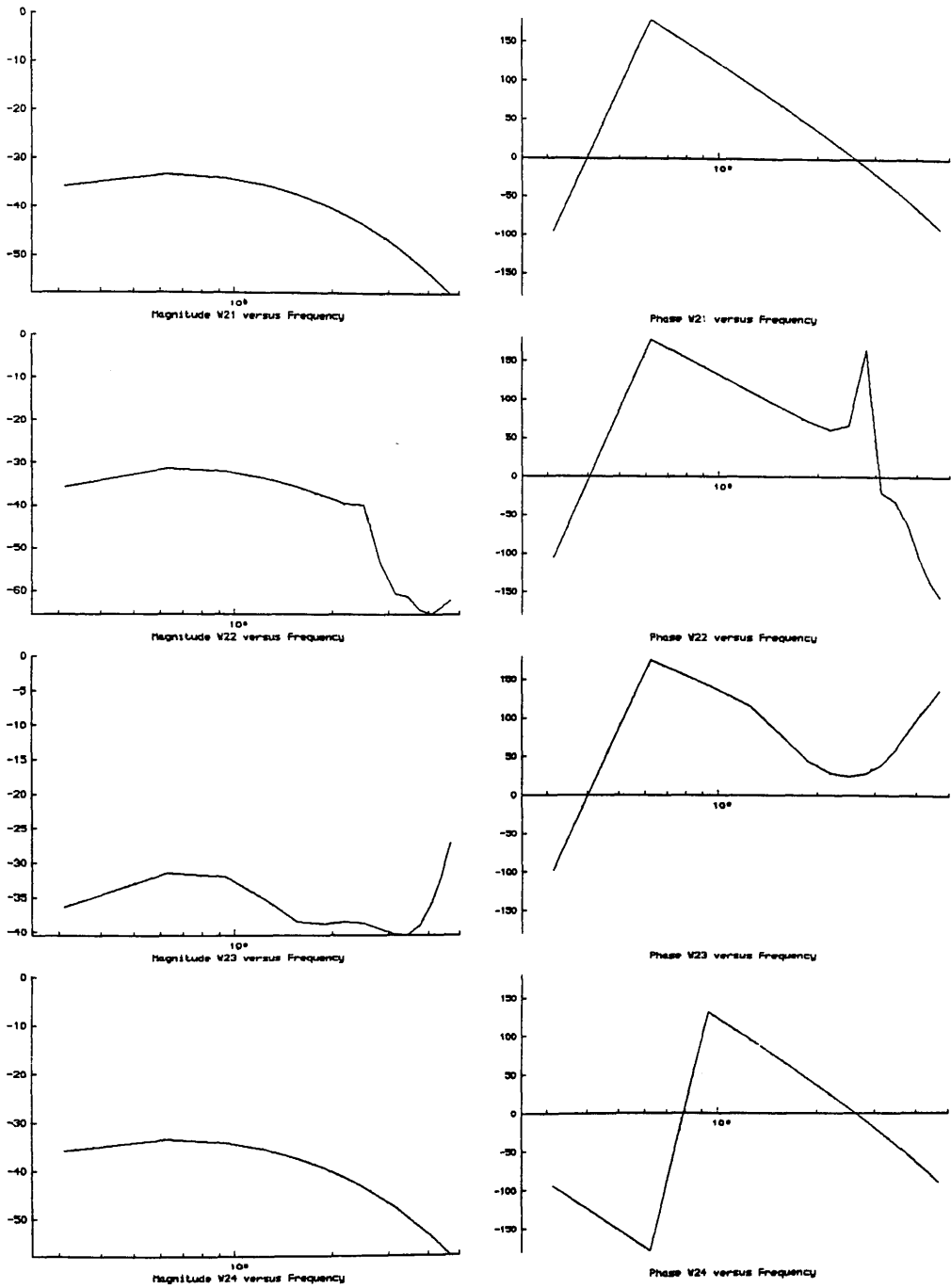
Figure 3.8: Vertical Velocity Transfer Function Sensitivities, Flight Path Controller, Magnitude and Phase.
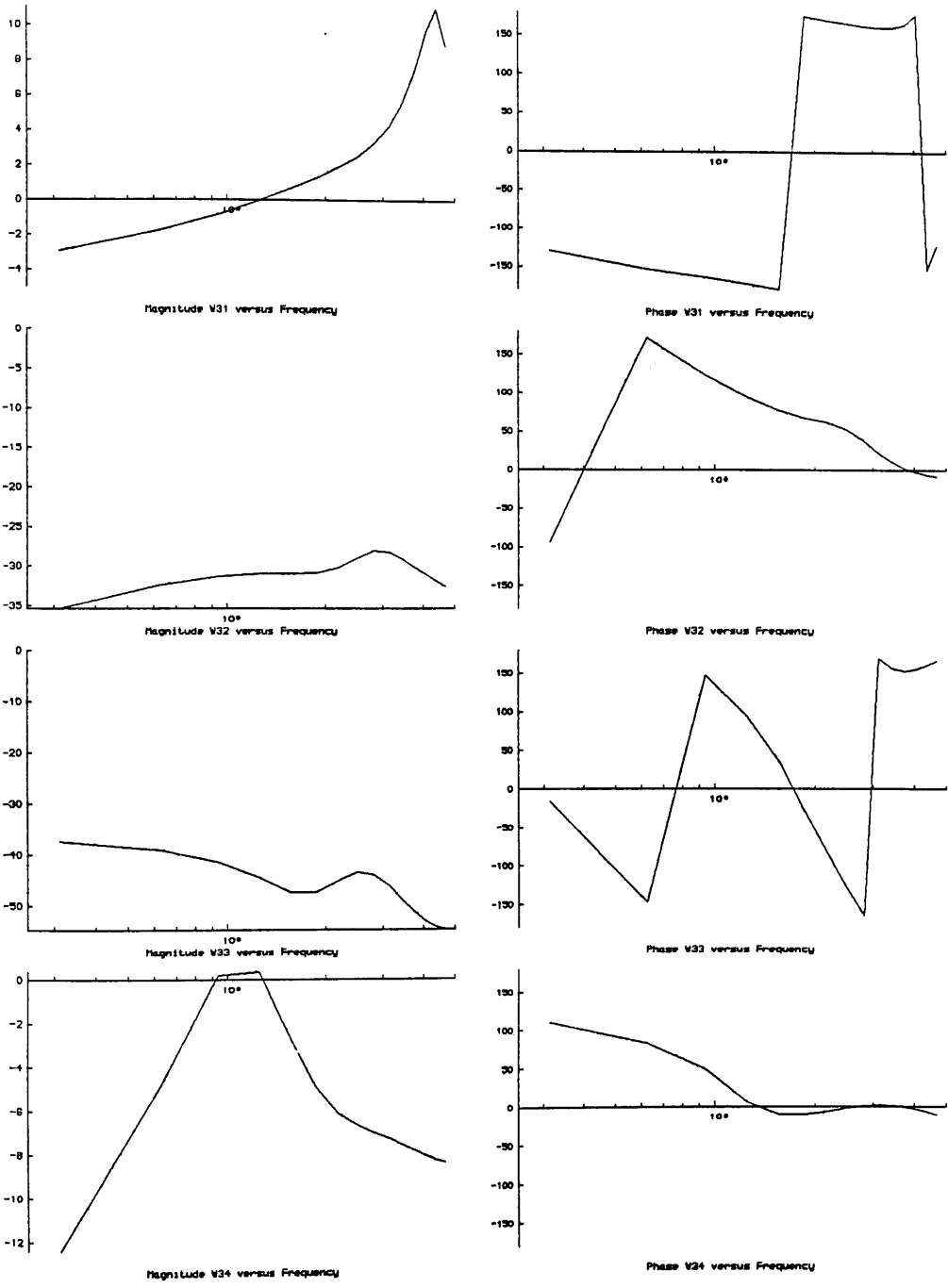
Figure 3.9: Pitch Rate Transfer Function Sensitivities, Flight Path Controller, Magnitude and Phase.
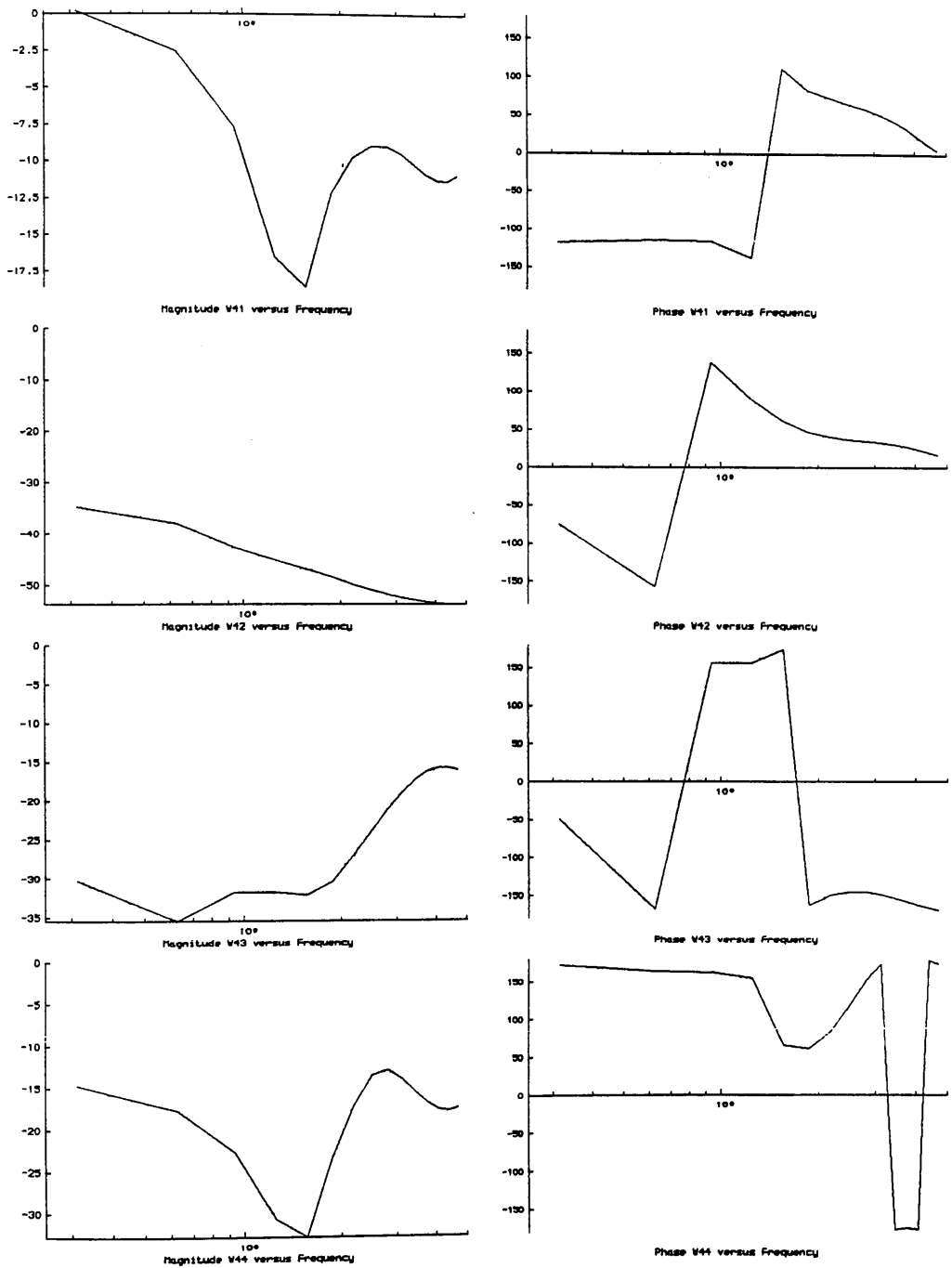
Figure 3.10: Pitch Angle Transfer Function Sensitivities, Flight Path Controller, Magnitude and Phase.
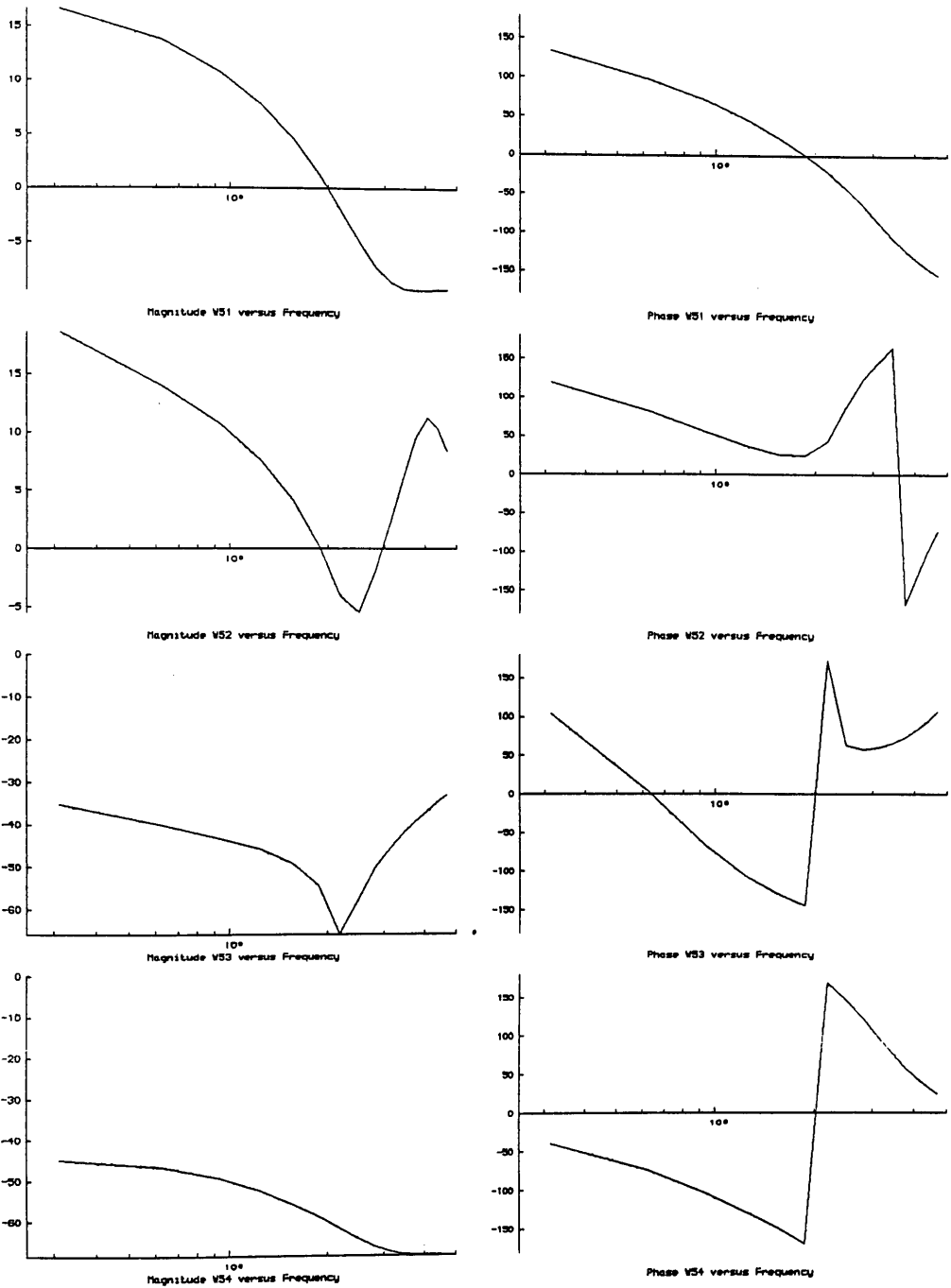
Figure 3.11: Lateral Velocity Transfer Function Sensitivities, Flight Path Controller, Magnitude and Phase.
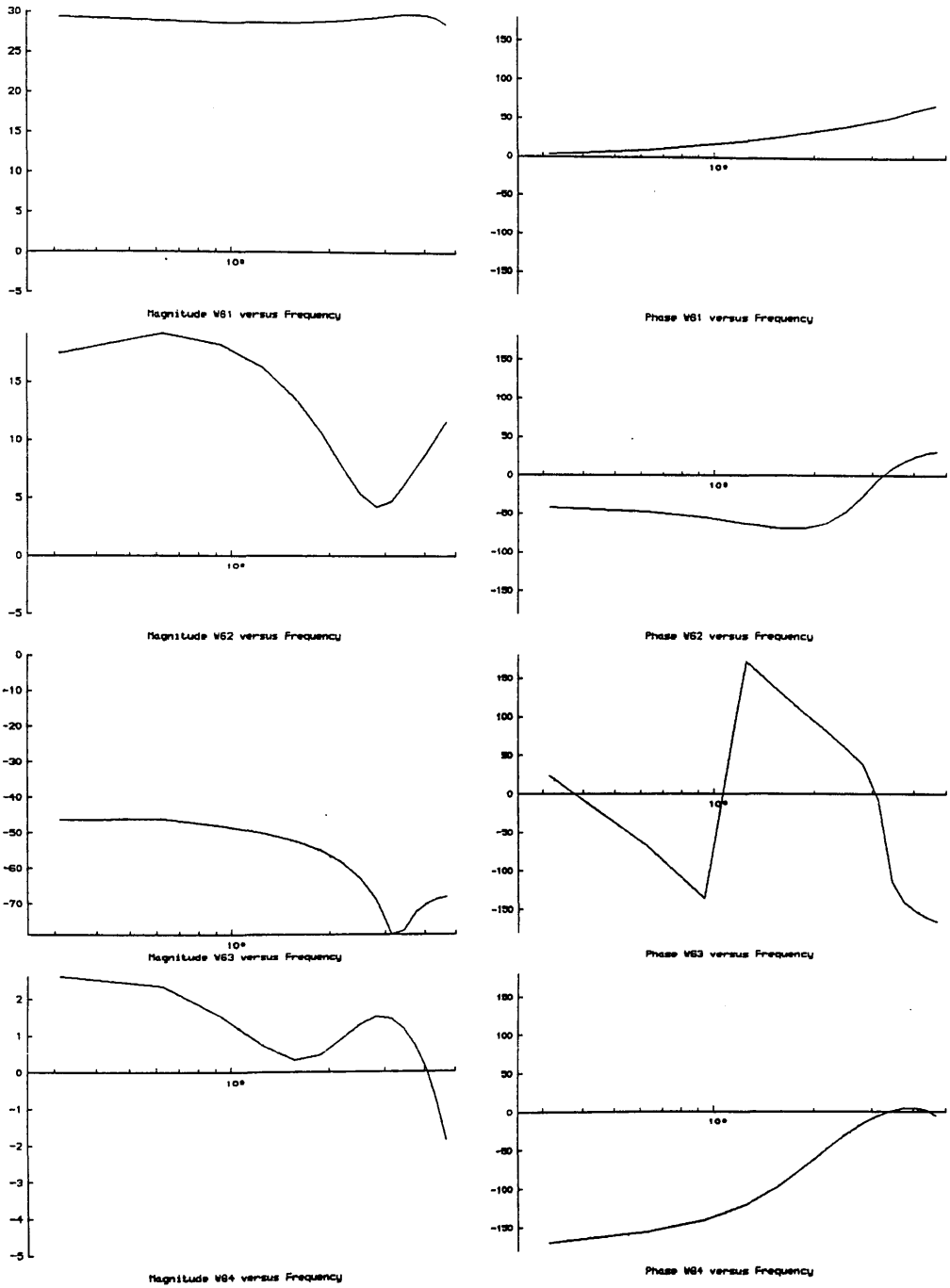
Figure 3.12: Roll Rate Transfer Function Sensitivities, Flight Path Controller, Magnitude and Phase.
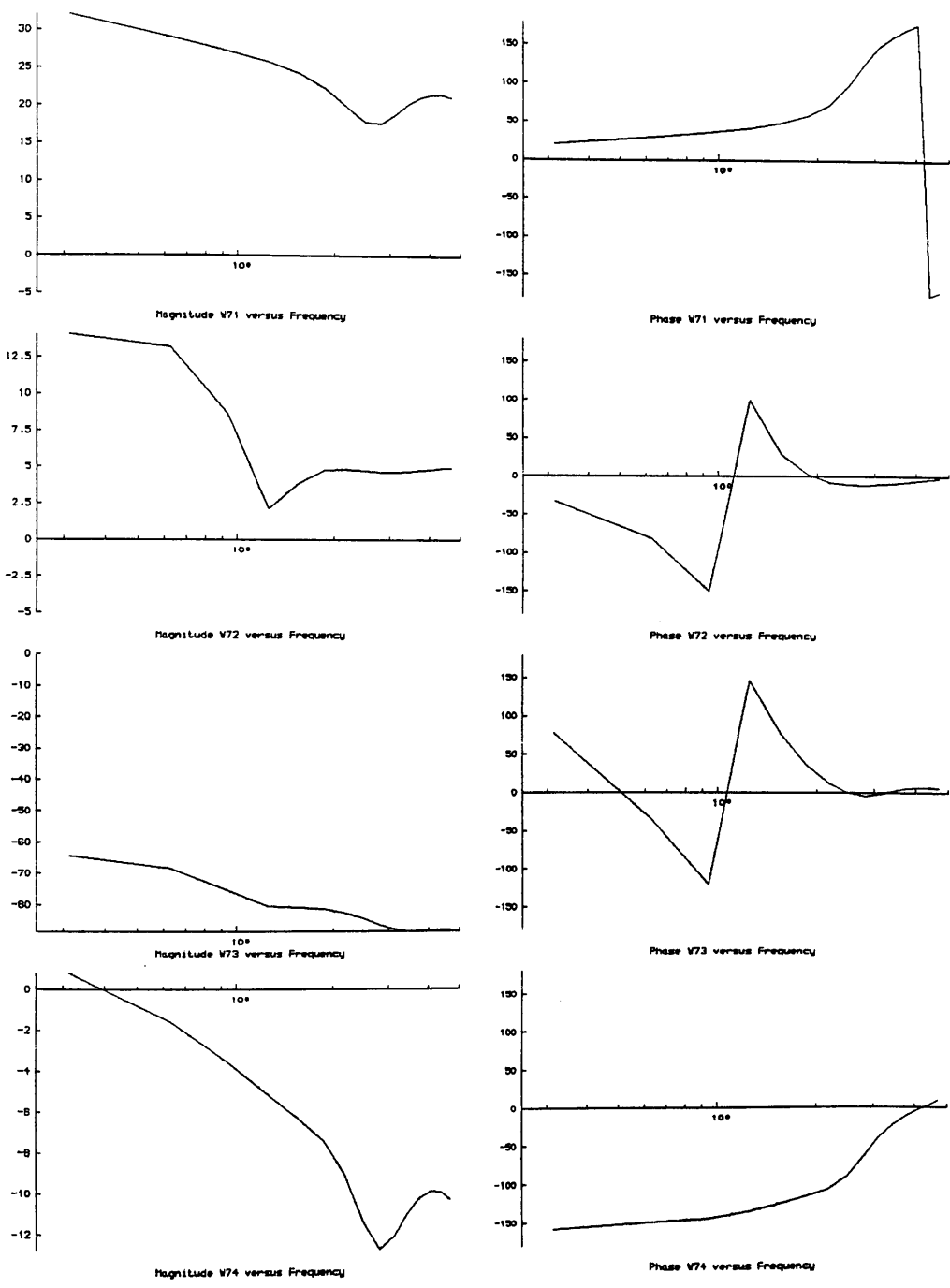
Figure 3.13: Roll Angle Transfer Function Sensitivities, Flight Path Controller, Magnitude and Phase.
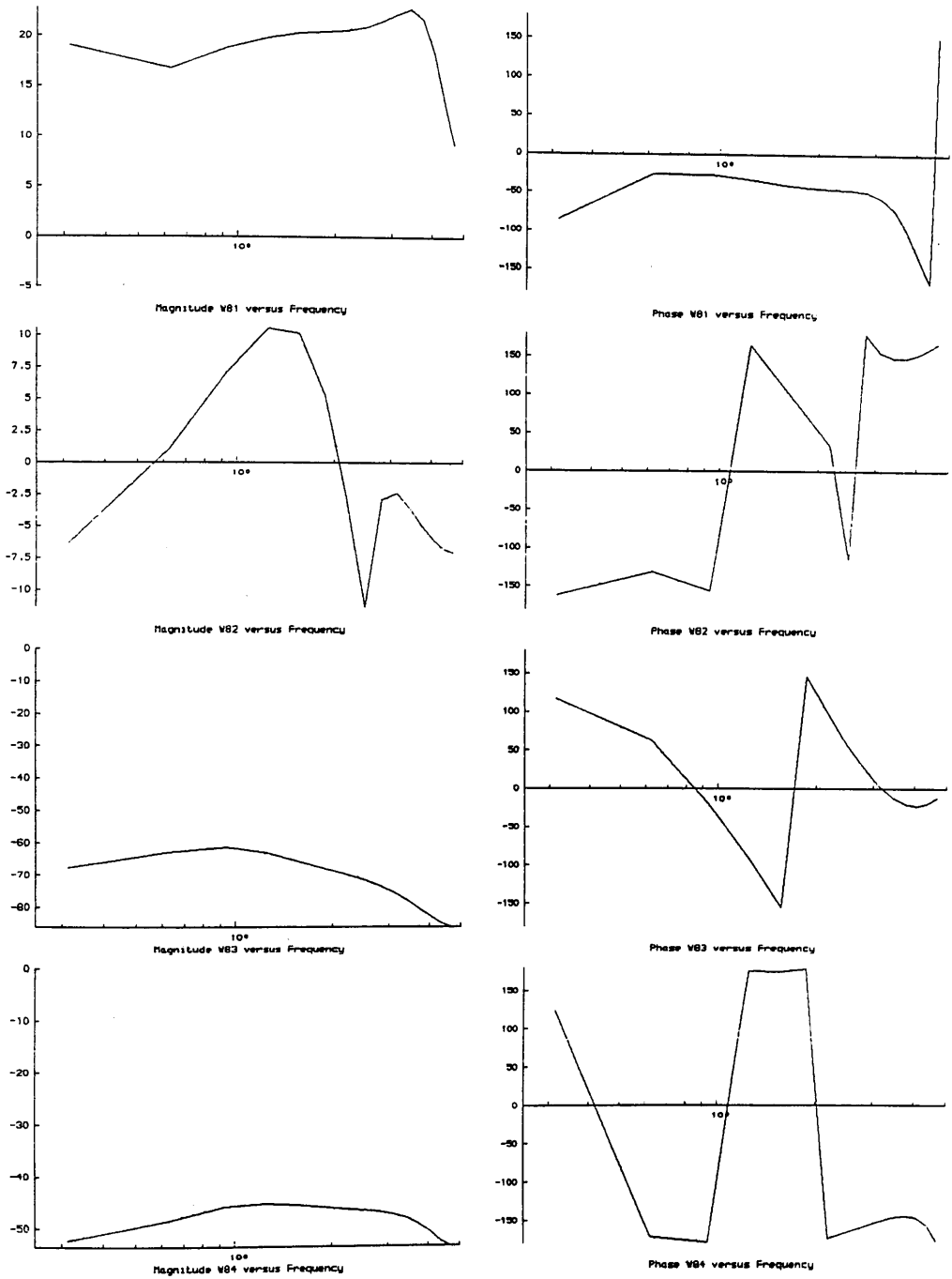
Figure 3.14: Yaw Rate Transfer Function Sensitivities, Flight Path Controller, Magnitude and Phase.

From the above list it is clear that P_{31} plays a significant role in determining the amount of coupling in the system since most of the entries are the responses of lateral states to longitudinal inputs.

Another effect of any increase in P_{31} would be to encourage resonances on the following responses:

$W_{11}(s)$ — Forward velocity due to vertical inceptor
$W_{31}(s)$ — Pitch rate due to vertical inceptor
$W_{34}(s)$ — Pitch rate due to pedal inceptor
$W_{44}(s)$ — Pitch angle due to pedal inceptor
$W_{51}(s)$ — Lateral velocity due to vertical inceptor
$W_{64}(s)$ — Roll rate due to pedal inceptor
$W_{81}(s)$ — Yaw rate due to vertical inceptor

It is concluded that resonances would be encouraged because all of these transfer function sensitivities show large amplitude peaks at certain frequencies, particularly at high frequencies. In contrast, $W_{61}(s)$ which is the transfer function from the vertical inceptor to the roll rate, p, shows a band—reject quality at about 1.8 Hertz.

An initial study of transfer function sensitivities was made for the Parry Modal Controller [50]. These tests have shown that transfer functions are visibly changed by parameters whose normalized sensitivity functions have amplitudes greater than 0 dB for a 10% parameter change. Even if the sensitivity amplitude is of the order of 0 dB, the relative phase of the change can have a large bearing on the amount of change in the response. A second point which was considered in the analysis was the question of whether a parameter affects the structure of the response or whether it can be interpreted simply as a gain in the system.

The first deduction which can be made from the results is that some transfer functions are far more sensitive than others to parameter variations. For example, the sensitivities of $W_{72}(s)$ (Parry Modal Controller) with respect to 24 parameters have magnitudes greater than 0 dB. In contrast, $W_{63}(s)$ (Parry Modal Controller) is insensitive to parameter changes, as shown by the lack of any sensitivities with amplitudes above 0 dB.

The second observation was that changing parameters generally changes the structure of a transfer function, not just its amplitude. A parameter can be considered as a pure gain if the normalized transfer function sensitivity magnitude is flat over most of the frequency bandwidth of interest. Some parameters come close to acting purely as a gain in terms of the magnitude plots but the phase plots vary in a nonlinear fashion. Therefore, it is concluded a change in any

parameter will affect the structure of the system's response.

If one considers the problem of adjusting the system's dynamics, the transfer function sensitivities are both encouraging and cause for concern. Some of the sensitivities have amplitudes of over 30 dB which may be useful for minimizing the amplitude of parameter adjustments. If one makes use of parameters which give large transfer function sensitivity magnitudes, then the necessary amount of change in parameters can be kept to a minimum. A 30 dB sensitivity means that for every 1% change in a parameter, there will be a 31% change in the transfer function. In this way, it may be possible to significantly improve system dynamics and handling qualities without major excursions from the theory used to design the controller. At the same time, the large sensitivities are alarming if they are an indication of the deviations which can be expected from errors in the implementation of the controller. When the controller is built, it will not be identical to its paper counterpart since there may be slight variations in parameter settings resulting from finite word-length considerations. Furthermore, if one also considers that the sensitivity magnitudes can vary over a range of 30 dB between 0 Hz. and 2 Hz., it becomes apparent that changing a parameter can introduce resonances to the system.

Transfer function sensitivities can be calculated without knowledge of the helicopter plant using signal convolution techniques. Normalized sensitivities show that altering parameters will affect the structure in addition to the amplitude of the system's response, with some transfer functions being more affected than others. However, the large sensitivity amplitudes with respect to some parameters may be either beneficial or detrimental in terms of adjusting the system's response. The computational cost of generating the transfer function sensitivities is high, but the information that they provide for the small amount of inflight testing needed is important to the adjustment algorithm as will be seen in the next section.

3.3) The Identification of Adjustment Parameters

A modern ACT flight control system will contain many parameters. At times, it will not be practical to try to optimize the setting of each parameter at every flight condition. It was felt that if adjustments to the system were to be minimized, then those parameters which significantly affect the system's performance should be used. Hence, one of the major problems involved in the development of the tuning process has been the identification of parameters which

will be useful in terms of altering the system's dynamics and performance.

Originally, it was hoped that the state sensitivity functions would give an indication of those parameters which would be useful in the adjustment algorithm — the adjustment parameters. Unfortunately, the state sensitivity functions have various forms, making it difficult to compare two sets of sensitivities for two different parameters and decide conclusively that one parameter has more of an influence on system dynamics than another.

The controller which is being used in the study was designed using modal control techniques. It was a logical extension to the ideas present in this design technique to the consideration of how the eigenstructure parameters (the eigenvalues, eigenvectors, and principal angles) are affected by shifts in the controller parameters. The theory and results of this study are presented in Section 3.4. Unfortunately, because the eigenstructure sensitivities require knowledge of the system plant, they are unsuitable for use with a tuning algorithm which relies solely on information extracted from system outputs.

Transfer function sensitivities measure the rate of change of transfer functions between the four pilot inceptors and the output states with respect to parameter changes in the controller. Since the magnitude of the transfer function sensitivities can be normalized by dividing through by the magnitude of the transfer functions, it is a relatively straightforward task to compare several system transfer function sensitivities. If a normalized transfer function sensitivity magnitude to a particular parameter is large, then it can be said that changes in that parameter will have a large effect on the system's dynamics. A simplistic search for peak frequency domain sensitivity amplitudes can be made much more successfully than a search for peak amplitudes in the time domain due to the success of the frequency domain normalization. Time domain normalization was not helpful because the normalized state variable sensitivities were dominated by zeros in the state response. The peak transfer function sensitivity amplitudes can be ordered in terms of either the transfer functions or the output states to provide a ranking of the adjustment parameters.

As stated previously, it is possible to calculate the transfer function sensitivities without knowledge of the system plant through the use of signal convolution techniques. Therefore, unlike eigenstructure sensitivities, the transfer function sensitivities can be used with actual helicopters.

To normalize the transfer function sensitivities, the individual elements of $\partial[W(s)]/\partial\alpha_i$ are divided by their respective transfer functions and multiplied by the value of the parameter α_i.

$$\left| \frac{\partial W_{jk}(s)}{\partial \alpha_i} \right|_{normalized} = \frac{\alpha_i}{W_{jk}(s)} \frac{\partial W_{jk}(s)}{\partial \alpha_i} \qquad \text{Equation 3.42}$$

For the purposes of identifying the adjustment parameters, the maximum amplitude, $(W_{jki})_{max}$, of each normalized transfer function sensitivity to each parameter across the frequency range of interest is catalogued.

$$(W_{jki})_{max} = \left| \left| \frac{\partial W_{jk}(s)}{\partial \alpha_i} \right|_{normalized} \right|_{\substack{max \\ s}} \qquad \text{Equation 3.43}$$

The various $(W_{jki})_{max}$ are then sorted into decreasing order and the highest valued entries, $(W_{jka})_{max}$, in each list are used to identify the adjustment parameters α_a.

The sorting of the $(W_{jki})_{max}$ can be used to choose adjustment parameters based on either individual transfer functions or groups of transfer functions which are related by having the same output state. Depending on how many adjustment parameters are to be used, the top one, two, or three parameters from each sorted list of $(W_{jki})_{max}$ values are identified for use.

When the most significant parameters for each of the eight states are identified from transfer function sensitivities, six parameters are chosen. This means that some parameters are significant in terms of more than one output state. The six parameters with greatest influence on the output states of the Flight Path Controller are P_{11}, P_{22}, P_{23}, P_{31}, P_{32}, and P_{33}. It is comforting to note that the eigenstructure sensitivities for the same helicopter computer model also identified P_{11}, P_{22}, P_{23}, P_{32}, and P_{33} as being important. These consistent results can be used as justification for the hypothesis that parameters which greatly affect the magnitudes of system transfer functions will also affect the system eigenvalues to a large degree. Hence, the system dynamics are greatly affected by parameters with large transfer function sensitivity magnitudes.

It should be noted that all of the above theory ignores how the phase of the system will respond to parameter changes. It was considered beyond the scope of the current study to attempt to analyse and use phase sensitivity information for the purposes of choosing which parameters to adjust. This is largely because of a lack of knowledge about how a pilot in the flight control loop will react to different phase margins. Pilot induced oscillations are a common undesirable flight handling quality on high performance aircraft, both fixed and rotary winged and are the result of insufficient phase margins. The crux of the problem is that the pilot is an adaptive controller and as such will

have various phase characteristics.

3.4) Eigenstructure Sensitivities

This section briefly describes the motivation behind looking at the eigenstructure sensitivities of helicopter simulation models and the results which were obtained from the study. Eigenstructure will be used to collectively refer to the system's eigenvalues, eigenvectors, and principal angles. The term, eigenstructure sensitivity will be defined as the first partial derivative of an eigenstructure parameter (an eigenvalue, eigenvector, or principal angle) with respect to one of the controller or compensator parameters.

3.4.1) Eigenstructure Sensitivities Motivation and Theory

As previously stated, the large number of adjustable gains in modern flight control systems generates a need for an algorithm which will identify the parameters which are to be used to adjust system dynamics. The design of the flight control systems being studied is based on modal control theory. Since the flight controller design is based on eigenvalue and eigenvector placement it made sense to base the adjustment procedure in some way on the structure of the response — its eigenvalues, eigenvectors, and principal angles. Those controller parameters which signficantly affect the eigenstructure parameters will have a large influence on the system's performance. It was for these reasons that the eigenstructure sensitivities of the helicopter model were examined as a means of identifying those parameters which would prove useful in the adjustment algorithm.

Although it is possible to generate the state sensitivity functions without knowledge of the system plant, this is not so for the eigenstructure sensitivities. The eigenvalues and eigenvectors for the Flight Path Controller (Section 2.2.4) are defined by Equation 3.44.

$$([A] - [B][K] - [B][P][\xi]) [V] = [V] [\Lambda]$$

<div align="right">Equation 3.44</div>

Rearranging equation 3.44 gives,

$$[A] - [B][K] - [B][P][\xi] = [V][\Lambda][V]^{-1}$$

<div align="right">Equation 3.45</div>

If this equation is differentiated with respect to the control system parameters it can be shown that,

$$- [B]\frac{\partial[K]}{\partial\alpha_i} - [B]\frac{\partial[P]}{\partial\alpha_i}[\xi] - [B][P]\frac{\partial[\xi]}{\partial\alpha_i} =$$

$$\frac{\partial[V]}{\partial\alpha_i}[\Lambda][V]^{-1} + [V]\frac{\partial[\Lambda]}{\partial\alpha_i}[V]^{-1} + [V][\Lambda]\frac{\partial[V]^{-1}}{\partial\alpha_i}$$

<div align="right">Equation 3.46</div>

Equation 3.46 shows that the eigenvalue and eigenvector sensitivities with respect to the control system parameters cannot be determined without knowledge of the input distribution matrix, [B] and the system's eigenstructure. For this reason it is impossible to consider using these eigenstructure sensitivities in the same way as the state sensitivity functions and the transfer function sensitivities. Eigenstructure sensitivities can only be used in support of a state sensitivity function based optimization algorithm.

Assuming that the derivatives of the feedback distribution matrix, $\partial[\xi]/\partial\alpha_i$, are zero (Equation 3.6), then the state sensitivities of Equation 3.10 can be described by,

$$\frac{\partial\underline{X}(s)}{\partial\alpha_i} = \left\{ s[I] - [A] + [B][K] + [B][P][\xi] \right\}^{-1} \times$$

$$\left\{ \left[\frac{\partial[V]}{\partial\alpha_i}[\Lambda][V]^{-1} + [V]\frac{\partial[\Lambda]}{\partial\alpha_i}[V]^{-1} + [V][\Lambda]\frac{\partial[V]^{-1}}{\partial\alpha_i} \right] \underline{X}(s) + \right.$$

$$\left. [B]\frac{1}{s}\frac{\partial[P]}{\partial\alpha_i}[\eta][G]\underline{R}(s) \right\}$$

<div align="right">Equation 3.47</div>

Equation 3.47 clearly shows how the state sensitivity functions are influenced by the eigenstructure sensitivities. Not only do the eigenstructure sensitivities show how the fundamental modes of the system will change with adjustments of

the control system gains, they are also much simpler to work with than state sensitivity functions because they are time invariant for the simulation models.

3.4.2) Eigenstructure Sensitivity Observations and Results

A comprehensive study of the eigenstructure sensitivities for the parameters of the feedback matrix has been made for the Parry Modal Controller [51]. The eigenstructure sensitivities were calculated using the SAM computer module. The sensitivities are approximated by performing a difference quotient between a standard set of values and a perturbed set of values. Further documentation concerning these routines can be found in Reference [46].

It was found that a perturbation ratio of 0.0001 gave the best results with these routines. Larger pertubations caused the method to loose accuracy and a smaller pertubation was seen to cause no change in the sensitivities. The one area of concern with the use of parameter perturbation techniques for the calculation of eigenstructure sensitivities centres around the generation of eigenvector sensitivities. The sensitivity calculations are extremely sensitive to inaccuracies in the smaller elements of the eigenvector. Two NAG computer routines [52] using different algorithms returned differing values of the eigenvectors [51]. Eventually it was decided that the eigenvalue/eigenvector routine used in the design would be used for the sake of consistency. As will be seen, this also led to a self-consistent set of results.

The slight differences in eigenvectors from the two NAG routines resulted in a significant change in the eigenstructure sensitivities. The major contribution to this difference came from the smaller elements of the eigenvectors which although they might be shifted by a small amount in terms of the length of the vector, their change was large in terms of the value of the element. If the eigenvector sensitivities are sensitive to changes in the smaller elements of the eigenvectors, then it might also be the case that any event or influence which shifts the smaller elements of the eigenvector by any amount, which is large in relation to that element, will have a significant bearing on the dynamics of the system. The control systems currently under study are design using a linear eighth order HELISTAB model. It has been shown that a controller designed with this model and subsequently used with a simulation model (or indeed a system) of higher order, such as HELISIM3, will exhibit a degraded level of performance. This deterioration might be seen as a result of shifts in the smaller elements of the eigenvectors which would change their orientation.

In order to discuss which parameters are important for which modes, it was beneficial to set up a classification scheme for the parameters. A parameter was classified as having strong cross coupling tendencies if the eigenstructure derivatives with respect to that parameter are present for more than one mode at a discernable amplitude. A discernable sensitivity amplitude is one which is large enough to be seen on the plots of the modulus of the eigenstructure sensitivities. The following table shows five categories which were used to classify feedback parameters from their eigenstructure sensitivities.

Table 3.1: Categories for Adjustment Parameter Identification

Eigenstructure Sensitivity Amplitude	Parameter affects only one mode	Parameter has strong cross coupling tendencies
Amplitude greater than 50% of the maximum sensitivity amplitude	A	B
Amplitude of discernable size	C	D
Negligible amplitude	E	

The eigenstructure sensitivity data for the control system parameters of the Flight Path Controller — HELISTAB plant model system are displayed in Figures 3.15 through 3.26. Figure 3.15 shows the modulus of normalized eigenvalue sensitivities with respect to the feedback gains. The sensitivity of each mode's eigenvalue to the feedback parameters is plotted as a histogram. This two dimensional representation of the data is useful for showing which parameters affect which modes. For example, the fast pitch mode is sensitive to K_{12} and K_{13}. The data presented in Figure 3.15 is grouped together to form the three dimensional histogram of Figure 3.16 which plots the modulus of normalized eigenvalue sensitivity above a grid of mode numbers and feedback gains. Figure 3.16 shows that the slow pitch and phugoid modes are more sensitive than the
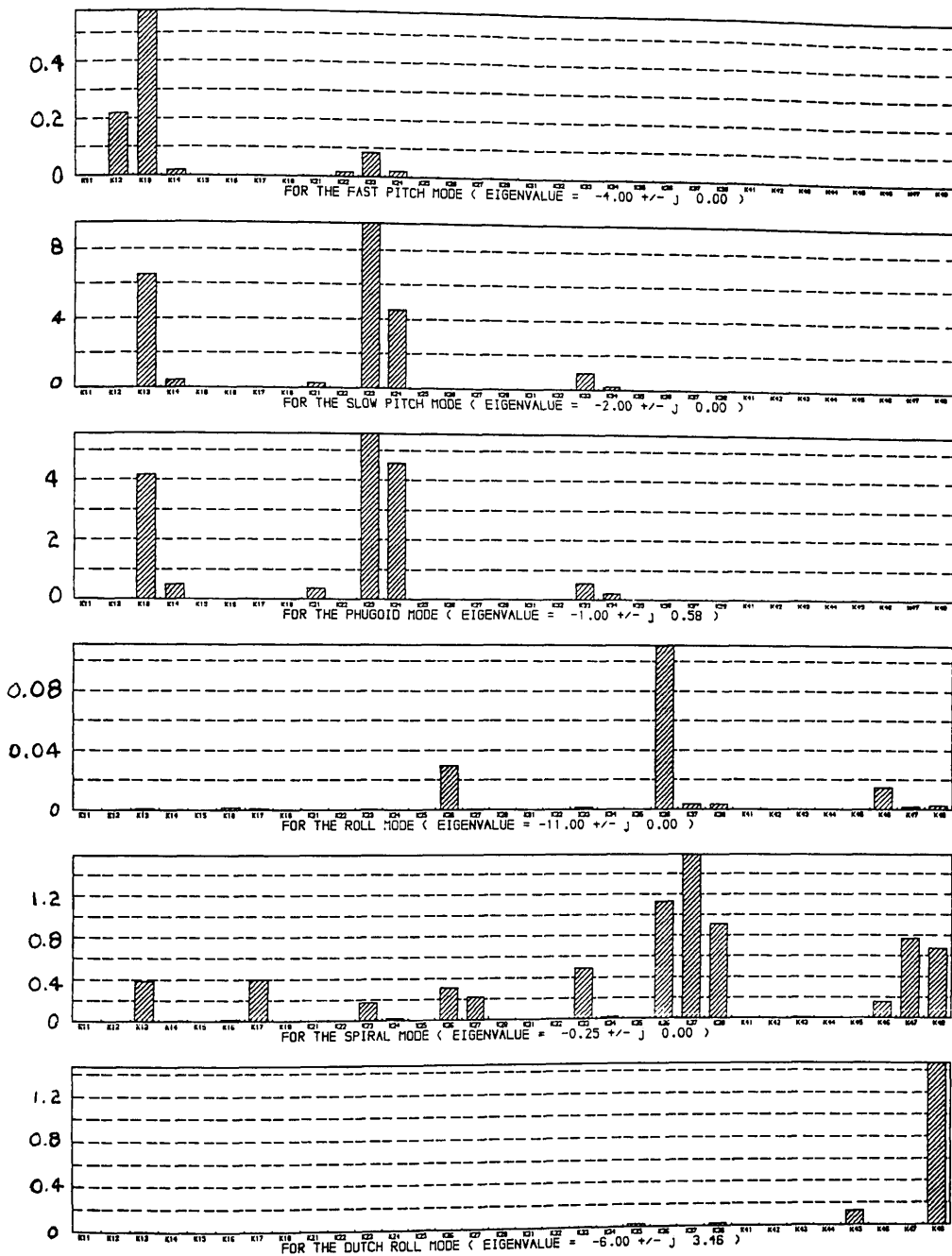
Figure 3.15: Modulus of Normalized Eigenvalue Sensitivities Against Flight Path Controller Feedback Gains.
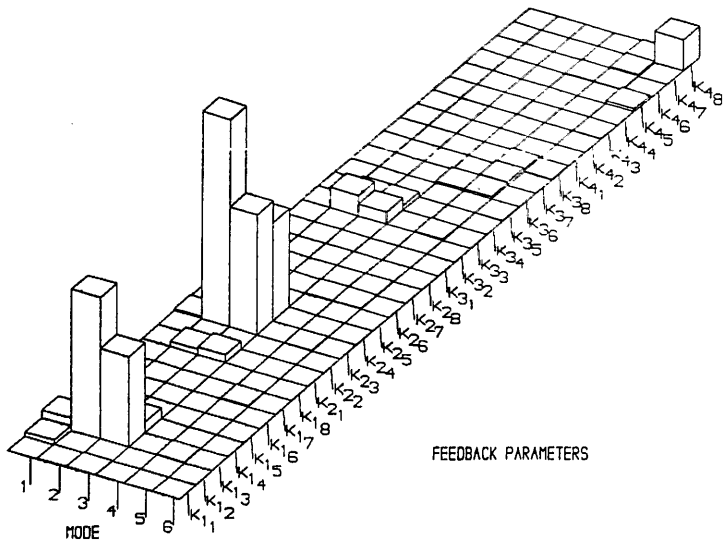
Figure 3.16: Modulus of Normalized Eigenvalue Sensitivities Against Flight Path
Controller Feedback Gains and Mode Numbers.
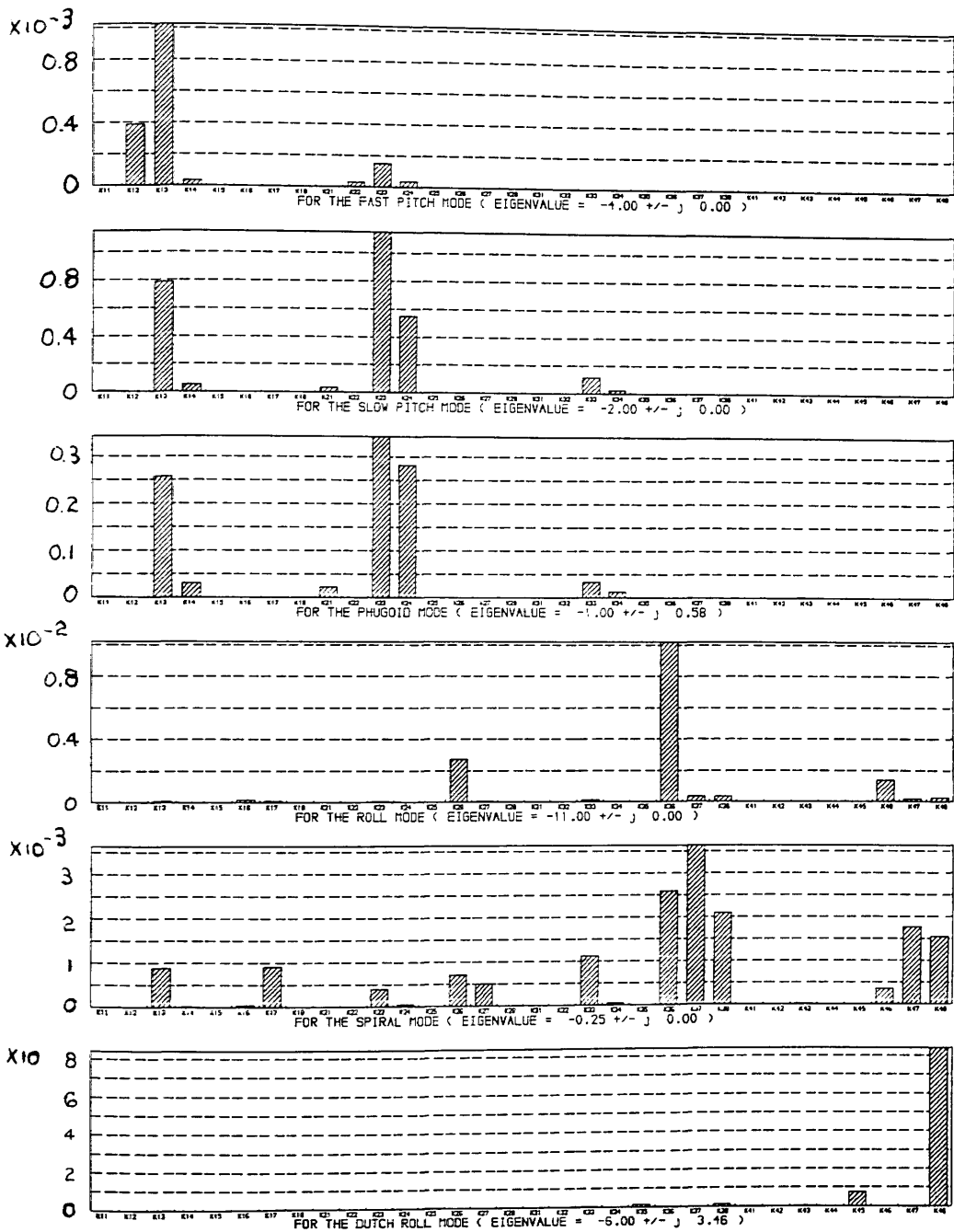
Figure 3.17: Modulus of Normalized Eigenvector Sensitivities Against Flight Path Controller Feedback Gains.

MODE NUMBERS
1 - FAST PITCH MODE (EIGENVALUE = -4.00 +/- j 0.00)
2 - SLOW PITCH MODE (EIGENVALUE = -2.00 +/- j 0.00)
3 - PHUGOID MODE   (EIGENVALUE = -1.00 +/- j 0.58)
4 - ROLL MODE   (EIGENVALUE = -11.00 +/- j 0.00)
5 - SPIRAL MODE   (EIGENVALUE = -0.25 +/- j 0.00)
6 - DUTCH ROLL MODE (EIGENVALUE = -6.00 +/- j 3.46)
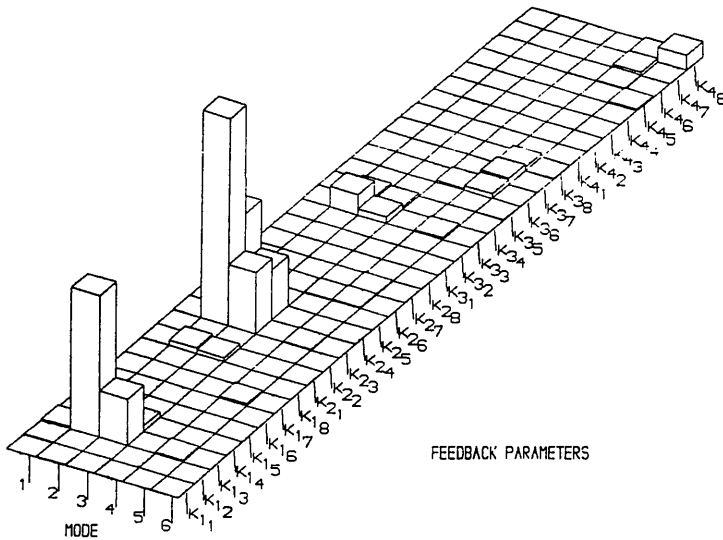
Figure 3.18: Modulus of Normalized Eigenvector Sensitivities Against Flight Path Controller Feedback Gains and Mode Numbers.
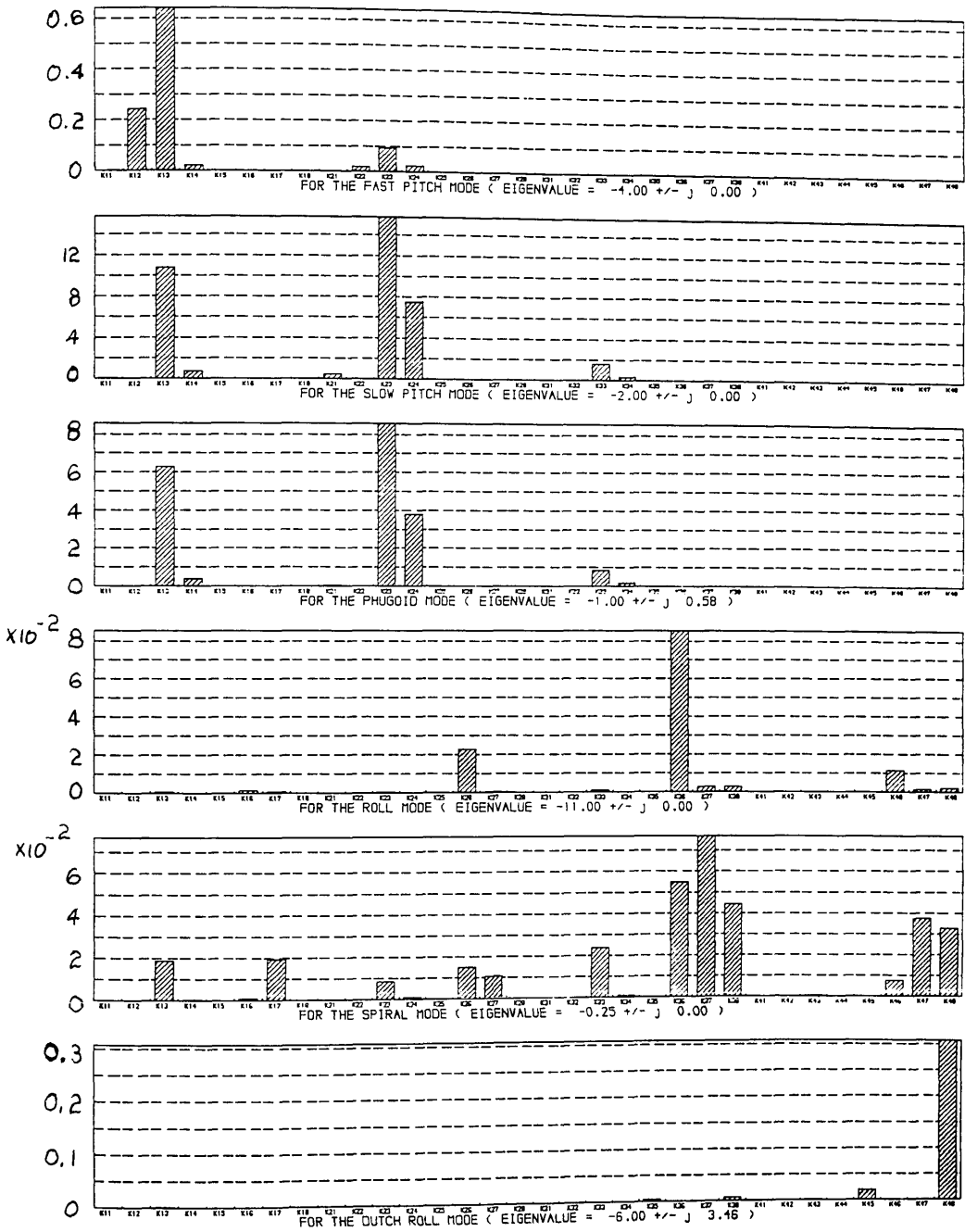
Figure 3.19: Modulus of Normalized Principal Angle Sensitivities Against Flight Path Controller Feedback Gains.

MODE NUMBERS
1 - FAST PITCH MODE (EIGENVALUE = -4.00 +/- J 0.00)
2 - SLOW PITCH MODE (EIGENVALUE = -2.00 +/- J 0.00)
3 - PHUGOID MODE (EIGENVALUE = -1.00 +/- J 0.58)
4 - ROLL MODE (EIGENVALUE = -11.00 +/- J 0.00)
5 - SPIRAL MODE (EIGENVALUE = -0.25 +/- J 0.00)
6 - DUTCH ROLL MODE (EIGENVALUE = -6.00 +/- J 3.46)
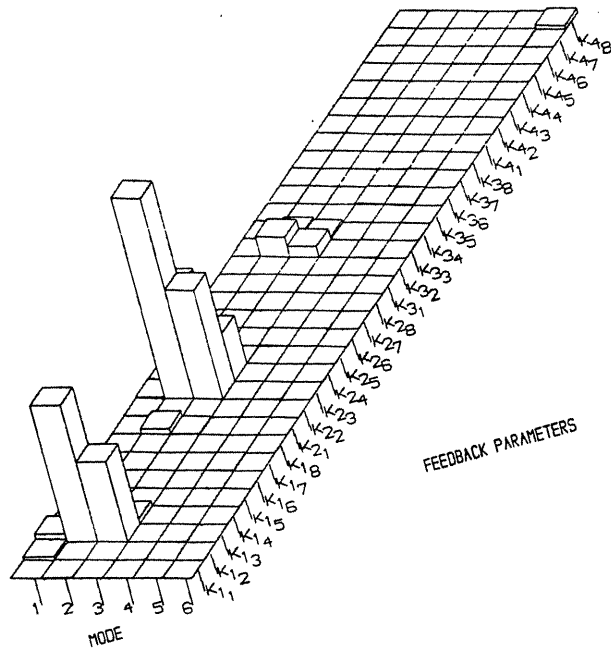
Figure 3.20: Modulus of Normalized Principal Angle Sensitivities Against Flight Path Controller Feedback Gains and Mode Numbers.
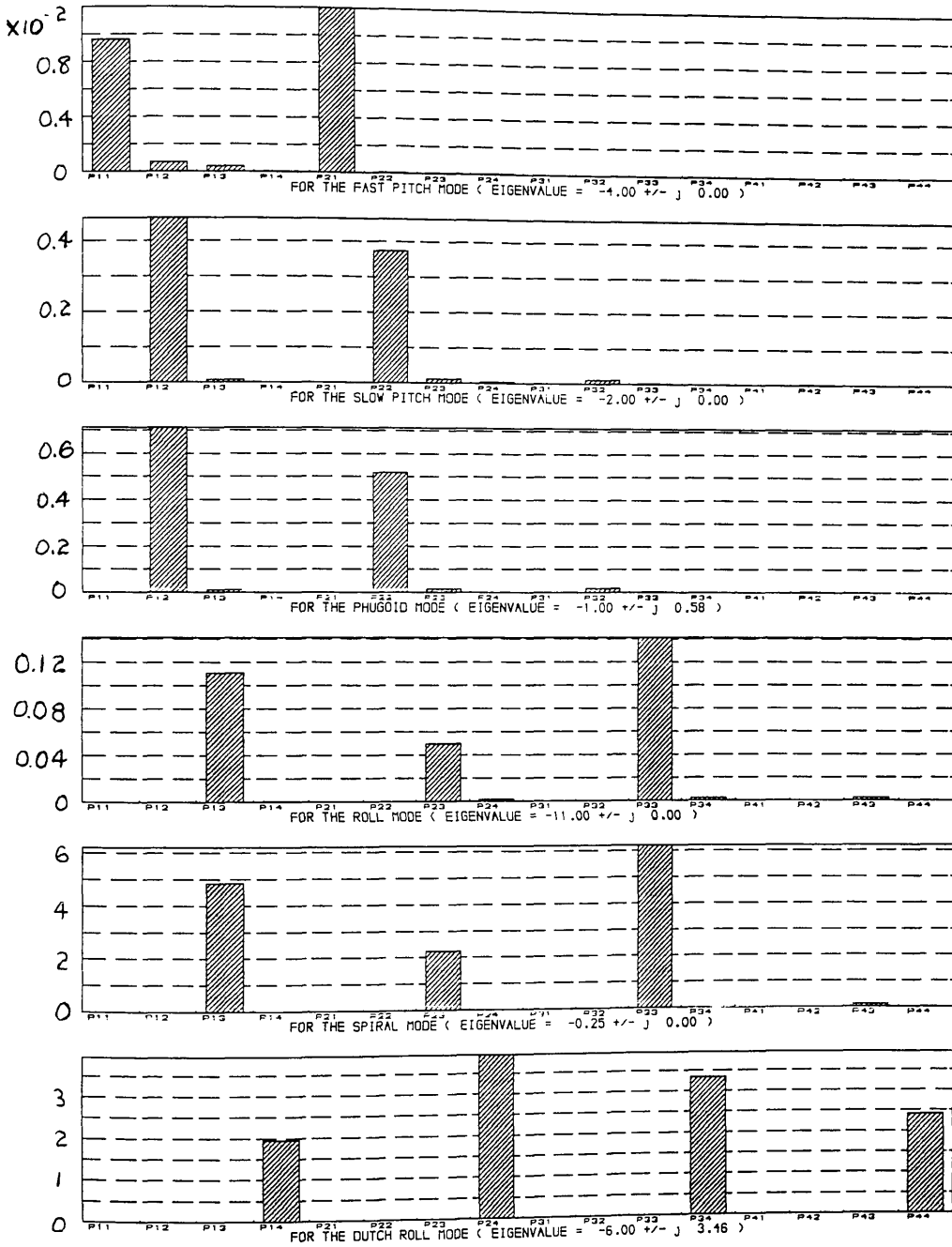
Figure 3.21: Modulus of Normalized Eigenvalue Sensitivities Against Flight Path Controller Precompensator Gains.

MODE NUMBERS
1 - FAST PITCH MODE (EIGENVALUE = -4.00 +/- j 0.00)
2 - SLOW PITCH MODE (EIGENVALUE = -2.00 +/- j 0.00)
3 - PHUGOID MODE   (EIGENVALUE = -1.00 +/- j 0.58)
4 - ROLL MODE   (EIGENVALUE = -11.00 +/- j 0.00)
5 - SPIRAL MODE   (EIGENVALUE = -0.25 +/- j 0.00)
6 - DUTCH ROLL MODE (EIGENVALUE = -6.00 +/- j 3.46)
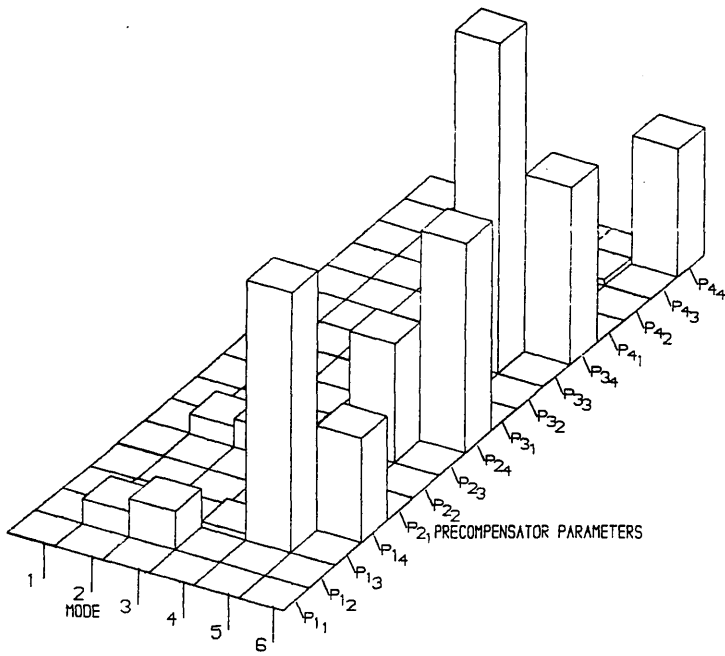
Figure 3.22: Modulus of Normalized Eigenvalue Sensitivities Against Flight Path
Controller Precompensator Gains and Mode Numbers.
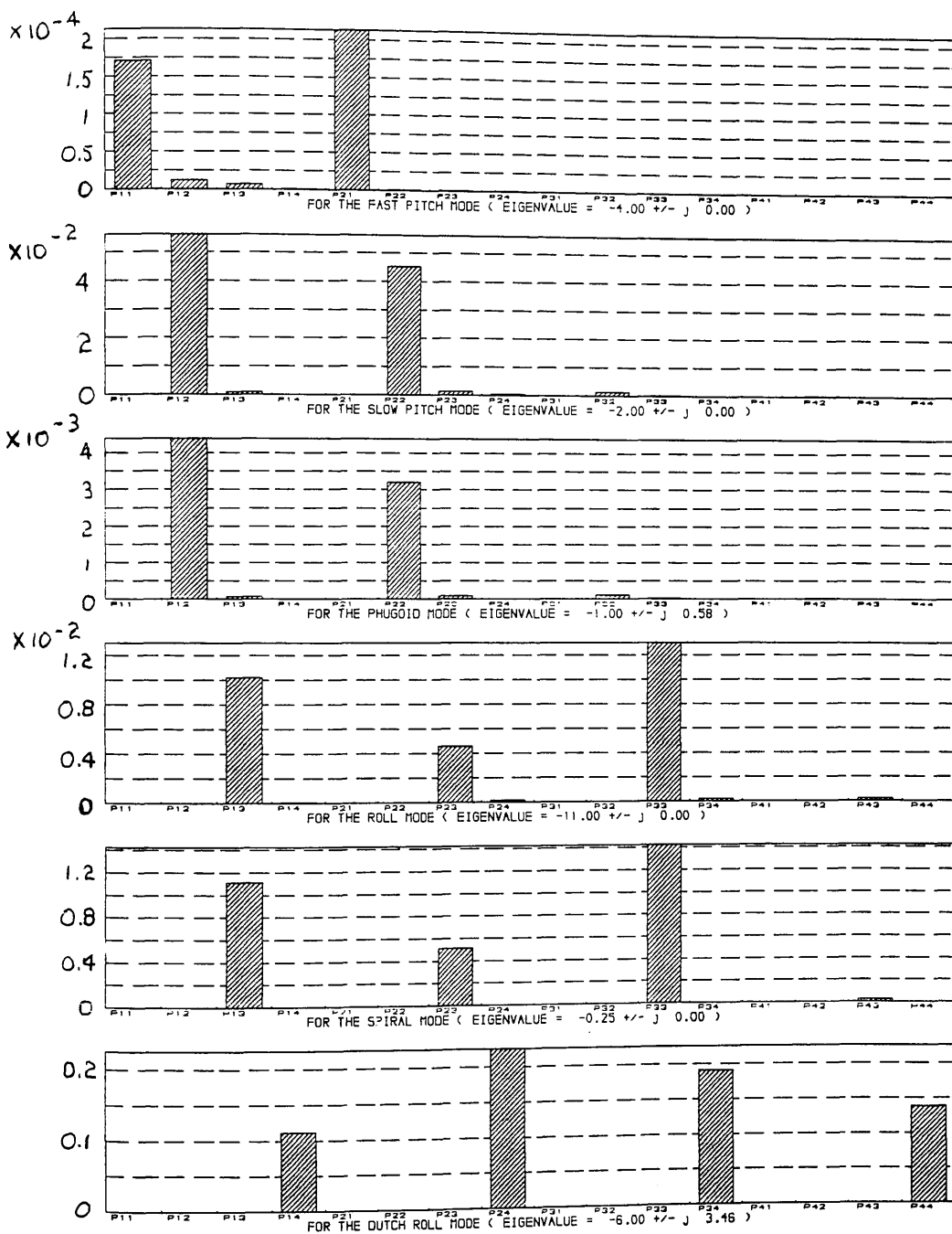
Figure 3.23: Modulus of Normalized Eigenvector Sensitivities Against Flight Path Controller Precompensator Gains.

MODE NUMBERS
1 - FAST PITCH MODE (EIGENVALUE = -4.00 +/- j 0.00)
2 - SLOW PITCH MODE (EIGENVALUE = -2.00 +/- j 0.00)
3 - PHUGOID MODE   (EIGENVALUE = -1.00 +/- j 0.58)
4 - ROLL MODE   (EIGENVALUE = -11.00 +/- j 0.00)
5 - SPIRAL MODE   (EIGENVALUE = -0.25 +/- j 0.00)
6 - DUTCH ROLL MODE (EIGENVALUE = -6.00 +/- j 3.46)
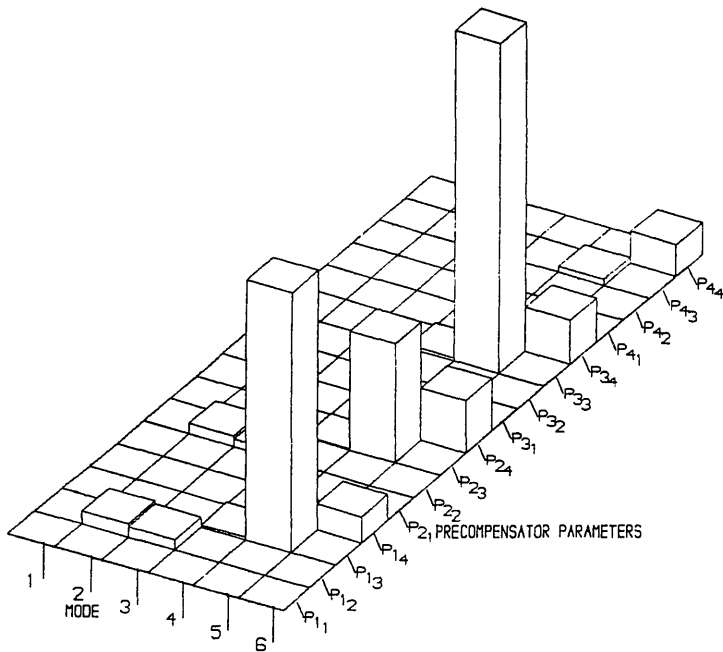
Figure 3.24: Modulus of Normalized Eigenvector Sensitivities Against Flight Path Controller Precompensator Gains and Mode Numbers.

— 117 —
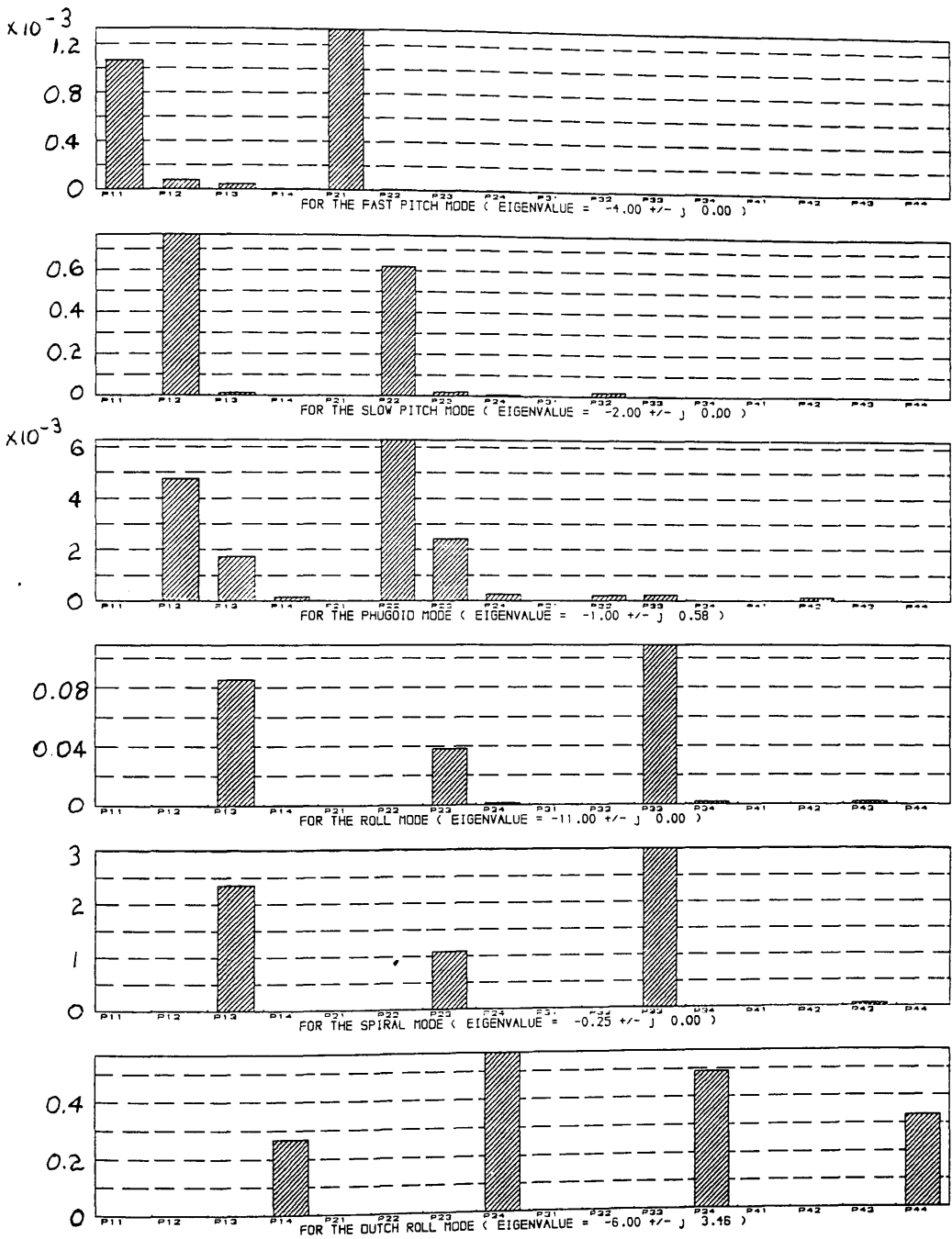
Figure 3.25: Modulus of Normalized Principal Angle Sensitivities Against Flight Path Controller Precompensator Gains.

MODE NUMBERS
1 - FAST PITCH MODE (EIGENVALUE = -4.00 +/- j 0.00)
2 - SLOW PITCH MODE (EIGENVALUE = -2.00 +/- j 0.00)
3 - PHUGOID MODE (EIGENVALUE = -1.00 +/- j 0.58)
4 - ROLL MODE (EIGENVALUE = -11.00 +/- j 0.00)
5 - SPIRAL MODE (EIGENVALUE = -0.25 +/- j 0.00)
6 - DUTCH ROLL MODE (EIGENVALUE = -6.00 +/- j 3.46)
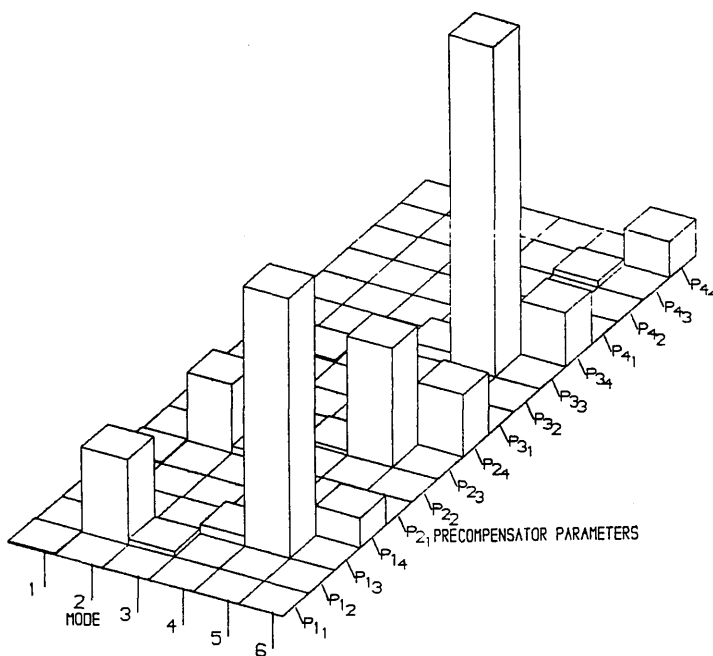
Figure 3.26: Modulus of Normalized Principal Angle Sensitivities Against Flight Path Controller Precompensator Gains and Mode Numbers.

fast pitch and lateral modes with respect to feedback parameter variations. Figure 3.17 shows the eigenvector sensitivities of the Flight Path Controlled system with respect to the feedback gains. The eigenvector sensitivity histograms for each mode are identical to the eigenvalue sensitivity histograms (Figure 3.15). The scales on the histograms may be different but both sets of plots show the modes being affected by a consistent set of parameters. The self—consistency of the eigenstructure sensitivity results even holds for the principal angle sensitivities shown in Figure 3.19. The eigenstructure sensitivities uniquely identify which feedback parameters are important in terms of each system mode, its stability and coupling. The three dimensional histograms of eigenstructure sensitivities to feedback parameters (Figures 3.16, 3.18 and 3.20) show similar trends but they are not identical. All of these graphs show that the slow pitch mode is the most sensitive followed by the phugoid mode and the Dutch roll mode, for feedback parameters. However, Figures 3.16, 3.18, and 3.20 show differences in the relative sensitivity of each mode. The eigenvector sensitivity plot in Figure 3.18 shows the slow pitch mode to be much more sensitive in relation to the other modes than either the eigenvalue sensitivities or the principal angle sensitivities. In contrast, the eigenvalue sensitivities in Figure 3.16 show the Dutch roll mode to be more sensitive to K_{48} than is shown in Figures 3.18 or 3.20 in a relative sense.

The eigenvalue sensitivities to precompensator gains are shown in Figures 3.21 and 3.22. As was the case for the feedback gains, the histograms of eigenvalue sensitivity versus precompensator gains can be used to identify easily which parameters influence each of the modes. The eigenstructure sensitivities with respect to precompensator gains are self—consistent for a given mode. The eigenvector and principal angle sensitivities plotted in Figures 3.23 and 3.25 show the same precompensator parameters affecting each mode. Ignoring the scaling factor, the graphs are identical. The reason why the eigenstructure sensitivities are self—consistent for each mode becomes clear once one remembers that it is the eigenvalues in conjunction with the principal angles which govern the choice in eigenvectors. Therefore, one would expect that a control system gain which strongly affects the eigenvalues will also have a strong influence on the eigenvectors and principal angles. The consistency of the sensitivity results between modes breaks down again for the precompensator parameters as shown in Figures 3.22, 3.24, and 3.26. In relation to other modes, the Dutch roll mode eigenvalue is more sensitive to precompensator changes than is the Dutch roll eigenvector or principal angle, while the slow pitch mode's principal angle appears more sensitive than the mode's eigenvalue or eigenvector in comparison with the

spiral mode sensitivities. The spiral mode appears to be influenced to the greatest extent by the precompensator parameters.

The following table shows how the parameters have been classified for each of the modes.

Table 3.2: Classification of Flight Path Controller Parameters

Mode	Category			
	A	B	C	D
Fast Pitch Mode	P_{11}, P_{21}	K_{13}	K_{12}, K_{22}	K_{14}, K_{23}, K_{24}, P_{12}, P_{13}
Slow Pitch Mode		K_{13}, K_{23}, P_{12}, P_{22}		K_{14}, K_{21}, K_{24}, K_{33}, K_{34}, P_{13}, P_{23}, P_{24}
Phugoid Mode		K_{13}, K_{23}, K_{23}, P_{12}, P_{24}		K_{14}, K_{21}, K_{33}, K_{34}, P_{13}, P_{23}, P_{32}
Roll Mode		K_{36}, P_{13}, P_{33}		K_{16}, K_{26}, K_{27}, K_{33}, K_{37}, K_{38}, K_{46}, K_{47}, K_{48}, P_{23}, P_{24}, P_{34}, P_{43}
Spiral Mode		K_{36}, K_{37}, K_{38}, K_{47}, P_{13}, P_{33}	K_{18}, K_{28}	K_{13}, K_{16}, K_{17}, K_{23}, K_{24}, K_{26}, K_{27}, K_{33}, K_{34}, K_{46}, K_{48}, P_{23}, P_{43}
Dutch Roll Mode	P_{44}	K_{48}, P_{24}, P_{34}	K_{35}, K_{45}, P_{14}	K_{38}

Considering the set of adustment parameters as chosen using transfer function sensitivities; P_{11}, P_{22}, and P_{33} strongly affect the eigenstructure, P_{23} and P_{32} weakly affect the eigenstructure, and P_{31} is not seen to influence the eigenstructure greatly. The results of the two identification procedures are similar

in spite of the different sensitivity measures used to classify the parameters. Although eigenstructure sensitivities cannot be used in the adjustment algorithm, the results of this section support the procedures which are being used in the selection of parameters to adjust.

CHAPTER 4: CONTROLLER OPTIMIZATION THEORY

4.1) Present Optimization Techniques

The need to adjust the flight systems of helicopters is not a new problem. However, the trial and error techniques which are presently being used will undoubtedly be inadequate for full—authority fly—by—wire flight controllers. The trial and error approach involves making a series of test flights with slightly different parameter settings and then choosing the best set of controller values. For flight controllers which have been developed using classical techniques in a loop by loop analysis, this approach can give good results because of the relatively small set of controller parameters which can be adjusted. However, the fundamental difficulty with this approach is that it suffers from a lack of quantitative information concerning how parameters should be adjusted. Trial and error tuning can be highly iterative in consequence. Modern, fully integrated controllers will have many parameters, and it will be difficult to know which of these parameters will significantly affect the system's response and the manner in which they will do so. The tuning procedure must address these two related problems.

4.2) The Use of Sensitivity Functions for Tuning Flight Controllers

Sensitivity functions provide information concerning the two aspects of the tuning problem. First, sensitivity functions can be used to provide a measure of the extent to which the system response will be altered by changing control system parameter values. As previously stated (Section 3.3), transfer function sensitivities can be normalized to yield valuable information concerning the significance of various parameters. A parameter which shows dominance with regard to a particular transfer function will also be important in terms of the time domain response of the corresponding output state to the appropriate input. Thus, transfer function sensitivities help to answer the question of which parameters to use in the tuning process. The second aspect of the tuning problem, that of knowing how parameters will affect system response, is also answerable through the use of information from the sensitivity functions. If one is performing a time domain optimization, then the state variable sensitivities show

how the state responses will be affected by control system parameter shifts. In the frequency domain, equivalent information is contained in the transfer function sensitivities.

Since the state variable sensitivities and the transfer function sensitivities provide equivalent information, tuning can be completely carried out in the time domain. That is, all adjustments to controller parameters will be based on state variable sensitivities and transfer function sensitivities will only be used to select which parameters to adjust. The decision to work in the time domain is based on the fact that state variable sensitivities can be generated with fewer calculations than transfer function sensitivities.

The adjustment algorithm is based on the idea that from the sensitivity functions, it is possible to predict the changes which will occur to the system response, as a result of changing the parameter values in the flight control system. The prediction of what the modified state response will be is generated using Newton—Raphson techniques. The predicted system response after parameter shifts, to second order accuracy, is given by,

$$\underline{x}_m(t) = \underline{x}_a(t) + \left[\frac{\partial \underline{x}_a(t)}{\partial \alpha} \right] \underline{\Delta A}_1 + \left[\frac{\partial^2 \underline{x}_a(t)}{\partial \alpha \partial \beta} \right] \underline{\Delta A}_2$$

Equation 4.1

Where $\underline{x}_m(t)$ is the predicted or modified system response
$\underline{x}_a(t)$ is the measured or actual system response
$[\partial \underline{x}_a(t)/\partial \alpha]$ is the matrix of first order sensitivity funtions
of the actual system response
$[\partial^2 \underline{x}_a(t)/\partial \alpha \partial \beta]$ is the matrix of second order sensitivity
functions of the actual system response
$\underline{\Delta A}_1 = [\Delta \alpha_1 \ \Delta \alpha_2 \ \dots \ \Delta \alpha_n]^T$
$\underline{\Delta A}_2 = [\Delta \alpha_1 \Delta \alpha_1 \ \Delta \alpha_1 \Delta \alpha_2 \ \dots \ \Delta \alpha_n \Delta \alpha_n]^T$

The modified response can be predicted using both first and second order sensitivity functions or solely from first order sensitivities. The first order equivalent of Equation 4.1 can be obtained simply by setting $[\partial^2 \underline{x}_a(t)/\partial \alpha \partial \beta]$ to equal zero. As will be seen in Chapter 5, the use of second order sensitivities can enhance the convergence properties of the tuning process by allowing a more accurate prediction of the effects of various parameter changes.

4.3) Performance Indices

In order to systematically tune a flight control system, there must be a criterion by which improvements in system response can be measured. Sensitivity functions allow the prediction of what the structure of the modified system response will be, but this information is virtually useless if it is not possible to say quantitatively that one response is better than another. For each set of possible control system parameter values, a figure of merit must be assigned to the system response. By comparing the figures of merit associated with various sets of parameter perturbations, it is possible to identify a set of changes to make to the existing values which will lead to the greatest improvement in system response.

The figures of merit used to compare the possible sets of parameter values can take many forms. Each figure of merit will be calculated using a performance index, J, which in general will simply be a function of the modified state response, $\underline{x}_m(t)$.

$$J = J \left[\underline{x}_m(t) \right] \qquad \text{Equation 4.2}$$

Since any performance index can be described such that the best solution yields a minimum, the tuning problem reduces to using the sensitivity functions to predict a new set of controller parameter values which will minimize the given performance index, J.

Two distinct performance indices have been considered in the present study. The first is the Least Integral Error Square Performance Index, J_{MR}, described in Chapter 5, which attempts to tune the system response towards an ideal system response. It is a model reference technique. The second performance index is the Handling Qualities Performance Index, J_{HQ}, which attempts to improve system handling qualities directly (Chapter 6). As will be seen, both of these performance indices rely for their calculation on information which is not provided by the system to be tuned. In the model reference case, J_{MR} relies on a description of the 'ideal' system response. The handling qualities index, J_{HQ}, on the other hand, makes use of specifications of desirable handling qualities. Therefore, although the structure of the tuning process is equivalent in the two cases, the nature of the tuning can be completely different if the 'ideal' response does not possess desirable handling qualities.

It was decided at an early stage in the development of the adjustment algorithm that perturbations to the designed controller parameter values should be

kept to a minimum. This led to the decision to restrict the range over which parameter values could migrate, motivated by the fact that during the tuning process, attempts were to be made to maintain the underlying control strategy as much as possible. There seems little point in letting the tuning process move the controller's dynamics significantly away from those which it was designed to have. The easiest method of accomplishing this objective was to restrict control system parameter movement. The optimization methods which are used allow bounds to be placed on the range over which controller parameters may be adjusted.

4.3.1) Minimization Routine Theory

The search for the set of control system parameter values which minimize the chosen performance index is performed on the computer using the routine E04JAF of the Numerical Algorithm Group (NAG) Libraries [53]. This algorithm calculates values of the performance index with various parameter sets subject to bounds on the parameters. Quasi–Newton methods are used by the algorithm to select the control system parameter sets for which the performance index is evaluated. The theoretical basis for the quasi–Newton algorithm which is employed is given by Gill and Murray [54].

Let the Hessian matrix of the performance index be [H] where the elements of [H] are the second order partial derivatives of the performance index with respect to the adjustable controller parameters.

$$H_{ij} = \frac{\partial^2 J}{\partial \alpha_i \partial \alpha_j} \qquad \qquad \text{Equation 4.3}$$

The feature which distinguishes quasi–Newton methods from Newton–type methods is in how the Hessian matrix, [H], is updated from iteration to iteration in the optimization algorithm. In Newton–type methods, [H] is explicitly calculated during each iteration, while in quasi–Newton methods, [H] is an updated version of the previous estimate of [H] [54]. Since the Hessian matrix, [H], cannot be calculated in closed form in the present application, the adjustment algorithm was forced to use quasi–Newton techniques. Similarly, the gradient of the performance index, $\underline{h}$, must also be approximated by finite differences at each iteration since it cannot be calculated in closed form. The data used in the finite difference calculations for $\underline{h}$ are the previous estimates of the performance index, J, for the various parameter sets. The elements of the

gradient, $\underline{h}$, are given by,

$$h_i = \frac{\partial J}{\partial \alpha_i} \approx \frac{\Delta J}{\Delta \alpha_i}$$

Equation 4.4

Five distinct steps are involved in each iteration of the optimization algorithm. In the first step, any variables which are on their bounds are tested using gradient information (from $\underline{h}$) to decide if they should be held at their current positions or allowed to move away. A search direction for the minimum in terms of parameter changes is made during the second step on the basis of the gradient, $\underline{h}$, and the Hessian, [H]. The third step is to determine how far to move the evaluation point for J in the search direction. The evaluation of the performance index is implicit at this stage of the calculations. Next is a calculation of the new control system parameter perturbations. The problem of tuning flight contol systems has been formatted such that the NAG optimization algorithm works with perturbations to the starting set of controller parameter values rather than their absolute values. The last step, during an iteration, involves finding the matrix elements of the Cholesky decompostion of the Hessian, [H]. These factors of [H] are then available for the next iteration. The search terminates when the norm of the gradient, $\underline{h}$, is sufficiently small and the Lagrange multipliers used by the algorithm are larger than a prescribed tolerance. A more in depth discussion of the calculations and their theoretical basis is provided by Gill and Murray [54].

CHAPTER 5: MODEL REFERENCE TUNING

5.1) Least Integral Error Square Performance Index

The objective of the Least Integral Error Square Performance Index is to make the system responses as similar as possible to desired or *'ideal'* system responses. These *'ideal'* responses can be generated by any means, but are in general just the responses which one generates from the simulation model used for the design of the control system [55].   When the simulation model and the actual system are excited by the same inputs, there will be differences in the responses which one observes from the two systems.   With the Least Integral Error Square Performance Index, the difference between the two signals is squared and integrated to yield a measure of the difference between the two responses.   The difference between the two signals is squared in order to avoid positive and negative excursions of the difference signal cancelling each other.

In the past, single–input single–output systems have been successfully tuned using a Least Integral Error Square Performance Index.   For these systems, the time domain adjustment algorithm is given by Winning et.al. [41]. The necessary changes to the controller parameters, α_i, can be determined if the actual system response, $x_a(t)$, the desired system response, $x_d(t)$, and the system's sensitivity functions, $\partial x_a(t)/\partial \alpha_i$, are known.   The first order adjustment equation used by Winning et.al. [41] is given by,

$$x_d(t) = x_a(t) + \sum_i \frac{\partial x_a(t)}{\partial \alpha_i} \Delta \alpha_i + R_e(t) \qquad \text{Equation 5.1}$$

Where $R_e(t)$ is a residual error
   $\Delta \alpha_i$ is the required change in parameter α_i

Equation 5.1 can be rearranged to solve for the residual error $R_e(t)$. Winning et.al. [41] then proceed to substitute for $R_e(t)$ into the integral least square error given as,

$$J = \int_0^T \left[R_e(t) \right]^2 dt \qquad \text{Equation 5.2}$$

By minimizing Equation 5.2, it is possible to find the set of controller

parameters α_i which is optimal in terms of minimizing the difference between the desired response and the actual system response. In practice, the process required a small number of iterations to obtain the closest fit to the desired response.

The primary constraint on the expansion of the single-input single-output tuning theory [41] towards multivariable systems is in the generation of sensitivity functions. For single-input single-output systems, sensitivity functions can be generated by either a sensitivity cosystem or the signal convolution method in real time. For multivariable systems, only a sensitivity cosystem can yield the state variable sensitivity functions without offline signal processing. The possibility of using a sensitivity cosystem with a Least Integral Error Square Performance Index to tune an Advanced Boiling Water Reactor with multivariable controller has been successfully explored by Winkelman [55]. Unfortunately, dynamic modelling of helicopters is not sufficiently accurate for a sensitivity cosystem to be employed to tune flight control systems. Indeed, lack of information concerning the helicopter plant produces the need for tuning in the first place and one of the fundamental constraints on the project is that the plant must be treated as a 'black box'. The decision to use signal convolution techniques is based on this fact and forces one to accept that tuning will not be performed in real time.

The multivariable nature of helicopter flight control also forces changes in the manner in which the Least Integral Error Square Performance Index is calculated. The second order, multivariable equivalent of Equation 5.1 is,

$$\underline{x}_d(t) = \underline{x}_a(t) + \left[\frac{\partial \underline{x}_a(t)}{\partial \alpha} \right] \Delta A_1 + \left[\frac{\partial^2 \underline{x}_a(t)}{\partial \alpha \partial \beta} \right] \Delta A_2 + \underline{R}_e(t)$$

Equation 5.3

Adopting the notation of Equation 4.1 for the modified system response, $\underline{x}_m(t)$, it is possible to express Equation 5.3 in terms of the projected residual error vector, $\underline{R}_e(t)$.

$$\underline{R}_e(t) = \underline{x}_d(t) - \underline{x}_m(t) \qquad\qquad \text{Equation 5.4}$$

In analogy with Equation 5.2, the performance index to be minimized becomes the time integral of the inner product of the residual error vector.

$$J = \int_0^T \left[\underline{R}_e(t), \underline{R}_e(t) \right] dt \qquad\qquad \text{Equation 5.5}$$

For helicopter applications, it is necessary to tune with regard to dynamics which are excited by all four pilot inceptors. Therefore, the performance index must be capable of optimizing with regard to more than one input signal. For example, if the actual aircraft system has undesirable phugoid and fast pitch characteristics, it is beneficial to be able to tune the controller with respect to these two modes simultaneously to avoid improving one mode at the possible expense of the other. If the phugoid dynamics are excited by an input confined to the longitudinal inceptor and the fast pitch dynamics are excited by an input on the vertical inceptor, it makes sense to stimulate the system with separate inputs on each of these inceptors. The response to each of these separate inputs is then to be used as data for the tuning process. It is beneficial to take the data in two distinct test sequences rather than using the two inputs in close succession in a single test. The problem with performing a single data run in which the longitudinal inceptor is excited followed by the vertical inceptor is that the fast pitch mode excitation would occur at a time when the phugoid was already excited. The phugoid mode would then add dynamics to the fast pitch section of the measured time history and this would create a bias towards phugoid tuning at the expense of fast pitch tuning. Therefore, the Least Integral Error Square Performance Index, J_{MR}, is the sum over Ω distinct time histories.

$$ J_{MR} = \sum_{\Omega} \left\{ \int_0^T \left[\underline{R}_e(t), \underline{R}_e(t) \right] \, dt \right\} \qquad \text{Equation 5.6} $$

When one remembers that the residual error vector is a function of the control system parameters, α_i, Equation 5.6 helps to make it clear that the α_i's must be optimized in a three dimensional sense: changes in parameters, $\Delta\alpha_i$, must not only be chosen to minimize the relative error on a state with time, but also to minimize error across the various output states and with respect to the Ω time histories as well. This is particularly true in a highly coupled system such as a helicopter because each control parameter may influence each state in a fully integrated, multivariable flight control system.

Although J_{MR} allows tuning of parameters with respect to time, across all of the output states, and across several inputs, there are problems associated with model reference tuning for flight control systems. One of the fundamental concerns regarding the use of this performance index is the question of how one ensures that the 'ideal' response is in fact ideal. By using the design model to generate the 'ideal' signal, one is probably coming as close to ideal as possible,

provided that care has been taken to ensure that the response of the design model with controller satisfies the performance specifications for the design. In the case of helicopters, these performance specifications are found in Reference [56]. One of the motivating factors in the development of the Handling Qualities Performance Index, J_{HQ}, is the fact that the design process of using computer simulation models does not preclude a design from having poor handling qualities. If a control system is tuned towards a design model with unsatisfactory handling qualities, then the result will be a helicopter flight controller which yields poor handling characteristics. The second concern over the use of a Least Integral Error Square Performance Index is that the system response may only be tuned for the input sequences used during the tuning process. In helicopter applications, it will be impossible to tune the controller with regard to the infinite set of pilot inputs which may be used throughout the flight envelope. It is, therefore, important that tuning on helicopters relies on input signals which are representative of as many manouevres as possible. Chapter 3 showed that sensitivity functions for nonlinear systems can be inaccurate when generated using signal convolution techniques. In light of such results, it will not be possible to use the algorithm to tune some manoeuvres because the pilot inputs which are used will lead to erroneous calculations of the sensitivity functions.

5.2) Linear System Results

In order to test the Least Integral Error Square Performance Index, J_{MR}, using simulation models, it was necessary to have a system which yields a desirable response and one which yields the actual response. The desirable response is provided by the design model with the designed set of controller values, while the actual response is also provided by the design model, but with a perturbed set of controller parameters. The task for the tuning process is then to retrieve the original design parameters working only with the outputs of the desirable system and the actual system (perturbed parameters).

Preliminary trials were conducted using the Parry Modal Controller of Section 2.2.3. The feedback parameter K_{13} was perturbed by over 9% in the actual system to yield a perturbed feedback matrix, $[K_p']$. The tests demonstrated that the output responses of the actual system could be effectively tuned. The actual system's feedback matrix, $[K_p']$, did converge towards the desired feedback matrix, $[K_p]$, with successive passes of the tuning process.

During these initial tests, three rules of thumb were identified which, when employed, help to improve the performance of the adjustment algorithm. First, the system should be tuned with respect to the response to pilot input signals which involve all four of the pilot inceptors. By using all of the inceptors to excite the system, the system responses provide more information to the adjustment algorithm than that gained if the tuning was based on system responses to pilot inputs on a single inceptor, such as the vertical velocity inceptor. In all of the tests which are reported, four time histories of the system response were collected as data − one for each of the pilot inceptors.

Secondly, it is advantageous to use as many parameters as possible during the adjustment. Allowing a large number of parameters to move helps decrease the size of the parameter perturbations which are made. It was found that improvements could be made by changing a few parameters by a large amount or alternatively by moving a large number of parameters by a small amount. As perturbations to parameter values are to be kept to a minimum, as many parameters as possible should be used. Due to limited space on the VAX 11−750 computer which was used for the work, the number of adjustment parameters which can be used is restricted to eight.

Finally, a sampling rate of at least 8 Hz. and preferably 32 Hz. or more should be used. The accuracy of the calculations of the performance index improves with higher sampling rates. This is undoubtedly due to the increased accuracy of the time histories which are used to provide information concerning the system's dynamics. Increasing the sampling frequency above 32 Hz. does not significantly improve the tuning and this would seem to indicate that most of the dynamics of the system have been adequately represented by sampling at 32 Hz.

Two tests of model reference tuning were performed using linear models to show the difference between the use of first and second order sensitivity information. The Flight Path Controller − eighth order HELISTAB plant system was used both as the desired and the actual system. In order to test the convergence properties of model reference tuning, three of the precompensator parameters of the Flight Path Controller were perturbed in the simulation model representing the actual system.

Figures 5.1 through 5.4 show the improvements which are made to the system response with one pass of the model reference tuning algorithm using only first order sensitivity functions. The desired responses on these plots, as in all of the following plots, is shown as a solid line. The original response of the actual system is shown by asterisks and the tuned response is shown by the dashed lines. The four figures show the responses to: a 0.5 second pulse on the vertical

Figure 5.1: Flight Path Controlled Linear System Tuning, First Order Sensitivities, Vertical Inceptor Pulse Input, —— Desired Response, * * Untuned Response, – – Tuned Response, Initially Perturbed Parameters: P_{11}, P_{22}, P_{33}.

Figure 5.2: Flight Path Controlled Linear System Tuning, First Order Sensitivities, Longitudinal Inceptor Pulse Input, —— Desired Response, * * Untuned Response, – – Tuned Response, Initially Perturbed Parameters: P_{11}, P_{22}, P_{33}.

U (Ft/sec) versus TIME (sec)

V (Ft/sec) versus TIME (sec)

V (Ft/sec) versus TIME (sec)

P (rad/sec) versus TIME (sec)

Q (rad/sec) versus TIME (sec)

PHI (rads) versus TIME (sec)

THETA (rads) versus TIME (sec)

R (rad/sec) versus TIME (sec)

Figure 5.3: Flight Path Controlled Linear System Tuning, First Order Sensitivities, Lateral (Roll) Inceptor Doublet Input, —— Desired Response, * * Untuned Response, – – Tuned Response, Initially Perturbed Parameters: P_{11}, P_{22}, P_{33}.

U (ft/sec) versus TIME (sec)

V (ft/sec) versus TIME (sec)

V (ft/sec) versus TIME (sec)

P (rad/sec) versus TIME (sec)

Q (rad/sec) versus TIME (sec)

PHI (rads) versus TIME (sec)

THETA (rads) versus TIME (sec)

R (rad/sec) versus TIME (sec)

Figure 5.4: Flight Path Controlled Linear System Tuning, First Order Sensitivities, Pedal (Lateral Velocity) Inceptor Pulse Input, —— Desired Response, * * Untuned Response, – – Tuned Response, Initially Perturbed Parameters: P_{11}, P_{22}, P_{33}.

inceptor (Figure 5.1); a 0.5 second pulse on the longitudinal inceptor (Figure 5.2); a doublet of 1.0 second period (no deadband) on the roll inceptor (Figure 5.3); and a 0.5 second pulse on the lateral velocity inceptor (Figure 5.4). In response to the vertical inceptor pulse, the differences between the dynamics of the untuned system and the desired system are primarily evident in the lateral velocity, v, response (Figure 5.1). The lateral velocity responses are also different for the two systems excited by a longitudinal inceptor pulse and a roll inceptor doublet (Figures 5.2 and 5.3 respectively). The responses of the two systems differ the most for the doublet input on the roll inceptor and differ the least for the pulse input on the lateral velocity inceptor (Figure 5.4). The large differences on the lateral velocity channel and for responses to the roll inceptor are most likely due to the previously described deficiencies of the Flight Path Controller in terms of roll authority. Since roll authority is weak for the desired system, any changes to the controller values are likely to further aggravate the coupling of energy into other states, thereby illuminating the differing dynamics of the untuned system. One fact which is clear from the results shown in Figures 5.1 to 5.4 is that the responses of the states are all improved at each instant of time and for each pilot input. Indeed, the dashed lines indicating the tuned response are, in general, indistinguishable from the desired response, with the lateral velocity response to vertical inceptor (Figure 5.1) as the only noticable exception. The value of the model reference performance index, J_{MR}, confirms this result since it has been reduced from the initial value of 0.30 to 1.0×10^{-3}. After a second iteration of the adjustment algorithm, J_{MR} is further reduced to 4.3×10^{-6}.

Table 5.1 shows the desired set of adjustment parameter values, the untuned values, and the tuned values after each iteration of the tuning process. By an iteration of the tuning process, it is meant that the adjustment algorithm is applied to new, updated system responses generated with the improved parameter values of the previous iteration. The precompensator parameters P_{33}, P_{11}, and P_{22} were all perturbed by 10% initially while P_{23}, P_{31}, P_{32}, and P_{44} were set to their desired values. During the first pass of the tuning process, all three of the perturbed parameters are moved closer to their designed values, P_{31} and P_{32} are held at their correct values, and P_{23} and P_{44} are shifted by -0.25% and 0.05% respectively. The adjustment algorithm is correctly identifying those parameters which require changing and those which are at their proper values. The very small deviations in parameters which remain after the second pass of the tuning process shows that the sensitivity functions are accurately predicting the changes which will be made to system dynamics and that the parameters converge

rapidly to their proper values.

Table 5.1: The Improvement in Tuned System Response with First Order Sensitivities

Parameter	Desired Values	Untuned Values	Tuned Values Pass 1	Tuned Values Pass 2	Final % Deviation
P_{33}	-.01728	-.01555	-.01719	-.01727	-.056
P_{11}	-.01140	-.01026	-.01124	-.01139	-.088
P_{23}	-.00405	-.00405	-.00404	-.00405	.000
P_{22}	-.00316	-.00348	-.00319	-.00316	.000
P_{31}	-.00301	-.00301	-.00301	-.00301	.000
P_{32}	.00069	.00069	.00069	.00069	.000
P_{44}	.01989	.01989	.01990	.01990	.050

The improved results of using both first and second order sensitivities is shown in Figures 5.5 to 5.8, which are the second order counterparts of Figures 5.1 to 5.4. The use of second order sensitivities results in a faster convergence to the designed controller values. After one iteration of the tuning process the performance index is reduced from 0.30 to 6.5×10^{-4}. The second iteration reduces the performance index to 1.8×10^{-6}. In general, the reduction in performance index per iteration is greater when using second order sensitivites in addition to using solely first order sensitivities since the use of the former allows a better prediction of the value of the performance index for a given set of parameter variations. For the first order optimization (Figures 5.1 to 5.4), the ratio between the actual performance index for the tuned system and the projected final performance index, as estimated by the algorithm, was 11:1 for the first iteration and 13:1 for the second iteration. In contrast, the ratio of actual to projected performance index for second order sensitivities was 8.0:1 for the first iteration and 9.3:1 for the second iteration. In terms of the parameter variations during this test, the individual parameter values also converge to their proper (designed) values at a faster rate with the use of second order sensitivities.

An argument against the use of second order sensitivities is that the
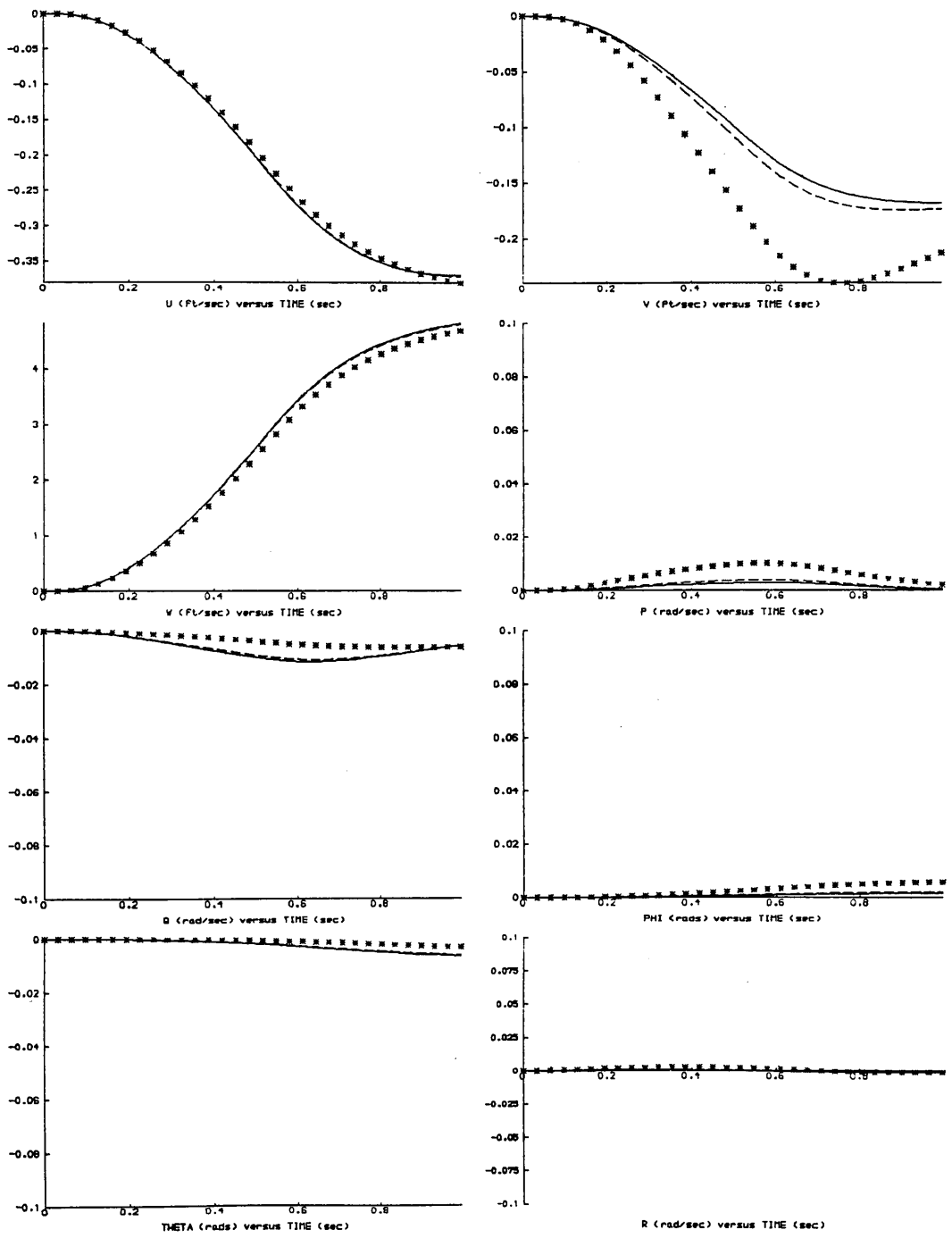
Figure 5.5: Flight Path Controlled Linear System Tuning, Second Order Sensitivities, Vertical Inceptor Pulse Input, —— Desired Response, * * Untuned Response, – – Tuned Response, Initially Perturbed Parameters: P_{11}, P_{22}, P_{33}.
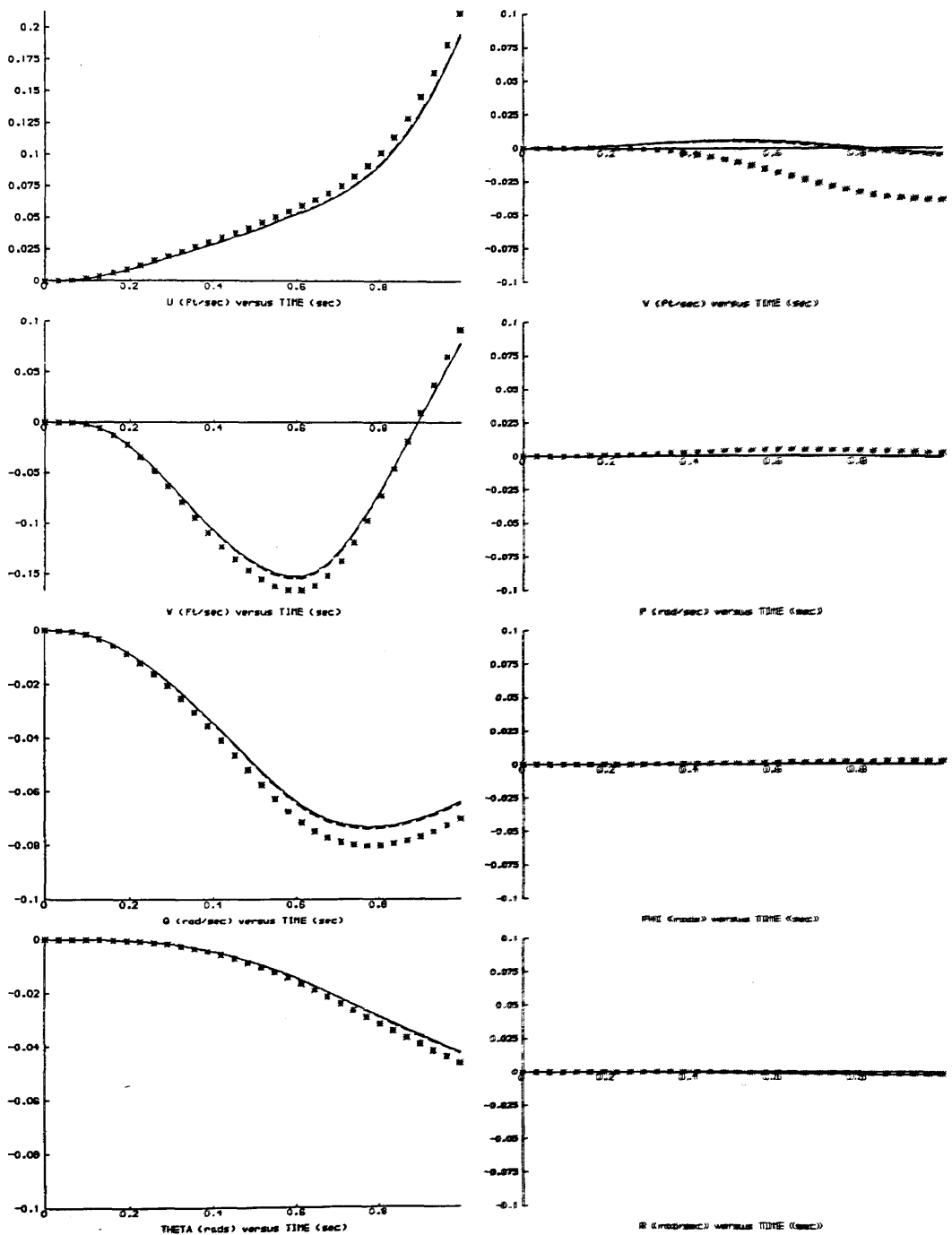
Figure 5.6: Flight Path Controlled Linear System Tuning, Second Order Sensitivities, Longitudinal Inceptor Pulse Input, —— Desired Response, * * Untuned Response, — — Tuned Response, Initially Perturbed Parameters: P_{11}, P_{22}, P_{33}.
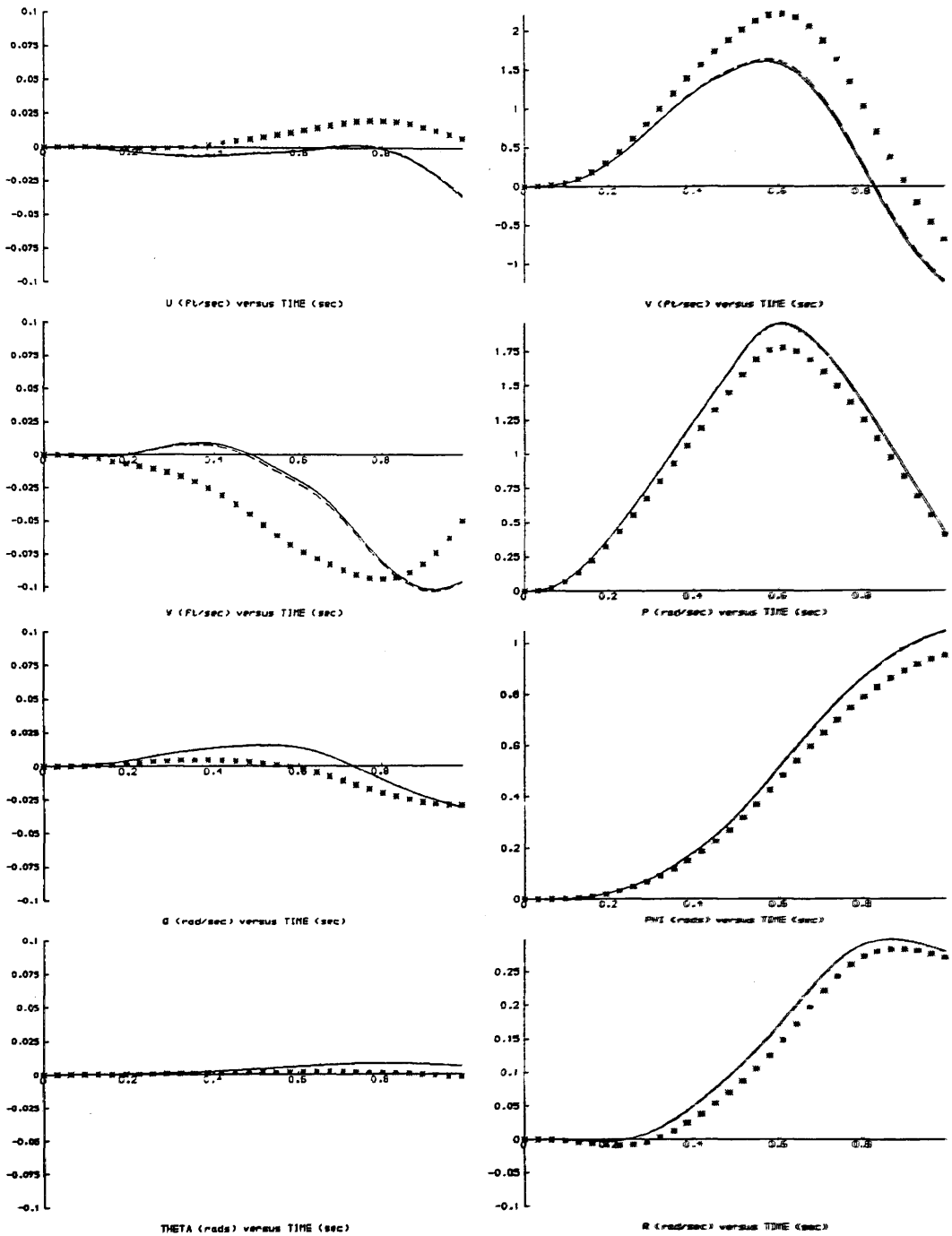
Figure 5.7: Flight Path Controlled Linear System Tuning, Second Order Sensitivities, Lateral (Roll) Inceptor Doublet Input, —— Desired Response, * * Untuned Response, – – Tuned Response, Initially Perturbed Parameters: P_{11}, P_{22}, P_{33}.
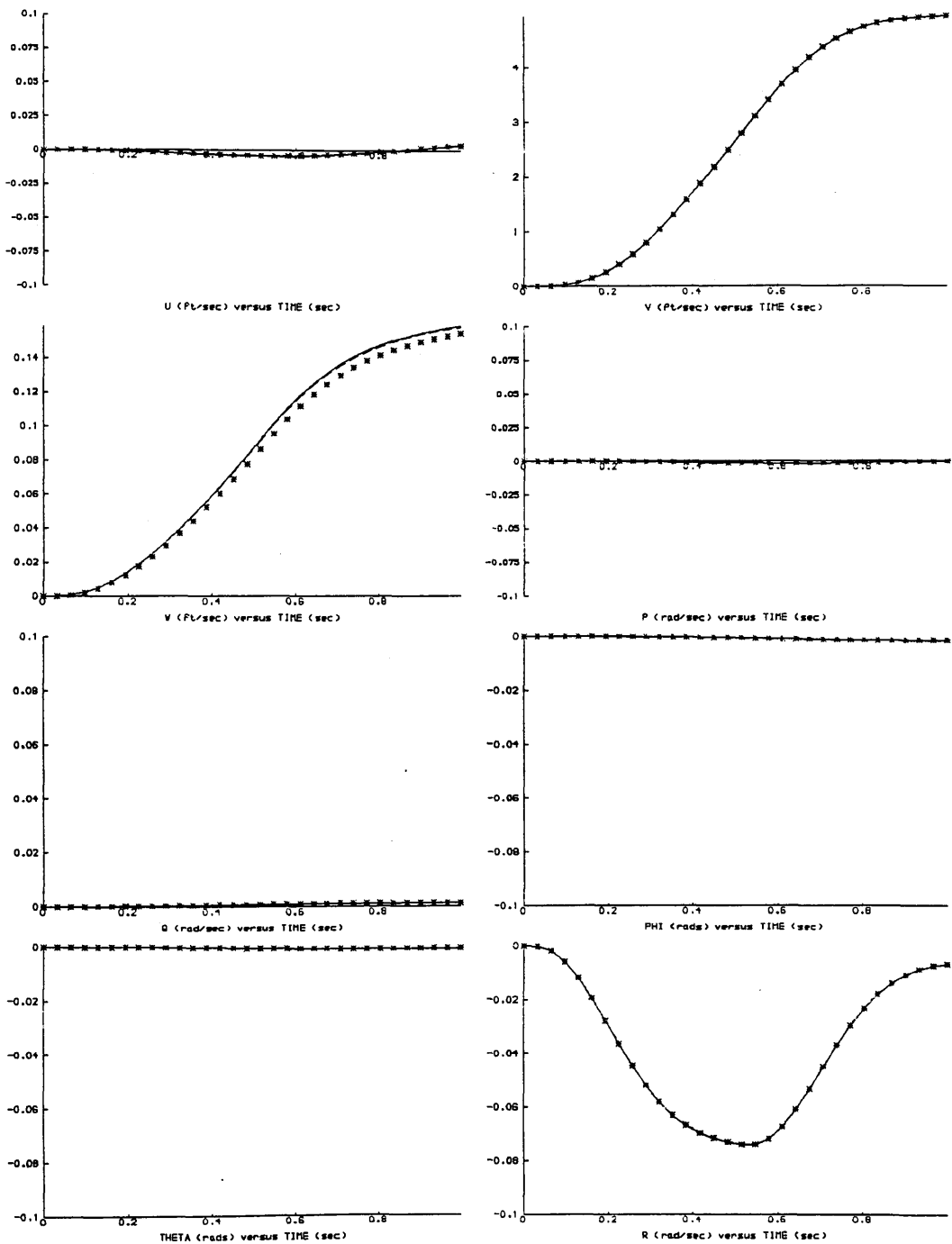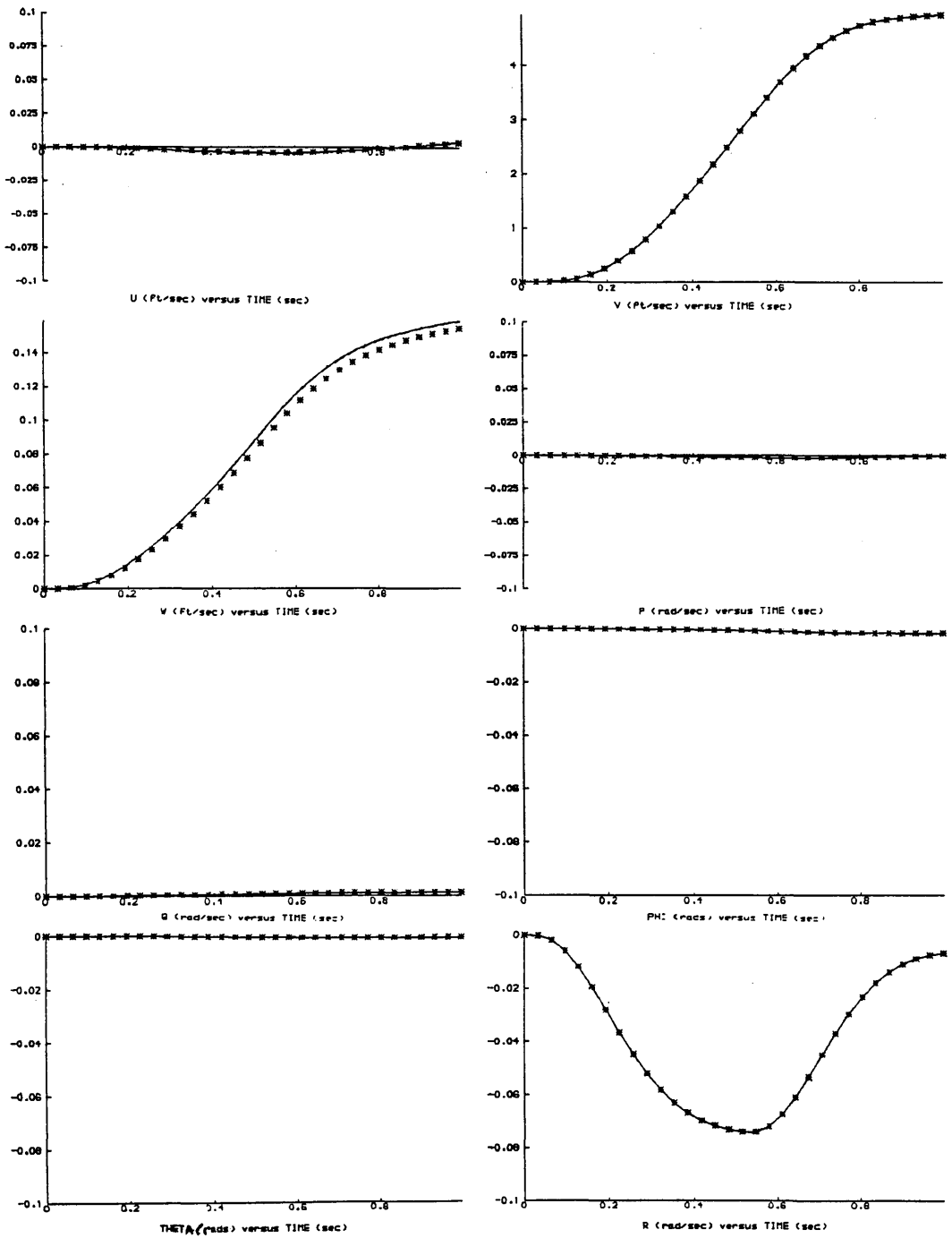
Figure 5.8: Flight Path Controlled Linear System Tuning, Second Order Sensitivities, Pedal (Lateral Velocity) Inceptor Pulse Input, —— Desired Response, * * Untuned Response, — — Tuned Response, Initially Perturbed Parameters: P_{11}, P_{22}, P_{33}.

improvement in the convergence properties of the adjustment algorithm might not be significant enough to compensate for the extra computations involved in generating the second order sensitivities. However, having considered the costs of inflight testing, the extra computational overhead of using second order sensitivities becomes less significant. Inflight testing must be kept to a minimum, and for this reason alone, one should take advantage of any improvements in the tuning process offered by second order sensitivities.

5.3) Nonlinear System Results

The results of Chapter 3 indicated that using signal convolution techniques to generate the sensitivity functions of nonlinear systems can lead to erroneous results. However, if the test inputs are such that the system operates in a linear region about the initial flight condition for the test, then improvements in response can be made. Figures 5.9 through 5.12 show the responses of two nonlinear systems. The solid lines on the graphs depict the desired system response generated from a system using the Flight Path Controller and a HELISIM3 plant without rotor dynamics. The asterisks represent the response of the same system with rotor dynamics included in the plant model. The task for the adjustment algorithm was to find a new set of controller values which would decrease the differences between the dynamics of the two systems as caused by the rotor dynamics. A sampling period of 64 Hz. was used in this test to ensure that all high order dynamics were adequately sampled. The input signal for each of the four inceptors was a doublet of 10% amplitude and a period of 1.0 seconds with no deadband. The doublet on the vertical inceptor and the lateral velocity inceptor produces responses which are virtually identical for the two systems (Figures 5.9 and 5.12 respectively). The effects of the rotor dynamics are more in evidence on the vertical velocity, w, and lateral velocity, v, responses to the longitudinal inceptor input (Figure 5.10) and on most state responses to the doublet input on the roll inceptor (Figure 5.11). The tuned response of the actual system shown by dashed lines is largely hidden on the graphs by the untuned response. The improvements in response are most in evidence on the lateral velocity, v, and roll rate, p, states of the response to a roll inceptor doublet (Figure 5.11). For the roll rate response, p, the tuned system is closer to the desired system from 0.6 seconds onwards. Between 0.4 and 0.6 seconds the tuned response is marginally worse than the untuned response. The lateral velocity, v, shows a similar trend: the tuned response is
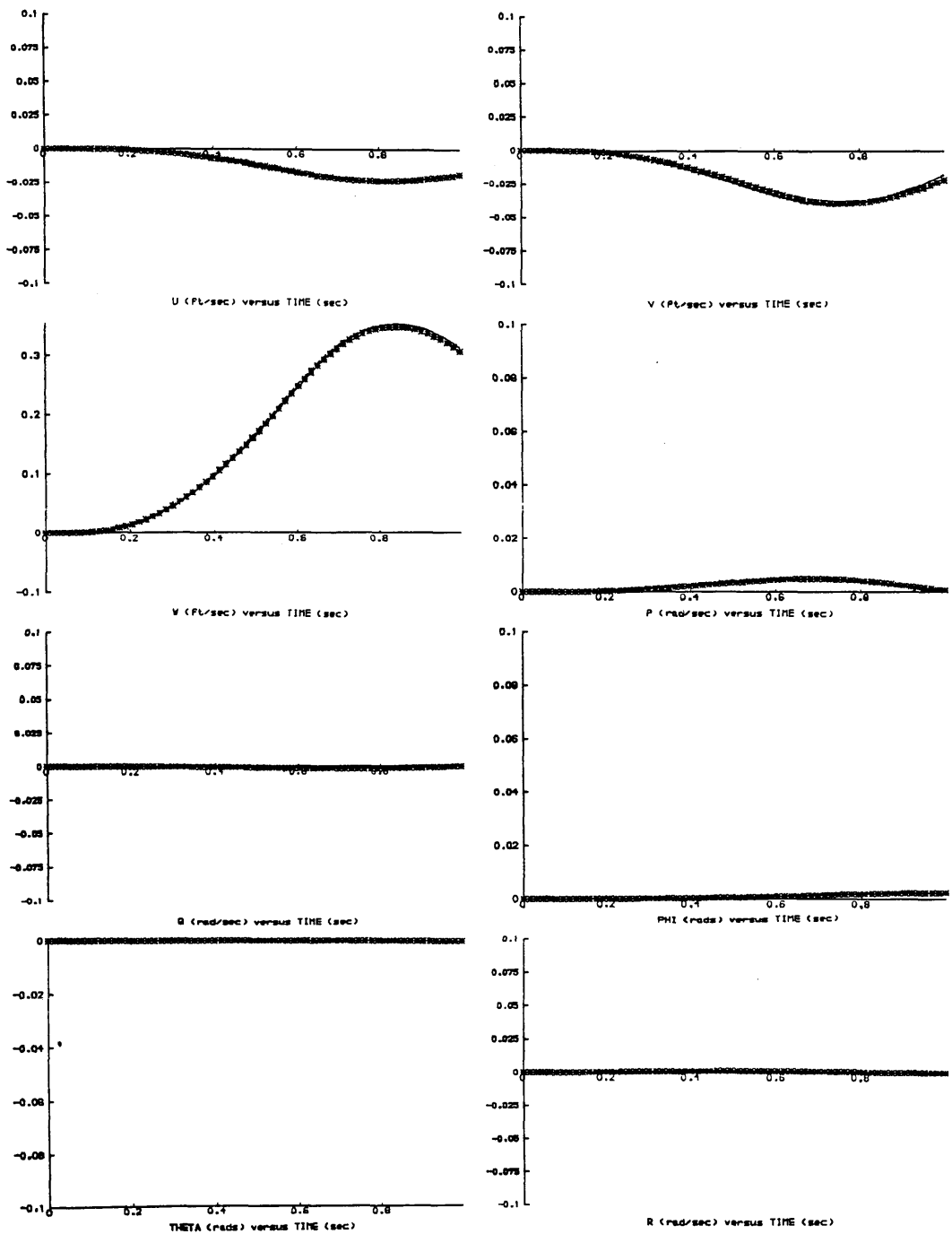
Figure 5.9: Rotor Dynamics Tuning, Flight Path Controlled Nonlinear System, Second Order Sensitivities, Vertical Inceptor Doublet Input, —— Desired Response, * * Untuned Response, — — Tuned Response.
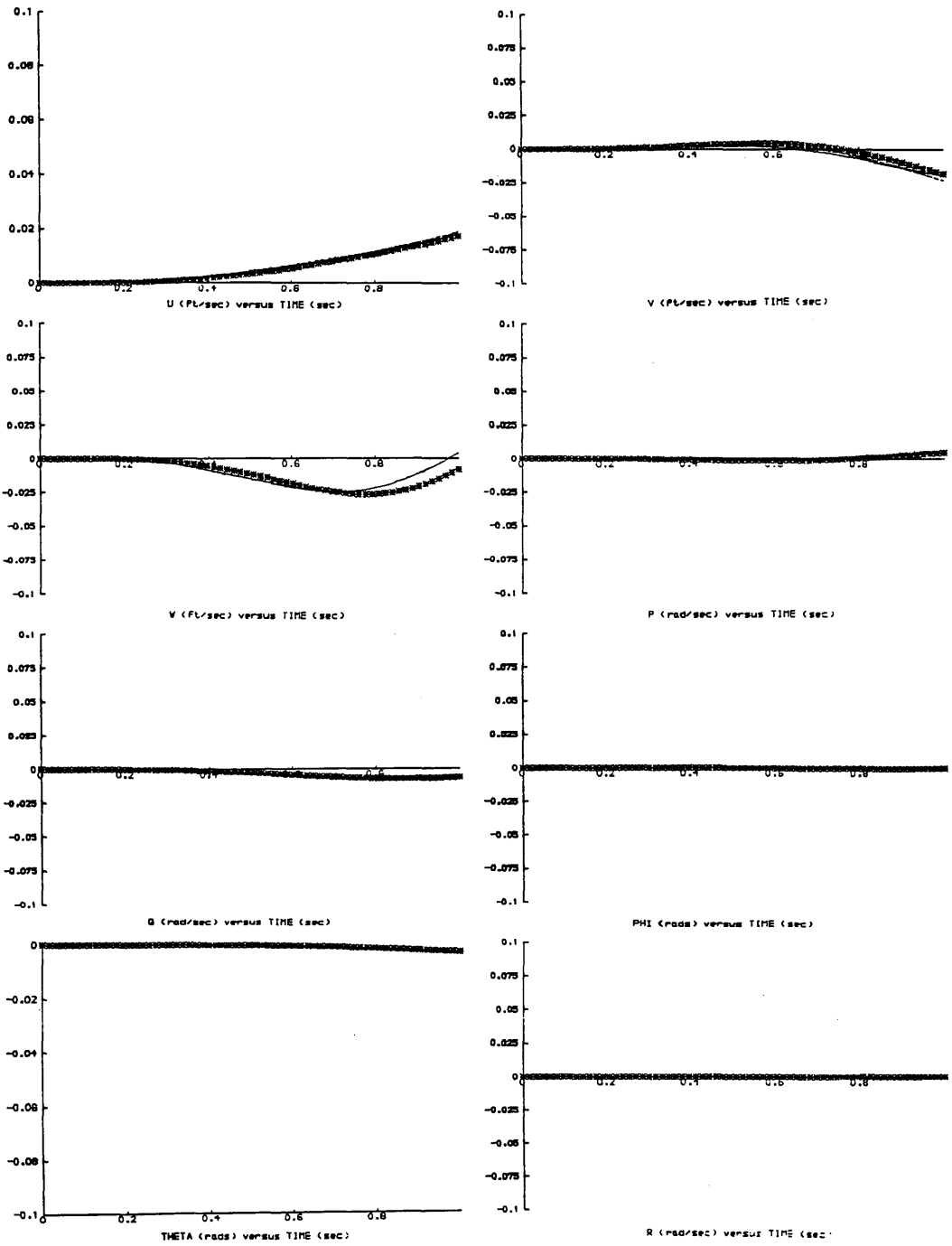
Figure 5.10: Rotor Dynamics Tuning, Flight Path Controlled Nonlinear System, Second Order Sensitivities, Longitudinal Inceptor Doublet Input, —— Desired Response, * * Untuned Response, − − Tuned Response.
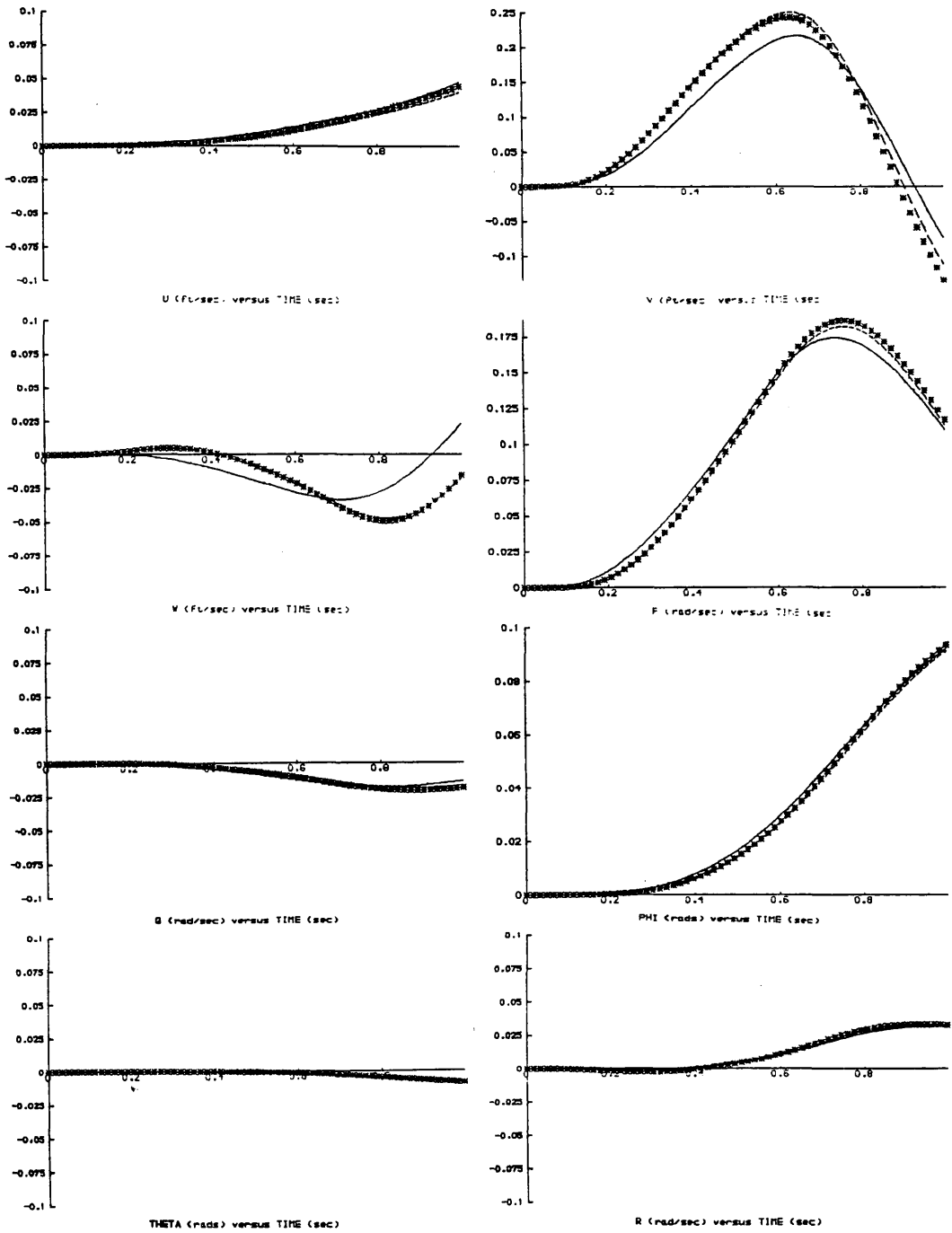
Figure 5.11: Rotor Dynamics Tuning, Flight Path Controlled Nonlinear System, Second Order Sensitivities, Lateral (Roll) Inceptor Doublet Input, —— Desired Response, * * Untuned Response, – – Tuned Response.
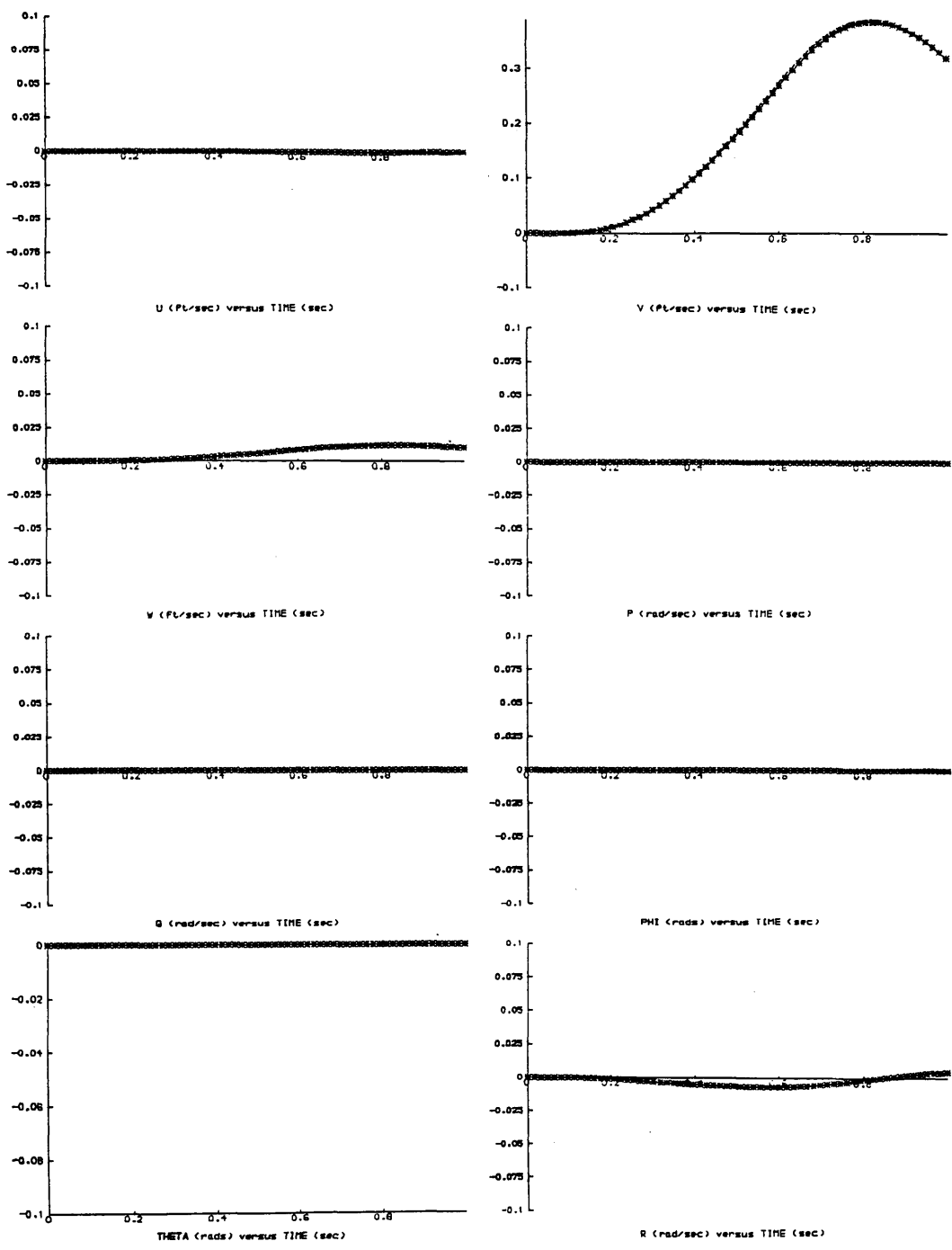
Figure 5.12: Rotor Dynamics Tuning, Flight Path Controlled Nonlinear System, Second Order Sensitivities, Pedal (Lateral Velocity) Inceptor Doublet Input, —— Desired Response, * * Untuned Response, — — Tuned Response.

worse than the untuned response between 0.6 and 0.8 seconds and better than the untuned response after 0.8 seconds. The marginal improvement in the response of the system with rotor dynamics is recorded by the performance index as a decrease from 1.2×10^{-3} to 1.0×10^{-3} for the responses shown. A second iteration of the optimization reduced J_{MR} to 0.96×10^{-3}. Although the tuning process does not seem to cope well with the problem of optimizing the controller in the presence of rotor dynamics in a nonlinear system, it is highly probable that the results could be improved by adjusting more control system parameters. Because of the memory restrictions of the Vax $11-750$ computer, it was not possible to test this hypothesis. However, the fact that the performance index was consistently reduced by the adjustment algorithm is significant. Even if the improvements in performance were marginal, the method could be applied to nonlinear systems.

When used in earnest, the model reference adjustment algorithm will attempt to move the dynamics of one system towards those of a desired system. The closest representation of this task allowable within the size constraints of the computer was an attempt to tune a nonlinear system with rotor dynamics towards the linear design model. In order to ease the problem slightly, the design model was altered such that the actuator dynamics of the nonlinear system were used in the linear simulation. The results of this test are presented in Figures 5.13 to 5.16. The input on each inceptor is again a doublet of 10% amplitude, a period of 1.0 seconds and no deadband. For the state responses to a vertical velocity inceptor input, tuning appears successful for the vertical velocity, w, and lateral velocity, v, over portions of the time history (Figure 5.13). In the case of the responses to the longitudinal inceptor doublet (Figure 5.14), the tuned response is marginally worse than the untuned response on the vertical velocity channel. Marginal improvements in the tuned responses to the roll inceptor (Figure 5.15) and the lateral velocity inceptor (Figure 5.16) can also be seen. The improvement in performance index is a slight decrease from 1.1×10^{-2} to 0.72×10^{-2}.

In both of the tests involving nonlinear systems, improvements in system response during part of the time history were made at the expense of detuning the response at other times. This fact, combined with the knowledge that the performance index was decreased, means that the sensitivity functions were valid for the nonlinear systems. In the tests with linear systems the improvement in the tuned response was universal because the algorithm was moving the perturbed parameters back to their designed positions. Similarly contrived tuning problems with nonlinear systems also show universal improvement in the system response of
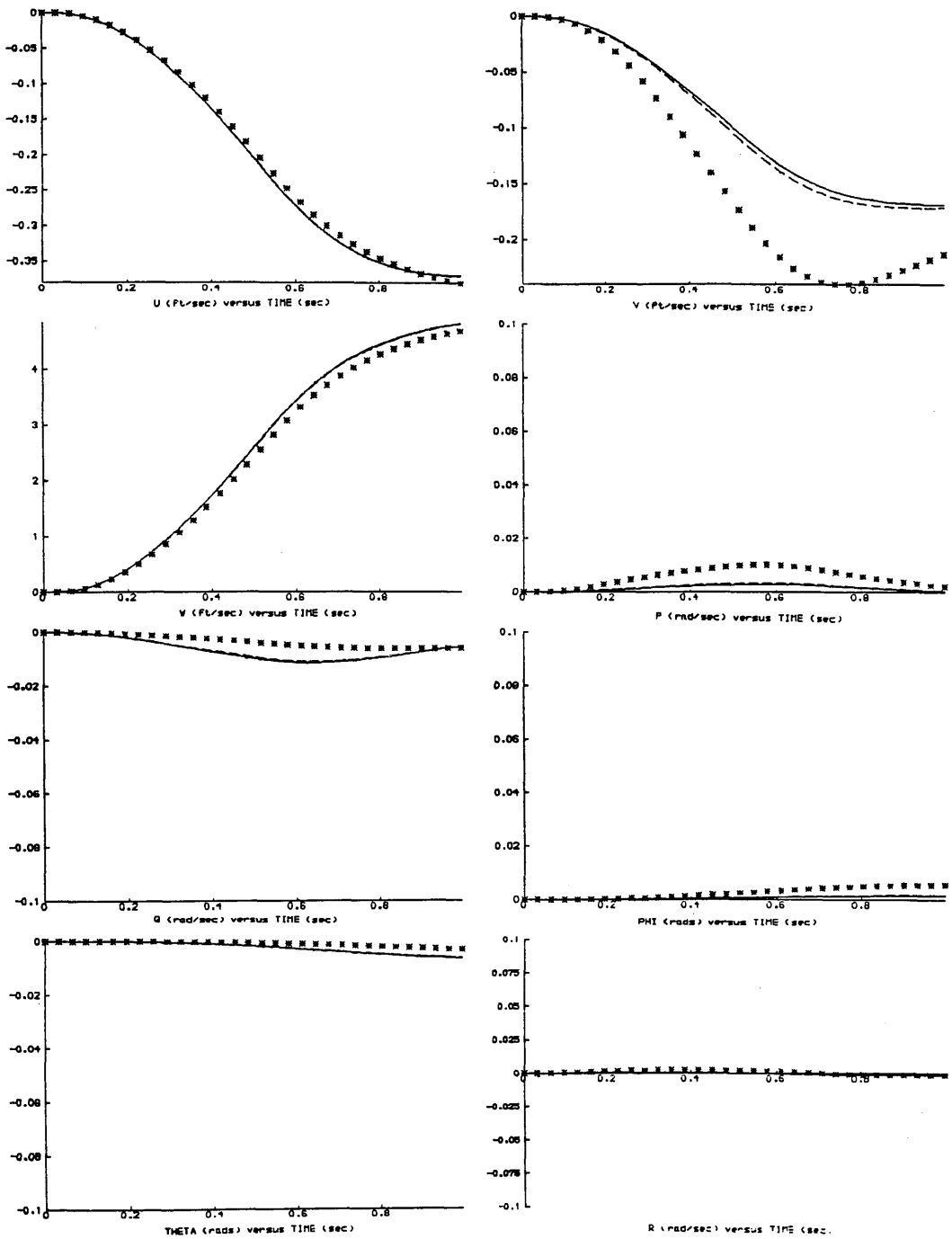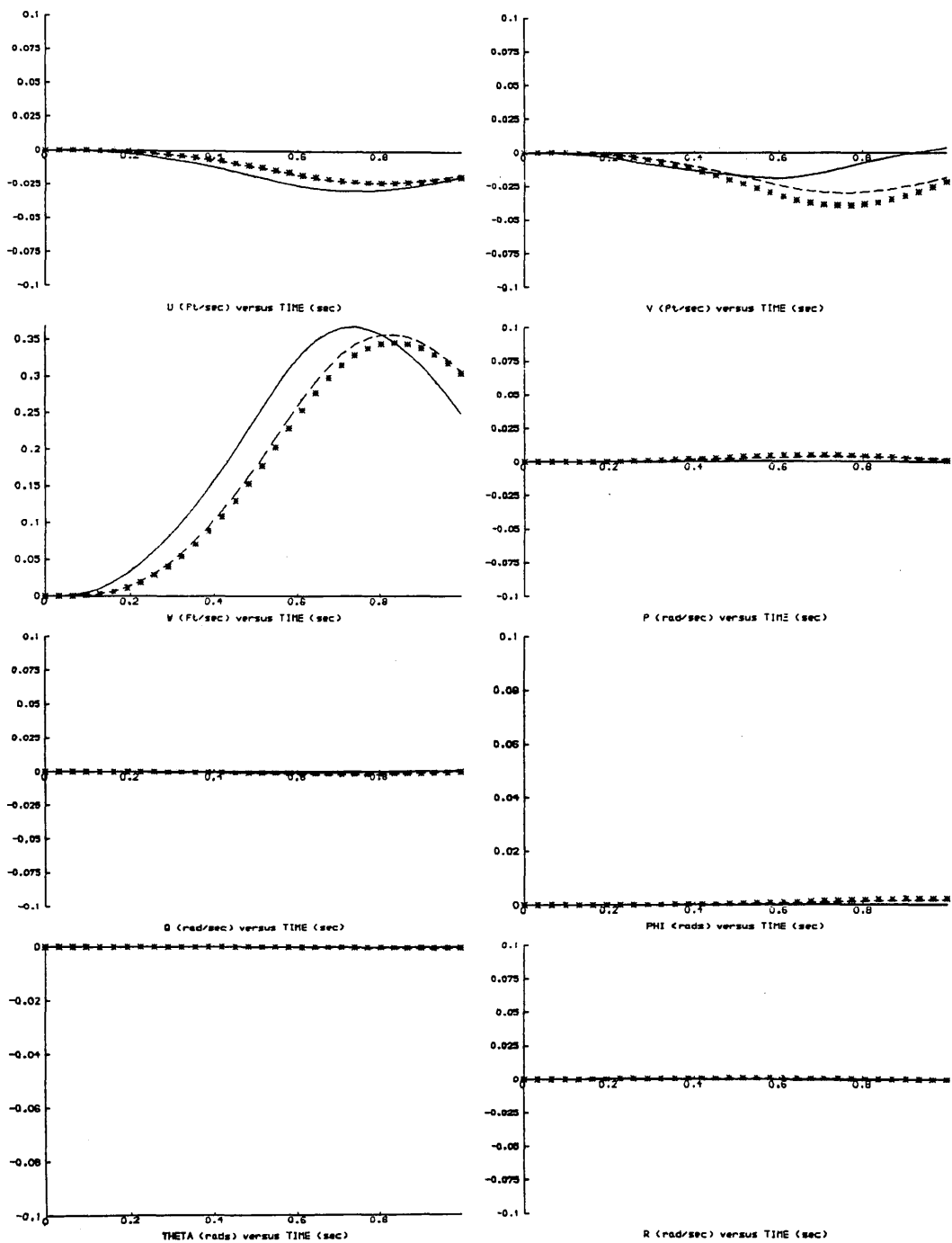
Figure 5.13: Nonlinear to Linear Tuning, Flight Path Controller, Second Order Sensitivities, Vertical Inceptor Doublet Input, ——— Desired Response, * * Untuned Response, – – Tuned Response.

— 149 —

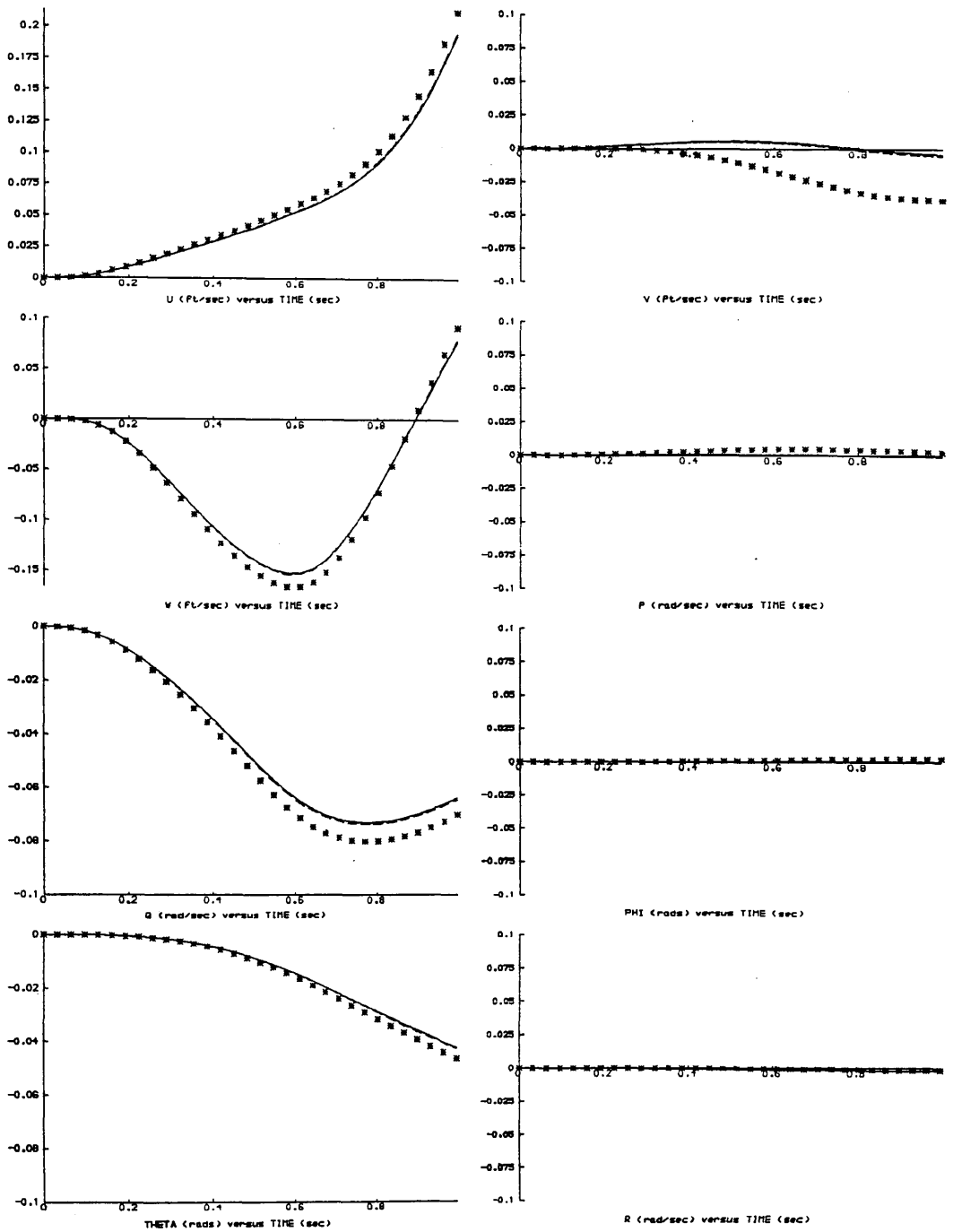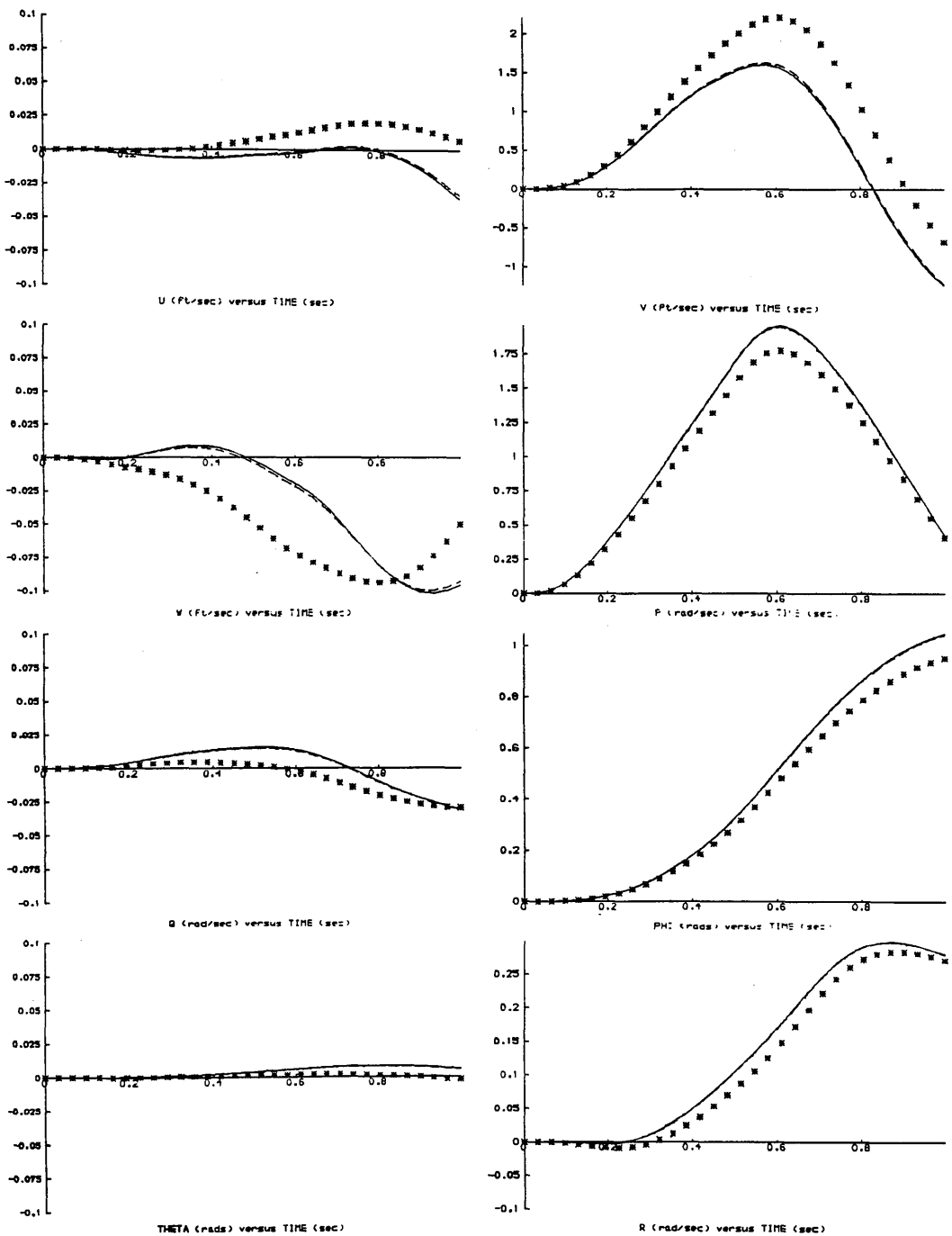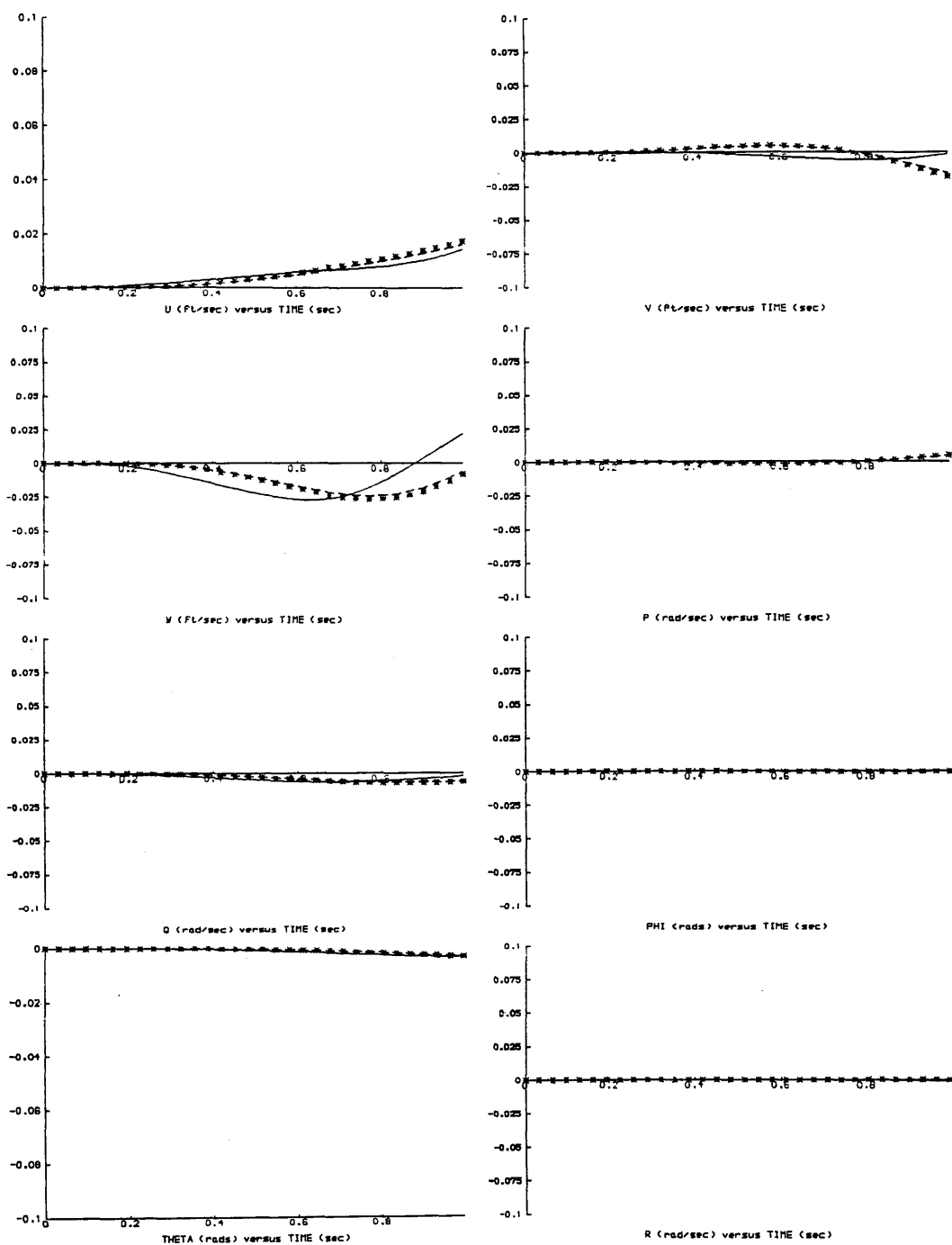Figure 5.14: Nonlinear to Linear Tuning, Flight Path Controller, Second Order Sensitivities, Longitudinal Inceptor Doublet Input, —— Desired Response, * * Untuned Response, – – Tuned Response.
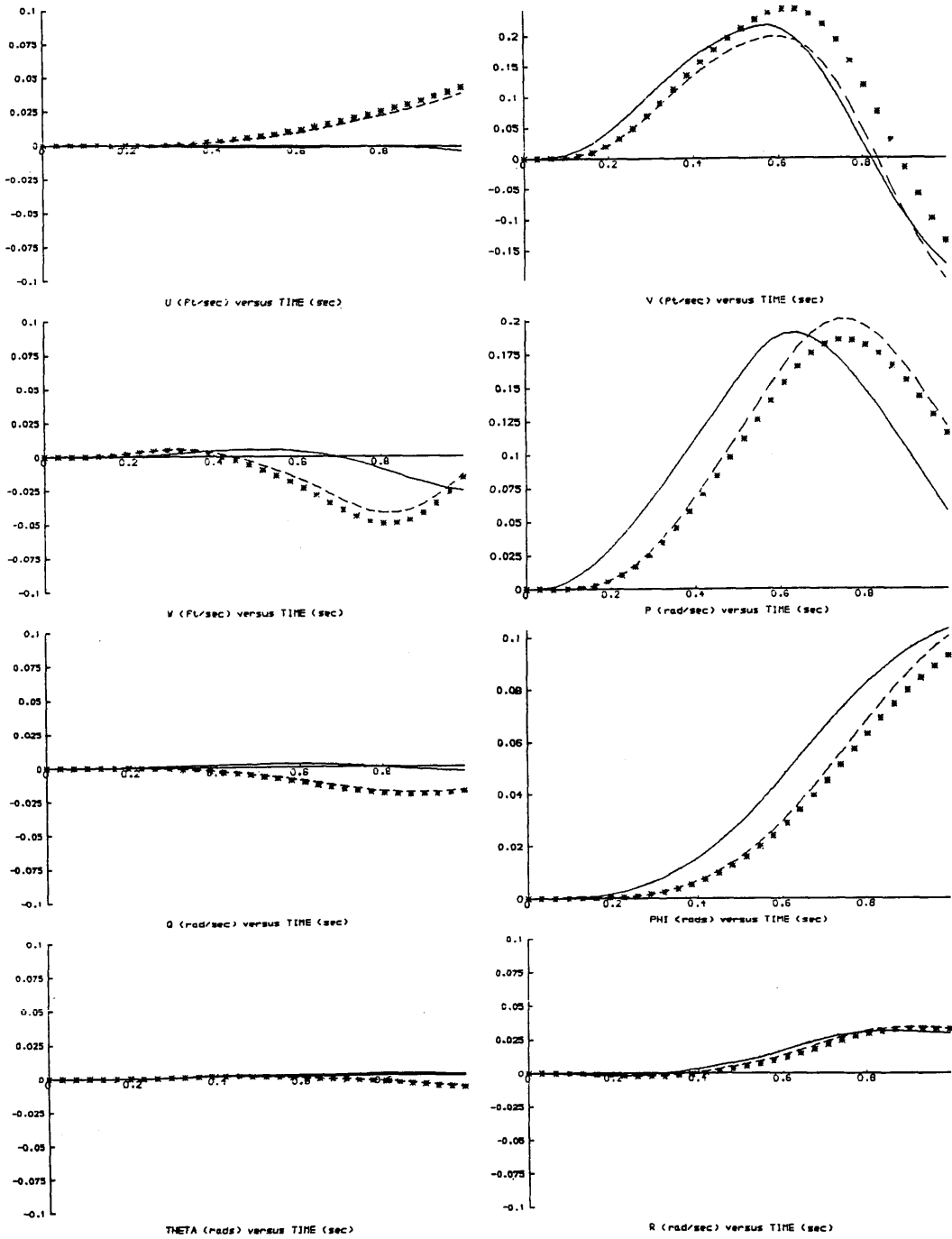
Figure 5.15: Nonlinear to Linear Tuning, Flight Path Controller, Second Order Sensitivities, Lateral (Roll) Inceptor Doublet Input, —— Desired Response, * * Untuned Response, – – Tuned Response.
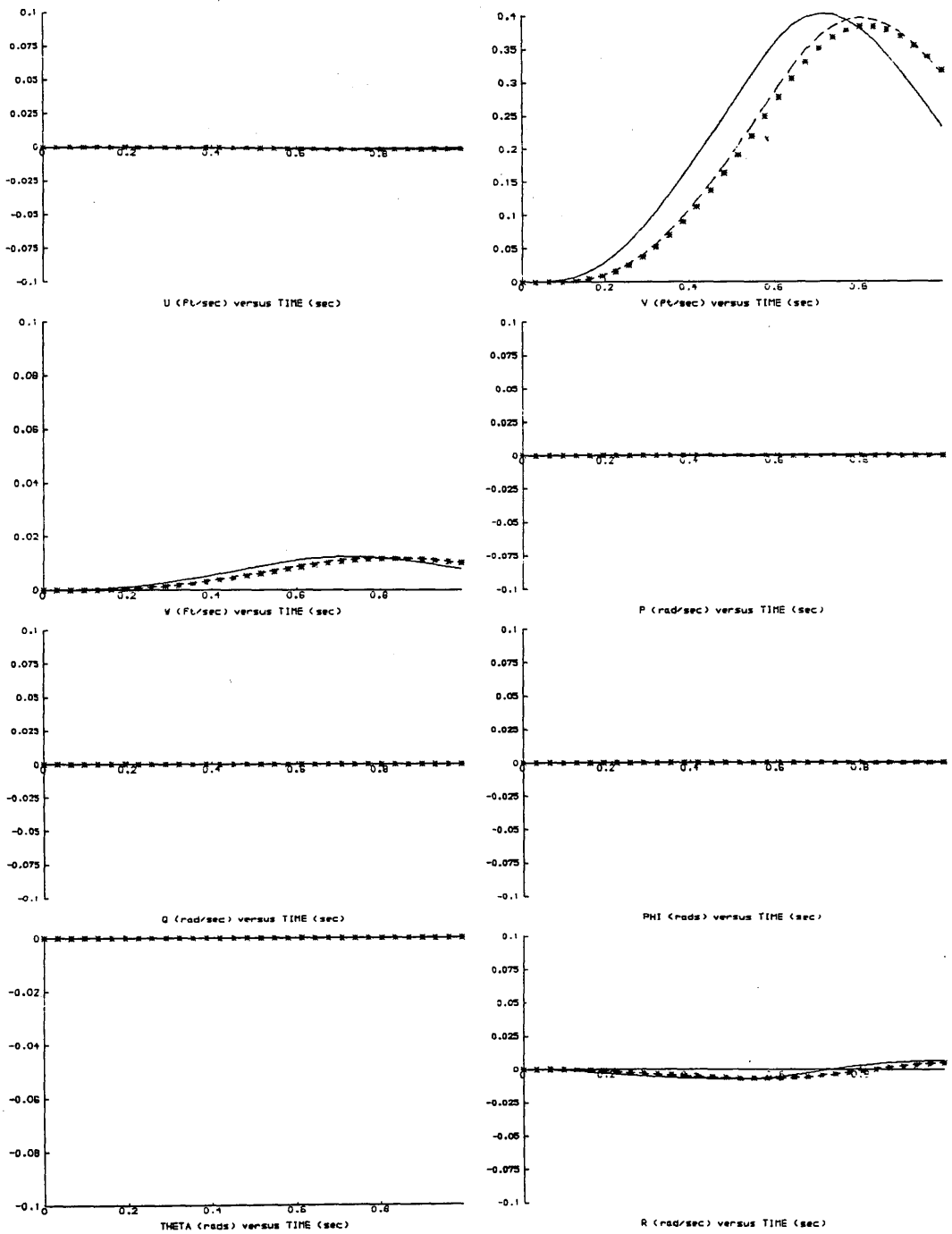
Figure 5.16: Nonlinear to Linear Tuning, Flight Path Controller, Second Order
Sensitivities, Pedal (Lateral Velocity) Inceptor Doublet Input,
—— Desired Response, * * Untuned Response, – – Tuned
Response.

the actual system. If it were possible to simultaneously adjust a larger number of control system parameters, the algorithm might then find a set of changes which would yield a universal improvement in the actual system's response. The use of a greater number of parameters would, at the least, give the adjustment algorithm more degrees of freedom in terms of using the effects of more parameters on the response. Each control system parameter has a unique influence on the system dynamics. Although it is possible that the dynamics might not be universally improved by using a greater number of parameters, it is concluded that the model reference tuning process works in simulation studies, since the adjustment algorithm minimizes the performance index, and pilot inputs can be chosen to yield valid sensitivity functions even in the presence of nonlinearities. One aspect of helicopter applications which will need to be addressed in the future is whether or not low amplitude test signals can be used in the presence of measurement noise. With nonlinear systems the adjustment algorithm only made slight changes to the performance index. Any system noise in the measurements could seriously affect the calculation of the performance index and turn marginal improvements of the controller into degradations.

CHAPTER 6: FLIGHT HANDLING QUALITIES TUNING

6.1) Flight Handling Quality Specifications

The flight handling quality specifications of aircraft provide a means of describing how easily the vehicle can be piloted. During the commissioning trials of new designs, test pilots will judge the performance of the aircraft during particular manoeuvres and assign a rating in terms of the Cooper—Harper scale (Section 6.1.1). The handling characteristics of aircraft depend on several factors in addition to the aircraft dynamics. Secondary characteristics include: the control sensitivity, the cockpit environment (man—machine interface), the pilot's view of the outside world, and the pilot's workload [57]. Although handling quality specifications attempt to cover all aspects of aircraft design, for the purposes of tuning flight controllers it will only be necessary to consider those relating to the aircraft's dynamic response. This chapter aims to demonstrate which handling quality criteria are applicable and how they can be used to tune flight control systems.

As previously stated, the application of active control technology to helicopters promises to improve handling qualities and increase mission effectiveness. However, fixed wing experience has shown that the introduction of active control technology does not guarantee an improvement in handling qualities if the criteria are not accounted for during the design of the flight control systems [10].

Traditionally, handling quality specifications have been seen as more important during the preliminary design of aircraft than at any other time [58]. It is, however, the author's opinion that the criteria should be used as a check at every stage of the development of new aircraft from the initial paper design concepts through computer simulation and even onto the commissioning trials stage. The use of ACT for implementing the flight control system allows alterations to the controller at late stages of development and this flexibility should be used to its full in attempting to improve the vehicle's handling qualities. These ideas led to a study of handling quality specifications in the hope that parts of the requirements could be incorporated into the tuning process for helicopter flight control systems. As previously stated, the purpose of the tuning process is to improve the performance of the flight control system in the presence of dynamics which were not modelled during the design. It was hoped

that handling quality specifications could be used in some way as a measure of the improvement in the settings of the controller parameters. Ideally, the controller parameters would be chosen to provide a Level 1 rating on the Cooper—Harper scale. In this way, it might also be possible to overcome performance deficiencies of flight controllers which were designed on the basis of control theory without adequate reference to the specifications.

The report which has been used as the source for the flight handling quality specifications is the May 1988 draft of the NASA—Technical Memorandum, USAAVSCOM Technical Report 87—A—4 "PROPOSED SPECIFICATION FOR HANDLING QUALITIES OF MILITARY ROTORCRAFT, Volume I — Requirements" [56]. A few points concerning the current state of the flight handling quality specifications are in order. The specifications are derived from experimental measurements which are correlated to pilot opinions in order to determine what range of handling quality parameters is acceptable for each particular aspect of the aircraft performance. Since flight trials are continually being conducted, the data base for the handling quality specifications is constantly in flux. This is particularly true at present because a major revision of the specifications is being carried out in the United States, Great Britain, and Canada. The aim of the work is to develop a systematic database for the handling quality specifications. This task has a two—fold nature. First, past specifications have lacked structure [59] and the next generation of specifications will be related to 'Mission Task Elements' (MTE's). These mission oriented criteria should cover the tasks which a helicopter performs during a mission, which for military rotorcraft include: take—off and landing, ground manoeuvres, low level contour flight, NOE flight, precision hover, air—to—air combat manoeuvres, night flight, and adverse weather flight [2]. Each particular manoeuvre and subtask performed will be assigned its own handling quality specifications and will be individually rated by pilots as possessing a particular handling qualities level. The second aspect of the current updating exercise is the collection of experimental results for the database. Helicopter idiosyncracies such as cross—coupling, nonlinearities, and high—order dynamics mean that the fixed wing handling quality criteria (including VSTOL specifications) cannot, in general, be used for rotorcraft [58]. It has been necessary to collect data from which helicopter handling quality criteria can be developed. The state of the present criteria can be judged by the fact that static and dynamic stability criteria are still subject to controversy. For example, recent work at the Royal Aerospace Establishment (Bedford) [12] has shown that pilot handling quality ratings for an Aerospatiale Puma do not correlate with the level which one would

expect from previous specifications of handling quality requirements. Other work that has recently been undertaken has expanded the database in the areas of rotor system design parameters [60],[61], and side—arm pilot inceptors [37],[62],[63]. Helicopter handling qualities are still maturing and hence the tuning process will need to be updated to keep pace with improvements in the specifications.

6.1.1) Handling Quality Levels and Ratings

The trend towards mission oriented handling quality specifications has led to ideas concerning levels of helicopter response. Key [58] explains that the level concept is designed to achieve:

1) *High probability of good flying qualities under conditions in which the helicopter is expected to be used.*
2) *Acceptable flying qualities in reasonably likely yet infrequently expected conditions.*
3) *A performance floor to ensure, to the greatest extent possible, at least a flyable helicopter, no matter what failures occur.*
4) *A process to ensure that all the ramifications of reliance on powered controls, stability augmentation, etc., receive proper attention.*

A Level 1 rating means that the aircraft is satisfactory for the task being tested. If a test pilot returns a rating of Level 2 or Level 3 then the aircraft is unsatisfactory or unacceptable respectively. In the context of tuning aircraft flight control systems, the objective is to give the aircraft Level 1 flight handling characteristics. An implicit assumption in this work on tuning is that the flight controller is not experiencing any failures.

When a pilot performs a series of test manoeuvres he will give more feedback on the vehicle's response than merely classifying it as satisfactory, unsatisfactory, or unacceptable. The Cooper—Harper scale attempts to take into account pilot opinions with greater precision than just a three level classification. Figure 6.1 is taken directly from the flight handling quality specifications report [56] and shows the logic used by a pilot in assigning a rating to a particular aircraft for each task. The vehicle will be rated in the range 1 to 10 depending on how well it performs. A rating of 1 means that the task is performed easily without taxing the pilot. On the other hand a redesign is in order if a rating of 10 is returned for any of the tasks. It should be remembered that rating a helicopter's handling qualities is a subjective problem and pilots will have different

ADEQUACY FOR SELECTED TASK OR REQUIRED OPERATION*

AIRCRAFT CHARACTERISTICS	DEMANDS ON THE PILOT IN SELECTED TASK OR REQUIRED OPERATION*	PILOT RATING
Excellent Highly desirable	Pilot compensation not a factor for desired performance	1
Good Negligible deficiencies	Pilot compensation not a factor for desired performance	2
Fair — Some mildly unpleasant deficiencies	Minimal pilot compensation required for desired performance	3
Minor but annoying deficiencies	Desired performance requires moderate pilot compensation	4
Moderately objectionable deficiencies	Adequate performance requires considerable pilot compensation	5
Very objectionable but tolerable deficiencies	Adequate performance requires extensive pilot compensation	6
Major deficiencies	Adequate performance not attainable with maximum tolerable pilot compensation. Controllability not in question.	7
Major deficiencies	Considerable pilot compensation is required for control	8
Major deficiencies	Intense pilot compensation is required to retain control	9
Major deficiencies	Control will be lost during some portion of required operation	10

LEVEL 1 — 3½ — LEVEL 2 — 6½ — LEVEL 3 — 8½

Pilot decisions

Is it satisfactory without improvement?
Yes — No — Deficiencies warrant improvement

Is adequate performance attainable with a tolerable pilot workload?
Yes — No — Deficiencies require improvement

Is it controllable?
Yes — No — Improvement mandatory

Cooper Harper   Ref NASA TND 5153

*Definition of required operation involves designation of flight phase and/or subphases with accompanying conditions

Figure 6.1: The Cooper Harper Scale (Reference 56)

— 157 —

opinions depending on several factors, not least of which are past experience and familiarity with the configuration being tested.

One of the difficult tasks in establishing quantitative criteria is that qualitative pilot assessments must be correlated with design parameters. An example of the assignment of a handling qualities level in terms of aircraft parameters is given by Baillie and Morgan [64]. For Level 1, helicopters should have a thrust to weight ratio of at least 1.08 while the Level 2 limit is 1.04. In addition the minimum heave damping is -0.20 sec^{-1} for Level 1. Values such as these are found by systematically adjusting the parameters of interest on variable stability helicopters or on ground—based simulators. Pilot opinions for each configuration are used to position the boundaries of the handling levels. It is important to note that the description of handling quality levels in terms of aircraft parameters is given by minimum boundaries. The levels are defined in terms of response characteristics such as damping ratios and natural frequencies, in addition to design constants, such as the thrust to weight ratio. The term, *handling quality parameter*, will be used to refer to any quantity which is used to define the boundaries of handling quality levels.

6.2) Review of Applicable Flight Handling Quality Specifications

There are several factors which influence the applicability of the flight handling quality specifications for use in a tuning process. Since the tuning process is quantitative, those handling quality specifications which are qualitative will prove difficult to describe in the software. Furthermore, the relatively simple computer simulation models will also place restrictions on the quantitative requirements which can be used effectively. In the following discussion, references to sections in the flight handling quality specifications report [56] will be given in italics to avoid confusion with the section numbers of this thesis.

The computer simulation models currently in use provide information dealing with the output state responses to pilot inputs. Other information, such as load factors, control stick charactersitics, limits of the *Operational Flight Envelope* (OFE) (see *section 1.6.1)*, and performance with failures is not available. Any requirements in [56] which make use of this information cannot be readily used in the tuning process. Therefore, as a first step, it will only be necessary to consider those specifications that give limits on the output response to pilot inputs.

The next area of concern with the models is that of accuracy. Since the

generation of sensitivity functions (Chapter 3) relies on the helicopter plant being linear, it was decided to limit the handling qualities analysis to dealing with a perturbation type of analysis rather than one based on complex flight manoeuvers. The *'Mission Task Elements'* (MTE) described in the report [56] (*section 1.4.1*) are relatively complex subtasks which a pilot must perform to successfully complete a mission. These MTE's can be further broken up into a series of discrete pilot inputs. With the simulation models currently available it is a great deal easier to study the vehicle response to a lateral cyclic pulse input, for example, than it is to study a slalom manoeuver which could excite system nonlinearities. In addition, it is assumed that the errors in the simulation of the lateral cyclic input will be less due to the shorter length of the simulation. Simulation errors may be significant for complex manoeuvers such as the slalom.

Another constraint imposed on the work by the accuracy of the simulation models occurs at low speeds. The values of plant parameters at low speeds are suspect (Chapter 2) and this is can lead to errors in simulated responses. Because of this weakness of the model, only those handling quality requirements relevant to the forward flight regime will be considered. Forward flight is defined by *section 1.4.6.3* of the handling criteria report [56] as,

> *1.4.6.3 Forward Flight. Forward Flight is defined as all operations with a ground speed greater than 45 knots (23 m/sec).*

A large part of the specifications are related to the *'Response—Type'* (*section 3.2*) being used and some requirements even dictate a particular response—type. The simulation models describe a single rotor helicopter with rate demand structures for the flight control systems and hence the number of relevant specifications is further reduced. Specifications concerning attitude or altitude hold functions may be difficult to test with the simulation models. Of the two flight controllers discussed in Chapter 2, only the Parry Modal Controller has a pilot input strategy which is appropriate for use with the specifications.

6.2.1) The Structure of the Handling Quality Specifications Report

The report [56] is divided into four sections. The first section *'Scope and Definitions'* gives purely background information and does not contain specific requirements. Similarly, the next section, *'Applicable Documents'* is again aimed at providing background information in the form of referencing the 'Background

Information and User's Guide' [65]. Most of the relevant handling qualities are given in *section 3* which is titled *'Requirements'*. The final section discusses *'Flight Test Manoeuvers'* and lists the desired minimum performance for each manoeuver. Unfortunately, the information in *section 4* is more readily applicable to flight tests or piloted real—time simulations than to the models with which we are working. Therefore, the search for relevant handling quality data can be restricted to *section 3*.

In the report [56], *section 3 'Requirements'* is broken down into several subsections. The following table lists the subsections which are included and indicates if the information in each subsection is relevant (i.e. those subsections with limits on system parameters).

Table 6.1: The Subsections of Requirements of the Handling Quality Specifications

Subsection	Relevant Information
3.1 General	- generally qualitative in nature - 3.1.11 limits residual oscillations
3.2 Required Response-Type	- qualitative background information
3.3 Hover and Low Speed	- due to simulation inaccuracies, no directly relevant data
3.4 Forward Flight	- all subsections relevant but some require information not available from the simulation model
3.5 Transition of a Variable Configuration Rotorcraft Between Rotor-Borne and Wing-Borne Flight	- not relevant
3.6 Controller Characteristics	- deals with the man—machine interface which is not simulated with enough detail to include the data
3.7 Specific Failures	- the current model does not simulate system failures
3.8 Transfer Between Response-Types	- not relevant with the current flight control system
3.9 Ground Handling and Ditching Characterisitics	- not relevant

From Table 6.1 it is clear that much of the handling qualities report [56] can be put aside. *Section 3.4 'Forward Flight'* contains the parameters which can be used with our present helicopter models.

6.2.2) The Forward Flight Handling Quality Specifications

The *'Forward Flight'* section of the handling qualities report [56] contains 32 individual requirements. Each of these sections has been reviewed to determine its usefulness to a tuning process for flight controllers. A requirement is considered applicable to the present study of tuning if it contains parameter limits which can be used to classify the handling qualities on the basis of the state response of the system with respect to pilot inputs. It is hoped that simple pilot inputs can be used to show compliance with as many of the requirements as possible. Information of this type allows the use of sensitivity functions for the purpose of optimizing the controller. The results of the review of *'Forward Flight'* handling qualities is presented in Appendix 3. Many of the requirements can be disregarded in the context of the tuning process because they are either qualitative or the simulation models are lacking in sophistication.

Three of the requirements (*3.4.3, 3.4.4.1.1,* and *3.4.4.1.2*) involve testing with step inputs on the vertical velocity inceptor. Requirement *3.4.3* places restrictions on the shape of the vertical response. Requirements *3.4.4.1.1* and *3.4.4.1.2* give bounds for the allowable levels of collective to pitch attitude coupling.

There are two requirements (*3.4.1.1* and *3.4.4.2*) which involve the longitudinal pilot inceptor. In order to comply with *3.4.1.1*, which classifies the pitch attitude response to the longitudinal inceptor, it will need to be assumed, or preferably shown, that the longitudinal cyclic needed to yield ±5° of pitch is within the limits imposed by load factors and the OFE. Requirement *3.4.4.2* is concerned with the pitch to roll coupling.

The roll inceptor response is classified by seven requirements (*3.4.4.2, 3.4.5.1, 3.4.5.2, 3.4.5.3, 3.4.6.1, 3.4.6.2,* and *3.4.8.2*). Coupling to pitch from commands on the roll inceptor is assigned a handling qualities level according to the information presented in requirement *3.4.4.2*. Requirements *3.4.5.1, 3.4.5.2,* and *3.4.5.3* are concerned with ensuring that the roll response of the aircraft is adequate. Roll—sideslip coupling is considered in requirements *3.4.6.1* and *3.4.6.2* while the degree of spiral stability is assigned to a Cooper—Harper level in *3.4.8.2*.

The system response to the yaw control is classified by three specifications (*3.4.7.1*, *3.4.7.2*, and *3.4.8.1*). Requirements *3.4.7.1* and *3.4.7.2* are designed to ensure that the aircraft's yaw inceptor has adequate authority and that the response has acceptable dynamics. System oscillations to yaw inceptor inputs are specifically considered by requiremenet *3.4.8.1*.

Simple pilot inputs can be used with the simulation models to show compliance with several handling quality requirements. There are 14 requirements which are in a form suitable for use with a tuning process.

6.3) The Handling Qualities Performance Index

It is desirable that the tuned helicopter display Level 1 handling qualities for all MTE's and therefore beneficial to have Level 1 handling quality requirements embedded in the adjustment algorithm. Hence, the question becomes one of how best to incorporate the requirements in the adjustment scheme. Examination of the handling quality requirements [56] has shown that the parameters which could be used in a tuning process (those relying on output responses) are related to parameters common in classical linear control theory. These requirement parameters are a mix of time domain characteristics, such as response peaks and damping ratios, and frequency domain characteristics, such as bandwidth and phase delay (Appendix 3). The time/frequency domain mix of the relevant parameters led to the conclusion that attempting to incorporate the handling quality requirements in a model reference algorithm would be inappropriate.

In model reference tuning, the controller parameters are adjusted on the premise that; given the present and desired system responses, and a set of sensitivity functions, it is possible to predict an improved set of control system parameter values. Controller parameters are changed to minimize the difference between the responses, hence the Integral Error Squared Performance Index. If it is necessary to improve the handling qualities of the vehicle, then it seems appropriate to use a *per*formance index which is based on handling quality parameters rather than strictly on time responses. Given a set of desirable handling quality parameters and the present set of handling quality parameters for the system, the objective of the tuning could be to reduce the error between the two sets. However, the handling quality criteria *do* not give desirable handling quality parameters, instead the levels are described by parameter regions.

The following theory shows *how* system parameters are being adjusted towards a handling qualities level. If a handling qualities level is defined by n

parameters in the space Γ over all handling quality parameters, then define it to be an n dimensional handling qualities level. Let B_{L1} be the boundary for Level 1 handling qualities in the n dimensional handling qualities parameter space. Similarly, B_{L2} will define the Level 2 boundaries.

Systems are tested to provide estimates of the relevant handling quality parameters and the response is assigned to a particular level on the basis of these estimates. Let γ_{est} be the estimated position of the current system in the handling qualities space Γ. The value of γ_{est} will be determined as a function, F_{HQ}, of the state responses, both time domain $\underline{x}(t)$ and frequency domain $\underline{X}(\omega)$.

$$\gamma_{est} = F_{HQ} \left[\underline{x}(t), \underline{X}(\omega) \right] \qquad \text{Equation 6.1}$$

As parameters are changed, $\underline{x}(t)$ and $\underline{X}(\omega)$ will change and hence γ_{est} will also migrate in Γ. Sensitivity functions can predict the change in $\underline{x}(t)$ and $\underline{X}(\omega)$ resulting from parameter changes, and from the perturbed responses, it will be possible to use F_{HQ} to predict a change in γ_{est}. This will allow a prediction of the effects of changing a controller parameter on handling qualities.

Assume that the aim of the optimization is to minimize the distance between γ_{est} and Γ_{L1} (the region bounded by B_{L1}). Define γ_{L1} to be the point on the Level 1 boundary, B_{L1}, which is closest to γ_{est}. By studying the effects of changing controller parameters on γ_{est}, it will be possible to find a set of controller parameters which minimizes the performance index of Equation 6.2.

$$J = \left[\gamma_{est} - \gamma_{L1} \right]^2 \qquad \text{Equation 6.2}$$

If the distance measurement from γ_{est} to the boundary, B_{L1}, is minimized according to the performance index in Equation 6.2, then the handling quality parameters will migrate towards the Level 1 boundary, B_{L1}. If γ_{est} is initially inside the boundary, B_{L1}, then the use of the performance index in Equation 6.2 will cause γ_{est} to move towards the Level 1 boundary, B_{L1}, and the Level 2 region, Γ_{L2}, which will possibly lead to a deterioration of the vehicle's handling qualities. Therefore, if γ_{est} is initially an element of Γ_{L1}, the performance index should be such that γ_{est} is pushed even farther into the Level 1 region, Γ_{L1}. One solution might be to minimize the following performance index whose description depends on whether γ_{est} is interior to the Level 1 region, Γ_{L1}.

$$J = \begin{cases} \left[\gamma_{est} - \gamma_{L1} \right]^2 & , \ \gamma_{est} \notin \Gamma_{L1} \\ -\left[\gamma_{est} - \gamma_{L1} \right]^2 & , \ \gamma_{est} \in \Gamma_{L1} \end{cases}$$

<div align="right">Equation 6.3</div>

Assuming that there are several handling quality requirements, i, then it will be necessary to minimize with respect to all of these requirements simultaneously. Thus the performance index would become,

$$J = \sum_i \begin{cases} \left[\gamma_{est}^i - \gamma_{L1}^i \right]^2 & , \ \gamma_{est}^i \notin \Gamma_{L1}^i \\ -\left[\gamma_{est}^i - \gamma_{L1}^i \right]^2 & , \ \gamma_{est}^i \in \Gamma_{L1}^i \end{cases}$$

<div align="right">Equation 6.4</div>

There is one problem with Equation 6.4 which is readily apparent. Suppose that the jth requirement is described by a handling qualities space Γ_{L1}^j which is much larger in absolute terms than any of the other spaces. In this case γ_{est}^j could be pushed deeply into Γ_{L1}^j at the expense of other handling qualities. Therefore, it is proposed that the distances are normalized before being used in the performance index of Equation 6.4.

Define γ_{L2} to be the point on the Level 2 boundary, B_{L2}, which intersects with the line drawn through the points γ_{est} and γ_{L1}. The proposed factor of normalization to be used with Equation 6.4 is the distance beween the points γ_{L1} and γ_{L2}. The performance index in Equation 6.5 will measure the relative distance of each of the system's handling qualities (given as γ_{est}^i) from their respective Level 1 boundaries, B_{L1}^i, and will attempt to drive the γ_{est}^i into their associated Level 1 regions, Γ_{L1}^i.

$$J = \sum_i \begin{cases} \left[\dfrac{\gamma_{est}^i - \gamma_{L1}^i}{\gamma_{L2}^i - \gamma_{L1}^i} \right]^2 & , \ \gamma_{est}^i \notin \Gamma_{L1}^i \\[4mm] -\left[\dfrac{\gamma_{est}^i - \gamma_{L1}^i}{\gamma_{L2}^i - \gamma_{L1}^i} \right]^2 & , \ \gamma_{est}^i \in \Gamma_{L1}^i \end{cases}$$

<div align="right">Equation 6.5</div>

In addition, there may be physical justification for placing greater emphasis on certain handling qualities than on others. The importance of various handling qualities may be taken into account in the optimization of controller parameters by including a weighting factor, W_i, for each handling quality in the performance index. Therefore, the proposed performance index to be used in the adjustment algorithm to tune the helicopter handling qualities is given by Equation 6.6.

$$
J_{HQ} = \sum_i W_i \left\{ \begin{array}{ll} \left[\dfrac{\gamma^i_{est} - \gamma^i_{L1}}{\gamma^i_{L2} - \gamma^i_{L1}} \right]^2 & , \quad \gamma^i_{est} \notin \Gamma^i_{L1} \\[4em] -\left[\dfrac{\gamma^i_{est} - \gamma^i_{L1}}{\gamma^i_{L2} - \gamma^i_{L1}} \right]^2 & , \quad \gamma^i_{est} \in \Gamma^i_{L1} \end{array} \right.
$$

Equation 6.6

The performance index J_{HQ} can be used to *tune directly* the helicopter flight controller with respect to several handling qualities simultaneously. There are a total of 19 tests which can be conducted on the simulation models in an attempt to show compliance with the 14 handling quality requirements discussed in Section 6.2.2.

6.4) Results for Linear Systems

The development of the Handling Qualities Performance Index is still at an early stage due to implementation difficulties. The problems which have been encountered in attempts to use the 19 tests as part of the handling qualities adjustment algorithm have largely been attributable to the nature of the simulated system responses. As mentioned previously, the requirements are only applicable to the input strategy employed with the Parry Modal Controlled system. Because of the deficiencies of this controller in terms of command authority (response amplitude) and turn coordination/roll control, the system responses differed greatly from the responses on which the handling quality criteria are based. In some cases, such as requirements *3.4.6.1* and *3.4.6.2*, the responses from the simulation model were inconsistent with the specifications. In another instance, the low response levels of the Parry Modal Controlled system were responsible for failures of the algorithms checking the degree of pitch attitude response to the longitudinal inceptor (*3.4.1.1* and *3.4.1.2*), and the roll attitude response to roll

inceptor (*3.4.5.2*).   Algorithms used to evaluate F_{HQ} (Equation 6.1) in the calculation of the Handling Qualities Performance Index should be developed with error checking in order to allow the system response to be compared with an expected response type so as to ensure that the test for compliance with a requirement is valid.   The computer code must be robust to different system responses.

The implementation of the Handling Qualities Performance Index was also hampered by the constraint of available memory on the VAX $11-750$.   In order to use frequency domain criteria, it is necessary to calculate transfer function sensitivities so that the changes in frequency response with control system parameter shifts can be calculated.   Transfer function sensitivities require a considerable amount of storage space when they are to be held in program arrays.   They must be stored internally so that the computer processing time needed to perform the tuning process is reasonable (a few hours rather than a number of days).   It was, therefore, impossible to obtain sufficient resolution of the frequency responses for an accurate assessment of the frequency domain criteria (*3.4.4.1*, *3.4.5.1*, and *3.4.7.1*).

In spite of these difficulties, the Handling Qualities Performance Index has been used successfully for a limited number of criteria.   The two criteria which have been used during the tuning exercise depicted by Figures 6.2 and 6.3 are requirements *3.4.1.1* — *Pitch Attitude Response to Longitudinal Controller, Short—Term Response* and *3.4.5.1* — *Roll Attitude Response to Lateral Controller, Small—Amplitude Roll Attitude Response to Control Inputs.*   Figure 6.2 shows the response of the Parry Modal controlled system to an impulse on the longitudinal inceptor.   The dashed line indicates the untuned response and the solid line indicates the tuned response.   The impulse on the longitudinal inceptor is used to exite the system in an attempt to determine effective damping ratios for the system.   For Level 1, the system must have effective damping ratios of at least 0.35 while the Level 2 limit is 0.25.   The tuning algorithm has increased the system damping to this input from a Level 3 value of 0.20 to 0.344 which is probably within experimental error of the Level 1 boundary (Figure 6.4).   Figure 6.3 shows the response of the same system to an impulse on the roll inceptor, with the dashed and solid lines again indicating untuned and tuned responses respectively.   The impulse on the roll inceptor is also used to excite natural oscillations in the system which are classified according to the graphical criteria shown in Figure 6.5.   As demonstrated, the untuned response was Level 2 and the tuned response is an improved Level 1.   In terms of the performance index, J_{HQ}, the value has been reduced from 2.59 to -0.35.
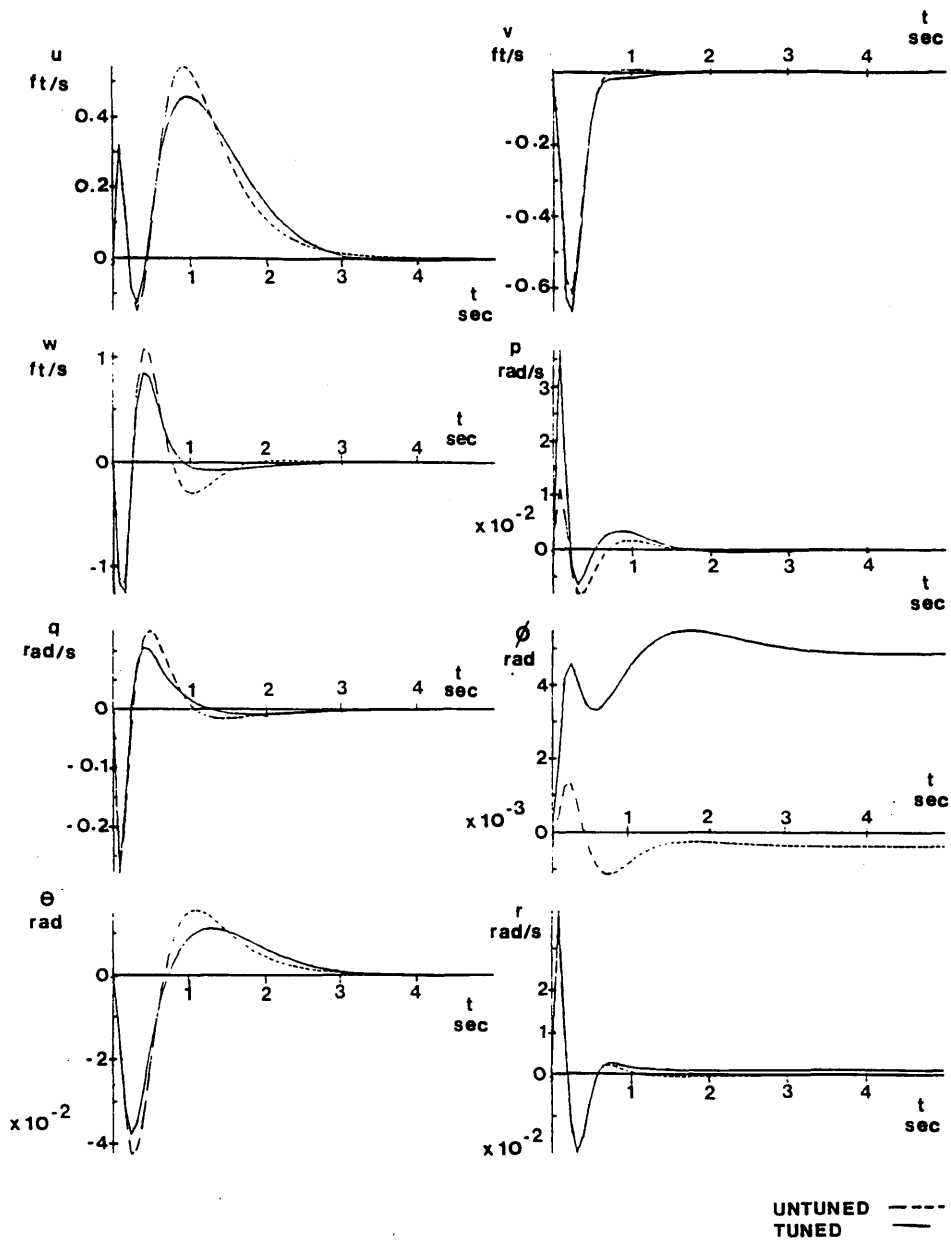
Figure 6.2: Handling Qualities Tuning, Parry Modal Controller, Longitudinal Inceptor Pulse.
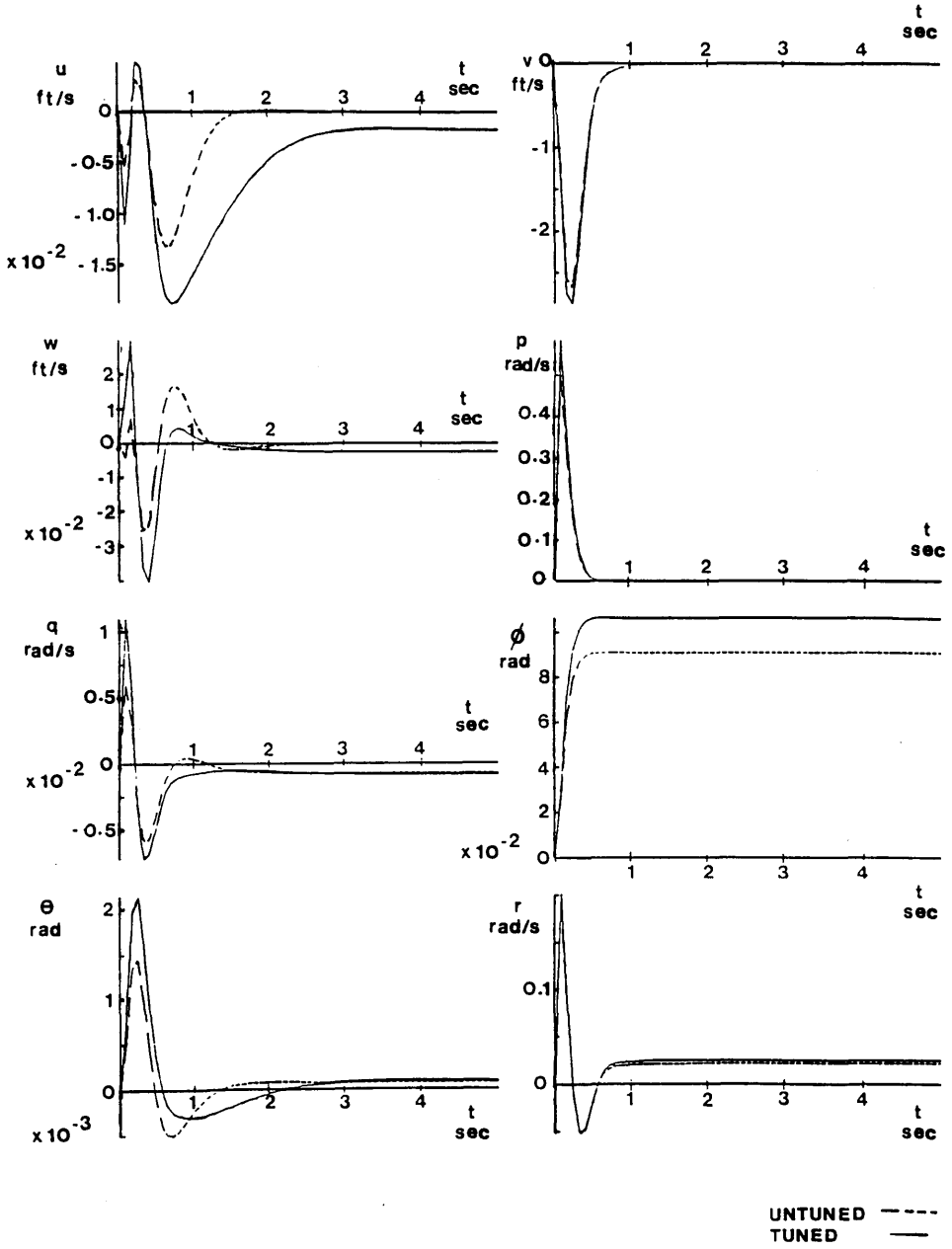
Figure 6.3: Handling Qualities Tuning, Parry Modal Controller, Roll Inceptor Pulse.

$\zeta = 0.0$　　　　0.25　　0.35　　　　　　　　　　$\zeta = 1.0$

Level 3　　Level 2　　　　　Level 1

Untuned Response　　　　Tuned Response
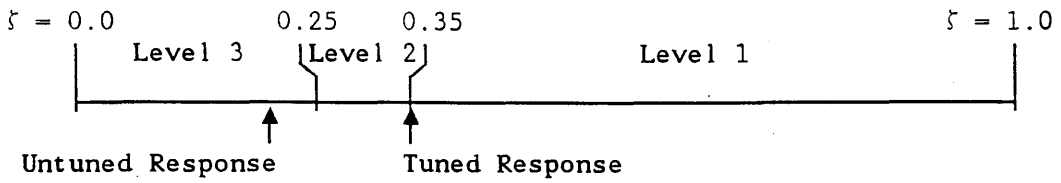
Figure 6.4: Damping Ratio to a Longitudinal Controller Pulse Input (*Requirement 3.4.1.1*).

Level 3

$\zeta \leq 0.19$

Level 2

$\zeta \leq 0.35$

$\omega_n \sqrt{1 - \zeta^2}$

Level 1

⊙ Untuned Response
△ Tuned Response

$\zeta \omega_n \geq .35$

$\omega_n \geq 1.0$

$-\zeta \omega_n$
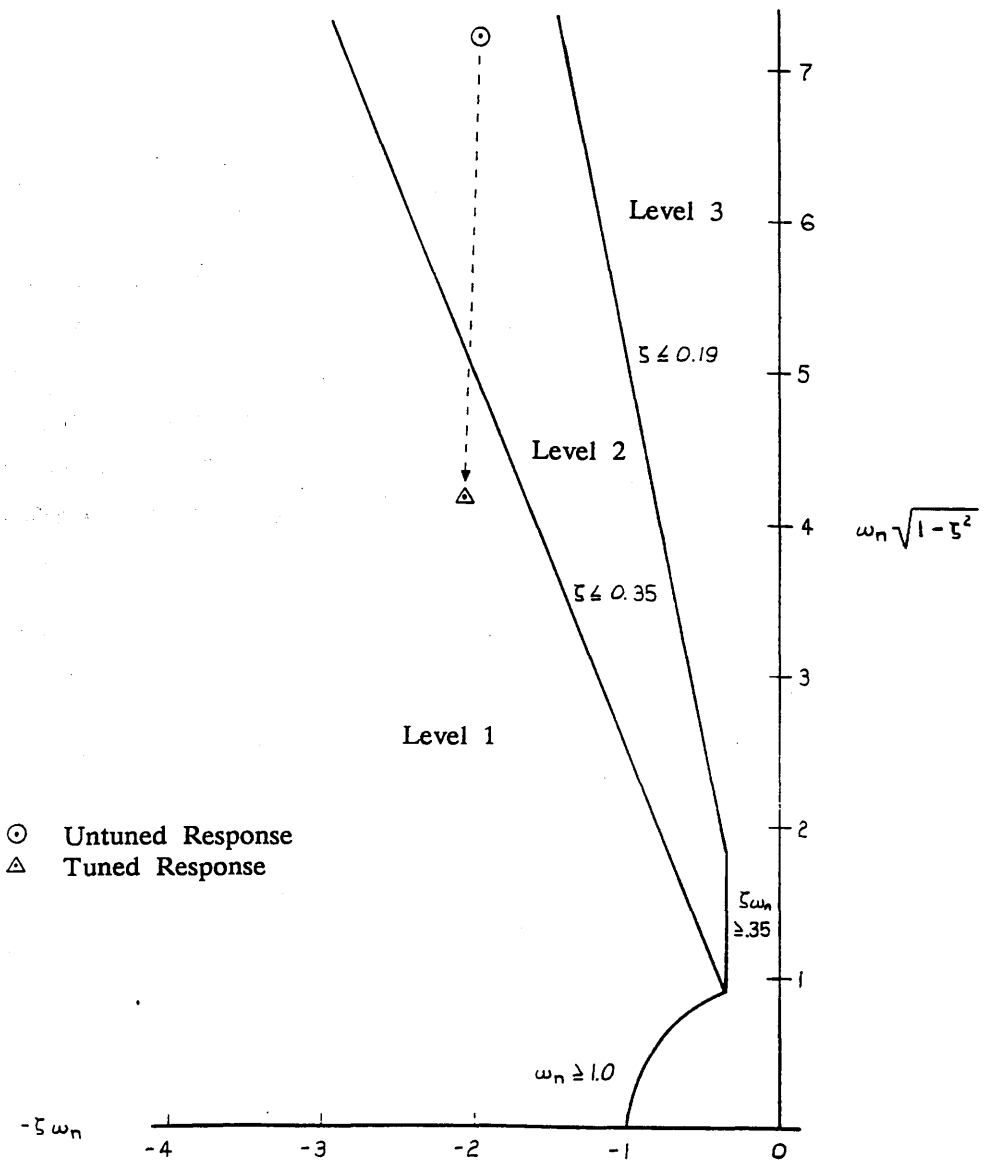
Figure 6.5: Lateral–Directional Oscillatory Requirements (*Requirement 3.4.5.1*) (Reference 56).

These initial tuning results are informative in several ways. First, it is possible to tune simultaneously the system with respect to more than one handling qualities requirement. In addition, the test is illustrative of the varied nature of the criteria and the fact that the Handling Qualities Performance Index, J_{HQ}, is universally applicable to requirements linking system response to pilot inputs. The improvement in handling qualities was effectively recorded by J_{HQ}. However, Figure 6.2 shows an increased level of coupling of the longitudinal inceptor input to roll angle, which is undesirable. It will clearly be necessary to use as many of the handling quality criteria in the calculation of J_{HQ} as possible, in order to avoid the situation in which one facet of the system response is improved at the expense of another.

6.5) Future Improvements in Flight Handling Qualities Tuning

The use of the Handling Qualities Performance Index, J_{HQ}, is a tuning technique for the future. Advances in the processing power and memory capacity of computers will eliminate a large stumbling block which is currently preventing a more successful application of J_{HQ} in tuning problems. It should also be possible to develop efficient and robust algorithms to determine the estimated handling quality parameters, γ_{est}. The robustness problem will also be reduced if the controlled systems which are being optimized are more in tune with the handling specifications.

The use of J_{HQ} allows a system's handling qualities to be enhanced in a much more direct manner than is possible with the model reference performance index, J_{MR}. Indeed, it is conceivable that the Handling Qualities Performance Index could be used as part of a design technique rather than just as a tool for eliminating the problems caused by other control theories. Issues concerning the implementation and use of the Handling Qualities Performance Index, J_{HQ}, deserve much closer scrutiny than has been possible in the current study.

CHAPTER 7: FLIGHT SIMULATION RESULTS

7.1) Objective of Flight Simulation Trials

The Advanced Flight Simulator (AFS) at the Royal Aerospace Establishment (Bedford) was made available for a trial of the Flight Path Controller and the tuning procedures which have been previously discussed. The AFS is a real−time facility which allows control laws to be flown from a moving base cockpit or by using joysticks at the control desk. Because of modifications which were being carried out to both the cockpit and the visual systems of the AFS, the trial was somewhat restricted. The control law was flown using the joysticks at the control desk with a Head Up Display (HUD) (Figure 7.1) as the only visual cue available.

The use of the AFS allows a validation of contol laws in an environment which is much closer to a real helicopter than is possible during computer simulation. During real−time simulations on the AFS, it is possible to study a pilot's interface with the controlled aircraft system. This interface is both explicit in terms of the pilot moving inceptors to manoeuvre the vehicle and implicit in terms of the strategy used by the pilot for control. The fact that the control strategy used for ACT systems is intimately related to the type of inceptors which the pilot must use cannot be overstressed. The change from the traditional collective lever and cyclic stick to sidearm controllers has repercussions in terms of control system design. It is only with real−time simulation that deficiencies in this critical area of flight control will become apparent.

The results of the real−time simulation trial are both limited and mixed. Much of the time allocated for the simulation slot was used to convert the control law from HELISIM3 format to a form which linked into the Rationalized Helicopter Model (RHM) on the Gould Concept−32 processors. In consequence, useful data was only collected during four sorties, each lasting approximately one hour. This data highlighted several problems with the structure .of the controller and particularly the pilot input command strategy used. Qualitative results pertaining to modal control theory are inconclusive, yet they are promising. The tuning procedures were only used once and hence it is premature to draw conclusions.

The problems with the acceleration demand strategy used by the Flight Path Controller which were very much in evidence during real−time simulation had

Airspeed

080

Altimeter

1500

Compass

| 355° | 0° | 5° | 10° | 15° |

Accelerometer

Velocity
Vector
Indicator

15°

10°

5°

0°

-5°

-10°

-15°

-20°

Helicopter Symbol

Artificial Horizon

Height Rate Indicator
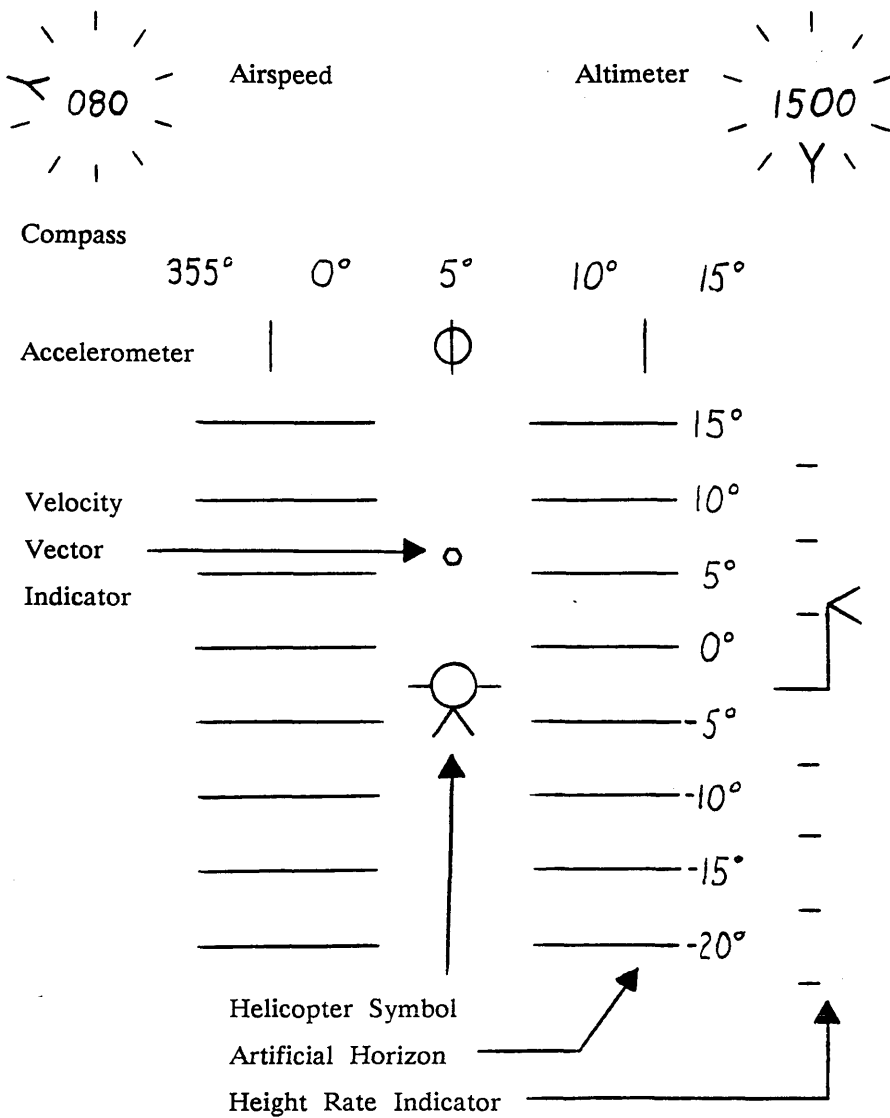
Figure 7.1: Typical Head Up Display (HUD) Symbology

only been hinted at previously. Because of these problems, the lack of a moving base cockpit and television system was inconsequential. A need exists for a real—time facility somewhere between the extensive capabilities of the real—time AFS and the computer simulations used for design. A real—time system with a simple HUD for visual cueing and joysticks for pilot control inputs, could allow the input strategy to be tested before a control law is thrown against other problems presented by the AFS. The AFS is an excellent facility for evaluating the performance (handling qualities) of controllers in specific manoeuvres common to NOE flying such as the dolphin or slalom, but before moving onto the AFS, tests should be conducted to ensure that the controller will *fly* in the first place.

7.2) Trimming the Controlled System

In any simulation consisting of a nonlinear element such as a helicopter plant, an equilibrium operating point is needed to properly initialize the simulation. For flight simulation, this translates into a steady state flight condition which was chosen to be the same as the design point of the controller — 80 knots level flight. A considerable amount of effort was expended during attempts to achieve a trim of the Flight Path Controller — RHM system using the TSIM trimming utility. TSIM is the simulation language which has been used to generate time histories of the controlled helicopter system during the computer simulations on the VAX 11–750 computer. Unfortunately, when these trim values for the actuator blade angles and states were used to initialize a simulation on either the VAX using TSIM or the Gould Concept—32 processors, the system was given a push which drove the controller's integrators to a new trim condition.

Using TSIM, the problem on the VAX was traced to the values of the linear accelerations of the helicopter's centre of gravity. During the trim, the values of the X, Y, and Z components of linear acceleration in earth axes (including gravity) were as shown below:

$$A_{XE} = -5.885 \times 10^{-6} \ \frac{ft}{s^2}$$

$$A_{YE} = 1.961 \times 10^{-6} \ \frac{ft}{s^2}$$

$$A_{ZE} = -3.815 \times 10^{-6} \ \frac{ft}{s^2}$$

However, when a time response was initiated these same variables were seen to be reassigned to:

$$A_{XE} = 0.3696 \; \frac{ft}{s^2}$$

$$A_{YE} = 0.0411 \; \frac{ft}{s^2}$$

$$A_{ZE} = 1.6608 \; \frac{ft}{s^2}$$

Since the Flight Path Controller of Section 2.2.4 relies on acceleration feedback, there is little wonder that the system was given an initial *'kick'*. The controller will integrate these errant accelerations and drive the system to a new trim.

Three independent pieces of evidence indicate that the problem is related to the RHM. First, the transient is present both on the VAX using TSIM and on the Gould Concept−32 processor. Thus, it can be assumed that the problem is not a TSIM bug nor a hardware problem. In addition to this, a different controller designed at the Royal Aerospace Establishment (Bedford) using Linear Quadratic Gaussian (LQG) theory shows a similar initial transient at the start of a time history simulation. The LQG controller does not use acceleration feedback so the control stategy can be ruled out as a cause for the transient. Finally, the only part of the simulations common to both machines is the RHM and SESAME [38]. SESAME is a 'System of Equations for the Simulation of Aircraft in a Modular Environment'. It has been developed in order to facilitate the modelling of various aircraft during real−time simulations and contains modules which are common to all aircraft models. The AFS user must write modules which are specific to his aircraft and contol system design and subsequently link these modules into SESAME in order to build the full real−time simulation model. SESAME is unlikely to be the cause of the nonzero accelerations because it is used by HELISIM3 and the transients are not present in a HELISIM3 generated time history. Another piece of evidence relating to the trim problem is that when the system is flown back to the desired trim state, the values of the actuator blade angles are equal to the trim values used to initialize the system. This leads to the conclusion that the TSIM trim utility does correctly locate the equilibrium flight condition.

In fairness to the RHM, it must be stated that the Flight Path Controller of Section 2.2.4 was difficult to retrim at an arbitrary flight condition. The use of

acceleration feedback complicates the pilot input strategy which must be used. At a trimmed forward flight state, the roll rate, vertical velocity and lateral velocity will ideally be zero and the actuator blade angles will have constant values. In order to trim a flight path controller with acceleration feedback, the pilot must ensure that all accelerations are zero and that all velocities other than the forward speed are also zero. There are, implicitly, two levels of integration between the pilot's acceleration demands and the actuator blade angles.

It was relatively easy to zero system accelerations by zeroing the pilot inceptors. However, the pilot would have to plan ahead as to when to zero his inputs such that the resulting helicopter velocities were those desired for trim. With the imperfect decoupling of modes, this retrimming task was a highly iterative procedure. The input strategy of the Flight Path Controller does not provide for a tight control of speed, height, and heading which is necesary in NOE manouevres.

An alternative input strategy (employed on the LQG system), which was easy to trim, was to have the pilot inceptors controlling the three linear velocities and roll rate. The forward speed inceptor was of a position hold type in contrast to the other three inceptors which were sprung loaded. For this configuration, it is assumed that nonzero vertical and lateral velocities, as well as roll rates, will only be used for transient manoeuvres between one level flight condition and another. The position hold nature of the forward velocity inceptor allows the pilot to choose a speed by positioning the inceptor accordingly and then to forget about that inceptor until a change in speed is required.

The real-time simulation demonstrated the importance of the ability to retrim the aircraft quickly in terms of control input strategy. If the vehicle will not retrim easily, the pilot will then need to execute a much more complicated set of inputs in performing manoeuvres. Because the input strategy is intimately related to the structure of the controller, it can be concluded that the Flight Path Controller should be restructured to allow the pilot direct control of velocities rather than accelerations. These results essentially confirm the conclusions of Chapter 2, showing that the command augmentation of the Flight Path Controlled system was inadequate.

7.3) Flight Path — Fuselage Attitude Decoupling

Although the HUD was used primarily as a means of identifying a trim state, it also showed that the helicopter fuselage attitude was significantly

decoupled from the flight path. The HUD symbology shows both the attitude of the vehicle and a velocity vector indicator. During the simulations, the velocity vector indicator rarely had a conventional position in relation to the body attitude. Even in a level flight trimmed condition, as indicated by the velocity vector, the aircraft often had significant sideslip and bank angle indicating that the fuselage was not aligned with the flight path. Any steady—state wind acting on the aircraft would further complicate the fuselage attitude — flight path relation. Pilots would undoubtedly find this decoupling unacceptable.

The decoupling was also present in a dynamic sense because commands for an increase in forward speed led to an upward pitching of the nose. This non—minimum phase behavior was particularly noticable when operating at any speeds greater than 10 knots away from the design point of the controller. Depending on the distance of the operating point from the design point, the non—minimum phase pitching moment resulted in between 5° and 10° of nose up attitude.

It is assumed that the fuselage attitude — flight path coupling would be improved by having the pilot control velocities as he would be one stage closer to controlling the attitude. With acceleration commands, the pilot is essentially two integrations removed from controlling the fuselage attitude. Because the decoupling of lateral and longitudinal states is not perfect, part of the energy which is input to the system will be used to push the vehicle into unconventional attitudes.

7.4) Pilot Command Effectiveness

The problems with trimming the aircraft and the decoupling of fuselage attitude from flight path can largely be attributed to the acceleration demand structure. Unfortunately, these deficiencies eclipsed the fact that the controller performed reasonably well in terms of regulating the three linear accelerations which were designed to be controlled by the pilot inputs. The velocity vector indicator on the HUD showed that precise control of vertical and lateral velocity was being achieved. Moving the vertical or pedal inceptor caused the indicator to move in the desired direction at a rate which appeared to be linearly related to input amplitude. In addition, vertical and lateral movements of the velocity vector were nicely decoupled near the design point in the flight envelope. Away from the design point, the decoupling was not as good and this will be due, in part, to the invariant axes transformation matrix $[\eta]$.

While vertical and lateral acceleration was quick and precise with no discernable velocity overshoots, forward acceleration was slow and often less than precise as discussed above. The difference is undoubtedly a result of the slower phugoid and slow pitch modes which are present on the forward velocity channel. Moving the inceptor to demand forward acceleration was often followed by a considerable time delay before the HUD started to show an appreciable increase in speed. Release of the inceptor was followed by a period in which the forward speed continued to build up before stabilizing.

Roll control was poor as a result of basing part of the acceleration feedback signal on bank angle rather than roll rate. Lateral cyclic authority is much greater for roll rate than for bank angle as shown by the elements of the input distribution matrix, [B], in Appendix 1. Because the roll command effectiveness (lateral cyclic to bank angle authority) was low, much of the input energy was coupled into other modes, with the result that roll commands produced both sideslip and pitching moments. It is possible that the deficiencies encountered in the command effectiveness over roll are largely responsible for the difficulties in retrimming the aircraft.

From the point of view of evaluating modal control theory as applied to helicopters, it is difficult to draw conclusions. There is insufficient data to say that the problems experienced by the controller were wholly a consequence of its structure. The vertical and lateral responsiveness of the system is cause for some degree of optimism about the effectiveness of modal control, but the forward speed and roll responses show that implementation issues will have a strong influence on the controller's performance.

CHAPTER 8: CONCLUSIONS AND RECOMMENDATIONS

The ACT flight control systems which are being developed to meet the demands of NOE flight will undoubtedly require tuning to eliminate, as far as possible, adverse response characteristics on the controlled helicopter. The tuning requirement arises because of two problems inherent in the use of computer simulation for flight controller design. The practice of using a mathematical model of the helicopter plant introduces errors into the design since descriptions of high order dynamics, particularly those of the rotor, are inaccurate. The effects of these dynamics will be noticeable to the pilot in terms of a decrease in system stability and undesirable cross—couplings. The other aspect of current design techniques which might generate a need for tuning is the use of control laws which are based on control system performance measures, rather than on the flight handling quality specifications. It is unlikely that control system design techniques, such as modal control or optimal control, can yield systems which satisfy the handling requirements without some modifications which are application specific.

8.1) Tuning Process Conclusions and Recommendations

The preferred means of addressing the tuning requirement of ACT helicopter flight controllers is through a sensitivity analysis of the system's response with respect to control system gains. Sensitivity functions provide the partial derivatives which are used in a Newton—Raphson extrapolation scheme to predict the changes in system response arising from variations in the values of controller parameters. The advantage of using sensitivity functions in the tuning process lies in the fact that they provide information concerning the way in which controller parameters affect the amplitude and frequency content of the system's responses. Trial and error tuning techniques are highly iterative and inefficient because they lack this quantitative information.

The signal convolution method has been shown to be an efficient and accurate technique for the generation of sensitivity functions for multivariable closed—loop control systems. Of the two methods of generating the sensitivity functions of controller parameters in systems with unknown plants, the amount of inflight testing required by the signal convolution method is an order of

magnitude smaller than that involved in the use of parameter perturbation techniques. This difference in the necessary amount of inflight testing will only increase as the sophistication of flight controllers is enhanced. In terms of accuracy, signal convolution techniques help to filter the noise which can seriously degrade the results obtained with parameter perturbation methods. Although the theory is only valid for linear systems, signal convolution techniques have been successfully used to generate sensitivities with nonlinear systems, in limited circumstances.

A further testament to the accuracy of the signal convolution method is the rapid convergence of perturbed parameters to their designed values in tuning tests with the Least Integral Error Square Performance Index. Systems are optimised with two passes of the tuning process as the performance index is decreased by a factor of up to 10^5. Tuning of linear systems with the Least Integral Error Square Performance Index has been highly effective as a consequence of the availability of accurate sensitivities. The work reported herein has demonstrated the feasibility of tuning helicopter flight control systems and should prove to be a useful starting point for future investigations.

Unfortunately, there are a few aspects of the tuning problem which still remain to be solved. The main difficulty, at present, is that plant nonlinearities severely limit the circumstances under which the algorithms discussed in this thesis can be applied. Nonlinearities affect the validity of the signal convolution method of generating sensitivity functions and, without accurate sensitivity measures, the optimization procedures cannot guarantee an improvement in the system's response. It is anticipated that this problem will remain as the primary obstacle to the implementation of the technique, since the success or failure will depend on the availability of sensitivity information for nonlinear systems. Thus, further work on nonlinear sensitivity analysis in the helicopter context is needed.

Knowing which control system parameters should be used in the adjustment algorithm is also an area of concern. The method of using normalized transfer function sensitivities to choose the adjustment parameters does isolate those parameters with large sensitivity magnitudes, but, it is not necessarily these parameters which will have the greatest effect in terms of controlling instabilities caused by the high order system dynamics. The tests conducted on linear systems with the Least Integral Error Square Performance Index demonstrated that the adjustment algorithm correctly identified those parameters requiring alterations in systems with perturbed controller gains. If one also recalls the result that allowing a greater number of parameters to be moved will improve the outcome of the optimization, it can be concluded that it is best to use all of the flight

control system parameters when trying to optimize in the presence of unknown dynamics.

In the contrived tests in which the model reference tuning process was presented with the task of retrieving the designed controller matrices from an initially perturbed set, the improvement in system response was universal. That is, when perturbed parameters are moved closer to their desired values, the tuned response is closer than the untuned response to the desired response at all instants of time, for each state, and for all of the test inputs. In tests attempting to optimize the controller gains in the face of unmodelled dynamics, the improvement in response was not universal, as the tuned response would be closer to the desired response for limited times and for a subset of the system's states, but, at other times and on other states the tuned response was worse than the untuned response. These two results lead to the conclusion that the algorithm might have been working with the wrong parameters in the unmodelled dynamics optimization tests, and strengthens the argument that all of the controller's parameters must be available for use in the adjustment algorithm.

If the controller parameters are all allowed to change, the quasi—Newton methods of the adjustment algorithm can be relied upon to alter only those gains which will improve the value of the performance index being used. Controller gains which do not need to be changed will be ignored during the tuning process if the sensitivity functions are valid. In this way, the gains which will be used to counter adverse dynamics will be those having the biggest influence in terms of the required system changes. Unfortunately, the computer used in the study restricted the algorithm to working with only a few parameters and it would be beneficial to use the adjustment algorithm on a larger machine to validate the methods further. However, this is not a fundamental problem and advances in the capabilities of computer hardware will eliminate this barrier. Furthermore, it is conceivable that an optimization could be performed and validated during a single test flight using portable equipment onboard the aircraft.

A fundamental flaw of trial and error tuning is that improvements in system performance with changing control system parameter values are subjectively measured by the pilot. Since different test pilots will have different opinions on what constitutes an ideal response, a system which is tuned for one pilot may not be suitable for another. Improvements in system response must be clearly defined and this implies quantifying the desirability of responses through the use of performance indices. However, the problem is not entirely resolved because in the same way as different pilots have differing opinions, different performance indices will also yield different optimized system characteristics. In terms of flight

control systems work, the ultimate criteria by which performance should be measured is the flight handling quality requirements and this tends to justify the use of the Handling Qualities Performance Index, J_{HQ}, in preference to the Model Reference Performance Index, J_{MR}.

In model reference tuning, the figure of merit assigned to a particular set of controller gains is calculated by the integral of the error squared, the error being defined as the difference between the actual system response and a model response. Although tuning is carried out with respect to several pilot inputs, across all of the system's output states, and with regard to time, there are problems arising from the helicopter application. The optimization of a system with this technique will only be as good as the reference model. In consequence, it is recommended that model reference tuning be used only when it has been demonstrated that the ideal response satisfies the handling quality requirements.

In terms of finding pilot inputs which will expose the system dynamics without unduly exciting nonlinearities, research is currently under way into test input design methods from a system identification point of view [66], and the results of this work will undoubtedly be of benefit to model reference tuning. The possibility of optimizing the pilot's test inputs gives model reference tuning a distinct advantage, in terms of applicability, over handling qualities tuning because the latter requires accurate measures of the sensitivity functions with respect to large amplitude inputs.

Although the robustness problem encountered in attempts to develop the Handling Qualities Performance Index will be solved by developing sophisticated computer algorithms with error checking, the nonlinearities of helicopter flight will severely restrict the use of J_{HQ} for the purposes of tuning. Consequently, at present, it would appear that model reference tuning with specially designed test inputs is most applicable to flight tests. Since this method is best suited to making small changes in the control system gains, large amplitude deficiencies in system dynamics may prove untunable using sensitivity analysis at present. However, with advances in system identification leading to an improvement of the simulation models used in design, the gap between the available tuning authority and the dynamics needing optimization will decrease. The applicability of the tuning procedures will also be enhanced if the robustness of the sensitivity calculations to nonlinearities can be strengthened.

8.2) Flight Control System Conclusions and Recommendations

Athough the aim of the research being reported in this thesis was to develop a tuning algorithm for flight controllers, the development of the Flight Path Controller has illustrated several aspects of the control system design process. The Flight Path Controller was developed in an attempt to enhance the command augmentation features of the controlled system. The acceleration demand structure of the Flight Path Controller was adopted because it allowed a direct transfer of the eigenstructure of the Parry Modal Controller. This structure is not recommended for further development since the pilot is too far removed from control over the vehicle's attitude and because the acceleration feedback signals will be more heavily corrupted by sensor noise than velocity feedback signals.

Active control allows extensive tailoring of the helicopter's stability and control dynamics, but while stability issues can largely be resolved with many control techniques which are becoming standard, the best choice of control dynamics linking the pilot's inceptors to the aircraft's response is not clear. Indeed, the possibilities offered by ACT systems are far more extensive than the present knowledge concerning desirable pilot control strategies. Although the handling quality specifications deal with desired *'response—types'* for different manoeuvres and with pilot inceptor characteristics, such as force gradients, the success of command augmentation strategies will largely depend on how these two areas come together in terms of the structure of the flight control system. Of particular importance is the distribution of inceptor energy on to the various modes of the system. This is shown by the different coupling of input signals into the stability loops of the Parry Modal Controller and the Flight Path Controller, which resulted in different degrees of coupling of the states in response to pilot commands. When one speaks of decoupling system modes, it must be remembered that simply decoupling the plant is not sufficient; one also wants to decouple the control channels linking output states to the pilot's inceptors.

If the state vector of the system plant is extended to include any control system states, the modal control theory of Parry and Murray—Smith [18] could then be used to achieve *'system decoupling'*, rather than just *'plant decoupling'*. For full flight envelope, rate demand systems, it is necessary to have at least four integrations prior to the actuator inputs. These integrators will hold the actuator blade angles at nonzero steady state values even when the rate demand inputs are zero, thereby maintaining the direction and magnitude of the main and tail rotor thrust vectors which is necessary for trimmed flight. In addition, if one

is looking for system decoupling, the work has confirmed the fact that rotor and actuator states should also be included in the analysis because these high order dynamics can have a strong influence on stability and couplings. Therefore, it is proposed that, in the future, the state vector, $\underline{x}(t)$, should be extended to the form given in Equation 8.1 which will have upwards of 23 elements.

$$
\underline{x}(t) =
\begin{bmatrix}
\begin{array}{ll}
u & \text{- forward velocity} \\
w & \text{- vertical velocity} \\
q & \text{- pitch rate} \\
\theta & \text{- pitch angle} \\
v & \text{- lateral velocity} \\
p & \text{- roll rate} \\
\varphi & \text{- roll angle} \\
r & \text{- yaw rate} \\
\psi & \text{- yaw angle} \\
\text{BTA0} & \text{- main rotor coning angle} \\
\text{B1S} & \text{- main rotor longitudinal flapping angle} \\
\text{B1C} & \text{- main rotor lateral flapping angle} \\
\text{BT0DT} & \text{- main rotor coning rate} \\
\text{B1SDT} & \text{- main rotor longitudinal flapping rate} \\
\text{B1CDT} & \text{- main rotor lateral flapping rate} \\
\tau_{0E} & \text{- collective actuator blade angle} \\
\tau_{1S} & \text{- longitudinal cyclic actuator blade angle} \\
\tau_{1C} & \text{- lateral cyclic actuator blade angle} \\
\tau_{0TR} & \text{- tail rotor collective actuator blade angle} \\
\left.\begin{array}{l}
\text{CS1} \\
\text{CS2} \\
\text{CS3} \\
\text{CS4} \\
\vdots
\end{array}\right\} & \text{- flight control system states ($\geq$4)}
\end{array}
\end{bmatrix}
$$

<div align="right">Equation 8.1</div>

In addition to illustrating the importance of command augmentation issues, the development of the Flight Path Controller for real—time simulation trials on the Advanced Flight Simulator (AFS) also revealed that simulation facilities are lacking. When attempting to produce a flight controller, it is necessary to build up the system in a step by step manner rather than by making large jumps, such as that made in transferring from TSIM computer simulation to the AFS. A real—time simulator with simple visual cueing and joysticks for use as pilot inceptors would allow a much more gradual development of the control law. A designer wishes to address problem areas such as real—time excitation of the system and pilot inceptor dynamics in isolation, rather than collectively. The

increase in simulation hardware capabilities should be gradual in a similar vein to the use of the candidate controller on simulation models of increasing complexity. The availability of HELISIM3, modelling nonlinearities, does not eliminate the need for HELISTAB which provides linear descriptions of the same helicopter plant, and the use of the latter will remain as a fundamental component in the initiation of new controller designs. In the future, it is hoped that HELISTAB and HELISIM3 trials will be followed by real—time simulation and then by full moving—base, piloted flight simulation.

As an example of the fundamental problems which the piloted real—time flight simulation results showed, which were not apparent in the computer simulation results of Chapter 2, the AFS illuminated the importance of easily trimming the aircraft which essentially precludes an acceleration demand control strategy. In addition, the undesirable decoupling of the flight path from body attitude of the Flight Path Controller did not appear in the computer simulation results because simple pilot inputs were initiated from a trimmed state. Both of these problems should have been detected well before attempts were made to fly the controller on the AFS.

8.3) Handling Qualities Performance Index Conclusions and Recommendations

Although the Handling Qualities Performance Index, J_{HQ}, does not appear suitable for implementation in a tuning algorithm for helicopters at the present time, it has considerable potential from a control system design standpoint. One application might be that of tuning control system parameters at the computer simulation stage using J_{HQ} on a design developed using a control theory, such as modal control. Alternatively, consider the facts that J_{HQ} allows a continuous measurement of the desirability of a system's handling qualities, and that through the minimization of J_{HQ}, a system's handling qualities are optimized. Since requirements on a system's handling quality parameters can often be transformed into eigenvalue requirements, it may be possible to use a form of the Handling Qualities Performance Index to give a measure of the desirability of particular eigenvalues or pole positions. Thus, it seems possible that eigenstructure assignment for decoupling as espoused by Parry and Murray—Smith [18] might be transformed into eigenstructure assignment for Level 1 flight handling qualities. Instead of plotting principal angles versus eigenvalues, the relevant handling qualities as measured by J_{HQ} could be plotted against eigenvalues. The desired eigenvalues would be those which minimized J_{HQ}, their associated eigenvectors

being those which would minimize the system's principal angles and hence coupling. Although these ideas are tenuous at present, the ability of J_{HQ} to continuously measure handling qualities should at least allow a greater insight into eigenstructure assignment in terms of desirable pole positions. With suitable development, the Handling Qualities Performance Index might bridge the gap between the fields of flight control system development and research into handling qualities. Indeed, the unification of these two areas of expertise is of paramount importance for the production of helicopters which will meet today's demands.

REFERENCES

1. Fry, C.A., "Army 21 — Aviation", *Proceedings of the IEEE 1985 National Aerospace and Electronics Conference*, pp. 1046—1049, 1985.

2. Steward, W., "Operational Criteria for the Handling Qualities of Combat Helicopters", *AGARD — Criteria for Handling Qualities of Military Aircraft*, Paper No. 13, June 1982.

3. Houston, S.S., "On the Analysis of Helicopter Flight Dynamics During Manoeuvres", *Eleventh European Rotorcraft Forum*, London England, Paper No. 80, September 10—13, 1985.

4. Buresh, J.A., Parlier, C.A., and Wilson, W.E., "AH—64A Apache: Development of Capabilities For The Aerial Combat Role", *Vertiflite*, Vol. 34, No. 4, pp. 42—50, July/August 1988.

5. Warwick, G., "For agile read active", *Flight International*, November 9 1985.

6. Winter, J.S., Padfield, G.D., and Buckingham, S.L., "The Evolution of ACS for Helicopters — Conceptual Simulation Studies to Preliminary Design", *NATO — AGARD Conference Proceedings No. 384 Active Control Systems — Review, Evaluation and Projections*, Toronto Canada, Paper No. 7, October 15—18, 1984.

7. Morgan, J.M., "Some Piloting Experience With Multi Function Isometric Side—Arm Controllers in a Helicopter" in *Helicopter Handling Qualities, NASA Conference Publication 2219*, Moffett Field California, pp. 109—120, April 14—15, 1982.

8. Ellis, C.W., "Effects of Articulated Rotor Dynamics on Helicopter Automatic Control System Requirements", *Aeronautical Engineering Review*, pp. 30—38, July 1953.

9. Chen, R.T.N., and Hindson, W.S., "Influence of High—Order Dynamics on Helicopter Flight—Control System Bandwidth", *Eleventh European Rotorcraft Forum*, London England, Paper No. 83, September 10—13, 1985.

10. Berry, D.T., "Flying Qualities Criteria and Flight Control Design", *AIAA Guidance and Control Conference,* Albuquerque, New Mexico, AIAA Paper No. 81—1823, August 19—21, 1981.

11. Padfield, G.D., A Theoretical Model of Helicopter Flight Mechanics for Application to Piloted Simulation, Royal Aircraft Establishment, Technical Report 81048, 1981.

12. Houston, S.S., and Horton, R.I., "The Identification of Reduced Order Models of Helicopter Behavior for Handling Qualities Studies", *Thirteenth European Rotorcraft Forum*, Arles France, Paper No. 7.9, September 8—11, 1987.

13. Hansen, A.S., "Toward a Better Understanding of Helicopter Stability Derivatives", *Journal of the American Helicopter Society*, January 1984.

14. Smith, J., An Analysis of Helicopter Flight Mechanics Part 1, Users Guide to the Software Package Helistab, Royal Aircraft Establishment (Bedford), TM FS(B) 569, 1984.

15. Etkin, B., Dynamics of Flight — Stability and Control, Second Edition, John Wiley and Sons, Toronto Canada, 1982.

16. Bramwell, A.R.S., Helicopter Dynamics, Edward Arnold, London England, 1976.

17. Saunders, G.H., Dynamics of Helicopter Flight, Wiley—Interscience, London England, 1975.

18. Parry, D.L.K., and Murray—Smith, D.J., "The Application of Modal Control Theory to the Single Rotor Helicopter", *Eleventh European Rotorcraft Forum*, London, Paper No. 78, September 10—13, 1985.

19. Hall, W.E. Jr., and Bryson, A.E. Jr., "Inclusion of Rotor Dynamics in Controller Design for Helicopters", *Journal of Aircraft*, Vol. 10, No. 4, pp. 200—206, April 1973.

20. Sobel, K.M., and Shapiro, E.Y., "A Design Methodology for Pitch Pointing Flight Control Systems", *Journal of Guidance*, Vol. 8, No. 2, pp. 181—187, March—April 1985.

21. Leyendecker, H., "The Model Inverse as an Element of a Manoeuvre Demand System for Helicopters", *Twelfth European Rotorcraft Forum*, Garmisch—Partenkirchen, Federal Republic of Germany, Paper No. 54, September 22—25, 1986.

22. Richards, R.J., An Introduction to Dynamics and Control, Longman Group Limited, London England, 1979.

23. Murphy, R.D., and Narendra, K.S., "Design of Helicopter Stabilization Systems Using Optimal Control Theory", *Journal of Aircraft*, Volume 6, Number 2, pp. 129—136, March—April 1969.

24. Miyajima, K., "Analytical Design of a High Performance Stability and Control Augmentation System for a Hingeless Rotor Helicopter", *34TH Annual National Forum of the American Helicopter Society*, pp. 29—36, May 1978.

25. Smith, G.A., and Meyer, G., "Aircraft Automatic Digital Flight Control System with Inversion of the Model in the Feed—Forward Path", *Sixth Digital Avionics Systems Conference*, Baltimore Maryland, pp. 140—150, December 3—6, 1984.

26. Gill, F.R., and Rosenberg, K.W., "Variable Control Policies For Future Aerospace Vehicles", *IEEE National Aerospace and Electronics Conference Proceedings*, Dayton Ohio, pp. 500—506, May 20—24, 1985.

27. Ohta, H., Yokokura, S., Nikiforuk, R.N., and Gupta, M.M., "Adaptive Flight Control of Unstable Helicopters During Transition", *Bridge Between Control Science and Technology, Proceedings of the Ninth Triennial World Congress of IFAC*, Budapest Hungary, pp. 1045—1050, 1984.

28. Simon, J.D., and Mitter, S.K., "A Theory of Modal Control", *Information and Control*, Vol. 13, pp. 316—353, 1968.

29. Srinathkumar, S., and Rhoten, R.P., "Eigenvalue/Eigenvector Assignment For Multivariable Systems", *Electronics Letters*, Vol. 11, No. 6, pp. 124—125, March 20, 1975.

30. Shah, S.L., Fisher, D.G., and Seborg, D.E., "Eigenvalue/Eigenvector Assignment For Multivariable Systems And Further Results For Output Feedback Control", *Electronics Letters*, Vol. 11, No. 16, pp. 388—389, August 7, 1975.

31. Moore, B.C., "On the Flexibility Offered by State Feedback in Multivariable Systems Beyond Closed Loop Eigenvalue Assignment", *IEEE Transactions on Automatic Control*, pp. 689—692, 1976.

32. Sinswat, V., and Fallside, F., "Eigenvalue/Eigenvector Assignment by State—Feedback", *International Journal of Control*, Vol. 26, No. 3, pp. 389—403, 1977.

33. Andry, A.N. Jr., Shapiro, E.Y., and Chung, J.C., "Eigenstructure Assignment for Linear Systems", *IEEE Transactions on Aerospace and Electronic Systems*, Vol. 19, No. 5, pp. 711—724, 1983.

34. Afriat, S.N., "Orthogonal and Oblique Projectors and the Characteristics of Pairs of Vector Spaces", *Proceedings of the Cambridge Philosophical Society*, Vol. 53, pp. 800—816, 1957.

35. Björck, A., and Golub, G.H., "Numerical Methods for Compution Angles Between Linear Subspaces", *Mathematics of Computation*, Vol. 27, No. 123, pp. 579—594, 1973.

36. Klema, V.C., and Laub, A.J., "The Singular Value Decomposition: Its Computation and Some Applications", *IEEE Transactions on Automatic Control*, Vol. AC—25, No. 2, pp. 164—176, April 1980.

37. Morgan, J.M., and Sinclair, S.R.M., "The Use of Integrated Side— Arm Controllers in Helicopters", *AGARD — The Man—Machine Interface in Tactical Aircraft Design and Combat Automation*, Paper No. 27, Stuttgart, Federal Republic of Germany, September 1987.

38. Tomlinson, B.N., <u>SESAME — A System of Equations for the Simulation of Aircraft in a Modular Environment</u>, Royal Aircraft Establishment Technical Report 79008, January 1979.

39. Tomovic, R., <u>Sensitivity Analysis of Dynamic Systems</u>, McGraw— Hill Book Company, Inc., London, 1963.

40. El— Shirbeeny, E.H.T., Murray— Smith, D.J., and Winning, D.J., "Technique for direct evaluation of parameter sensitivity functions", *Electronics Letters*, Vol. 10, No. 25/26, pp. 530— 531, December 12, 1974.

41. Winning, D.J., El–Shirbeeny, E.H.T., Thompson, E.C., and Murray— Smith, D.J., "Sensitivity method for online optimisation of a synchronous— generator excitation controller", *Proc. IEE*, Vol. 124, pp. 631— 638, 1977.

42. Murray–Smith, D.J., "Investigations of methods for the direct assessment of parameter sensitivity in linear closed— loop control systems", in Tzafestas, S. and Borne, P. (eds), <u>Complex and Distributed Systems: Analysis, Simulation and Control</u>, North Holland, Amsterdam, pp. 323— 328, 1986.

43. Soudant, S., <u>Investigations of Methods for the Direct Assessment of Parameter Sensitivity in Closed— Loop Control Systems</u>, Final Year Report, University of Glasgow, Scotland, June 1985.

44. Manness, M.A., and Murray— Smith, D.J., "Direct Assessment of Parameter Sensitivity in Multivariable Closed— Loop Control Systems", *Proceedings of the United Kingdom Simulation Council Triennial Conference 1987*, University College of North Wales, pp. 149— 153, September 9— 11, 1987.

45. Oppenheim, A.V., and Schafer, R.W., "The Discrete Fourier Transform", <u>Digital Signal Processing</u>, Prentice— Hall, Inc. Englewood Cliffs, New Jersey, pp. 110— 115, 1975.

46. Manness, M.A., <u>SAM — Sensitivity Analysis Module Documentation</u>, Version 2, Department of Electronics and Electrical Engineering, University of Glasgow, July 1, 1987.

47. Manness, M.A., <u>The Sensitivity Functions of the State Variables of a Linear Helicopter Model</u>, Department of Electronics and Electrical Engineering, University of Glasgow, Internal Report, Flight Systems Series FS87002, July 24, 1987.

48. Hildebrand, F.B., <u>Introduction to Numerical Analysis</u>, Edition 2, McGraw—Hill, New York, 1974.

49. Barker, H.A., and Davy, R.W., "System identification using pseudorandom signals and the discrete Fourier transform", *Proc. IEE*, Vol. 122, No. 3, pp. 305—311, March 1975.

50. Manness, M.A., <u>The Transfer Function Sensitivities of a Linear Helicopter Model</u>, Department of Electronics and Electrical Engineering, University of Glasgow, Internal Report, Flight Systems Series FS87003, August 5, 1987.

51. Manness, M.A., <u>The Eigenstructure Sensitivity of a Linear Helicopter Model</u>, Department of Electronics and Electrical Engineering, University of Glasgow, Internal Report Flight Systems Series FS87001, April 8, 1987.

52. Documentation for the routines F02AGF and F02AXF in Numerical Algorithm Group Fortran Library Manual, Mark 12, Vol.4, Numerical Algorithms Group Ltd., NAG Central Office, Mayfield House, 256 Banbury Road, Oxford England, 1987.

53. Documentation for the routine E04JAF in Numerical Algorithm Group Fortran Library Manual, Mark 12, Vol.3, Numerical Algorithms Group Ltd., NAG Central Office, Mayfield House, 256 Banbury Road, Oxford England, 1987.

54. Gill, P.E., and Murray, W., <u>Minimization Subject to Bounds on the Variables</u>, National Physical Laboratory — NPL Report NAC 72, December 1976.

55. Winkelman, J.R., "A Tuning Algorithm for a Multivariable Controller", *IFAC Congress Preprints*, Vol. 10, pp. 177−182, August 1987.

56. Hoh, R.H., Mitchell, D.G., et. al., <u>Proposed Specification for Handling Qualities of Military Rotorcraft, Volume I − Requirements</u>, Draft, NASA − Technical Memorandum, US Army AVSCOM Technical Report 87−A−4, May 1988.

57. O'Hara, F., "Handling Criteria", *Journal of The Royal Aeronautical Society*, Vol. 71, No. 676, pp. 271−291, April 1967.

58. Key, D.L., "A Critique of Handling Qualities Specifications for U.S. Military Helicopters", *Atmospheric Flight Mechanics Conference*, Danvers Mass., pp. 305−319, August 11−13, 1980.

59. Key, D.L., "The Status of Military Helicopter Handling Qualities Criteria", *Proceedings of a Specialists Meeting on Helicopter Handling Qualities, NASA Conference Publication 2219 Helicopter Handling Qualities*, Paper No. 11, April 14−15 1982.

60. Chen, R.T.N., and Talbot, P.D., "An Exploratory Investigation of the Effects of Large Variations in Rotor System Dynamics Design Parameters on Helicopter Handling Characteristics in Nap−of−the−Earth Flight", *Journal of the American Helicopter Society*, pp. 22−36, July 1978.

61. Chen, R.T.N., "Unified Results of Several Analytical and Experimental Studies of Helicopter Handling Qualities in Visual Terrain Flight", *Proceedings of a Specialists Meeting on Helicopter Handling Qualities, NASA Conference Publication 2219 Helicopter Handling Qualities*, April 14−15 1982.

62. Sinclair, S.R.M., and Morgan, M., "An Evaluation of a 4−Axis Displacement Side−Arm Controller in a Variable Stability Helicopter", National Aeronautical Establishment, National Research Council, Ottawa Canada, 1987.

63. Sinclair, S.R.M., and Morgan, M., <u>An Investigation of Multi-Axis Isometric Side-Arm Controller in a Variable Stability Helicopter</u>, National Research Council of Canada, National Aeronautical Establishment, Aeronautical Report LR-606 NRC No. 19629, August 1981.

64. Baillie, S.W., and Morgan, J.M., <u>The Impact of Vertical Axis Characteristics on Helicopter Handling Qualities</u>, National Research Council Canada, National Aeronautical Establishment, Aeronautical Report LR-619 NRC No. 28133, August 1987.

65. Hoh, R.H., Mitchell, D.G., et. al., <u>BACKGROUND INFORMATION AND USER'S GUIDE FOR PROPOSED HANDLING QUALITIES REQUIREMENTS FOR MILITARY ROTORCRAFT</u>, Systems Technology Inc. Technical Report No. 1194-3, 20 December 1985.

66. Leith, D.J., and Murray-Smith, D.J., "Experience with Multi-step Test Inputs for Helicopter Parameter Identification", *Fourteenth European Rotorcraft Forum*, Milan Italy, Paper No. 68, September 20-23, 1988.

APPENDIX 1: THE PLANT AND CONTROL SYSTEM MATRICES USED IN THE SIMULATION STUDY

The plant of the single rotor helicopter which formed the basis of the computer simulations was represented by the stability and control derivatives generated by HELISTAB. The values of these derivatives are presented in the [A] and [B] matrices shown below for the 80.0 knots level flight condition which was used as the design point.

$$
[A] \; = \;
\begin{bmatrix}
-0.03221 & 0.04038 & -0.73663 & -32.17915 \\
-0.00954 & -0.80272 & 134.81477 & -0.69159 \\
0.00825 & 0.00878 & -2.33976 & 0.00000 \\
0.00000 & 0.00000 & 0.99946 & 0.00000 \\
0.00433 & 0.01430 & -0.42178 & 0.02275 \\
-0.01136 & 0.07148 & -1.99888 & 0.00000 \\
0.00000 & 0.00000 & -0.00071 & 0.00000 \\
-0.00786 & 0.00075 & -0.08946 & 0.00000
\end{bmatrix}
$$

$$
\begin{bmatrix}
-0.00211 & -0.35668 & 0.00000 & 0.00000 \\
-0.01941 & -1.48180 & 1.05781 & 0.00000 \\
0.00316 & 0.41067 & 0.00000 & 0.00000 \\
0.00000 & 0.00000 & 0.00000 & 0.03287 \\
-0.16671 & 0.64606 & 32.16176 & -133.48404 \\
-0.04971 & -10.52839 & 0.00000 & -0.28668 \\
0.00000 & 1.00000 & 0.00000 & 0.02149 \\
0.03095 & -1.79190 & 0.00000 & -1.35013
\end{bmatrix}
$$

$$
[B] \; = \;
\begin{bmatrix}
14.29279 & -25.03464 & 6.74727 & 0.00000 \\
-386.93283 & -99.82667 & 0.00000 & 0.00000 \\
14.07609 & 28.53878 & -5.85112 & 0.00000 \\
0.00000 & 0.00000 & 0.00000 & 0.00000 \\
4.92125 & -5.00933 & -30.58006 & 22.04102 \\
32.09763 & -25.00369 & -153.22520 & -1.34353 \\
0.00000 & 0.00000 & 0.00000 & 0.00000 \\
13.95295 & -5.94894 & -26.80758 & -18.09545
\end{bmatrix}
$$

The matrices of the Parry Modal Controller are given by Reference [18] as,

$$
[P] = \begin{bmatrix}
-0.00224 & 0.00855 & 0.00037 & 0.00002 \\
-0.00134 & -0.03313 & -0.00144 & -0.00009 \\
-0.00025 & 0.00719 & -0.00614 & -0.00037 \\
-0.00015 & 0.00054 & -0.00892 & 0.04483
\end{bmatrix}
$$

$$
[K_P] = \begin{bmatrix}
0.00708 & -0.00876 & -0.44078 & -0.28431 \\
-0.02733 & 0.00191 & 0.35800 & 1.10894 \\
0.00591 & -0.00259 & -0.13537 & -0.23683 \\
0.00701 & -0.00327 & -0.24124 & -0.26660
\end{bmatrix}
$$

$$
\begin{bmatrix}
-0.00005 & 0.00047 & -0.00330 & -0.00035 \\
0.00038 & 0.01303 & 0.00221 & 0.00135 \\
0.00010 & -0.00616 & -0.00275 & 0.00657 \\
0.01711 & 0.11690 & 0.15166 & -0.56884
\end{bmatrix}
$$

Using the theory presented in Section 2.2.4, the following matrices were developed for the Flight Path Controlled system at 80.0 knots.

$$
[G] = \begin{bmatrix}
10.000 & 0.000 & 0.000 & 0.000 \\
0.000 & 10.000 & 0.000 & 0.000 \\
0.000 & 0.000 & 19.293 & 0.000 \\
0.000 & 0.000 & 0.000 & 10.000
\end{bmatrix}
$$

$$
[\eta] = \begin{bmatrix}
0.99923 & 0.02149 & 0.00000 & 0.03287 \\
-0.02150 & 0.99977 & 0.00000 & 0.00000 \\
0.00000 & 0.00000 & 1.00000 & 0.00000 \\
-0.03286 & -0.00071 & 0.00000 & 0.99946
\end{bmatrix}
$$

$$
[\xi] = \begin{bmatrix}
0.000 & 1.000 & 0.000 & 0.000 \\
1.000 & 0.000 & 0.000 & 0.000 \\
0.000 & 0.000 & 0.000 & 0.000 \\
0.000 & 0.000 & 0.000 & 0.000
\end{bmatrix}
$$

$$
\begin{bmatrix}
0.000 & 0.000 & 0.000 & 0.000 \\
0.000 & 0.000 & 0.000 & 0.000 \\
0.000 & 0.000 & 1.000 & 0.000 \\
1.000 & 0.000 & 0.000 & 0.000
\end{bmatrix}
$$

$$[P] = \begin{bmatrix} -0.01140 & 0.00815 & 0.00105 & -0.00001 \\ 0.00412 & -0.00316 & -0.00405 & 0.00004 \\ -0.00301 & 0.00069 & -0.01728 & -0.00019 \\ -0.00523 & 0.00072 & 0.02467 & 0.01989 \end{bmatrix}$$

$$[K] = \begin{bmatrix} -0.00010 & 0.00226 & -0.40867 & -0.05522 \\ 0.00048 & -0.00070 & 0.23352 & 0.22096 \\ -0.00003 & 0.00011 & -0.10867 & -0.04735 \\ 0.00024 & 0.00160 & -0.21136 & -0.05018 \end{bmatrix}$$

$$\begin{bmatrix} 0.00001 & 0.00054 & -0.00332 & -0.00002 \\ 0.00016 & 0.012177 & 0.00228 & 0.00009 \\ 0.00032 & -0.00776 & -0.00277 & 0.00683 \\ -0.00274 & 0.11912 & 0.15165 & -0.56852 \end{bmatrix}$$

APPENDIX 2: THE EQUATIONS GOVERNING THE SIGNAL CONVOLUTION METHOD AS APPLIED TO THE PARRY MODAL CONTROLLER

The following theory presents the application of signal convolution techniques to the Parry Modal Controller. While it is not necessary to repeat the steps involved in the generation of sensitivity functions using the signal convolution method (Section 3.2.1), this appendix will demonstrate that the form of the sensitivity signals differs from Equations 3.13 and 3.23 which are specific to the Flight Path Controller.

Recall Equation 2.24 which governs the Parry Modal Controller.

$$\dot{\underline{x}}(t) = \left[\ [A] - [B][K_p] \ \right] \underline{x}(t) + [B][P] \ \underline{r}(t) \qquad \text{Equation 2.24}$$

After rearrangement in the Laplace transform domain, this equation becomes,

$$\underline{X}(s) = \left[\ s[I] - [A] + [B][K_p] \ \right]^{-1} [B][P] \ \underline{R}(s)$$

$$\text{Equation A2.1}$$

The closed loop transfer function matrix of the Parry Modal Controlled system is given by,

$$[W(s)] = \left[\ s[I] - [A] + [B][K_p] \ \right]^{-1} [B][P] \qquad \text{Equation A2.2}$$

Equation A2.1 can be rearranged into,

$$\left[\ s[I] - [A] + [B][K_p] \ \right] \underline{X}(s) = [B][P] \ \underline{R}(s) \qquad \text{Equation A2.3}$$

The sensitivity functions are given by implicit differentiation of Equation A2.3 with respect to the control system parameter, α_i.

$$\left[\ [B]\frac{\partial[K_p]}{\partial\alpha_i} \ \right] \underline{X}(s) + \left[\ s[I] - [A] + [B][K_p] \ \right] \frac{\partial\underline{X}(s)}{\partial\alpha_i} = [B]\frac{\partial[P]}{\partial\alpha_i}\underline{R}(s)$$

$$\text{Equation A2.4}$$

Simplification gives,

$$\frac{\partial \underline{X}(s)}{\partial \alpha_i} = \left[s[I] - [A] + [B][K_P] \right]^{-1} [B] \left[\frac{\partial [P]}{\partial \alpha_i} \underline{R}(s) - \frac{\partial [K_P]}{\partial \alpha_i} \underline{X}(s) \right]$$

<div align="right">

Equation A2.5

</div>

Equation A2.5 can be put into the standard form of a multiplication of the closed loop transfer function matrix and a sensitivity signal if the latter is given by,

$$\underline{Z}_{\alpha_i}(s) = [P]^{-1} \left[\frac{\partial [P]}{\partial \alpha_i} \underline{R}(s) - \frac{\partial [K_P]}{\partial \alpha_i} \underline{X}(s) \right] \qquad \text{Equation A2.6}$$

The theory concerning the generation of the sensitivities follows that presented in Section 3.2.1 from this point onwards.

In terms of the second order sensitivity signal of the Parry Modal Controller, if one differentiates Equation A2.4 with respect to a second control system parameter, α_j, it is possible to generate Equation A2.7.

$$\left[[B] \frac{\partial [K_P]}{\partial \alpha_i} \right] \frac{\partial \underline{X}(s)}{\partial \alpha_j} + \left[[B] \frac{\partial [K_P]}{\partial \alpha_j} \right] \frac{\partial \underline{X}(s)}{\partial \alpha_i} +$$

$$\left[s[I] - [A] + [B][K_P] \right] \frac{\partial^2 \underline{X}(s)}{\partial \alpha_j \partial \alpha_i} = 0 \qquad \text{Equation A2.7}$$

Since the control system matrices are both first order in terms of their elements, their second order differentials are zero (Equations 3.17 and 3.18). Equation A2.7 can be simplified to Equation A2.8.

$$\frac{\partial^2 \underline{X}(s)}{\partial \alpha_j \partial \alpha_i} = - \left[s[I] - [A] + [B][K_P] \right]^{-1} [B] \times$$

$$\left[\frac{\partial [K_P]}{\partial \alpha_i} \frac{\partial \underline{X}(s)}{\partial \alpha_j} + \frac{\partial [K_P]}{\partial \alpha_j} \frac{\partial \underline{X}(s)}{\partial \alpha_i} \right]$$

<div align="right">

Equation A2.8

</div>

Thus, the second order sensitivity signal for the Parry Modal Controller is,

$$\underline{Z}^2_{\alpha_j \alpha_i}(s) = - [P]^{-1} \left[\frac{\partial [K_P]}{\partial \alpha_i} \frac{\partial \underline{X}(s)}{\partial \alpha_j} + \frac{\partial [K_P]}{\partial \alpha_j} \frac{\partial \underline{X}(s)}{\partial \alpha_i} \right]$$

Equation A2.9

APPENDIX 3: THE FORWARD FLIGHT HANDLING QUALITY
SPECIFICATIONS

In the following table each of the subsections of *section 3.4* of the flight handling quality specifications report [56] is examined for parameters which can be used in the tuning process. A subsection is considered applicable to the present work if it contains quantitative parameter limits which can be used to classify the handling qualities on the basis of the state response of the system with respect to pilot inputs.

Table A3.1: The Applicability of the Forward Flight Handling Qualities for
the Tuning of Flight Control Systems

Section   Data

3.4.1   Title: *Pitch Attitude Response to Longitudinal Controller*

3.4.1.1   Title: *Short-Term Response*
                 Applicability: Applicable
                 Relevant Parameters: ω_{BW} – bandwidth
                                      $\tau_{p\theta}$ – pitch phase delay
                                      ζ – effective damping ratio
                 Inputs: longitudinal inceptor to yield ±5° of pitch or
                         limited by the load factors and the OFE

3.4.1.2   Title: *Mid-Term Response — Maneuvering Stability*
                 Applicability: Not applicable
                 Comments: This requirement is not applicable because it
                           depends on knowledge of the inceptor forces and
                           the OFE.

3.4.2   Title: *Pitch Control Power*
                 Applicability: Not applicable
                 Comments: This requirement is not applicable because it
                           depends on knowledge of the load factors and
                           the OFE.

3.4.3   Title: *Flight Path Control*

Applicability: Applicable
Relevant Parameters: w   - vertical velocity
T_{heq} - response time constant
τ_{heq} - response time constant
r^2 - coefficient of determination
Inputs: step input on the vertical inceptor

3.4.4   Title: *Interaxis Coupling*

Applicability: Parts are applicable
Comments: This paragraph outlines the situations in which the subsequent paragraphs in *section 3.4.4* are applicable.

3.4.4.1   Title: *Collective-to-Attitude Coupling*

3.4.4.1.1 Title: *Small Collective Inputs (Less Than 20% of Full Control)*

Applicability: Applicable
Relevant Parameters: θ_{peak} - peak change in pitch attitude
n_{zpeak} - peak normal acceleration
t   - time
Inputs: step input on the vertical inceptor of less than 20% of full control
Comments: It will be necessary to know the full control authority of the collective in order to use this requirement.

3.4.4.1.2 Title: *Large Collective Inputs (Greater Than or Equal to 20% of Full Control)*

Applicability: Applicable
Relevant Parameters: θ_{peak} - peak change in pitch attitude
n_{zpeak} - peak normal acceleration
t   - time
Inputs: step input on the vertical inceptor of greater than 20% of full control
Comments: It will be necessary to estimate the full control authority of the collective in order to use this requirement. Parts of this requirement dealing with autorotation and the OFE cannot be used.

3.4.4.2   Title: *Pitch-to-Roll and Roll-to-Pitch Coupling During Aggressive Maneuvering*

Applicability: Applicable
Relevant Parameters: q_{peak} - peak pitch rate
P_{step} - step change in roll rate
P_{peak} - peak roll rate
q_{step} - step change in pitch rate
Inputs: step on the longitudinal inceptor for rate
response-types
step on the roll inceptor for rate response-types

3.4.5   Title: *Roll Attitude Response to Lateral Controller*

3.4.5.1   Title: *Small-Amplitude Roll Attitude Response to Control Inputs*

Applicability: Applicable
Relevant Parameters: ω_{BW} - bandwidth
$\tau_{p\varphi}$ - roll phase delay
ζ - damping ratio
ω_n - frequency
Φ - roll attitude
Inputs: roll inceptor to yield ±10° of roll

3.4.5.2   Title: *Moderate-Amplitude Attitude Changes*

Applicability: Possibly
Relevant Parameters: P_{peak} - peak roll rate
$\Delta\Phi$ - change in bank angle
Inputs: roll inceptor to yield between 10° and 40° of
roll both positive and negative
Comments: This requirement should be related to an MTE.

3.4.5.3   Title: *Large Amplitude Roll Attitude Changes*

Applicability: Applicable
Relevant Parameter: p - roll rate
Inputs: a full amplitude step on the roll inceptor
Comments: It may not be possible to use this test with
nonlinear simulation models since the
sensitivity functions may not be valid.

3.4.5.4   Title: *Linearity of Roll Response*

Applicability: Not applicable
Comments: This requirement is purely qualitative.

3.4.6   Title: *Roll-Sideslip Coupling*

3.4.6.1   Title: *Bank Angle Oscillations*

Applicability: Applicable
Relevant Parameters: Φ_{OSC} – a bank angle parameter
Φ_{AV} – a bank angle parameter
Φ – change in bank angle
p – roll rate
β – sideslip
δ_{AS} – lateral control position from trim
t – time
Inputs: a pulse roll control command for rate response-types

3.4.6.2   Title: *Turn Coordination*

Applicability: Applicable
Relevant Parameters: $\Delta\beta$ – maximum change in sideslip
$t_{\Delta\beta}$ – a time constant
Φ_1 – a feature on the roll attitude response
Φ – the roll attitude response
$|\Phi/\beta|_d$ –
t – time
Inputs: an abrupt pulse roll control command for rate response-types.

3.4.7   Title: *Yaw Response to Yaw Control Input*

3.4.7.1   Title: *Small Amplitude Yaw Response for Air Combat*

Applicability: Applicable
Relevant Parameters: ω_{BW} – bandwidth
$\tau_{p\psi}$ – yaw phase delay
ψ – heading angle
Inputs: pedal inceptor to produce $\pm 10°$ in yaw.

3.4.7.2   Title: *Large Amplitude Heading Changes*

Applicability: Applicable
Relevant Parameters: Ψ – the heading
t – time
Inputs: an abrupt step displacement of the yaw control
Comments: In order to use this requirement it must be assumed that the sideslip limits of the OFE are not exceeded.

3.4.7.3   Title: *Linearity of Response*

Applicability: Not applicable
Comments: This requirement is purely qualitative.

3.4.7.4   Title: *Yaw Control with Speed Changes*

Applicability: Not applicable
Comments: This requirement should be tested with a real-time simulation facility.

3.4.8   Title: *Lateral Directional Stability*

3.4.8.1   Title: *Lateral-Directional Oscillations*

            Applicability: Applicable
            Relevant Parameters: ω_n - frequency
                                 ζ - damping ratio
            Inputs: a doublet on the yaw controller

3.4.8.2   Title: *Spiral Stability*

            Applicability: Applicable
            Relevant Parameter: φ - bank angle
            Inputs: a pulse on the roll inceptor

3.4.9   Title: *Lateral-Directional Characteristics in Steady Sideslips*

            Applicability: Not applicable
            Comments: The requirement calls for testing to the limits
                      of the OFE.

3.4.9.1   Title: *Yaw Control in Steady Sideslips*

            Applicability: Not applicable
            Comments: The requirement depends on knowledge of the
                      control forces.

3.4.9.2   Title: *Bank Angle in Steady Sideslips*

            Applicability: Not applicable
            Comments: The requirement is purely qualitative.

3.4.9.3   Title: Lateral Control in Steady Sideslips

            Applicability: Not applicable
            Comments: The requirement depends on knowledge of the
                      control forces.

3.4.9.3.1   Title: *Positive Effective Dihedral Limit*

            Applicability: Not applicable
            Comments: The requirement depends on knowledge of the
                      control forces.

3.4.10   Title: *Pitch, Roll and Yaw Response to Disturbance Inputs*

            Applicability: Not applicable
            Comments: This requirement calls for direct excitation
                      of the control actuators.